NOTICE

The quality of this microform is heavily dependent upon the quality of the original thesis submitted for microfilming. Every effort has been made to ensure the highest quality of reproduction possible.

If pages are missing, contact the university which granted the degree.

Some pages may have indistinct print especially if the original pages were typed with a poor typewriter ribbon or if the university sent us an inferior photocopy.

Reproduction in full or in part of this microform is governed by the Canadian Copyright Act, R.S.C. 1970, c. C-30, and subsequent amendments.

AVIS

La qualité de cette microforme dépend grandement de la qualité de la thèse soumise au microfilmage. Nous avons tout fait pour assurer une qualité supérieure de reproduction.

S'il manque des pages, veuillez communiquer avec l'université qui a conféré le grade.

La qualité d'impression de certaines pages peut laisser à désirer, surtout si les pages originales ont été dactylographiées à l'aide d'un ruban usé ou si l'université nous a fait parvenir une photocopie de qualité inférieure.

La reproduction, même partielle, de cette microforme est soumise à la Loi canadienne sur le droit d'auteur, SRC 1970, c. C-30, et ses amendements subséquents.

ISBN 0-315-53807-4

A NEW METHOD FOR THE CRITICAL SPEED CALCULATION OF ROTOR-BEARING SYSTEMS

BY

PAUL YOUNG-IL KIM

A THESIS PRESENTED TO
THE SCHOOL OF GRADUATE STUDIES
UNIVERSITY OF OTTAWA
IN PARTIAL FULFILLMENT OF
THE REQUIREMENTS FOR THE DEGREE OF
DOCTOR OF PHILOSOPHY
IN
THE MECHANICAL ENGINEERING DEPARTMENT

OTTAWA, ONTARIO, CANADA
FEBRUARY, 1987

ABSTRACT

A new approach to the critical speed calculation of practical industrial rotors is presented. The Euler beam equation is applied to each segment of a rotating shaft to find a solution for each single-segment with a uniform cross-section. The solution is applied to a practical rotor-bearing system satisfying all the boundary conditions. This eventually generates homogeneous equations which form the set of governing equations for the critical speeds of the system. Within the framework of Euler beam theory, the set of governing equations is completely analytical and explicit. That is, it is explicit, not implied as in the Transfer Matrix Method, and it does not include any approximations such as discretization of shaft mass, polynomial approximations, etc.

The set of governing equations appears in the form of a sparse and banded determinant, the value of which is to vanish. By solving for specific values of ω (the rotational speed of the shaft) which makes the value of the determinant vanish, the critical speeds of the rotor-bearing system are found. The elements of the determinant form a special shape and they can be arranged in partitions. Each partition can be related to a specific boundary of the rotor. This permits an automatic generation of the system matrix using a computer. The theory and procedures involved in this new method are straightforward thus allowing novice engineers to create their own computer program with extreme ease.

A simple rotor-bearing system is used to illustrate the theory and procedures step-by-step. Then, a two-disc rotor-bearing system is solved for its critical speeds using the new simplified method. The results are compared with other analytical as well as experimental results. Finally, as a general case of practical rotors, the socalled "Prohl's rotor" is solved for its critical speeds using the present method as well as the Transfer Matrix Method, and the results are compared with each other. Comparisons are also made with the results by Urban, available from an open literature.

ACKNOWLEDGEMENTS

The author expresses his appreciation to Dr. R.C. Flanagan, Professor, Department of Mechanical Engineering, University of Ottawa, and Dr. I.R.G. Lowe, Section Head, Low Temperature Laboratory, Division of Mechanical Engineering, National Research Council, for their constant encouragement and supervision throughout the complete program. He also wishes to express his sincere gratitude to Mr. E.H. Dudgeon, Vice-President (Engineering), and Mr. J. Ploeg, Director, Division of Mechanical Engineering, National Research Council, for their generous support and encouragement throughout the development of this program and dissertation.

He also wishes to thank Mrs. H.S. Cuccaro and Mrs. Linda Charbonneau for typing many drafts of the manuscripts.

Finally, the author extends his deepest appreciation to his family for their support and encouragement.

TABLE OF CONTENTS

List of Figures

List of Figures

List of Figures

List of Figures

List of Tables

Nomenclature

Many methods for critical speed calculation have been reviewed and summarized in this thesis. Each method has its own conventional notations signifying functional roles or physical meanings. In order not to disturb this, the list of notations are separated for each section in Chapter II. Therefore, their notations are not valid beyond each section of Chapter II. From Chapter III on, one body of notation system has been adopted throughout this thesis.

Section II.2.3

a_i	Parameters
$q(t)$	A function of time t
x	Coordinate parallel to shaft axis
t	Time
u	Deflection of beam
γ_i	Generating set
Ψ	An assumed mode shape

Section II.2.4

g	Acceleration due to gravity
k_e	Equivalent spring constant
W_1	Weight of first disc
W_2	Weight of second disc
ω_i	ith critical speed
ω_{jj}	Critical speed of jth sub-rotor
ω_{total}	The first critical speed of the total system

Section II.2.6

C_i	Constant
G	$= K^{-1}M$
H	$= G^{-1}$
K	Stiffness matrix of the system
M	Mass matrix of the system
p	A principal mode
$\{q\}$	Generalized coordinates
S_1	Sweeping matrix for first mode
$\{u\}$	A modal vector
$[u]$	Modal matrix
$\{V\}$	Arbitrary vector
$[v]$	$= [u]^{-1}$
ω	Natural frequency

Section II.2.9

A,B,C,D	Constants
D_D	Diameter of disc
D_S	Diameter of shaft
EI	Flexural rigidity of beam
g	Acceleration due to gravity
h	Thickness of disc
$\{H_c\}$	Moment of momentum of disc about its center
$[I]$	Inertia matrix of disc
I'	Net moment of disc; eq. (2-26) $(= I_\xi - I_\eta)$

I_ξ, I_η, I_ζ	Moment of inertia of disc about ξ, η, and ζ axes, respectively; Fig. 2-2
k_B	Spring constant of bearing
ℓ	Length of shaft segment
M	Bending moment of beam
$\{M\}$	Moment vector of disc
m	$= [\frac{\rho\omega^2}{EI}]^{\frac{1}{4}}$
m_D	Mass of disc
n	Number (ordinal) of station or segment
N	Total number of segments in the rotor-bearing system
q	Intensity of loading
$[S_1]$	Matrix defined by eq. (2-39)
$[S_2]$	Matrix defined by eq. (2-40)
$[S_3]$	Matrix defined by eq. (2-41)
$[S_4]$	Matrix defined by eq. (2-42)
$[T_a]$	Transfer matrix of shaft segment
$[T_n]$	Transfer matrix defined by eq. (2-37)
$[T_p]$	Point transfer matrix, eq. (2-34)
V	Shear force
w	Specific weight of disc material
x	Coordinate parallel to shaft axis
y	Deflection of beam
$\{Z\}$	State vector, eq. (2-33)
θ	Slope $[= \frac{dy}{dx}]$

ξ,η,ζ Principal coordinates of disc, Fig. 2-2

ρ Linear mass (mass per unit length) of shaft

ϕ Angle ($= \tan^{-1}\theta$), Fig. 2-2

$\{\Omega\}$ Angular velocity vector of disc

ω Angular velocity of rotation of the shaft

Section II.2.10

E Young's modulus

$[I]$ Inertia matrix of disc

I_D Diametral or transverse moment of inertia of disc

I_p Polar moment of inertia of disc

I_ξ, I_η, I_ζ Moment of inertia of disc about ξ, η, and ζ axes, respectively

i Used as a subscript, indicates either "ith" element or node "i"

j Used as a subscript, indicates node "j"

$[K_s]$ Stiffness matrix of shaft element

$[K_T]$ Total stiffness matrix of the whole system

k_B Spring constant of bearing

L Lagrangian ($= T_T - U_T$)

ℓ Length of element

$[M_s]$ Mass matrix of shaft element

$[M_T]$ Total mass matrix of the whole system

m_D Mass of disc

$\lfloor N \rfloor$ Shape function

q_i Generalized coordinates

T_D	Kinetic energy of disc
T_i	Kinetic energy of ith element
T_s	Kinetic energy of shaft element
T_T	Total kinetic energy of the whole system
U_B	Potential energy of bearing
U_i	Potential energy of ith element
U_s	Potential energy of shaft element
U_T	Total potential energy of the whole system
v	Lateral displacement of beam
y	Local coordinate, Fig. 2-5
$\alpha_1, \alpha_2, \alpha_3, \alpha_4$	Constants
$\{\delta\}$	Nodal displacement vector
ϵ	Strain
θ	Slope $\left[= \frac{dv}{dx}\right]$
ξ, η, ζ	Principal axes of disc
ρ	Linear mass of shaft element
σ	Stress
ϕ	Angle $(= \tan^{-1} \theta)$
$\{\Omega\}$	Angular velocity vector of disc
$\Omega_\xi, \Omega_\eta, \Omega_\zeta$	Components of $\{\Omega\}$ in the direction of ξ, η, and ζ axes, respectively
ω	Angular velocity of rotation of shaft

Chapter III

A,B,C,D	Constants, eq. (3-7)
A_1,B_1,C_1,D_1	Constants related to first segment
A_2,B_2,C_2,D_2	Constants related to second segment
•	•
•	•
•	•
A_6,B_6,C_6,D_6	Constants related to sixth segment
$[A]$	Matrix (partitioned), eq. (3-10), Fig. 3-4
a_{ij}	Elements of matrix [A]
$[B]$	Matrix, eq. (3-16), Fig. 3-4
b_{ij}	Elements of matrix [B]
$[C]$	Matrix, eq. (3-21), Fig. 3-4
c_{ij}	Elements of matrix [C]
$[D]$	Matrix, eq. (3-26), Fig. 3-4
D_D	Diameter of disc
D_S	Diameter of shaft
d_{ij}	Elements of [D]
$[E]$	Matrix, eq. (3-27), Fig. 3-4
EI	Flexural rigidity of beam
EI_1	Flexural rigidity of segment #1
EI_2	Flexural rigidity of segment #2
•	•
•	•
•	•
EI_6	Flexural rigidity of segment #6
e_{ij}	Elements of [E]
$[F]$	Matrix, eq. (3-28), Fig. 3-4
f_{ij}	Elements of [F]

[G]	Matrix defined by eq. (2-29), Fig. 3-4
g	Acceleration due to gravity
g_{ij}	Elements of [G]
h	Thickness of Disc
I'	Net moment of inertia of disc
[K]	Overall matrix, eq. (3-30)
$\ell_1,\ell_2,\ldots$	Distances along X direction from origin to first, second,...stations, respectively
M	Bending moment
$M_1,M_2,\ldots$	Bending moment of first, second,...segments, respectively
m	$= \left[\frac{\rho\omega^2}{EI}\right]^{\frac{1}{4}}$
$m_1,m_2,\ldots$	The values of m in first, second,...segments, respectively
p	Intensity of load (load per unit length of shaft)
SF	Some Finite value
V	Shear force
$V_1,V_2,\ldots$	Shear force of first, second,...segments, respectively
x	Horizontal coordinate axis, coincides with the centroidal axis of shaft when it is not deflected
y	Deflection of shaft
$y_1,y_2,\ldots$	Deflection of first, second,...segments, respectively
w	Linear weight (weight per unit length) of shaft
$\{\alpha_1\},\{\alpha_2\},\ldots$	Column matrix of constants $A_1,B_1,\ldots$ eqs. (3-10), (3-16), (3-21), (3-26), (3-27), (3-28), (3-29)
θ	Slope

$\theta_1, \theta_2, \ldots$	Slope of first, second,...segements, respectively
$\{\Lambda\}$	Column matrix of $A_1, B_1, \ldots C_6, D_6$
ρ	Linear mass of shaft
ω	Angular velocity of rotation of shaft

CHAPTER I

INTRODUCTION

I.1 Background Perspective

The first paper on Rotor Dynamics seems to be that of Rankine (Ref. 1) published in The Engineer in 1869. Ever since Rankine's paper, there has been a gradual increase in the number of publications in the field of Rotor Dynamics (Ref. 2) and by 1965 the number of publications reached 65 papers per year (Ref. 3). In April 1982, for the first time, ASME categorized 14 papers and published them, under the group title of Rotor Dynamics, in the Journal of Mechanical Design.

Meanwhile, the subjects of Rotor Dynamics have been expanded to include:

i) critical speed analysis

ii) unbalance responses

iii) flexible rotor balancing

iv) stability of rotor-bearing systems

v) transient analysis

vi) dynamics of fluid film bearings (Ref. 4) and rolling element bearings (Ref. 5).

The quality and quantity of publications, in terms of specialized physical phenomena as well as mathematical analyses (both analytical and numerical), have become so vast that it is almost impossible for anyone to master the complete field of Rotor Dynamics. Yet, judging by the number of papers published every year, it is still growing at an accelerated rate.

Interestingly, there is not a single textbook written in this field for undergraduate studies*. It is incredible that a field of technology could have grown so much without even a single textbook devoted to it. This is probably because interest in Rotor Dynamics was limited to only a few engineers and scientists in specialized fields such as the design of steam turbines, gas turbines, etc.

However, as demand for more efficient machinery grew in terms of higher output and lower weight, size and cost, machinery with bolder design features such as higher operating speeds, slender shafts, etc. entered the market place. Machinery, with such design features, became more sensitive to many external factors such as changes in balancing, foundation, lubrication, input and output conditions, etc. which will probably change with age. Consequently, the knowledge of Rotor Dynamics became essential not only to the specialist but also to many others such as installation/ commissioning engineers, maintenance engineers, plant engineers, and so on.

---

*There were two books published in the 1960's and one in 1983. They are:

i) "Flexural Vibrations of Rotating Shafts" by F.M. Dimentberg (Butterworths, London, 1961),

ii) "Some Problems of Rotor Dynamics" by A. Tondl (Chapman & Hall, London, 1965), and

iii) "Analytical Methods in Rotor Dynamics", by A.D. Dimarogonas and S.A. Paipetis (Applied Science Publishers, London, 1983).

The first two books are now out of print and all are beyond the undergraduate level.

However, it is not easy for self-educated field engineers to understand basic analytical techniques in Rotor Dynamics because, as mentioned earlier, not a single undergraduate level textbook has been written on this subject. Further, relevant references span several decades and are sometimes omitted in citations making them difficult to trace.

It is, therefore, essential to gain a new perspective and establish a more coherent and simplified approach to Rotor Dynamics. As a first step toward such a de-mystification, a completely new approach to the calculation of undamped critical speeds of practical rotors is proposed. This new approach to rotor critical speed analysis is the essential contribution of this thesis.

I.2 Thesis Overview

The Euler beam equation is applied to a rotating shaft to find a solution for each single-segment of the shaft with uniform cross-section. The solution is applied to a practical rotor-bearing system satisfying all the boundary conditions. This eventually generates homogeneous equations which constitute the set of governing equations for the critical speeds of the system. Within the framework of initial modelling, the set of governing equations is completely analytical and explicit. That is, it is explicit, not implied as in the Transfer Matrix Method, and it does not include any approximations such as discretization of mass of the shaft, polynomial approximations, etc.

The set of governing equations appears in the form of a sparse and banded determinant, the value of which is to vanish at any critical speed. By solving for the specific values of ω (the rotational speed of the shaft) which makes the value of the determinant vanish, the

critical speeds of the rotor-bearing system are found. Further, the elements of the determinant form a special shape and they can be arranged in partitions. Each partition can be related to a specific boundary of the rotor. This permits an automatic generation of the system matrix using a computer.

I.3 Thesis Structure

A comprehensive literature review on methods of critical speed calculation is given in Chapter II. Using a simple rotor-bearing system, the new approach for rotor critical speed analysis is developed in Chapter III. Here, a shaft with one disc in the midspan is used to illustrate the theory and procedures in a step-by-step manner. Thereafter, a two-disc rotor-bearing system is solved in Chapter IV for its critical speeds using the new simplified method presented in this dissertation. The results are compared with other analytical results. In Chapter V, a complete experimental investigation of this two-disc rotor-bearing system is presented. Finally, as a general case of practical rotors, Prohl's rotor is analysed in Chapter 6 using the present method and the Transfer Matrix Method. The results from the present method are also compared with those from Urban (Ref. 49). Benefits and advantages of the new method are recapitulated in Chapter VII, and conclusions are drawn in Chapter VIII.

CHAPTER II

LITERATURE REVIEW

II.1 Introduction

There seem to be many definitions of the critical speed of rotors (Ref. 3). For this dissertation, the definition given by Eshleman (Ref. 2) will be adopted, namely; "If the frequency of any harmonic component of a periodic forcing phenomenon is equal to, or approximates, the frequency of any mode of rotor vibration, a condition of resonance may exist; if resonance exists at a specific speed, that speed is called a critical speed". Critical speed calculation can be a very sensitive matter, especially in situations such as machinery commissioning, where responsibility can be shared between the owner, machinery manufacturer, installation or foundation contractors, etc.

A total of ten methods for critical speed prediction have been found in the open literature, and are reviewed in this chapter. They are:

i) Rayleigh's Method

ii) Galerkin's Method

iii) Rayleigh-Ritz Method

iv) Dunkerley's Method

v) Stodola Method

vi) Matrix Iteration Method

vii) Impedance Matching Technique

viii) Modal Analysis

ix) Transfer Matrix Method and

x) Finite Element Method

Although there are an abundance of methods for critical speed calculation, only two methods are extensively used for the analysis of practical rotors, namely the Transfer Matrix Method and the Finite Element Method (Ref. 6). The remainder of the above mentioned methods are inherently approximate for calculation of either the highest or the lowest critical speeds, or are not suitable for intermediate critical speeds, or are too cumbersome to be used for practical rotors of moderately complicated geometry.

II.2 Review of Methods for Critical Speed Calculation

II.2.1 Rayleigh's Method

Rayleigh's method is based on the equality of the maximum kinetic and potential energies of conservative systems. Theoretically, this method depends on the numerical equivalence of the natural frequency of beam vibrations and the critical speed of whirling rotors (Ref. 3).

This method is not suitable for critical speed calculations of practical rotors for the following reasons.

a) The system should be conservative, otherwise the analysis loses its validity. It is well known that no practical rotor-bearing system is truely conservative. However conservativeness can be approximately satisfied in special cases such as extremely lightly damped and relatively slow running rotor systems.

b) Since the potential energy of the rotor is the strain energy stored in the rotor, the potential energy is naturally a function of the deflection curve which should be assumed right from the start. That is, the accuracy of the result depends on the initially assumed deflection curve of the rotor. It is worthwhile noting that the critical speed obtained using this method is always higher than the correct value, excepting only the case where the initially assumed deflection curve happens to be the correct one.

c) Usually, the static deflection curve is used for the potential and kinetic energy calculations. However, there can be a gross difference between the static deflection curve and the dynamic response curve (Ref. 7). This could result in considerable errors in the computed value of the critical speed.

Because of the difficulty in assuming the correct dynamic deflection curve, the results from Rayleigh's method will not be accurate enough except when the rotor configuration is simple enough to allow reasonable prediction of the shape of the dynamic response curve. Therefore, Rayleigh's method has been used mainly for geometrically simple rotors such as rotors with a uniform cross-section over the entire length of the rotor.

II.2.2 Galerkin's Method

Galerkin's Method is an approximate method wherein a family of trial functions are used to approximate the deflected shape of the rotor (Ref. 8). The trial solutions include parameters which can be adjusted for minimizing the error in the solution of the governing differential equations.

In this method, there are four important conditions or steps which should be satisfied. They are: firstly, the trial family solution should satisfy all the boundary conditions, namely the kinematic and force boundary conditions; secondly, the trial family solution is substituted into the governing differential equation to find the "residual" function which should vanish for the exact case; thirdly, the method requires that the weighted average of the residual over a desired interval should vanish and fourthly, the weighting functions are the same as the functions which were used in constructing the original trial functions.

Willems and Holzer (Ref. 9) used Galerkin's method to determine the critical speeds of rotating shafts subject to bending, axial load, and torsion. Their shaft was of uniform diameter and did not have any discs. Application of this approach to situations where the shafts had many discs and segments with different diameters as in practical rotors in industry, would be very difficult.

This method is inherently an approximate method and it will be cumbersome and inaccurate. Therefore, the application of this method is limited to rotors with simple geometric configurations.

II.2.3 Rayleigh-Ritz Method

This is an extension of the Rayleigh's Method and provides improved results. Sometimes, this method is simply called the Ritz Method.

The Rayleigh's method requires an initial estimation of the dynamic deflection curve and the computed critical speed is always higher than the exact value. In the Rayleigh-Ritz Method, the deflection curve is given in the form of a linear combination of a "generating set" or "trial family" (Ref. 8) which consists of linearly independent functions satisfying all the kinematic boundary conditions, that is:

$$u(x,t) = \Psi(x) \cdot q(t) = \left[\sum_{i=1}^{n} a_i \gamma_i\right] \cdot q(t) \qquad (2\text{-}1)$$

where $u(x,t)$ is the deflection curve, $\Psi(x)$ is an assumed mode shape, $q(t)$ is a function of time (t), a_i's are parameters, and $\gamma_i(x)$ form the generating set which must satisfy the kinematic boundary conditions.

The procedure is essentially the same as Rayleigh's method except for the last step where a stationary value of the natural frequency is found by differentiating the resultant natural frequency with respect to the parameters a_i, and equating them to zero. That is, the parameters a_i are "adjusted" in such a way that the natural frequency would be of minimum value as far as the "trial family" functions would permit.

This method is extensively used in the process of finite element methods and definitely improves the results. However, it is worth noting that the most important step is the selection of the trial family. Good results cannot be obtained if good approximations are not included within the trial family (Ref. 8).

II.2.4 Dunkerley's Method

Dunkerley's method (Ref. 10) is an approximate method for finding the fundamental critical speed of a rotating shaft system.

It can be used for multi-rotor systems and is effective for the first critical speed only. The error is dependent upon the closeness of the first critical speed to the second and higher critical speeds. This is because Dunkerley's approximation formula is based on the assumption that the second and higher critical speeds are so high that the reciprocals of the squares of the second and higher criticals sum up to a negligible quantity compared with that of the fundamental critical speed.

The critical speed approximated using Dunkerley's method is always lower than the true value because:

i) the neglected terms in the evaluation of the critical speed are all positive, and

ii) they are located on the same side of the equation as the inverse term of the square of the first critical speed, that is:

$$\frac{1}{\omega_1^2} \approx \frac{1}{\omega_1^2} + \frac{1}{\omega_2^2} + \frac{1}{\omega_3^2} + \ldots + \frac{1}{\omega_n^2} = \frac{1}{\omega_{11}^2} + \frac{1}{\omega_{22}^2} + \ldots + \frac{1}{\omega_{nn}^2} \qquad (2\text{-}2)$$

where ω_1, ω_2, ... are first, second, ... critical speeds, respectively; and ω_{11}, ω_{12}, ... are the natural frequencies of equivalent mass-spring systems with M_1, M_2 ... acting alone at stations 1, 2, ..., respectively. The terms ω_{11}, ω_{22}, ... can be regarded in a multi-rotor system, as critical speeds of individual rotor sub-systems.

Dunkerley discussed 17 cases in his paper in 1894 (Ref. 10), among which only the last case had more than one disc in one span, (two discs). Although two discs occupied different locations along the shaft, Dunkerley preceded his discussion with a hypothetical

approximation where each disc occupied the identical location along the shaft, one at a time. Then he offered the natural frequency of the hypothetical case as the approximation for that of the real situation.

That is,

$$\omega_{11} = \sqrt{\frac{gk_e}{W_1}}$$

$$\omega_{22} = \sqrt{\frac{gk_e}{W_2}}$$

$$\omega_{total} = \sqrt{\frac{gk_e}{W_1+W_2}} = \frac{1}{\sqrt{\frac{1}{\omega_{11}^2} + \frac{1}{\omega_{22}^2}}} = \frac{\omega_{11}\omega_{22}}{\sqrt{\omega_{11}^2 + \omega_{22}^2}}$$

which is equivalent to

$$\frac{1}{\omega_{total}^2} = \frac{1}{\omega_{11}^2} + \frac{1}{\omega_{22}^2} \qquad (2\text{-}3)$$

where k_e is the equivalent spring constant; and ω_{11} and ω_{22} are the natural frequencies of the system when the first disc only, and the second disc only, respectively, was installed in the identical location along the shaft; ω_{total} is the fundamental natural frequency of the system with two discs installed. Stodola reports that the theoretical basis of the formula has been completed by Blaess (1914) and Hahn (1918) (Ref. 11).

Recapitulating, Dunkerley's method is inherently an approximate method and is limited to the first critical speed only. That is, higher critical speeds cannot be found by this method.

II.2.5 Stodola's Method

Stodola's Method is a graphical method for finding critical speeds by starting with an assumed deflection curve which is usually the static deflection curve (Ref. 11, 12, 13). While it is possible to find higher critical speeds, Stodola's method is practically limited to the first critical speed calculation because a complete elimination of the first mode shape is required for the next higher critical speed calculation. This "purification" process requires knowledge of the first mode with "sufficient accuracy" (Ref. 12).

The method requires the following steps:

1) Assume a "reasonable" mode shape of the system which is usually the static deflection curve as in Rayleigh's method.
2) Though it is not stated by Stodola explicitly, discretization of the rotor is necessary by dividing the rotor into a reasonable number of stations. The total system is then replaced by discretized and equivalent mass points located at each of the rotor stations.
3) The inertia loading at each station is then found by multiplying the concentrated mass, displacement at each station, and the square of the assumed critical speed.
4) A new deflection curve, due to the inertia loadings, can now be compared with the old one.
5) The magnitude of the critical speed is now adjusted such that the numerical values of two representative displacements from the new and old deflection curves (for example, midspan displacements) would be the same.

6) Repeat the whole procedure again, if necessary, starting with the new deflection curve.

Stodola stated that the centrifugal forces (that is, inertia loadings) and the elastic forces must be in equilibrium at the critical speed because "at the critical speed the shaft is in indifferent equilibrium for any deflection and it has a similar elastic curve" (Ref. 11).

Stodola's method is an early form of the matrix iteration method utilizing a flexibility matrix so that convergence to the lowest critical speed is assured. The "purification" procedure for calculation of higher critical speeds corresponds to the "sweeping matrix" procedure which will be discussed in the next section. In the matrix iteration methods, the second mode is found by "suppressing" the first mode by constructing the sweeping matrix (Ref. 7, 8, 14).

This method was used most extensively in industry in 1920's to 1940's until Prohl published a paper on a tabular form of the Transfer Matrix Method in 1944. Although both required the discretization of the rotor mass into lumped mass stations, Prohl's method did not require the assumed deflection curve while Stodola's did.

Stodola's method overcame the geometric complexities in the industrial rotors by the lumped mass system. However, it is still an approximate, graphical method using the assumed deflection curve of rotors and an approximate lumped mass system. Therefore, it suffers from inaccuracy. Moreover, it is practically limited to the calculation of the first critical speed only.

II.2.6 Matrix Iteration Method

This method is known to be developed by Schwarz (1885) and by Picard, and applied to technical eigenvalue problems by Vianello (1898) and to critical speeds of rotating shafts by Stodola (1904). The method was further applied to technical problems by Pohlhausen (1921), and by von Mises and Geiringer (1929) (Ref. 8). Duncan and Collar (1934) are reported to have given a number of practical applications to vibration problems using the matrix notation for the calculations (Refs. 7, 8).

This method yields, through iterations, one natural frequency and modal vector at a time. According to formulation, the iteration converges to either the lowest or the highest frequency and mode. Then this mode is suppressed by installing the "sweeping matrix", and the process is repeated to obtain the next mode.

The procedure can be described as follows. Let us assume oscillations of a multi-degree of freedom conservative system such that

$$M\{\ddot{q}\} + K\{q\} = 0 \tag{2-4}$$

where M and K are the mass and stiffness matrices of the system, respectively, and $\{q\}$ is the vector of the generalized coordinates.

Premultiplying by K^{-1}, eq. (2-4) becomes

$$K^{-1}M\{\ddot{q}\} + \{q\} = 0$$

$$G\{\ddot{q}\} + \{q\} = 0 \tag{2-5}$$

where $G = K^{-1}M$. Now assuming a sinusoidal solution as

$$\{q\} = \{u\}\sin \omega t$$

where $\{u\}$ are the amplitudes and ω is the circular frequency, we have

$$\{\ddot{q}\} = -\omega^2\{u\}\sin \omega t$$

Substituting into eq. (2-5), we find

$$\omega^2 G\{u\} = \{u\}$$

or

$$\frac{1}{\omega^2}\{u\} = G\{u\} \tag{2-6}$$

Now an arbitrary vector $\{V\}$, can be expanded in terms of the modal vectors as:

$$\{V\}_0 = \sum_{i=1}^{n} C_i\{u\}_i \tag{2-7}$$

where C_i's are constants. Now, a sequence of vectors can be generated using the iteration scheme as follows:

$$\{V\}_0$$

$$\{V\}_1 = G\{V\}_0$$

$$\{V\}_2 = G\{V\}_1 = G^2\{V\}_0$$

$$\vdots \qquad \vdots \qquad \vdots$$

Substituting the above into eq. (2-7) yields,

$$\{V\}_1 = G\{V\}_0 = \sum_{i=1}^{n} C_i G\{u\}_i = \sum_{i=1}^{n} C_i \frac{1}{\omega_i^2}\{u\}_i$$

$$\{V\}_2 = G\{V\}_1 = G^2\{V\}_0 = \sum_{i=1}^{n} C_i G^2\{u\}_i$$

$$= \sum_{i=1}^{n} C_i \frac{1}{\omega_i^2} G\{u\}_i = \sum_{i=1}^{n} C_i \left[\frac{1}{\omega_i^2}\right]^2 \{u\}_i$$

$$\{V\}_s = G^s\{V\}_0 = \sum_{i=1}^{n} C_i G^s\{u\}_i = \sum_{i=1}^{n} C_i \left[\frac{1}{\omega_i^2}\right]^s \{u\}_i$$

Assuming that the terms $1/\omega_i^2$ are distinct and that:

$$\frac{1}{\omega_1^2} > \frac{1}{\omega_2^2} > \cdots\cdots > \frac{1}{\omega_n^2},$$

and if 's' is sufficiently large, then

$$\left[\frac{1}{\omega_1^2}\right]^s >> \left[\frac{1}{\omega_i^2}\right]^s \text{ for } i = 2,3,\ldots,n,$$

thus:

$$\{V\}_s = G^s\{V\}_0 \approx C_1 \left[\frac{1}{\omega_1^2}\right]^s \{u\}_1$$

$$\{V\}_{s+1} \approx C_1 \left[\frac{1}{\omega_1^2}\right]^{s+1} \{u\}_1 = \frac{1}{\omega_1^2} \{V\}_s$$

Therefore, the iteration converges to the inverse of ω_1^2 and the first mode shape $\{u\}_1$. Note that, if an alternate form of eq. (2-6) is used then:

$$\omega^2\{u\} = H\{u\}$$

where $H = G^{-1}$. In this case the iteration converges to the highest natural frequency and mode.

The second mode is found by suppressing the first mode p_1, that is, by introducing the constraint $p_1 = 0$. To suppress the first mode, consider the transformation:

$$\{q\} = [u]\ \{p\}$$

where [u] is the modal matrix (Ref. 7).

$$\therefore \quad \{p\} = [u]^{-1}\ \{q\}$$

$$= [v]\ \{q\}$$

where $[v] = [u]^{-1}$. Since $p_1 = v_{11}q_1 + v_{12}q_2 + \cdots + v_{1n}q_n = 0$ (which is the constraint equation) and $q_i = q_i$, $i = 2,3,\cdots, n$ (because the rest of the coordinates remain unchanged), the total system equation becomes:

$$\begin{bmatrix} v_{11} & v_{12} & v_{13} & v_{14} & \cdots & v_{1n} \\ 0 & 1 & 0 & 0 & \cdots & 0 \\ 0 & 0 & 1 & 0 & \cdots & 0 \\ 0 & 0 & 0 & 1 & \cdots & 0 \\ \vdots & & & & & \vdots \\ 0 & 0 & 0 & 0 & \cdots & 1 \end{bmatrix} \begin{Bmatrix} q_1 \\ q_2 \\ q_3 \\ q_4 \\ \vdots \\ q_n \end{Bmatrix} = \begin{bmatrix} 0 & 0 & 0 & \cdots & 0 \\ 0 & 1 & 0 & \cdots & 0 \\ 0 & 0 & 1 & \cdots & 0 \\ \vdots & & & & \vdots \\ 0 & \cdots & \cdots & & 1 \end{bmatrix} \begin{Bmatrix} q_1 \\ q_2 \\ q_3 \\ q_4 \\ \vdots \\ q_n \end{Bmatrix}$$

$$\begin{Bmatrix} q_1 \\ q_2 \\ q_3 \\ \vdots \\ q_n \end{Bmatrix} = \begin{bmatrix} v_{11} & v_{12} & \cdots & v_{1n} \\ 0 & 1 & \cdots & 0 \\ \vdots & & & \vdots \\ 0 & \cdots & 0 & 1 \end{bmatrix}^{-1} \begin{bmatrix} 0 & 0 & 0 & \cdots & 0 \\ 0 & 1 & 0 & \cdots & 0 \\ 0 & 0 & 1 & \cdots & 0 \\ \vdots & & & & \vdots \\ 0 & \cdots & 0 & 1 & 0 \\ 0 & \cdots & 0 & 0 & 1 \end{bmatrix} \begin{Bmatrix} q_1 \\ q_2 \\ q_3 \\ \vdots \\ q_n \end{Bmatrix}$$

now, defining:

$$S_1 = \begin{bmatrix} v_{11} & v_{12} & \cdots & v_{1n} \\ 0 & 1 & \cdots & 0 \\ \vdots & & & \vdots \\ 0 & \cdots & 0 & 1 \end{bmatrix}^{-1} \begin{bmatrix} 0 & 0 & 0 & \cdots & 0 \\ 0 & 1 & 0 & \cdots & 0 \\ 0 & 0 & 1 & & \vdots \\ \vdots & & & & \vdots \\ 0 & \cdots & & 0 & 1 \end{bmatrix}$$

yields $\{q\} = S_1\{q\}$, where S_1 is called the "sweeping matrix".

The matrix G in eq. (2-6) is modified by S_1 to give a new matrix G_1 such that

$$G_1 = GS_1$$

Now, G_1 can be used in eq. (2-6) for the iteration of the second mode, since the first mode has been suppressed. All the rest of the original procedure can be used for the iterations as before (Ref. 7).

As stated in Section II.2.5, the matrix iteration method is an extension of Stodola's method. That is, the matrix iteration method is a modern version of Stodola's method in the sense that it is based on computerized iteration scheme as opposed to Stodola's method which is graphical. Due to this numerical iteration scheme, the matrix iteration method can be an excellent method for calculating the critical speeds. However, this method still suffers from two crucial shortcomings, namely:

i) There are no special provisions to accommodate geometric complexities of real-life industrial rotors except for converting them into lumped mass systems. This in turn introduces inaccuracies in the values of critical speeds and mode shapes.

ii) When higher critical speeds are sought, this method will suffer from inaccuracy due to the error accumulated by the "purification" or "sweeping" process.

II.2.7 Impedance Matching Technique

Impedance matching is a semi-graphical technique for determining system critical speeds.

It should be emphasized that this technique is not for critical speeds of a rotating shaft as a component but for critical speeds of the whole system which includes rotating shaft(s), pedestals, foundations, bearings, couplings, casings, etc. Dynamic characteristics of each component should be known beforehand.

There seems to be more than one definition for mechanical impedance and they can refer to element impedance or system impedance. According to Plunkett (Ref. 15), (mechanical) impedance is defined as a ratio of force to velocity. Tse et al. introduced a force- voltage analogy and in parallel, therefore, leading to possibilities of dual definitions of force/velocity and velocity/force (Ref. 7). Caruso (Ref. 16) and Ludwig (Ref. 17) referred to their method as the "dynamic stiffness method" and what they actually "matched" in order to find the system critical speeds was the dynamic stiffness of various components.

Though it can be done differently (Ref. 18), Caruso calculated the critical speeds of rotors as a function of bearing stiffness, using the Holzer-Myklestad-Prohl (HMP) method, and plotted them on a log-log scale graph, similar to a critical speed map. His abscissa was the rotational speed of the shaft and the ordinate was the dynamic stiffness, extending from negative infinity (at the top) to positive infinity (at the bottom) with the zero stiffness coinciding with the origin of the coordinate system. He then experimentally

determined the support stiffness, and plotted it on the same graph by superposing the coordinate of the support stiffness on that of the dynamic stiffness of the rotor (Ref. 16). In other words, he derived the bearing support dynamic stiffness curve from the calculated rotor dynamic characteristic and the measured critical speeds of the rotor-support system. Caruso showed the merits of the dynamic stiffness method by presenting many cases of correlations between factory tests and field data on various production steam turbine units.

Ludwig (Ref. 17) did not use experimental data, but calculated the support stiffness as a function of excitation frequency using a simple analytical model of the spring-damper-mass system. He also expanded the method to include symmetric and non-symmetric supports, symmetric and nonsymmetric casings, and couplings.

The advantage of this method over the classical approach of obtaining the formal solution of the governing differential equations is that this method permits the decoupling of a linear vibration system into subsystems and analysing each subsystem separately. Thus, the understanding of the dynamic behavior of a rotating machinery system can be assessed in terms of the separate dynamic characteristics of the rotor(s), casings, bearings, supports, couplings, etc.

A practical example of the above mentioned advantage is worth noting, namely the case of driver and driven equipment. Since driven and driver equipment are usually of different manufacture, substantial technical interchange of proprietary information may be required for the complete vibration analysis of the coupled system. The impedance method allows the matching of the two sets of equipment with a minimum of information interchange (Ref. 17).

The impedance matching technique is an effective method in determining dynamic characteristics of the whole system including rotors, casings, foundations, couplings, etc. However, it is not suitable for calculation of critical speeds of a rotating shaft as a component unless the geometric configuration of the rotor is extremely simple. This technique does not have any provisions to deal with geometric complexities of industrial turbo-rotors.

II.2.8 Modal Analysis

The method of modal analysis is based on the orthogonality relations, which exist amongst vibration modes of a linear system. A transformation from physical coordinates to modal coordinates allows decoupling of the system equations. Each equation can then be solved independently and with considerable ease. The technique can be used on its own (Ref. 19) or in combination with either the Transfer Matrix Method (Refs. 20, 21) or the Finite Element Method (Ref. 22).

When the modal analysis technique is used on its own on practical rotors, the objectives tend to be qualitative rather than quantitative, and the results are less accurate than those of the other techniques mentioned above (Ref. 20). However, this technique is claimed to be well suited for studying the rotor response under transient conditions such as stochastic loading conditions (Refs. 20, 22), and for studying the sensitivity of the rotor to mass-unbalance distributions (Ref. 20).

The basis of this technique is the orthogonality properties among the modal shapes (Ref. 20). Using these orthogonality relations, it is possible to acquire a decoupled set of system-governing equations. By solving these decoupled and, therefore, much simplified equations, any excitations of the rotor can be resolved into modal components; the resultant response is obtained from a summation of the response for the individual modes.

The modal analysis technique for a flexible rotor-bearing system was originally published by Gladwell and Bishop (Ref. 19) in 1959. Since then, a number of scientists such as Bishop, Gladwell, Parkinson and their co-workers at University College, London, published papers on the balancing application (Ref. 23-44). Probably because it is a qualitative rather than a quantitative technique (as discussed later in this section), the technique has not been used extensively (Ref. 45). Most of the practical applications have been limited to the field of flexible rotor balancing. Appropriately the balancing method is called the Modal Balancing Method, and is based on the orthogonality of the mode shapes. That is, after the first mode is balanced, the second mode can be balanced without affecting the previously balanced first mode.

The modal analysis technique, in its classical sense, has been used extensively for uniform cross-sectional shafts, and does not allow effective provisions for shafts with many segments of different diameters such as are found in practical rotors. The results therefore tend to be qualitative, and are thus often used for studying "sensitivity" distributions (Ref. 20). In order to improve such shortcomings, the modal analysis technique can be used in conjunction with either the Transfer Matrix Method or the Finite Element Method. A brief description of such "combined" techniques is given below. Transfer Matrix Methods or Finite Element Methods can be used for their effectiveness in accommodating stepped diameters, gyroscopic effects, etc. in the assembly stage of the governing equations. Coordinate

transformation of the modal analysis technique can then be used. Lund (Ref. 20, 21) used the Transfer Matrix Method in combination with the modal analysis method. His analyses included the effects of non-conservative systems with unsymmetrical stiffness and damping matrices, amplification factors related to each modal function, the transient reponse of an industrial multistage compressor rotor to selected unbalance distributions, and the transient response to a shock pulse.

Hashish and Sankar (Ref. 22) applied finite element and modal analyses on rotor-bearing systems under stochastic loading conditions, that is, stationary and Gaussian type random loading conditions. They used eight degree-of-freedom finite elements. As in the standard manner, the generalized coordinates are expressed in terms of the shape function and modal coordinates (element boundary points); kinetic and potential energy expressions are found and integrated over the element length; governing equations for the element are found by applying Lagrange's equations; and the element coordinates are rearranged such that total system governing equations are constructed by assembling the element equations. Up to this stage the procedure is identical to that of Finite Element Methods. However, instead of proceeding further by constructing a system stiffness matrix etc., a coordinate transformation is applied to decouple the coordinates. From this step on, the operations follow the usual procedures in the modal analysis technique.

II.2.9 Transfer Matrix Method

The Transfer Matrix Method does not describe a single method but rather a group of methods. They are the Holzer Method, HMP (Holzer-Myklestad-Prohl) Method and the Modified HMP Method. The Transfer Matrix Method is one of the most popular methods of calculating the critical speeds of practical rotors. Virtually all the critical speed and unbalance response calculations until the late 1970's have been based on this method alone. There is therefore an abundance of references on the use of this method.

However, there is no reference which describes the most up-to-date version of the method in a simple and straightforward manner. The best developed model is described in Lund's paper (Ref. 46) on unbalance response, which cites Prohl's work (Ref. 47) for a detailed and original explanation of the theory. Another pertinent reference is Urban's work (Ref. 48).

The most significant feature of Lund's model is that of the shaft with distributed mass over its length. This concept of distributed parameter had been developed originally by Urban in 1958. A brief description of the Transfer Matrix Method based on Urban's model is given in the following.

The vibration of a uniform cross-sectional beam subjected to a continuous loading, q, can be described by the fourth order linear differential equation:

$$EI \frac{d^4y}{dx^4} - q = 0 \qquad (2\text{-}8)$$

where EI is the flexural rigidity,

y is the deflection of the beam,

and

q is the intensity of loading. (Detailed derivation of eq. (2-8) is given in Section III.3.2)

This can also represent the differential equation for the deflection of a uniformly loaded rotating shaft with a proper evaluation of q, that is:

$$q = \rho \omega^2 y$$

where ρ is the mass per unit length of the shaft with uniform cross-section, and

ω is the angular velocity of the rotation of the shaft (Rad/sec).

Therefore, eq. (2-8) becomes

$$EI \frac{d^4y}{dx^4} - \rho \omega^2 y = 0 \qquad (2\text{-}9)$$

Substituting $m^4 = \frac{\rho \omega^2}{EI}$ into eq. (2-9) yields:

$$\frac{d^4y}{dx^4} - m^4 y = 0 \qquad (2\text{-}10)$$

The general solution of eq. (2-10) is

$$y = A \cosh mx + B \sinh mx + C \cos mx + D \sin mx \qquad (2\text{-}11)$$

where A,B,C, and D are constants to be determined by boundary conditions.

Differentiating eq. (2-11) three times consecutively with respect to x, and utilizing the relations

$$\theta = \frac{dy}{dx}$$

$$\frac{M}{EI} = \frac{d^2y}{dx^2}$$

$$\frac{V}{EI} = \frac{d^3y}{dx^3}$$

yield:

$$\theta = m\,(A \sinh mx + B \cosh mx - C \sin mx + D \cos mx) \qquad (2\text{-}12)$$

$$M = EIm^2\,(A \cosh mx + B \sinh mx - C \cos mx - D \sin mx) \qquad (2\text{-}13)$$

$$V = EIm^3\,(A \sinh mx + B \cosh mx + C \sin mx - D \cos mx) \qquad (2\text{-}14)$$

where θ, M, and V are the slope, the moment, and the shear force, respectively.

At x = 0, eqs. (2-11) to (2-14) become

$$y_o = A + C \qquad (2\text{-}15)$$

$$\theta_o = m(B + D) \qquad (2\text{-}16)$$

$$M_o = EIm^2(A - C) \qquad (2\text{-}17)$$

$$V_o = EIm^3(B - D) \qquad (2\text{-}18)$$

where y_o, θ_o, M_o, and V_o are the values of y, θ, M, and V at the point x = 0 as shown in Fig. 2-1. Solving eqs. (2-15) to (2-19) for the constants A,B,C, and D, yields:

$$\begin{Bmatrix} A \\ B \\ C \\ D \end{Bmatrix} = \frac{1}{2} \cdot \begin{bmatrix} 1 & 0 & 1 & 0 \\ 0 & 1 & 0 & 1 \\ 1 & 0 & -1 & 0 \\ 0 & 1 & 0 & -1 \end{bmatrix} \begin{Bmatrix} y_o \\ \frac{\theta_o}{m} \\ \frac{M_o}{EIm^2} \\ \frac{V_o}{EIm^3} \end{Bmatrix}$$

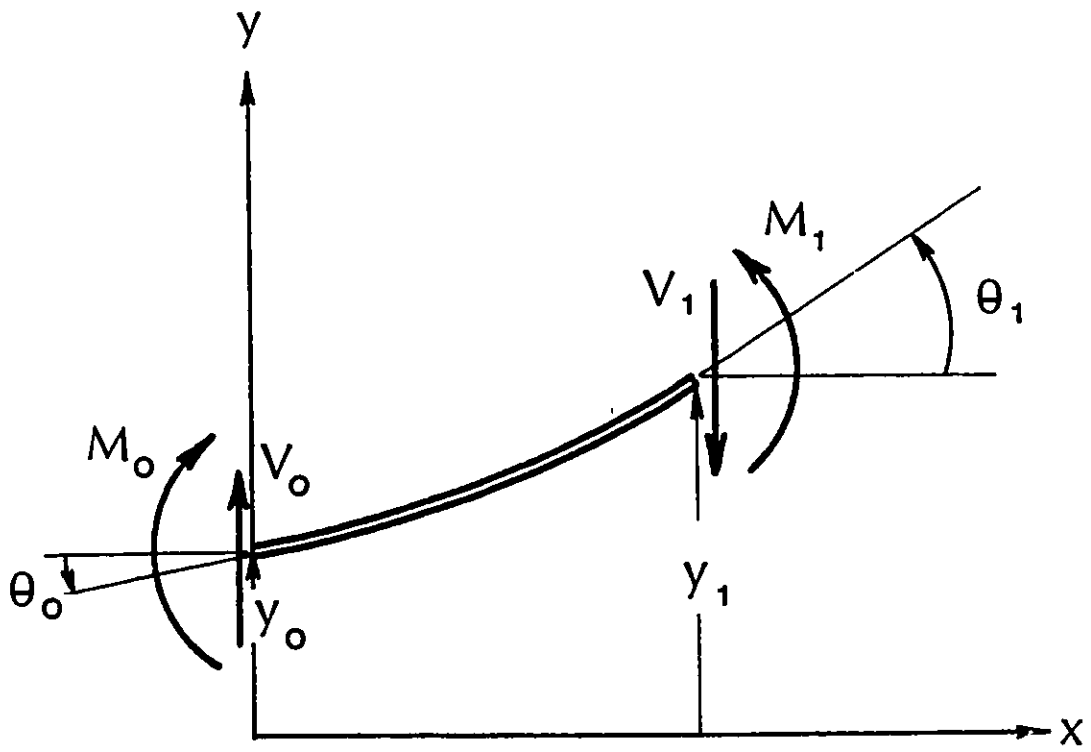

Fig. 2-1 A Shaft Segment

$$= \frac{1}{2} \cdot \begin{bmatrix} 1 & 0 & 0 & 0 \\ 0 & 1 & 0 & 1 \\ 1 & 0 & -1 & 0 \\ 0 & 1 & 0 & -1 \end{bmatrix} \cdot \begin{bmatrix} 1 & 0 & 0 & 0 \\ 0 & \frac{1}{m} & 0 & 0 \\ 0 & 0 & \frac{1}{EIm^2} & 0 \\ 0 & 0 & 0 & \frac{1}{EIm^3} \end{bmatrix} \begin{Bmatrix} y_o \\ \theta_o \\ M_o \\ V_o \end{Bmatrix} \qquad (2\text{-}19)$$

Substituting eq. (2-19) into eqs. (2-11) to (2-14), and designating the quantities y, θ, M, and V at the point $x = \ell_1$ as y_1, θ_1, M_1, and V_1 respectively, eqs. (2-11) to (2-14) yield:

$$\begin{Bmatrix} y_1 \\ \theta_1 \\ M_1 \\ V_1 \end{Bmatrix} = \frac{1}{2} \cdot \begin{bmatrix} 1 & 0 & 0 & 0 \\ 0 & m & 0 & 0 \\ 0 & 0 & EIm^2 & 0 \\ 0 & 0 & 0 & EIm^3 \end{bmatrix} \cdot \begin{bmatrix} \cosh m\ell_1 & \sinh m\ell_1 & \cos m\ell_1 & \sin m\ell_1 \\ \sinh m\ell_1 & \cosh m\ell_1 & -\sin m\ell_1 & \cos m\ell_1 \\ \cosh m\ell_1 & \sinh m\ell_1 & -\cosh m\ell_1 & -\sin m\ell_1 \\ \sinh m\ell_1 & \cosh m\ell_1 & \sin m\ell_1 & -\cos m\ell_1 \end{bmatrix}$$

$$\cdot \begin{bmatrix} 1 & 0 & 0 & 0 \\ 0 & 1 & 0 & 1 \\ 1 & 0 & -1 & 0 \\ 0 & 1 & 0 & -1 \end{bmatrix} \cdot \begin{bmatrix} 1 & 0 & 0 & 0 \\ 0 & \frac{1}{m} & 0 & 0 \\ 0 & 0 & \frac{1}{EIm^2} & 0 \\ 0 & 0 & 0 & \frac{1}{EIm^3} \end{bmatrix} \begin{Bmatrix} y_o \\ \theta_o \\ M_o \\ V_o \end{Bmatrix} \qquad (2\text{-}20)$$

or

$$\begin{Bmatrix} y_1 \\ \theta_1 \\ M_1 \\ V_1 \end{Bmatrix} = [T_a] \begin{Bmatrix} y_o \\ \theta_o \\ M_o \\ V_o \end{Bmatrix} \qquad (2\text{-}21)$$

where

$$[T_a] = \frac{1}{2} \begin{bmatrix} 1 & 0 & 0 & 0 \\ 0 & m & 0 & 0 \\ 0 & 0 & EIm^2 & 0 \\ 0 & 0 & 0 & EIm^3 \end{bmatrix} \cdot \begin{bmatrix} \cosh m\ell_1 & \sinh m\ell_1 & \cos m\ell_1 & \sin m\ell_1 \\ \sinh m\ell_1 & \cosh m\ell_1 & -\sin m\ell_1 & \cos m\ell_1 \\ \cosh m\ell_1 & \sinh m\ell_1 & -\cos m\ell_1 & -\sin m\ell_1 \\ \sinh m\ell_1 & \cosh m\ell_1 & \sin m\ell_1 & -\cos m\ell_1 \end{bmatrix}$$

$$\cdot \begin{bmatrix} 1 & 0 & 0 & 0 \\ 0 & 1 & 0 & 1 \\ 1 & 0 & -1 & 0 \\ 0 & 1 & 0 & -1 \end{bmatrix} \cdot \begin{bmatrix} 1 & 0 & 0 & 0 \\ 0 & \frac{1}{m} & 0 & 0 \\ 0 & 0 & \frac{1}{EIm^2} & 0 \\ 0 & 0 & 0 & \frac{1}{EIm^3} \end{bmatrix} \qquad (2\text{-}22)$$

As shown in Fig. 2-1, eq. (2-21) defines the quantities, y_1, θ_1, M_1, and V_1 at the point $x = \ell_1$ in terms of the quantities y_o, θ_o, M_o, and V_o at the point $x = 0$. That is, the deflection, slope, moment, and shear on the right end of the uniform shaft segment can be calculated by eq. (2-21) in terms of these quantities at the left end when there is no external forces or moments such as bearing reaction forces, gyroscopic effects due to discs, etc.

This is the general technique of the Transfer Matrix Method to develop a set of relationships between the variables of state at one end of a shaft segment and the variables of state at the other end. The matrix $[T_a]$, in eq. (2-21) is the "progression matrix" or "transfer matrix" which allows the analytical relationship to "progress" or "transfer" from one end to another end of a shaft segment, and therefore, eventually, from one end to the other end of the whole rotor-bearing system.

The matrix $[T_a]$ is also known as the "field" transfer matrix for a shaft segment with its mass uniformly distributed along the length of the segment, however, without any external forces or moments. When there are external forces or moments such as bearing reactions, inertia forces due to discs, gyroscopic moments due to discs, etc., the expressions for shear and bending moments should be modified by:

$$\Delta V = m_D \cdot \omega^2 \cdot y \quad \text{(disc)} \tag{2-23}$$

$$\Delta V = -k_B \cdot y \quad \text{(bearing)} \tag{2-24}$$

$$\Delta M = I' \omega^2 \theta \quad \text{(disc)} \tag{2-25}$$

where m_D is the mass of the disc, k_B is the spring constant of the bearing and I' is the net moment of inertia of the disc given as below:

$$I' = \frac{\pi w h}{64 g} \left[D_D^4 - D_S^4 - \frac{4}{3} h^2 (D_D^2 - D_S^2)\right] \tag{2-26}$$

and w : specific weight of disc material

h : thickness or width of the disc

D_D: disc diameter

D_S: shaft diameter

g : the constant of gravity

Equation (2-23) represents the centrifugal force due to the synchronous whirling motion of the disc. Equation (2-24) represents restoring force due to the compliant bearing element. Equation (2-25) can be drived by calculating the time rate of change of moment of momentum due to the synchronous motion of the disc. As shown in Fig. 2-2, the time rate of change of the moment of momentum of the disc about its center of mass is:

$$\begin{aligned} \{M\} &= \frac{d}{dt} \{H_c\} \\ &= \{\dot{H}_c\} + \{\Omega\} \times \{H_c\} \\ &= [I] \{\dot{\Omega}\} + \{\Omega\} \times [I] \{\Omega\} \end{aligned} \tag{2-27}$$

where $\{H_c\}$ is the moment of momentum of the disc with respect to its center of mass, $\{\Omega\}$ is the angular velocity vector of the disc, [I] is the inertia matrix of the disc, and the sign "×" means vector product or "cross product".

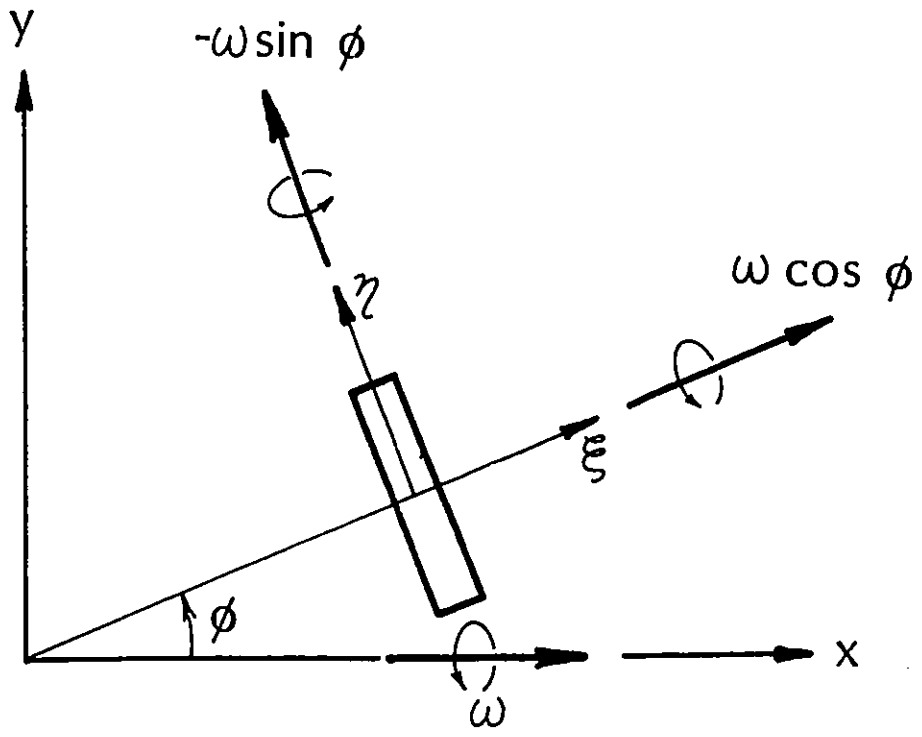

Fig. 2-2 A Disc Element and Angular Velocities

As shown in Fig. 2-2,

$$\{\Omega\} = \begin{Bmatrix} \omega \cos \phi \\ -\omega \sin \phi \\ 0 \end{Bmatrix} \tag{2-28}$$

$$[I] = \begin{bmatrix} I_\xi & 0 & 0 \\ 0 & I_\eta & 0 \\ 0 & 0 & I_\zeta \end{bmatrix} \tag{2-29}$$

Since ω and ϕ are constant with respect to time under steady state conditions; $\{\dot{\Omega}\} = 0$. Therefore, eq. (2-27) becomes

$$\begin{aligned} \{M\} &= \{\Omega\} \times [I] \{\Omega\} \\ &= \begin{Bmatrix} \omega \cos \phi \\ -\omega \sin \phi \\ 0 \end{Bmatrix} \times \begin{bmatrix} I_\xi & 0 & 0 \\ 0 & I_\eta & 0 \\ 0 & 0 & I_\zeta \end{bmatrix} \begin{Bmatrix} \omega \cos \phi \\ -\omega \sin \phi \\ 0 \end{Bmatrix} \\ &= \begin{Bmatrix} 0 \\ 0 \\ \omega^2 (I_\xi - I_\eta) \cos \phi \cdot \sin \phi \end{Bmatrix} \\ &\approx \begin{Bmatrix} 0 \\ 0 \\ \omega^2 I' \theta \end{Bmatrix} \end{aligned} \tag{2-30}$$

where $I' = I_\xi - I_\eta$,

$\cos \phi \approx 1$, and

$\sin \phi \approx \phi \approx \theta$ for a small angle ϕ.

Equation (2-30) completes the derivation of eq. (2-25).

Referring to eqs. (2-23), (2-24), (2-25), and Fig. 2-3, the governing equation for state vectors, y, θ, M, and V, across the disc becomes:

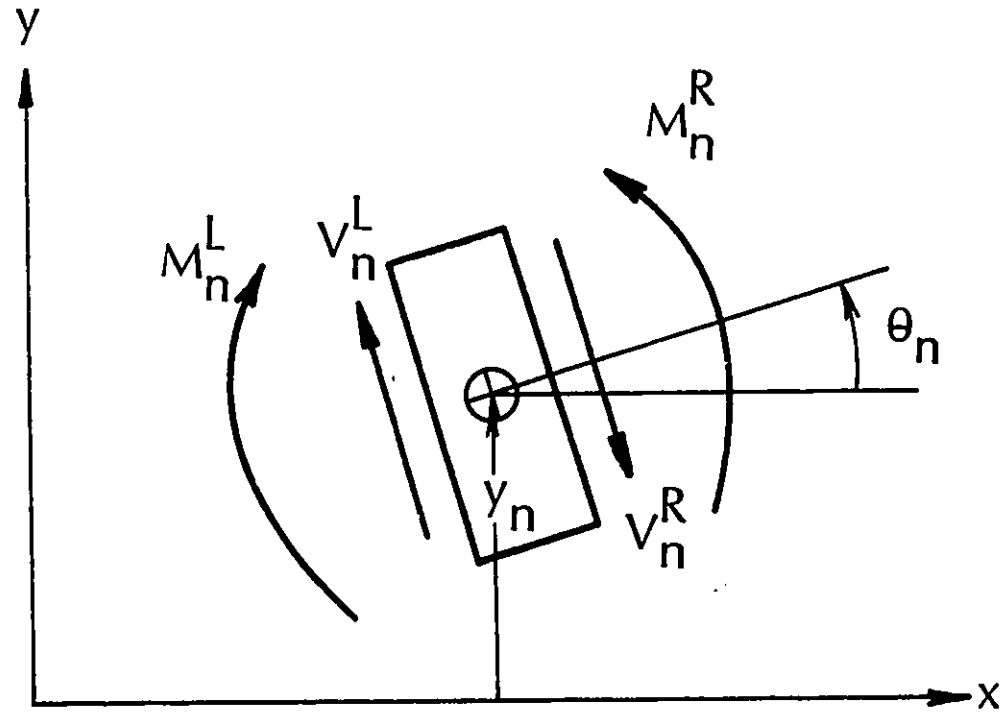

Fig. 2-3 A Disc Element and State Variables

$$\begin{Bmatrix} y \\ \theta \\ M \\ V \end{Bmatrix}_n^R = \begin{bmatrix} 1 & 0 & 0 & 0 \\ 0 & 1 & 0 & 0 \\ 0 & I'\omega^2 & 1 & 0 \\ (m_D\omega^2 - k_B) & 0 & 0 & 1 \end{bmatrix} \begin{Bmatrix} y \\ \theta \\ M \\ V \end{Bmatrix}_n^L \tag{2-31}$$

or

$$\{Z\}_n^R = [T_p]\ \{Z\}_n^L \tag{2-32}$$

where the superscripts R and L stand for right and left side, respectively, of the disc, the subscript n stands for the station number "n", and

$$\{Z\} = \begin{Bmatrix} y \\ \theta \\ M \\ V \end{Bmatrix} \tag{2-33}$$

$$[T_p] = \begin{bmatrix} 1 & 0 & 0 & 0 \\ 0 & 1 & 0 & 0 \\ 0 & I'\omega^2 & 1 & 0 \\ (m_D\omega^2 - k_B) & 0 & 0 & 1 \end{bmatrix} \tag{2-34}$$

It is worth noting that eq. (2-32) transfers simply over a "point" or station "n". Therefore, the matrix $[T_p]$ is known as the "point" transfer matrix.

In general form, the variables of state, y, θ, M, and V, for any station n can now be written in terms of these at station (n-1) by combining eq. (2-32) and a generalized form of eq. (2-21):

$$\begin{Bmatrix} y \\ \theta \\ M \\ V \end{Bmatrix}_n = [T_n] \begin{Bmatrix} y \\ \theta \\ M \\ V \end{Bmatrix}_{n-1} \tag{2-35}$$

or

$$\{Z\}_n = [T_n]\ \{Z\}_{n-1} \tag{2-36}$$

where $\{Z\}$ is the state vector defined by eq. (2-33), and

$$[T_n] = [T_S] \cdot [T_D] \tag{2-37}$$

$$[T_S] = \frac{1}{2} \cdot [S_1] \cdot [S_2] \cdot [S_3] \cdot [S_4] \tag{2-38}$$

$$[S_1] = \begin{bmatrix} 1 & 0 & 0 & 0 \\ 0 & m_n & 0 & 0 \\ 0 & 0 & EI_n(m_n)^2 & 0 \\ 0 & 0 & 0 & EI_n(m_n)^3 \end{bmatrix} \tag{2-39}$$

$$[S_2] = \begin{bmatrix} \cosh m_n \ell_n & \sinh m_n \ell_n & \cos m_n \ell_n & \sin m_n \ell_n \\ \sinh m_n \ell_n & \cosh m_n \ell_n & -\sin m_n \ell_n & \cos m_n \ell_n \\ \cosh m_n \ell_n & \sinh m_n \ell_n & -\cos m_n \ell_n & -\sin m_n \ell_n \\ \sinh m_n \ell_n & \cosh m_n \ell_n & \sin m_n \ell_n & -\cos m_n \ell_n \end{bmatrix} \tag{2-40}$$

$$[S_3] = \begin{bmatrix} 1 & 0 & 1 & 0 \\ 0 & 1 & 0 & 1 \\ 1 & 0 & -1 & 0 \\ 0 & 1 & 0 & -1 \end{bmatrix} \tag{2-41}$$

$$[S_4] = \begin{bmatrix} 1 & 0 & 0 & 0 \\ 0 & \frac{1}{m_n} & 0 & 0 \\ 0 & 0 & \frac{1}{EI_n(m_n)^2} & 0 \\ 0 & 0 & 0 & \frac{1}{EI_n(m_n)^3} \end{bmatrix} \tag{2-42}$$

Equation (2-36) is the essence of the Transfer Matrix Method to develop a set of relationships between the variables of state at one end of an element and the variables of state at the other end. The matrix $[T_n]$ in eq. (2-36) is the "progression matrix" or "transfer matrix" which allows the analytical relationship to "progress" or "transfer" from one station to the next, and therefore, eventually, from one end to the other end of the whole rotor-bearing system as below.

$$\{Z\}_1 = [T_1]\ \{Z\}_0$$

$$\{Z\}_2 = [T_2]\ \{Z\}_1$$

$$\{Z\}_3 = [T_3]\ \{Z\}_2$$

$$\{Z\}_N = [T_N]\ \{Z\}_{N-1}$$

$$\therefore \{Z\}_N = [T_N]\ [T_{N-1}] \cdots [T_3]\ [T_2]\ [T_1]\ \{Z\}_0 \qquad (2\text{-}43)$$

In eq. (2-43), $\{Z\}_0$ and $\{Z\}_N$ are "known" state vectors at the left end and the right end, respectively, of the rotor-bearing system. The multiplications of four-by-four transfer matrices can be carried out using digital computers. Except for the angular velocity of the shaft, ω, all the terms involved in the transfer matrices are known or measurable quantities such as the mass of the disc, length of the shaft segment, moments of inertia of the shaft cross-sections, etc.

Therefore, eq. (2-43) can be solved numerically for ω subject to boundary conditions using digital computers. The ωs which satisfy eq. (2-43) are the critical speed of the rotor-bearing system.

Holzer is reported to have developed a numerical method by which torsional critical speeds of rotors can be calculated (Ref. 2). However, this is only for torsional vibrations, not for lateral vibrations of rotating shafts. The governing differential equation for flexural vibration of beams is of fourth order while that of the torsional vibration of beams is of second order.

In 1944, Myklestad and Prohl, almost simultaneously published separate papers on a general method of calculating the natural frequencies of complicated wing structures and critical speeds of practical rotating shafts, respectively. Theoretically, both used the same concept, namely: an expansion of Holzer's theory from the second order system for torsion to fourth order system for beams. Therefore, some authors (Ref. 2, 48) refer to this scheme as the HMP (Holzer-Myklestad-Prohl) Method. In this scheme assumptions include:

i) a massless spring system and lumped mass to represent a typical portion of the shaft;

ii) lumped masses for discs and other types of loads; and

iii) a) solved mathematical relations somewhat similar to residual moments and shear force

b) using not-easily-understood "decoupling" properties between the slope and the shear force.

Many years later in 1958, Urban (Refs. 48, 49) improved upon Prohl's model by introducing a distributed mass system. Some authors call it a distributed "parameter" system (Ref. 2). This corresponds to the so called "consistent" parameter distribution system in the Finite Element Methods of Archer (Ref. 50).

Urban used distributed mass as well as distributed elastic characteristics for a representative portion of rotating shafts where Prohl had used a lumped mass and massless spring. Later in 1967, Lund and Orcutt (Ref. 46) used the same type of distributed parameter system in their unbalance response analysis. However, they did not quote Urban's work but cited only Prohl's work, repeating almost the same concepts as Urban. They also improved the mathematical model by introducing the shape factor for shear deformation, for the first time.

The second improvement upon the HMP Method was, not to solve the equations used by Prohl or Myklestad, but rather to solve a boundary condition in order to find the critical speeds. This accomplishes the same task as Prohl's and Myklestad's tabular method with the added advantage of simplicity of formulation. Thomson (Ref. 51) published this in 1950, but his work appears to have been overlooked by Urban (Ref. 48). Another possible reason why Thomson's result is widely used in practice, without being properly referenced (for example Ref. 46, 52), is the fact that Thomson described it in his textbook on vibrations (Ref. 53) without precise citation, merely listing its source at the end of a chapter.

Ever since Urban's development of the Modified Holzer-Myklestad-Prohl Method, this distributed parameter system has been used in numerous types of response analyses, very rarely with proper citation

(Ref. 54), and most of the time without being cited at all (Ref. 52). The application has been expanded to all types of practical rotors with various types of bearings and couplings (Ref. 55, 56), and even to a rotor partially filled with liquid (Ref. 2).

The improper or mis-recognition of references is partly due to the fact that:

i) References are scattered over many decades, that is from

Prohl in 1944

Thompson 1950

Urban . 1958

Lund 1967, etc.

ii) Not a single paper thoroughly reviewed and cited all the essential developments. It is therefore difficult for a novice scientist to acquire a balanced view in a reasonably short period of time.

iii) Omission of citation in Lund's unbalance response analysis could easily cause the reader to miss Thomson's and Urban's contributions. The most conspicuous development is the unbalance response analysis, and most of the recent publications are concentrated in this area. Tracing the literature from one of the recent unbalance response analysis discussions, it is most likely that both Thomson's and Urban's contributions will be missed since Lund's paper refers directly to Prohl's work.

Even if all major references were found , it is not easy for field engineers to understand these references except by long and careful study.

The Transfer Matrix Method is one of the two most extensively used methods in industry, however, it has two vital shortcomings in comparison with the new method which is proposed in this dissertation, namely:

1) The Transfer Matrix Method cannot accommodate couplings within its framework because the general relationship defined by eqs. (2-29) to (2-36) breaks down at the couplings. However, the new method can be applied to couplings without any modifications in its procedures or theory. Moreover, there is no theoretical limitations in the numbers of couplings.
2) The Transfer Matrix Method can calculate the deflection at the stations as discrete points, however, the new method provides the deflection of the shaft as a continuous curve. That is, the new method provides the deflection of shaft at any point along the shaft allowing an accurate stress calculation along the shaft.

II.2.10 Finite Element Methods

The Finite Element Method is a numerical analysis technique for obtaining approximate solutions to a wide variety of engineering problems such as stresses in complex structures, structural vibrations, lubrication problems, acoustics etc. (Ref. 64). The system is divided into a finite number of subregions or elements. And then, an interpolation function is introduced to describe (say) the displacement field over the element. In this way the governing differential equations are converted to a set of algebraic equations for each element. Finally by ensuring the continuity of displacements over the entire set of elements the global equations of the system are obtained in terms of the nodal parameters (the values of the interpolation functions evaluated at the nodal points of the elements) which are then solved on digital computers.

Because of the wide range of application of the Finite Element Method, the literature on the subject is enormous. The following discussion is restricted to the basic forms of the Finite Element Method of concern to the rotor dynamics problems with specific reference to the undamped critical speed calculations for the synchronous whirling motion of rotor-bearing systems. The method can be presented simply in terms of the following steps:

1) The rotor is divided by imaginary lines or surfaces into a finite number of elements. The elements are assumed to be interconnected at a discrete numbers of nodal points (or nodes) situated on their boundaries.
2) The generalized coordinates are chosen for the elements as the basic unknown parameters of the system. Usually

"generalized" displacements are chosen as the coordinates, for example, transverse displacements, slopes, etc.

3) Interpolating functions are chosen to define uniquely the state of displacements within each element. Using the interpolation functions, the state of displacements within each element can be expressed in terms of the nodal point displacements. When the interpolation functions are selected, considerations should be given to requirements of compatibility of displacements over the entire set of elements.

4) The displacement functions now define uniquely the state of strain and velocity within each element in terms of the nodal displacements. This allows the calculation of potential and kinetic energies of each element.

5) The potential energy and the kinetic energy of the whole system can be found by summation of the potential energy and the kinetic energy, respectively, of elements over the entire range of the whole system. The application of Lagrange's equations then allow the governing equations of the whole system expressed in terms of nodal displacements. This step is equivalent to superposition of the elemental mass matrices and the elemental stiffness matrices, respectively, to assemble the system mass matrix and the system stiffness matrix.

6) The governing equations of the whole system can be converted into a classical eigenvalue problem which can be solved numerically using digital computers.

A simple case of an Euler beam element will be utilized in the following to illustrate the actual steps involved.

For the first step, the rotor-bearing system is divided into a finite number of elements. The element shown in Fig. 2-4 has two nodes with two degrees of freedom at each node; namely, the lateral displacement, v, and the slope of the shaft axis, θ. That is, v and θ are chosen as the generalized coordinates.

The nodal displacement vector is

$$\{\delta\} = \begin{Bmatrix} v_i \\ \theta_i \\ v_j \\ \theta_j \end{Bmatrix} = \lfloor\, v_i,\ \theta_i,\ v_j,\ \theta_j \,\rfloor^t \qquad (2\text{-}44)$$

where the notation "{ }" is used to denote a column vector, "$\lfloor\ \rfloor$" is to denote a row vector, and the superscript t is to denote the transpose of the matrix involved. For Euler-Bernouli beam theory

$$\theta = \frac{dv}{dx} \qquad (2\text{-}45)$$

The interpolation function is chosen as a third order polynomial function with four constants namely α_1, α_2, α_3, and α_4, which are unknown at present:

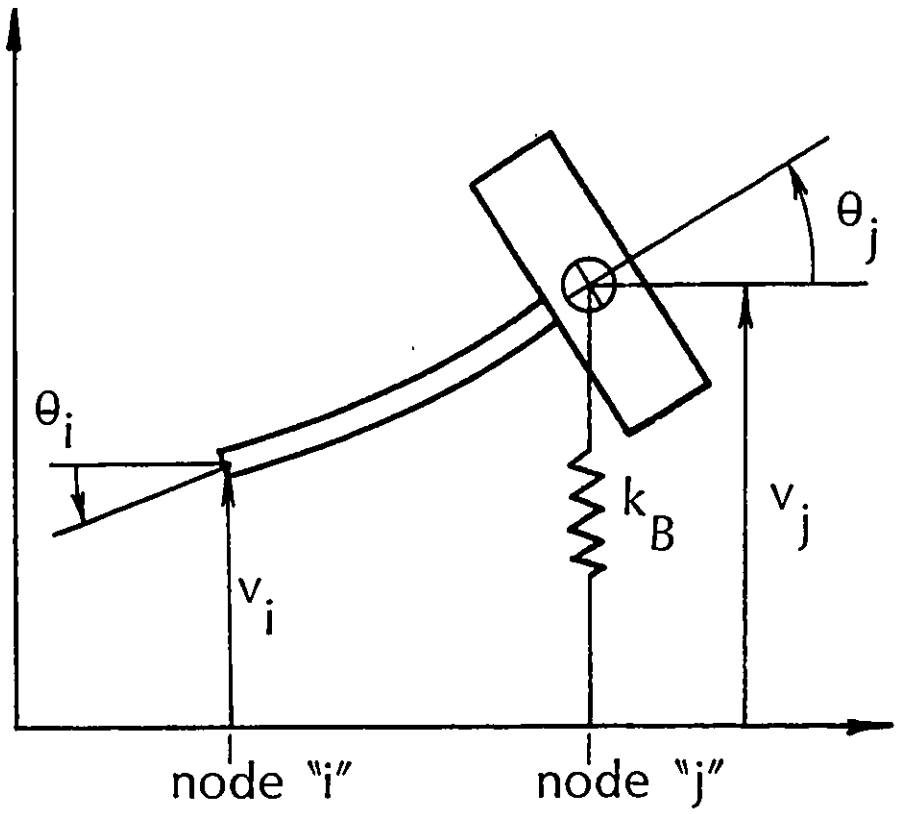

Fig. 2-4 Representative "i"th Element

$$v = \alpha_1 + \alpha_2 x + \alpha_3 x^2 + \alpha_4 x^3$$

$$= \lfloor 1,\ x,\ x^2,\ x^3 \rfloor \begin{Bmatrix} \alpha_1 \\ \alpha_2 \\ \alpha_3 \\ \alpha_4 \end{Bmatrix} \tag{2-46}$$

and $\theta = \frac{dv}{dx} = (\alpha_2 + 2\alpha_3 x + 3\alpha_4 x^2)$

$$= \lfloor 0,\ 1,\ 2x,\ 3x^2 \rfloor \begin{Bmatrix} \alpha_1 \\ \alpha_2 \\ \alpha_3 \\ \alpha_4 \end{Bmatrix}$$

At the node i, we have $x = 0$, therefore, $v_i = \alpha_1$ and $\theta_i = \alpha_2$. At the node j, we have $x = \ell$, therefore, we have $v_j = \alpha_1 + \alpha_2 \ell + \alpha_3 \ell^2 + \alpha_4 \ell^3$, and $\theta_j = (\alpha_2 + 2\alpha_3 \ell + 3\alpha_4 \ell^2)$.

$$\begin{Bmatrix} v_i \\ \theta_i \\ v_j \\ \theta_j \end{Bmatrix} = \begin{bmatrix} 1 & 0 & 0 & 0 \\ 0 & 1 & 0 & 0 \\ 1 & \ell & \ell^2 & \ell^3 \\ 0 & 1 & 2\ell & 3\ell^2 \end{bmatrix} \begin{Bmatrix} \alpha_1 \\ \alpha_2 \\ \alpha_3 \\ \alpha_4 \end{Bmatrix}$$

Solving for $\lfloor \alpha_1,\ \alpha_2,\ \alpha_3,\ \alpha_4 \rfloor^t$ yields

$$\begin{Bmatrix} \alpha_1 \\ \alpha_2 \\ \alpha_3 \\ \alpha_4 \end{Bmatrix} = \begin{bmatrix} 1 & 0 & 0 & 0 \\ 0 & 1 & 0 & 0 \\ 1 & \ell & \ell^2 & \ell^3 \\ 0 & 1 & 2\ell & 3\ell^2 \end{bmatrix}^{-1} \begin{Bmatrix} v_i \\ \theta_i \\ v_j \\ \theta_j \end{Bmatrix}$$

$$= \begin{bmatrix} 1 & 0 & 0 & 0 \\ 0 & 1 & 0 & 0 \\ \frac{-3}{\ell^2} & \frac{-2}{\ell} & \frac{3}{\ell^2} & \frac{-1}{\ell} \\ \frac{2}{\ell^3} & \frac{1}{\ell^2} & \frac{-2}{\ell^3} & \frac{1}{\ell^2} \end{bmatrix} \begin{Bmatrix} v_i \\ \theta_i \\ v_j \\ \theta_j \end{Bmatrix} \qquad (2\text{-}47)$$

Substituting eq. (2-47) into eq. (2-46), eq. (2-46) becomes:

$$v = \lfloor 1,\ x,\ x^2,\ x^3 \rfloor \begin{bmatrix} 1 & 0 & 0 & 0 \\ 0 & 1 & 0 & 0 \\ \frac{-3}{\ell^2} & \frac{-2}{\ell} & \frac{3}{\ell^2} & \frac{-1}{\ell} \\ \frac{2}{\ell^3} & \frac{1}{\ell^2} & \frac{-2}{\ell^3} & \frac{1}{\ell^2} \end{bmatrix} \begin{Bmatrix} v_i \\ \theta_i \\ v_j \\ \theta_j \end{Bmatrix}$$

$$= \lfloor N \rfloor \{\delta\} \qquad (2\text{-}48)$$

where

$$\lfloor N \rfloor = \lfloor 1,\ x,\ x^2,\ x^3 \rfloor \begin{bmatrix} 1 & 0 & 0 & 0 \\ 0 & 1 & 0 & 0 \\ \frac{-3}{\ell^2} & \frac{-2}{\ell} & \frac{3}{\ell^2} & \frac{-1}{\ell} \\ \frac{2}{\ell^3} & \frac{1}{\ell^2} & \frac{-2}{\ell^3} & \frac{1}{\ell^2} \end{bmatrix}$$

$$= \left\{ \begin{array}{l} \left[1 - \frac{3x^2}{\ell^2} + \frac{2x^3}{\ell^3}\right] \\ \left[x - \frac{2x^2}{\ell} + \frac{x^3}{\ell^2}\right] \\ \left[\frac{3x^2}{\ell^2} - \frac{2x^3}{\ell^3}\right. \\ \left[\frac{-x^2}{\ell} + \frac{x^3}{\ell^2}\right] \end{array} \right\}^t$$

$$= \lfloor n_1, n_2, n_3, n_4 \rfloor \qquad (2\text{-}49)$$

The functions $\lfloor N \rfloor$ are called as the shape function. The shape function is called upon when the "consistent" mass matrix is calculated directly without formalization of elemental and system kinetic energies.

Now, for the Euler-Bernouli beam theory, the axial strain ϵ becomes:

$$\epsilon = -y \frac{d^2v}{dx^2}$$

where y is the local coordinate shown in Fig. 2-5.

The potential energy of the shaft element, U_s, can be calculated as follows:

$$U_s = \frac{1}{2} \int_V \epsilon^t \cdot \sigma \, dV$$

$$= \frac{1}{2} \int_0^{\ell} \int_A \epsilon^t \, \sigma \, dA \cdot dx$$

$$= \frac{1}{2} \int_0^{\ell} \int_A \epsilon \cdot (E\epsilon) \, dA \cdot dx$$

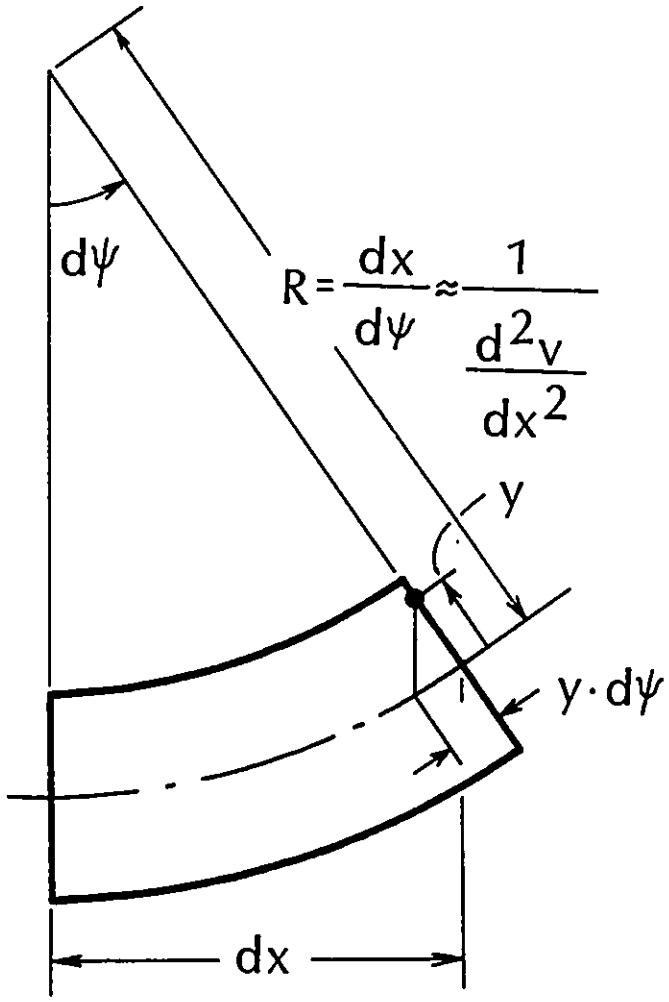

$$\epsilon = \frac{-y\, d\psi}{dx}$$

$$= -y \frac{d}{dx}\left(\frac{dv}{dx}\right)$$

Fig. 2-5 A Local Coordinate, y

$$= \frac{E}{2} \int_0^{\ell} \int_A \left\{-y \frac{d^2v}{dx^2}\right\}^2 \, dA \, dx$$

$$= \frac{E}{2} \int_0^{\ell} \left\{\frac{d^2v}{dx^2}\right\}^2 \int_A y^2 \, dA \cdot dx$$

$$= \frac{EI}{2} \int_0^{\ell} \left\{\frac{d^2v}{dx^2}\right\}^2 dx$$

$$= \frac{EI}{2} \int_0^{\ell} \frac{d^2}{dx^2} \left[(\lfloor N \rfloor \{\delta\})^t \right] \cdot \frac{d^2}{dx^2} \left[\lfloor N \rfloor \{\delta\} \right] dx$$

$$= \frac{EI}{2} \{\delta\}^t \left[\int_0^{\ell} \left[\frac{d^2}{dx^2} \{N\} \right] \cdot \left[\frac{d^2}{dx^2} \lfloor N \rfloor \right] dx \right] \{\delta\}$$

$$= \frac{EI}{2} \{\delta\}^t \int_0^{\ell} \begin{Bmatrix} n_1'' \\ n_2'' \\ n_3'' \\ n_4'' \end{Bmatrix} \lfloor n_1'', \; n_2'', \; n_3'', \; n_4'' \rfloor \, dx \cdot \{\delta\}$$

$$= \frac{EI}{2} \{\delta\}^t \int_0^{\ell} \begin{Bmatrix} -\frac{6}{\ell^2} + \frac{12x}{\ell^3} \\ \frac{-4}{\ell} + \frac{6x}{\ell^2} \\ \frac{6}{\ell^2} - \frac{12x}{\ell^3} \\ \frac{-2}{\ell} + \frac{6x}{\ell^2} \end{Bmatrix} \left\lfloor \left[-\frac{6}{\ell^2} + \frac{12x}{\ell^3}\right], \left[\frac{-4}{\ell} + \frac{6x}{\ell^2}\right], \left[\frac{6}{\ell^2} - \frac{12x}{\ell^3}\right], \left[\frac{-2}{\ell} + \frac{6x}{\ell^2}\right] \right\rfloor dx \{\delta\}$$

$$= \frac{EI}{2} \{\delta\}^t \int_0^{\ell} \frac{EI}{2} \{\delta\}^t \int_0^{\ell} \begin{bmatrix} \left[\frac{-6}{\ell^2} + \frac{12x}{\ell^3}\right]^2, \left[\frac{-6}{\ell^2} + \frac{12x}{\ell^3}\right]\left[\frac{-4}{\ell} + \frac{6x}{\ell^2}\right], \left[\frac{-6}{\ell^2} + \frac{12x}{\ell^3}\right]\left[\frac{6}{\ell^2} - \frac{12x}{\ell^3}\right], \left[\frac{-6}{\ell^2} + \frac{12x}{\ell^3}\right]\left[\frac{-2}{\ell} + \frac{6x}{\ell^2}\right] \\ \left[\frac{-4}{\ell} + \frac{6x}{\ell^2}\right]\left[\frac{-6}{\ell^2} + \frac{12x}{\ell^3}\right], \left[\frac{-4}{\ell} + \frac{6x}{\ell^2}\right]^2, \left[\frac{-4}{\ell} + \frac{6x}{\ell^2}\right]\left[\frac{6}{\ell^2} - \frac{12x}{\ell^3}\right], \left[\frac{-4}{\ell} + \frac{6x}{\ell^2}\right]\left[\frac{-2}{\ell} + \frac{6x}{\ell^2}\right] \\ \left[\frac{6}{\ell^2} - \frac{12x}{\ell^3}\right]\left[\frac{-6}{\ell^2} + \frac{12x}{\ell^3}\right], \left[\frac{6}{\ell^2} - \frac{12x}{\ell^3}\right]\left[\frac{-4}{\ell} + \frac{6x}{\ell^2}\right], \left[\frac{6}{\ell^2} - \frac{12x}{\ell^3}\right]^2, \left[\frac{6}{\ell^2} - \frac{12x}{\ell^3}\right]\left[\frac{-2}{\ell} + \frac{6x}{\ell^2}\right] \\ \left[\frac{-2}{\ell} + \frac{6x}{\ell^2}\right]\left[\frac{-6}{\ell^2} + \frac{12x}{\ell^3}\right], \left[\frac{-2}{\ell} + \frac{6x}{\ell^2}\right]\left[\frac{-4}{\ell} + \frac{6x}{\ell^2}\right], \left[\frac{-2}{\ell} + \frac{6x}{\ell^2}\right], \left[\frac{6}{\ell^2} - \frac{12x}{\ell^3}\right], \left[\frac{-2}{\ell} + \frac{6x}{\ell^2}\right]^2 \end{bmatrix} dx \cdot \{\delta\}$$

$$= \frac{1}{2} \{\delta\}^t \begin{bmatrix} k_{11} & k_{12} & k_{13} & k_{14} \\ k_{21} & k_{22} & k_{23} & k_{24} \\ k_{31} & k_{32} & k_{33} & k_{34} \\ k_{41} & k_{42} & k_{43} & k_{44} \end{bmatrix} \{\delta\}$$

$$= \frac{1}{2} \{\delta\}^t [K_s] \{\delta\} \qquad (2\text{-}50)$$

where $[K_s]$ is the stiffness matrix of the shaft element, and its element k_{ij} is defined as:

$$k_{ij} = EI \int_0^{\ell} n''_i \, n''_j \, dx, \quad i = 1,2,3,4$$

$$j = 1,2,3,4$$

$$n''_i = \text{ith element of } \frac{d^2}{dx^2} (\lfloor N \rfloor)$$

Therefore,

$$k_{11} = EI \int_0^{\ell} (n''_1)^2 \, dx$$

$$= EI \int_0^{\ell} \left[\frac{-6}{\ell^2} + \frac{12x}{\ell^3}\right]^2 dx$$

$$= EI \frac{12}{\ell^3}$$

$$k_{12} = EI \int_0^{\ell} n''_1 \, n''_2 \, dx$$

$$= EI \int_0^{\ell} \left[\frac{-6}{\ell^2} + \frac{12x}{\ell^3}\right] \cdot \left[\frac{-4}{\ell} + \frac{6x}{\ell^2}\right] dx$$

$$= EI \frac{6}{\ell^2}$$

Similar calculations lead to the stiffness matrix of the shaft element, $[K_s]$, as follows.

$$[K_s] = \frac{EI}{\ell^3} \begin{bmatrix} 12 & 6\ell & -12 & 6\ell \\ 6\ell & 4\ell^2 & -6\ell & 2\ell^2 \\ -12 & -6\ell & 12 & -6\ell \\ 6\ell & 2\ell^2 & -6\ell & 4\ell^2 \end{bmatrix} \qquad (2\text{-}51)$$

The kinetic energy of the shaft element, T_s, is:

$$T_s = \frac{1}{2}\int_o^{\ell} \rho \cdot A(\omega v)^2 \, dx$$

$$= \frac{\rho A \omega^2}{2}\int_o^{\ell} v^t \cdot v \, dx$$

$$= \frac{\rho A \omega^2}{2}\int_o^{\ell} (\lfloor N \rfloor \{\delta\})^t (\lfloor N \rfloor \{\delta\}) \, dx$$

$$= \frac{\rho A \omega^2}{2}\int_o^{\ell} \{\delta\}^t \{N\} \lfloor N \rfloor \{\delta\} \, dx$$

$$= \frac{\rho A \omega^2}{2} \{\delta\}^t \int_o^{\ell} \{N\} \lfloor N \rfloor \, dx \{\delta\}$$

$$= \frac{\omega^2}{2} \{\delta\}^t [M_s] \{\delta\} \qquad (2\text{-}52)$$

where $[M_s]$ is the consistence mass matrix of the shaft element, and its element m_{ij} is defined as:

$$m_{ij} = \rho A \cdot \int_o^{\ell} n_i \, n_j \, dx \quad (i = 1,2,3,4 \text{ and } j = 1,2,3,4)$$

where ρ is the linear mass (mass per unit length of the shaft element) and A the cross-sectional area of the shaft element.

Therefore,

$$m_{11} = \rho A \int_o^{\ell} (1 - \frac{3x^2}{\ell^2} + \frac{2x^3}{\ell^3})^2 \, dx$$

$$= \frac{156}{420} \rho A \ell$$

$$m_{12} = \rho A \int_o^{\ell} (1 - \frac{3x^2}{\ell^2} + \frac{2x^3}{\ell^3})(x - \frac{2x^2}{\ell} + \frac{x^3}{\ell^2}) \, dx$$

$$= \frac{22}{420} \rho A \ell^2$$

Similar calculations yield the mass matrix of the shaft element, $[M_s]$, as below.

$$[M_s] = \frac{\rho A \ell}{420} \begin{bmatrix} 156 & 22\ell & 54 & -13\ell \\ 22\ell & 4\ell^2 & 13\ell & -3\ell^2 \\ 54\ell & 13\ell & 156 & -22\ell \\ -13\ell & -3\ell^2 & -22\ell & 4\ell^2 \end{bmatrix} \tag{2-53}$$

So far, the analysis included the shaft element only. The effect of discs and bearings can be included by superposing their effect at the nodal point "j" in a similar way as described in the case of the shaft element. As shown in Fig. 2-6, a disc and a bearing is placed at the node "j". They can be placed either at the node "i" or both nodes "i" and "j". This is a matter of preference.

The kinetic energy of the disc, T_D, when it is subjected to synchronous whirling, has two portions, namely the kinetic energy due to translational motion and that due to rotational motion of the disc.

$$T_D = [T_D]_{translation} + [T_D]_{rotation} \tag{2-54}$$

$$[T_D]_{translation} = \frac{1}{2} m_D (\omega v_j)^2 \tag{2-55}$$

where m_D is mass of the disc

v_j is transverse displacement of the node "j" as shown in Fig. 2-6.

$$[T_D]_{rotation} = \frac{1}{2} \{\Omega\}^t [I] \{\Omega\} \tag{2-56}$$

where $\{\Omega\}$ is the angular velocity vector of the disc and $[I]$ is the inertia matrix of the disc. In the above equation, one of the most convenient coordinate system is that of the principal coordinate system

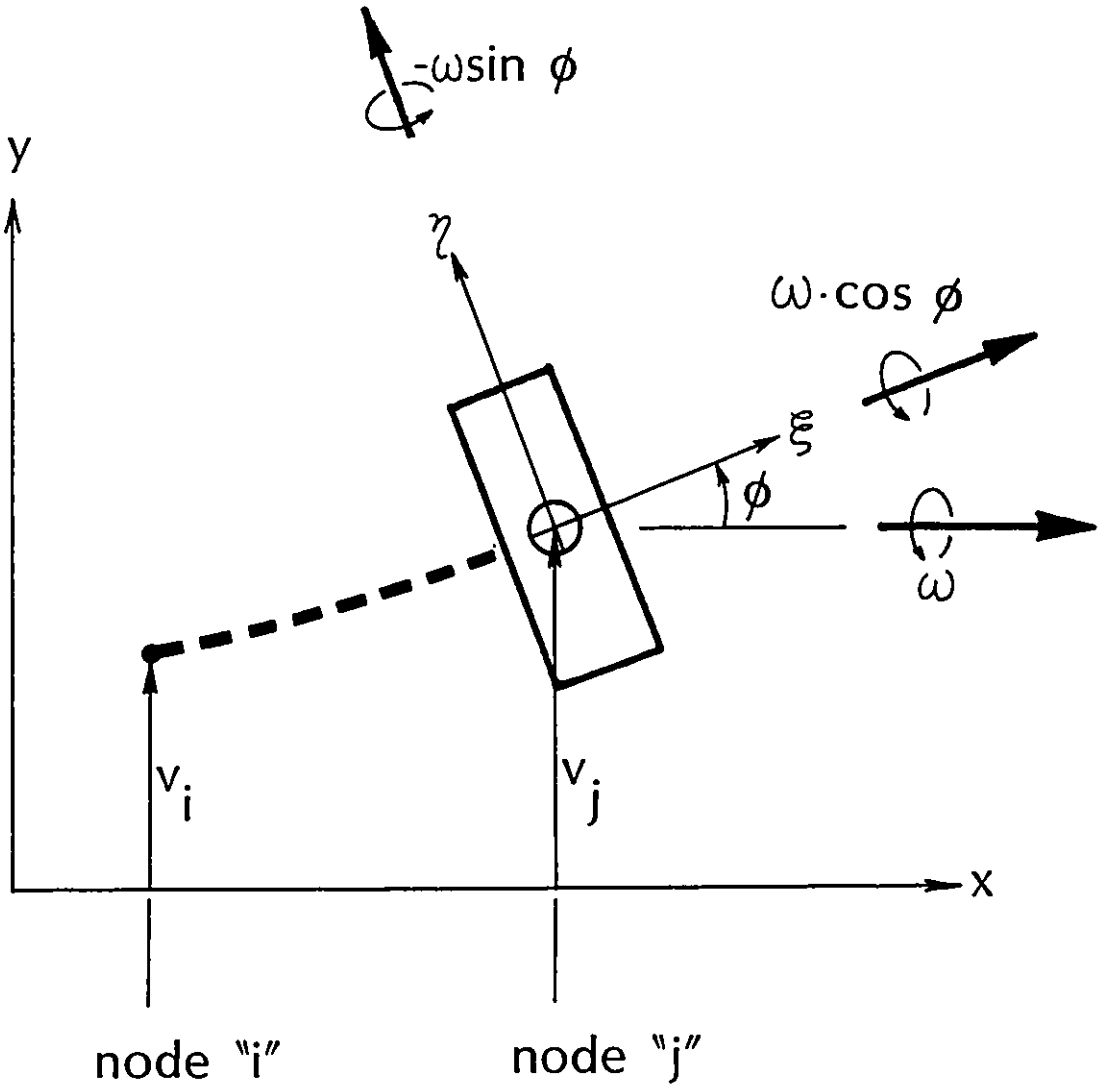

Fig. 2-6 A Disc Element

of the disc so that the terms of product moments of inertia vanish to leave only diagonal terms in the inertia matrix. Referring to Fig. 2-6, the angular velocity vector becomes:

$$\{\Omega\} = \begin{matrix}\Omega_\xi \\ \Omega_\eta \\ \Omega_\zeta\end{matrix} = \begin{matrix}\omega \cos\phi \\ -\omega \sin\phi \\ 0\end{matrix} \qquad (2\text{-}57)$$

where ω is the rotational speed (Rad/sec) of the shaft, and Ω_ξ, Ω_η and Ω_ζ are components of $\{\Omega\}$ along the principal coordinates of the disc as shown in Fig. 2-6.

Substituting eq. (2-57) into eq. (2-56) yields:

$$[T_D]_{\text{rotational}} = \frac{1}{2} \begin{matrix}\omega\cos\phi \\ -\omega\sin\phi \\ 0\end{matrix}^t \begin{matrix} I_\xi & 0 & 0 \\ 0 & I_\eta & 0 \\ 0 & 0 & I_\zeta \end{matrix} \begin{matrix}\omega\cos\phi \\ -\omega\sin\phi \\ 0\end{matrix}$$

$$= \frac{\omega^2}{2}\left[I_\xi \cos^2\phi + I_\eta \sin^2\phi\right]$$

$$= \frac{\omega^2}{2}\left[I_p \cos^2\phi + I_D \sin^2\phi\right] \qquad (2\text{-}58)$$

where $I_p = I_\xi$ is the polar moment of inertia and $I_D = I_\eta$ is the diametral or transverse moment of inertia, respectively, of the disc.

Comparing Fig. 2-6 with Fig. 2-4 and eq. (2-45), the relationship between the angle ϕ and the nodal variable θ_j is found as below.

$$\theta_j = \tan\phi$$

$$\therefore \phi = \tan^{-1}\theta_j$$

$$\therefore \cos^2\phi = \frac{1}{1+\theta_j^2} \qquad (2\text{-}59)$$

$$\therefore \sin^2\phi = \frac{\theta_j^2}{1+\theta_j^2} \tag{2-60}$$

Substituting eqs. (2-59) and (2-60) into eq. (2-58) yields:

$$[T_D]_{\text{rotational}} = \frac{\omega^2}{2} \frac{1}{1+\theta_j^2} [I_p + I_D \cdot \theta_j^2] \tag{2-61}$$

Substituting eqs. (2-55) and (2-61) into eq. (2-54), the total kinetic energy of the disc is:

$$T_D = \frac{\omega^2}{2} [m_D v_j^2 + \frac{I_p + I_D \cdot \theta_j^2}{1+\theta_j^2}] \tag{2-62}$$

It is worth noting that when T_D in eq. (2-62) is applied to the Lagrange's equation, the second term in the right hand side of eq. (2-62) generates

$$-\frac{\omega^2}{2} \cdot \frac{d}{d\theta_j} [\frac{I_p+I_D\cdot\theta_j^2}{1+\theta_j^2}] = \frac{-\omega^2}{2} \cdot \frac{2\theta_j(1+\theta_j^2) - (I_p+I_D\theta_j^2) \cdot (2\theta_j)}{(1+\theta_j^2)^2}$$

$$= \frac{\omega^2(I_p-I_D)\theta_j}{(1+\theta_j^2)^2}$$

$$= \omega^2(I_p-I_D)\theta_j \tag{2-63}$$

since $\theta_j << 1$.

Equation (2-63) indicates the identical results as eq. (2-30) where $I' = I_p - I_D$.

The potential energy due to a compliant bearing, U_B, can be expressed as:

$$U_B = \frac{1}{2} k_B v_j^2$$

where k_B is the spring constant of the bearing.

Therefore, the total kinetic energy of the ith element shown in Fig. 2-4, is the sum of the kinetic energy of shaft element and the kinetic energy of the disc:

$$T_i = T_s + T_D$$

$$= \frac{\omega^2}{2} \left[\{\delta\}^t [M_s] \{\delta\} + m_D v_j^2 + \frac{I_p + I_D \cdot \theta_j^2}{1+\theta_j^2} \right]$$

$$= \frac{\omega^2}{2} \left[\begin{Bmatrix} v_i \\ \theta_i \\ v_j \\ \theta_j \end{Bmatrix}^t [M_s] \begin{Bmatrix} v_i \\ \theta_i \\ v_j \\ \theta_j \end{Bmatrix} + m_D v_j^2 + \frac{I_p + I_D \cdot \theta_j^2}{1+\theta_j^2} \right] \qquad (2\text{-}64)$$

The total potential energy of the ith element is the sum of the strain energies of the shaft element and the bearing element:

$$U_i = U_s + U_B$$

$$= \frac{1}{2} \{\delta\}^t [K_s] \{\delta\} + \frac{1}{2} k_B v_j^2$$

$$= \frac{1}{2} \begin{Bmatrix} v_i \\ \theta_i \\ v_j \\ \theta_j \end{Bmatrix}^t [K_s] \begin{Bmatrix} v_i \\ \theta_i \\ v_j \\ \theta_j \end{Bmatrix} + \frac{1}{2} k_B v_j^2 \qquad (2\text{-}65)$$

Now, the total kinetic energy of the whole system T_T can be found by summing elemental kinetic energies over the range of the whole system:

$$T_T = \sum_{i=1}^{n} T_i \tag{2-66}$$

where n is the number of elements in the system.

Similarly, the total potential energy of the whole system, U_T, is

$$U_T = \sum_{i=1}^{n} U_i \tag{2-67}$$

The application of Lagrange's equation,

$$\frac{d}{dt}\left[\frac{\partial L}{\partial \dot{q}_i}\right] - \frac{\partial L}{\partial q_i} = 0$$

where $L = T_T - U_T$ and

q_i = generalized coordinates

yields the governing equation in matrix form

$$\omega^2 [M_T] = [K_T] \tag{2-68}$$

where $[M_T]$ and $[K_T]$ are the total mass and stiffness matrices, respectively, of the whole system.

Equation (2-68) is the classical algebraic eigenvalue-eigenvector problem which can be solved numerically using digital computers. It is worth nothing that the matrices $[M_T]$ and $[K_T]$ can be "assembled" directly without going through the formal process of application of Lagrange's equation, but by superposing elemental mass and stiffness matrices, respectively, according to the order of nodal points in the global numbering system (Ref. 64).

The first application of the Finite Element Method to rotor-bearing systems was described by Ruhl (Ref. 50) in 1970 in his Ph.D. thesis and then, in a summarized form, in the ASME Transactions (Ref. 57). Ruhl used four degrees-of-freedom finite elements with a uniformly distributed parameter system for a representative rotor segment. He did not dwell on the critical speed calculation but went at once to unbalance response analysis utilizing established information on dynamic stiffness and damping coefficients of fluid film bearings.

His generalized coordinates are the displacement and slope at each end of a cylindrical finite element, and his generalized external forces are the shear force and bending moment at each end of the element. Although he cited Prohl's paper (Ref. 47), he did not solve Prohl's rotor and, therefore, no direct comparison of the methods is available. Comparing it with Lund and Orcutt (Ref. 46), Ruhl's analysis does not include gyroscopic moments and shear deformation.

Since Ruhl's first application of Finite Element Methods to rotor-bearing systems, further work on rotor dynamics utilizing Finite Element Methods have started to appear.

Nelson and McVaugh (Ref. 58) introduced rotary inertia, gyroscopic moments and axial load in 1975. Zorzi and Nelson (Ref. 59) introduced internal damping, and later added axial torque (Ref. 60). Nelson introduced the effect of transverse shear effects by utilizing Timoshenko's beam theory to establish the shape functions.

Rouch and Kao (Ref. 61, 62) introduced a tapered beam finite element and applied a dynamic reduction technique to economize on the computational effort. Rouch (Ref. 62) examined the rotor of Lund and Orcutt (Ref. 46) and claimed "general agreement" both analytically and experimentally. Ozguven and Ozkan (Ref. 63) claimed a generalization of previous work by introducing the effects of rotary inertia, gyroscopic moment, axial load, internal viscous and hysteretic damping, and transverse shear deformations.

Although the Finite Elements Method appears to have covered many salient features, there are several items to be discussed seriously. Firstly, the Finite Element Method is inherently an approximate method.

Secondly, except for bearing analyses, there seems to be very little room in Rotor Dynamics, so far, for the Finite Element Method to take advantage of its most powerful capability - the capability to handle problems with extremely complicated geometric shapes. As can be seen in Fig. 2-4, the finite elements adoped so far in open literature are all basically "line" elements with material properties such as linear mass, length, flexural rigidity, etc. The line element is one of the simplest model. And the Transfer Matrix Method uses basically the same type of model as FEM. Moreover, the elements are usually connected to each other in one of the simplest form of all, namely the simple concatenation. Therefore, the FEM has little advantage over the Transfer Matrix Method in this regard.

Thirdly, while there is very little advantage over the Transfer Matrix Method, the theory and the procedures involved in the FEM are considerably more complicated as shown through the example at the beginning of this section than that of the Transfer Matrix Method.

This does not mean that the FEM is not effective in Rotor Dynamics. For example, the application of the FEM to the fluid film bearing analysis is very successful and effective comparing with other method such as the finite difference scheme. However, in this particular aspect of critical speed analysis, the FEM is not only approximate but also more complicated than the Transfer Matrix Method.

II.3 Summary

As reviewed in the previous section, there are many methods to calculate critical speeds of rotating shafts. However, they are either approximate or based on a theory difficult to understand. For example, the application of Finite Element Method (FEM) to the critical speed calculation of rotating shafts includes complicated formulation procedures. On the other hand, Dunkerley's method is simple and convenient to use, however, the results are too inaccurate to be used in industry for serious analyses; and the method is limited to the first critical speed only.

The rest of the methods discussed in the previous sections fall into either of the two categories as illustrated in the above two examples. That is, the methods are either inaccurate or difficult to understand.

Rayleigh's method has the limitation of being only applicable to conservative systems. Besides, the application of this method to a practical rotor will be enormously cumbersome, and the results will not be accurate enough due to the fact that this method requires one to assume the deflection curve for the entire system.

Galerkin's method, Rayleigh-Ritz method and Stodola's method are all inherently "approximate" methods. They suffer from inaccuracy and enormous unwieldiness if these are applied to a practical rotor for determination of higher critical speeds.

The matrix iteration method can be an excellent method for the fundamental critical speed calculation. However, when higher critical

speeds are sought, this method will suffer from inaccuracy due to the error accumulated by the "purification" or "sweeping" process as described in Sections II.2.6 and II.2.7.

The impedance matching technique is usually for "system" critical speed including the effect of foundations. Wright (Ref. 18) calculated the critical speed of a rotor with uniform diameter using an electrical analogy described in Section II.2.7. Ludwig (Ref. 17) used a rigid beam. Both of them did not have any discs nor stepped diameters on their rotors. Caruso (Ref. 16) used the critical speeds of rotors calculated by the HMP method. Caruso's rotors were practical rotors in actual production steam turbine units. This work illustrates the point very clearly that the impedance method is not practical for "component" critical speed calculation such as that of real-life rotors but is for "system" critical speeds.

The modal analysis, as described in detail in Section II.2.8, does not yield quantitatively accurate values of the rotor critical speeds, but rather qualitative information such as the sensitivity of the rotor to mass unbalanced distributions (Ref. 20).

The Transfer Matrix Method is one of the most effective methods for critical speed calculation of practical rotors. The other effective method for practical rotors is the Finite Element Method (FEM). In spite of its theoretical complexity, the FEM is very popular and useful. This is probably because of its outstanding capability in satisfying complicated (geometric) boundary conditions which are extremely difficult, if not impossible, to satisfy with other methods.

The popularity and usefulness of the Transfer Matrix Method probably lies in the fact that it can accommodate the conditions imposed by discs, stepped diameters, etc. and that it requires repeated calculation of only four-by-four (4×4) matrices. In other words, instead of building up a huge matrix as the FEM does, the Transfer Matrix Method allows smaller sized matrices but requires repeated multiplication of them. This had been considered the ingenuity of the Transfer Matrix Method, when the capacity in calculation was extremely limited at the time of Prohl in early 1940s. Therefore, the utmost importance was placed in not creating large matrices and devising a calculation scheme which was compatible with a tabular method.

Based on the summaries and the literature assessment discussed so far, it is concluded that existing methods are either inaccurate or too complicated for field engineers to understand. It is, therefore, essential to gain a renewed perspective, remove the theoretical detour, and establish a simplified approach to rotor dynamics. Conceptually the new approach is simple and straightforward. This thesis presents a new method in the critical speed calculation of practical rotors and establishes a more simplified approach for rotor dynamics.

The new approach being proposed in this dissertation is easy to understand because the theoretical development involved in the new method is straightforward. Moreover, it is extremely easy to apply to practical rotors in industrial environment due to its simplicity in the analytical and the procedural structure. It also yields accurate critical speeds because the new method is exact in theory within the limits of the assumptions in the general engineering theory of Euler beams.

CHAPTER III

A NEW METHOD FOR CRITICAL SPEED CALCULATION

III.1 Introduction

Rotors have been put to industrial uses in various shapes and manners for a long time. Mathematical analyses on rotor-bearing systems started over a century ago. Although the practical use and analytical investigation of rotor-bearing systems have been established for such a long time, there are no closed-form solutions available for practical rotors mainly because of their complexity in geometry. In fact, not only the solution, but also the set of governing equations for a general industrial rotor has not been previously written in analytical form. Typical rotor- bearing systems are too complex to allow a reasonably simple analytical description. Therefore, numerical methods only have been used successfully in the critical speed calculation of practical rotor- bearing systems.

One of the two most successful methods is the Transfer Matrix Method. The other is the Finite Element Method. Unfortunately, both of these require an advanced level of training to create one's own computer program for critical speed prediction of a rotor-bearing system.

A new method, based on structuring a set of governing equations, is proposed in this chapter. The theoretical development requires only a background in strength of materials, engineering

mechanics and ordinary differential equations. After a brief derivation of the governing equation for a single-segment system based on "Euler beam" theory, a simple rotor-bearing system will be introduced. This simplified system will be solved by the new method as a demonstration for the theoretical development and procedures. Although the system is "simplified" for convenience, there is no loss of generality. In fact, this "simplified" rotor-bearing system is still of such a complexity that, to the author's knowledge, neither a closed-form solution nor a complete set of governing equations is available in the open literature.

III.2 Physical Configuration of a General Rotor

A typical industrial turbo-rotor has a physical configuration as indicated in Fig. 3-1. The vertical lines drawn in Fig. 3-1 and enumerated from one to ten are referred to as stations. The intervals between the shaft stations are defined as segments.

As the stations are enumerated, so are the segments. That is, the segment between the stations i and (i+1) is defined as the ith segment or segment #i. For the sake of convenience, the deflection curve of the shaft can also be segmented and enumerated such that the deflection curve between the stations i and (i+1) is defined as y_i. Therefore, the ordinal number of the deflection curve and the segment number are identical.

The stations are to be introduced along the shaft whenever there is a geometric or dynamic discontinuity such as shoulders (or step changes in shaft diameter), bearing supports, discs, etc. That is, a rotor to be analysed for critical speed prediction will be divided into many segments of uniform cross-sections, and then analysed as a series of Euler beam segments connected at their boundaries (or stations). Appropriate boundary conditions will be applied at the relevant stations. Therefore, the words boundary and station are used synonymously in this thesis.

Though the physical configuration of industrial rotors can be very complex, it is possible to simplify the shape without loss of analytical generality. Therefore, a much simpler rotor is introduced in Fig. 3-2, and this rotor will be treated as an example for the purpose

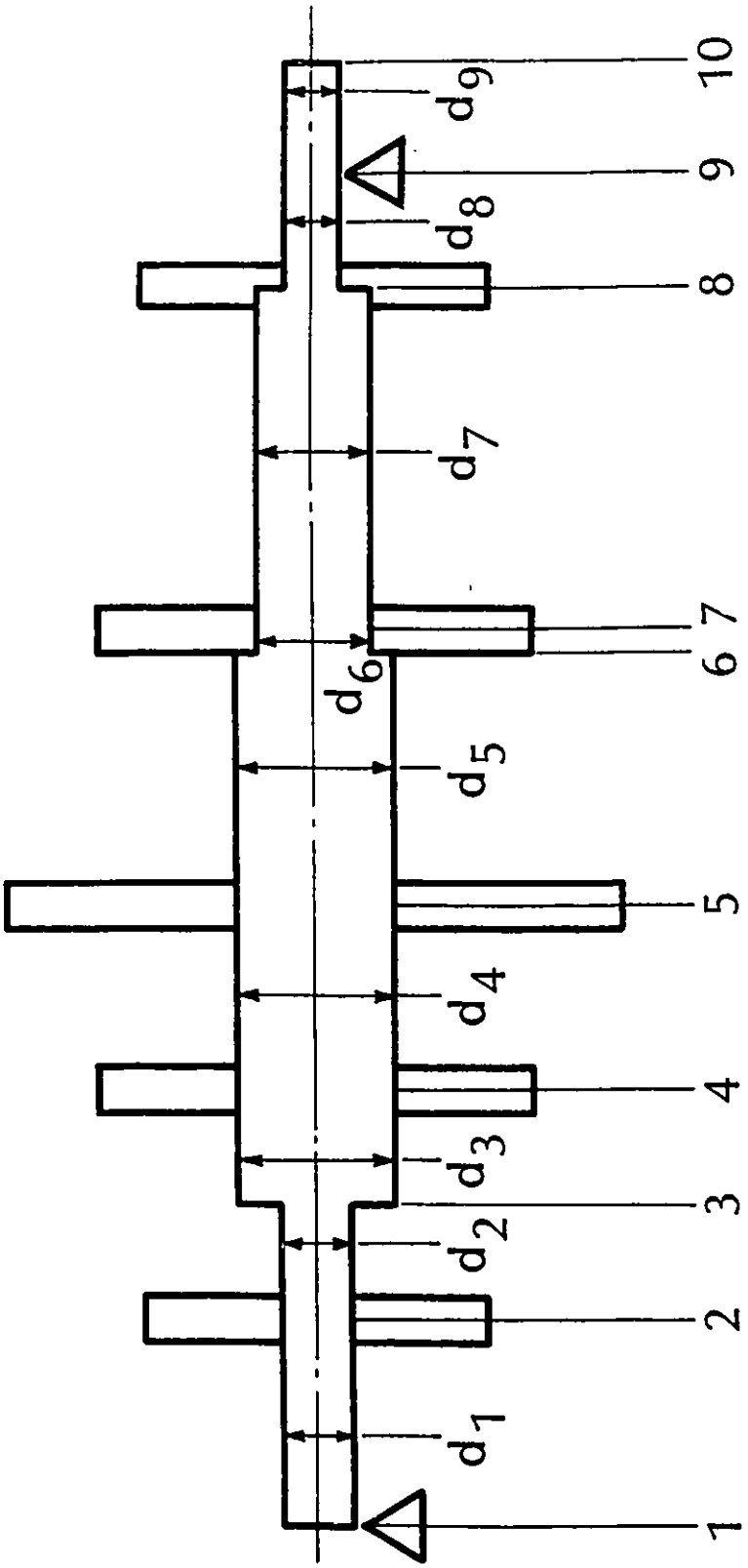

Fig. 3-1 General Configuration of Practical Rotors

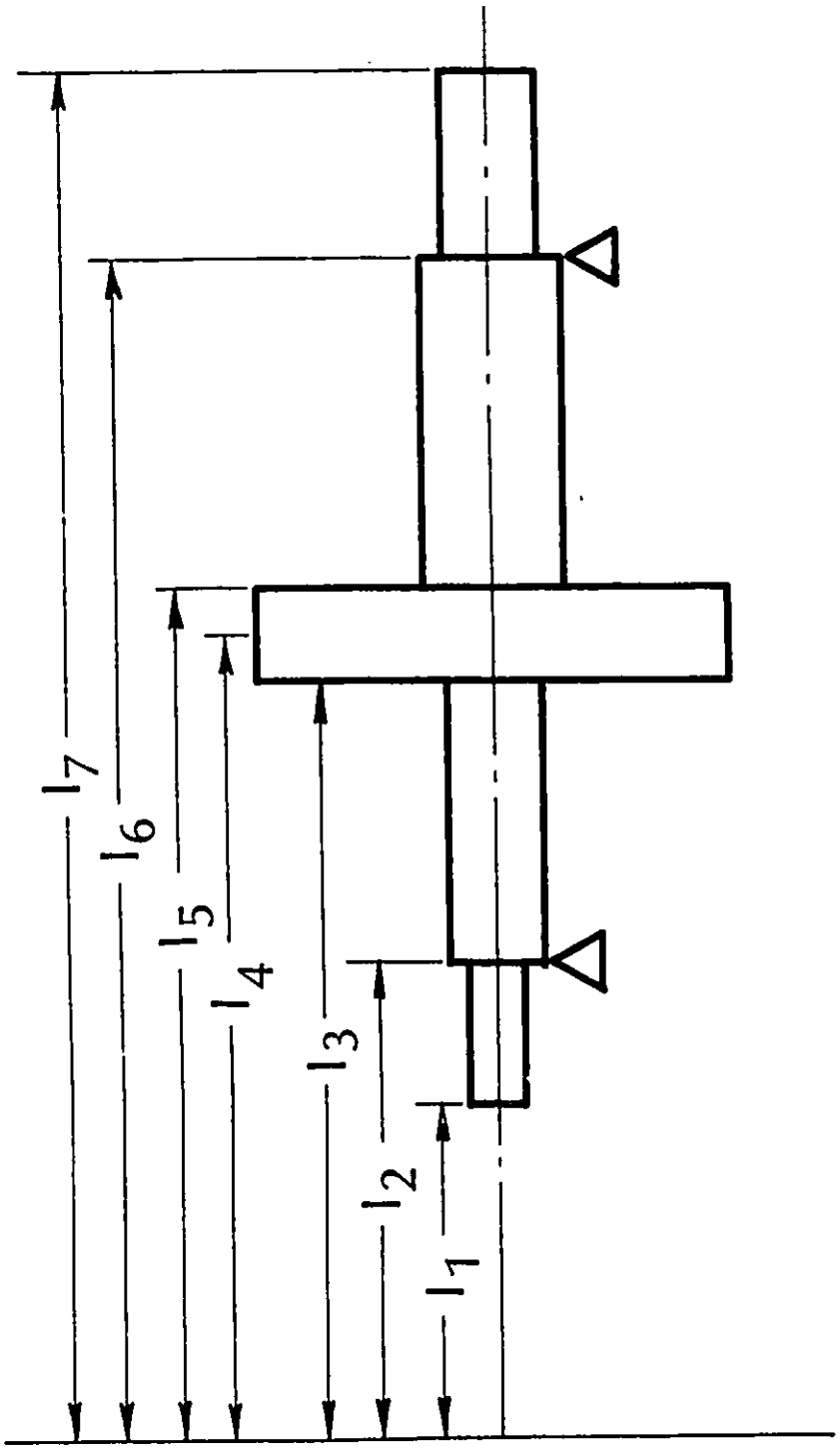

Fig. 3-2 Simple Rotor-Bearing System

of demonstrating the procedures of the new method for critical speed analysis.

The rotor shown in Fig. 3-2 has shaft segments with different diameters, a disc and two bearings. The disc will be treated as shrunk-fit on the shaft. That is, the shaft will be stiffer because of the effect of the shrink-fit. Other types of fit can be readily accommodated. Also the bearings are assumed rigid, however, elastic supports can be accomodated in the analysis with relative ease.

III.3 Theory

III.3.1 Introduction

For the sake of completeness, the governing equation of a single segment rotating shaft will be derived. The derivation is based on the "Euler beam" theory, and for the sake of brevity the inherent assumptions are not explicitly stated.

After the governing equation is derived, the general solution will be given without detailed intermediate procedures. The general solution for a single segment will be applied to the overall rotor-bearing system shown in Fig. 3-2, to derive the set of governing equations for the critical speeds of the system. Therefore, the governing equation of a single segment should be distinguished from the governing equation of the whole rotor-bearing system.

III.3.2 Governing Equation for a Single Segment Shaft

Figure 3-3 illustrates a free body diagram for a shaft element; where

V = shear

M = bending moment

p(x) = load per unit length of the beam

Summing forces in the y-direction yields

$$V - (V+dV) + p(x)dx = 0$$

$$dV = p(x)dx$$

$$\therefore \frac{dV}{dx} = p(x) \qquad (3\text{-}1)$$

Summing moments of the element yields

$$(M+dM) - M - Vdx - p(x)dx \cdot \frac{dx}{2} = 0$$

Neglecting higher order terms, the above equation becomes

$$\frac{dM}{dx} = V \qquad (3\text{-}2)$$

For the given coordinate system, the bending moment is related to the curvature by the flexure equation,

$$M = EI \frac{d^2y}{dx^2} \qquad (3\text{-}3)$$

For a rotating shaft element, the load per unit length of the shaft becomes,

$$p(x) = \rho\omega^2 y \qquad (3\text{-}4)$$

where ρ is the mass per unit length of the shaft.

Substituting eqs. (3-2) to (3-4) into eq. (3-1) yields

$$\frac{d^2}{dx^2}\left[EI \frac{d^2y}{dx^2}\right] - \rho\omega^2 y = 0 \qquad (3\text{-}5)$$

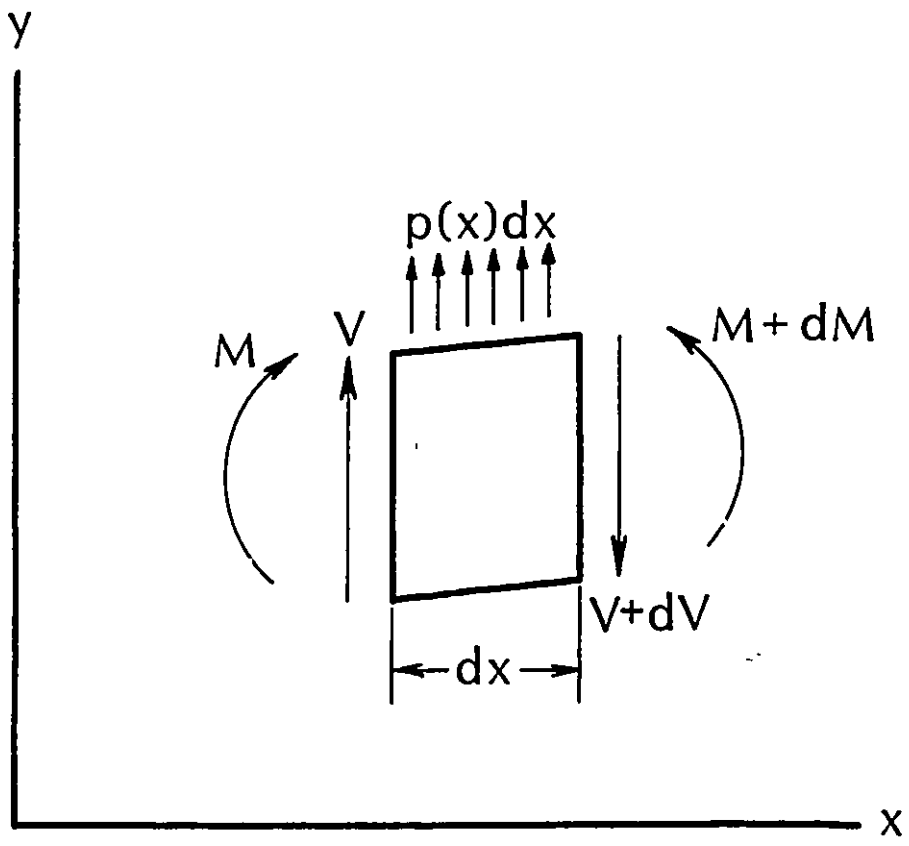

Fig. 3-3 Free Body Diagram of Rotor Element

In the special case of a rotor with a uniform cross-section, eq. (3-5) becomes

$$EI \frac{d^4y}{dx^4} - \rho\omega^2 y = 0$$

On substituting

$$m^4 = \rho \frac{\omega^2}{EI}$$

the final form of the governing equation becomes

$$\frac{d^4y}{dx^4} - m^4 y = 0. \tag{3-6}$$

The general solution of eq. (3-6) is

$$y = A \cosh mx + B \sinh mx + C \cos mx + D \sin mx \tag{3-7}$$

Constants A, B, C and D are to be determined through boundary conditions of the system.

Equation (3-7) is the general solution for a single-segment shaft with a uniform cross-section. This equation will be applied to boundary conditions at each boundary of the rotor shown in Fig. 3-2 in order to generate a set of governing equations for the critical speed of the rotor-bearing system. The detailed procedures will be illustrated in the following sections.

III.3.3 Governing Equations for a Rotor-Bearing System

The governing equations for critical speeds of the rotor-bearing system shown in Fig. 3-2 will be derived in order to demonstrate the procedures involved in this new method of critical speed prediction.

The procedure is straightforward. By applying the boundary conditions to equation (3-7) in the previous section, appropriate equations are found at each boundary of the whole rotor-bearing system. Combining all the equations yields the governing equations for critical speeds of the whole system. The set of the equations are completely analytical and no approximations are introduced within the frame work of the initial analytical modelling.

There are seven boundaries in the particular example problem shown in Fig. 3-2. A set of equations will be derived at each boundary by applying the appropriate boundary conditions to the general solution for a single segment shaft. Each of the equations can be re-arranged to yield a set of homogeneous equations. After a total of seven sets of homogeneous equations are derived, they will be combined together to form a determinant equation. This is the governing equation for the critical speeds of the whole rotor-bearing system.

III.3.3.1 Boundary Conditions at $x = \ell_1$

As shown in Fig. 3-2, the left end of the shaft starts from $x = \ell_1$. The left end of the shaft is a free end, i.e. there is neither a bending moment nor a shear force acting on the shaft at $x = \ell_1$. Therefore, the boundary conditions at this station are:

$$\left.\begin{array}{ll} \text{i)} & M = 0 \\ \text{ii)} & V = 0 \end{array}\right\} \text{at } x = \ell_1$$

Since the deflection curve between the stations $x = \ell_1$ and $x = \ell_2$ is defined as y_1, the above conditions can be expressed as:

$$M\Big|_{x=\ell_1} = EI_1 \frac{d^2y_1}{dx^2}\Big|_{x=\ell_1} = 0 \text{ , and}$$

$$V\Big|_{x=\ell_1} = EI_1 \frac{d^3y_1}{dx^3}\Big|_{x=\ell_1} = 0$$

where EI_1 stands for the rigidity of the shaft for the segment #1. The first condition that the bending moment vanishes yields

$$\frac{d^2y_1}{dx^2}\Big|_{x=\ell_1} = m_1^2[A_1 \cosh m_1x+B_1\sinh m_1x-C_1\cos m_1x-D_1\sin m_1x]\Big|_{x=\ell_1} = 0$$

$$\therefore A_1\cosh m_1\ell_1+B_1\sinh m_1\ell_1-C_1\cos m_1\ell_1-D_1\sin m_1\ell_1 = 0 \qquad (3\text{-}8)$$

The second condition that the shear force vanishes at $x = \ell_1$ yields

$$\frac{d^3y_1}{dx^3}\Big|_{x=\ell_1} = m_1^3[A_1\sinh m_1x+B_1\cosh m_1x+C_1\sin m_1x-D_1\cos m_1x]\Big|_{x=\ell_1} = 0$$

$$\therefore A_1\sinh m_1\ell_1+B_1\cosh m_1\ell_1+C_1\sin m_1\ell_1-D_1\cos m_1\ell_1 = 0 \qquad (3\text{-}9)$$

Combining equations (3-8) and (3-9) together yields

$$\begin{bmatrix} \cosh m_1\ell_1 & \sinh m_1\ell_1 & -\cos m_1\ell_1 & -\sin m_1\ell_1 \\ \sinh m_1\ell_1 & \cosh m_1\ell_1 & \sin m_1\ell_1 & -\cos m_1\ell_1 \end{bmatrix} \begin{Bmatrix} A_1 \\ B_1 \\ C_1 \\ D_1 \end{Bmatrix} = \begin{Bmatrix} 0 \\ 0 \end{Bmatrix}$$

For reasons, to be clarified later, the above equation can be rewritten as follows

$$[A]\ \{\alpha_1\} = \{0\} \text{ or}$$

$$\begin{bmatrix} a_{11} & a_{12} & a_{13} & a_{14} \\ a_{21} & a_{22} & a_{23} & a_{24} \end{bmatrix} \begin{Bmatrix} A_1 \\ B_1 \\ C_1 \\ D_1 \end{Bmatrix} = \begin{Bmatrix} 0 \\ 0 \end{Bmatrix} \tag{3-10}$$

where $a_{11} = \cosh m_1\ell_1$

$a_{12} = \sinh m_1\ell_1$

$a_{13} = -\cos m_1\ell_1$

$a_{14} = -\sin m_1\ell_1$

$a_{21} = \sinh m_1\ell_1$

$a_{22} = \cosh m_1\ell_1$

$a_{23} = \sin m_1\ell_1$

$a_{24} = -\cos m_1\ell_1$

In the special case where $\ell_1 = 0$, eq. (3-10) becomes

$$\begin{bmatrix} 1 & 0 & -1 & 0 \\ 0 & 1 & 0 & -1 \end{bmatrix} \begin{Bmatrix} A_1 \\ B_1 \\ C_1 \\ D_1 \end{Bmatrix} = \begin{Bmatrix} 0 \\ 0 \end{Bmatrix} \tag{3-11}$$

III.3.3.2 Boundary Conditions at $x = \ell_2$

The conditions at $x = \ell_2$ can be summarized as a "rigid support point" because the stiffness at the support point is idealized as infinitely rigid. Since the stiffness is infinite, the displacement vanishes and due to the continuity of the deflection curve, the slope and the bending moment are unique regardless of the direction of approach. These can be translated into four boundary conditions as below.

$$\left.\begin{aligned} y_1 &= 0 \\ y_2 &= 0 \\ \theta_1 &= \theta_2 \\ M_1 &= M_2 \end{aligned}\right\} \text{ at } x = \ell_2$$

where the subscripts 1 and 2 stand for the segments #1 and #2, respectively. The first condition represents the displacement at $x = \ell_2$, measured as a part of the segment #1, and thus vanishes.

$$y_1\Big|_{x=\ell_2} = A_1\cosh m_1\ell_2+B_1\sinh m_1\ell_2+C_1\cos m_1\ell_2+D_1\sin m_1\ell_2 = 0 \quad (3\text{-}12)$$

The second condition describes the same "zero displacement", but measured as a part of segment #2.

$$y_2\Big|_{x=\ell_2} = A_2\cosh m_2\ell_2+B_2\sinh m_2\ell_2+C_2\cos m_2\ell_2+D_2\sin m_2\ell_2 = 0 \quad (3\text{-}13)$$

The third condition describes the fact that the slope of the deflection curve at $x = \ell_2$ is the same whether it is measured as a part of segment #1 or segment #2, namely:

$$m_1[A_1\sinh m_1\ell_2+B_1\cosh m_1\ell_2-C_1\sin m_1\ell_2+D_1\cos m_1\ell_2]$$
$$= m_2[A_2\sinh m_2\ell_2+B_2\cosh m_2\ell_2-C_2\sin m_2\ell_2+D_2\cos m_2\ell_2]$$
$$\therefore A_1m_1\sinh m_1\ell_2+B_1m_1\cosh m_1\ell_2-C_1m_1\sin m_1\ell_2+D_1m_1\cos m_1\ell_2$$
$$-A_2m_2\sinh m_2\ell_2-B_2m_2\cosh m_2\ell_2+C_2m_2\sin m_2\ell_2-D_2m_2\cos m_2\ell_2 = 0 \quad (3\text{-}14)$$

The fourth boundary condition is that of uniqueness of the bending moment at $x = \ell_2$, thus:

$$EI_1m_1^2[A_1\cosh m_1\ell_2+B_1\sinh m_1\ell_2-C_1\cos m_1\ell_2-D_1\sin m_1\ell_2]$$
$$= EI_2m_2^2[A_2\cosh m_2\ell_2+B_2\sinh m_2\ell_2-C_2\cos m_2\ell_2-D_2\sin m_2\ell_2]$$
$$\therefore A_1EI_1m_1^2\cosh m_1\ell_2+B_1EI_1m_1^2\sinh m_1\ell_2-C_1EI_1m_1^2\cos m_1\ell_2$$
$$- D_1EI_1m_2^2\sin m_1\ell_2-A_2EI_2m_2^2\cosh m_2\ell_2-B_2EI_2m_2^2\sinh m_2\ell_2$$
$$+ C_2EI_2m_2^2\cos m_2\ell_2+D_2EI_2m_2^2\sin m_2\ell_2 = 0 \quad (3\text{-}15)$$

Rewriting the boundary conditions at $x = \ell_2$, eqs. (3-12) to (3-15), in matrix form, yields: $[B]\{\alpha_2\} = \{0\}$ or

$$\begin{bmatrix} b_{11} & b_{12} & b_{13} & b_{14} & 0 & 0 & 0 & 0 \\ 0 & 0 & 0 & 0 & b_{25} & b_{26} & b_{27} & b_{28} \\ b_{31} & b_{32} & b_{33} & b_{34} & b_{35} & b_{36} & b_{37} & b_{38} \\ b_{41} & b_{42} & b_{43} & b_{44} & b_{45} & b_{46} & b_{47} & b_{48} \end{bmatrix} \begin{Bmatrix} A_1 \\ B_1 \\ C_1 \\ D_1 \\ A_2 \\ B_2 \\ C_2 \\ D_2 \end{Bmatrix} = \begin{Bmatrix} 0 \\ 0 \\ 0 \\ 0 \end{Bmatrix} \quad (3\text{-}16)$$

where $b_{11} = \cosh m_1\ell_2$

$b_{12} = \sinh m_1\ell_2$

$b_{13} = \cos m_1\ell_2$

$b_{14} = \sin m_1\ell_2$

$b_{25} = \cosh m_2\ell_2$

$b_{26} = \sinh m_2 \ell_2$

$b_{27} = \cos m_2 \ell_2$

$b_{28} = \sin m_2 \ell_2$

$b_{31} = m_1 \sinh m_1 \ell_2$

$b_{32} = m_1 \cosh m_1 \ell_2$

$b_{33} = -m_1 \sin m_1 \ell_2$

$b_{34} = m_1 \cos m_1 \ell_2$

$b_{35} = -m_2 \sinh m_2 \ell_2$

$b_{36} = -m_2 \cosh m_2 \ell_2$

$b_{37} = m_2 \sin m_2 \ell_2$

$b_{38} = -m_2 \cos m_2 \ell_2$

$b_{41} = EI_1 m_1^2 \cosh m_1 \ell_2$

$b_{42} = EI_1 m_1^2 \sinh m_1 \ell_2$

$b_{43} = -EI_1 m_1^2 \cos m_1 \ell_2$

$b_{44} = -EI_1 m_1^2 \sin m_1 \ell_2$

$b_{45} = -EI_2 m_2^2 \cosh m_2 \ell_2$

$b_{46} = -EI_2 m_2^2 \sinh m_2 \ell_2$

$b_{47} = EI_2 m_2^2 \cos m_2 \ell_2$

$b_{48} = EI_2 m_2^2 \sin m_2 \ell_2$

III.3.3.3 Boundary Conditions at $x = \ell_3$

As shown in Fig. 3-2, a disc is located from $x = \ell_3$ to $x = \ell_5$. The center line of the disc thickness is located at $x = \ell_4$. When a disc is shrunk fit on the shaft, as in this example, the disc exerts three effects onto the shaft, namely

i) stiffening

ii) dead weight or additional mass, and

iii) gyroscopic effect.

The shaft is stiffened by the shrunk fit of the disc. If a disc is not shrunk fit but installed in such a way that the flexibility or stiffness of the shaft is not affected, the stiffening effect should be ignored. The disc also provides an additional mass to that of the shaft. This additional mass creates a tendency to decrease the critical speed of the shaft. These two effects can be modelled mathematically by introducing a "thick shaft section", that is, the shaft diameter is increased to that of the disc. This corresponds to the case where the disc is treated as an integral portion of the shaft.

Therefore, in order to account for the stiffening and the dead weight effects due to the disc, a "thickened" shaft segment will be introduced between $x = \ell_3$ and $x = \ell_5$. That is, a step increase in the shaft diameter will be introduced at $x = \ell_3$, and a step decrease in the shaft diameter at $x = \ell_5$.

Since the shaft is modelled after the "Euler beam" as opposed to the "Timoshenko beam theory", rotary inertia or gyroscopic effect of the disc should be introduced independent of the "additional mass". The

gyroscopic effect will be introduced at the center line station of the disc, i.e. at $x = \ell_4$. This corresponds to the fact that;

i) The disc is treated as a rigid body, and

ii) The gyroscopic effect of the rigid disc is applied at the center of gravity as a concentrated entity.

As illustrated before, the shaft goes through a step change in its diameter at $x = \ell_3$. Since there is no external shear, bend, or restrictions (such as a rigid support), there is no abrupt change at $x = \ell_3$ in the displacement, slope, bending moment, and shear. Further, it doesn't make any difference as to whether these quantities are measured as a part of segment #2 or segment #3.

It is worth noting that, although there is no external cause for abrupt changes in the deflection curve or its derivatives, there is a step change in the shaft diameter which causes abrupt changes in the values of m_is and EIs across the point $x = \ell_3$. Therefore, these will generate four equations as below.

$$\left.\begin{aligned} y_2 &= y_3 \\ \theta_2 &= \theta_3 \\ M_2 &= M_3 \\ V_2 &= V_3 \end{aligned}\right\} \quad \text{at } x = \ell_3$$

Therefore:

i) $y_2 = y_3$

$$A_2\cosh m_2\ell_3 + B_2\sinh m_2\ell_3 + C_2\cos m_2\ell_3 + D_2\sin m_2\ell_3 - A_3\cosh m_3\ell_3 - B_3\sinh m_3\ell_3 - C_3\cos m_3\ell_3 - D_3\sin m_3\ell_3 = 0 \qquad (3\text{-}17)$$

ii) $\theta_2 = \theta_3$

$$A_2m_2\sinh m_2\ell_3+B_2m_2\cosh m_2\ell_3-C_2m_2\sin m_2\ell_3$$
$$+ D_2m_2\cos m_2\ell_3-A_3m_3\sinh m_3\ell_3-B_3m_3\cosh m_3\ell_3$$
$$+ C_3m_3\sin m_3\rho_3-D_3m_3\cos m_3\ell_3 = 0 \qquad (3\text{-}18)$$

iii) $M_2 = M_3$

$$A_2EI_2m_2^2\cosh m_2\ell_3+B_2EI_2m_2^2\sinh m_2\ell_3-C_2EI_2m_2^2\cos m_2\ell_3$$
$$- D_2EI_2m_2^2\sin m_2\ell_3-A_3EI_3m_2^2\cosh m_3\ell_3-B_3EI_3m_3^2\sinh m_3\ell_3$$
$$+ C_3EI_3m_3^2\cos m_3\ell_3+D_3EI_3m_3^2\sin m_3\ell_3 = 0 \qquad (3\text{-}19)$$

iv) $V_2 = V_3$

$$A_2EI_2m_2^3\sinh m_2\ell_3+B_2EI_2m_2^3\cosh m_2\ell_3$$
$$+ C_2EI_2m_2^3\sin m_2\ell_3-D_2EI_2m_2^3\cos m_2\ell_3$$
$$- A_3EI_3m_3^3\sinh m_3\ell_3-B_3EI_3m_3^3\cosh m_3\ell_3$$
$$- C_3EI_3m_3^3\sin m_3\ell_3+D_3EI_3m_3^3\cos m_3\ell_3 = 0 \qquad (3\text{-}20)$$

Rearranging eqs. (3-17) to (3-20) in matrix form yields

$[C]\ \{\alpha_3\} = \{0\}$, or

$$\begin{bmatrix} c_{11} & c_{12} & c_{13} & c_{14} & c_{15} & c_{16} & c_{17} & c_{18} \\ c_{21} & c_{22} & c_{23} & c_{24} & c_{25} & c_{26} & c_{27} & c_{28} \\ c_{31} & c_{32} & c_{33} & c_{34} & c_{35} & c_{36} & c_{37} & c_{38} \\ c_{41} & c_{42} & c_{43} & c_{44} & c_{45} & c_{46} & c_{47} & c_{48} \end{bmatrix} \begin{Bmatrix} A_2 \\ B_2 \\ C_2 \\ D_2 \\ A_3 \\ B_3 \\ C_3 \\ D_3 \end{Bmatrix} = \begin{Bmatrix} 0 \\ 0 \\ 0 \\ 0 \end{Bmatrix} \qquad (3\text{-}21)$$

where $c_{11} = \cosh m_2 \ell_3$

$c_{12} = \sinh m_2 \ell_3$

$c_{13} = \cos m_2 \ell_3$

$c_{14} = \sin m_2 \ell_3$

$c_{15} = -\cosh m_3 \ell_3$

$c_{16} = -\sinh m_3 \ell_3$

$c_{17} = -\cos m_3 \ell_3$

$c_{18} = -\sin m_3 \ell_3$

$c_{21} = m_2 \sinh m_2 \ell_3$

$c_{22} = m_2 \cosh m_2 \ell_3$

$c_{23} = -m_2 \sin m_2 \ell_3$

$c_{24} = m_2 \cos m_2 \ell_3$

$c_{25} = -m_3 \sinh m_3 \ell_3$

$c_{26} = -m_3 \cosh m_3 \ell_3$

$c_{27} = m_3 \sin m_3 \ell_3$

$c_{28} = -m_3 \cos m_3 \ell_3$

$c_{31} = EI_2 m_2^2 \cosh m_2 \ell_3$

$c_{32} = EI_2 m_2^2 \sinh m_2 \ell_3$

$c_{33} = -EI_2 m_2^2 \cos m_2 \ell_3$

$c_{34} = -EI_2 m_2^2 \sin m_2 \ell_3$

$c_{35} = -EI_3 m_3^2 \cosh m_3 \ell_3$

$c_{36} = -EI_3 m_3^2 \sinh m_3 \ell_3$

$c_{37} = EI_3 m_3^2 \cos m_3 \ell_3$

$c_{38} = EI_3 m_3^2 \sin m_3 \ell_3$

$c_{41} = EI_2 m_2^3 \sinh m_2 \ell_3$

$$c_{42} = EI_2 m_2^3 \cosh m_2 \ell_3$$

$$c_{43} = EI_2 m_2^3 \sin m_2 \ell_3$$

$$c_{44} = -EI_2 m_2^3 \cos m_2 \ell_3$$

$$c_{45} = -EI_3 m_3^3 \sinh m_3 \ell_3$$

$$c_{46} = -EI_3 m_3^3 \cosh m_3 \ell_3$$

$$c_{47} = -EI_3 m_3^3 \sin m_3 \ell_3$$

$$c_{48} = EI_3 m_3^3 \cos m_3 \ell_3$$

III.3.3.4 Boundary Conditions at $x = \ell_4$

As discussed in the previous section, the gyroscopic effect of the disc is introduced at the station where the center line of the disc is located, i.e. at $x = \ell_4$. The gyroscopic effect appears in the form of external bending moment applied at $x = \ell_4$. The rest of the terms, displacement, slope and shear are not subject to any abrupt changes. Therefore, the boundaries conditions are:

$$\begin{cases} y_3 = y_4 \\ \theta_3 = \theta_4 \\ \Delta M = M_4 - M_3 = \omega^2 I' \theta_3 \\ V_3 = V_4 \end{cases}$$

where I' is the net mass moment of inertia of the disc;

$$I' = \frac{\pi w h}{64 g} \left[D_D^4 - D_S^4 - \frac{4}{3} h^2 [D_D^2 - D_S^2] \right]$$

w: specific weight of the disc material

h: thickness or width of the disc

D_D: diameter of the disc

D_S: diameter of the shaft

The above boundary conditions can be arranged to yield four homogeneous equations as below:

i) $y_3 = y_4$

$$A_3 \cosh m_3 \ell_4 + B_3 \sinh m_3 \ell_4 + C_3 \cos m_3 \ell_4 + D_3 \sin m_3 \ell_4$$
$$- A_4 \cosh m_4 \ell_4 - B_4 \sinh m_4 \ell_4 - C_4 \cos m_4 \ell_4 - D_4 \sin m_4 \ell_4 = 0 \qquad (3\text{-}22)$$

ii) $\theta_3 = \theta_4$

$$A_3m_3\sinh m_3\ell_4+B_3m_3\cosh m_3\ell_4-C_3m_3\sin m_3\ell_4+D_3m_3\cos m_3\ell_4$$
$$- A_4m_4\sinh m_4\ell_4-B_4m_4\cosh m_4\ell_4+C_4m_4\sin m_4\ell_4-D_4m_4\cos m_4\ell_5 = 0 \qquad (3\text{-}23)$$

iii) $M_4 - M_3 = \omega^2 I'\theta_3$

$$M_4 = EI_4 \frac{d^2y_4}{dx^2}$$

$$M_3 = EI_3 \frac{d^2y_3}{dx^2}$$

$$\theta_3 = \frac{dy_3}{dx}$$

$$\therefore EI_4 \frac{d^2y_4}{dx^2} - EI_3 \frac{d^2y_3}{dx^2} - \omega^2 I' \frac{dy_3}{dx} = 0$$

Substituting for y_3 and y_4, and carrying out the required differentiation yields:

$$\therefore EI_4m_4^2[A_4\cosh m_4\ell_4+B_4\sinh m_4\ell_4-C_4\cos m_4\ell 4-D_4\sin m_4\ell_4]$$
$$- EI_3m_3^2[A_3\cosh m_3\ell_4+B_3\sinh m_3\ell_4-C_3\cos m_3\ell_4-D_3\sin m_3\ell_4]$$
$$- \omega^2I'm_3[A_3\sinh m_3\ell_4+B_3\cosh m_3\ell_4-C_3\sin m_3\ell_4+D_3\cos m_3\ell_4] = 0$$

Rearranging the above equation for constants A_3, B_3, C_3, ..., C_4 and D_4, we find:

$$\therefore A_3[-EI_3m_3^2\cosh m_3\ell_4-\omega^2I'm_3\sinh m_3\ell_4]$$
$$+ B_3[-EI_3m_3^2\sinh m_3\ell_4-\omega^2I'm_3\cosh m_3\ell_4]$$
$$+ C_3(EI_3m_3^2\cos m_3\ell_4+\omega^2I'm_3\sin m_3\ell_4]$$
$$+ D_3(EI_3m_3^2\sin m_3\ell_4-\omega^2I'm_3\cos m_3\ell_4]$$
$$+ A_4EI_4m_4^2\cosh m_4\ell_4$$
$$+ B_4EI_4m_4^2\sinh m_4\ell_4$$
$$- C_4EI_4m_4^2\cos m_4\ell_4$$
$$- D_4EI_4m_4^2\sin m_4\ell_4 = 0 \qquad (3\text{-}24)$$

iv) $V_3 = V_4$

$$EI_3m_3^3[A_3\sinh m_3\ell_4+B_3\cosh m_3\ell_4+C_3\sin m_3\ell_4-D_3\cos m_3\ell_4]$$
$$= EI_4m_4^3[A_4\sinh m_4\ell_4+B_4\cosh m_4\ell_4+C_4\sin m_4\ell_4-D_4\cos m_4\ell_4]$$
$$\therefore A_3EI_3m_3^3\sinh m_3\ell_4+B_4EI_3m_3^3\cosh m_4\ell_4+C_3EI_3m_3^3\sin m_3\ell_4$$
$$- D_3EI_3m_3^3\cos m_3\ell_4-A_4EI_4m_4^3\sinh m_4\ell_4-B_4EI_4m_4^3\cosh m_4\ell_4$$
$$- C_4EI_4m_4^3\sin m_4\ell_4+D_4EI_4m_4^3\cos m_4\ell_4 = 0 \qquad (3\text{-}25)$$

Rewriting eqs. (4.a) to (4.d) in matrix form

$$[D]\ \{\alpha_4\} = \{0\} \text{ or}$$

$$\begin{bmatrix} d_{11} & d_{12} & d_{13} & d_{14} & d_{15} & d_{16} & d_{17} & d_{18} \\ d_{21} & d_{22} & d_{23} & d_{24} & d_{25} & d_{26} & d_{27} & d_{28} \\ d_{31} & d_{32} & d_{33} & d_{34} & d_{35} & d_{36} & d_{37} & d_{38} \\ d_{41} & d_{42} & d_{43} & d_{44} & d_{45} & d_{46} & d_{47} & d_{38} \end{bmatrix} \begin{Bmatrix} A_3 \\ B_3 \\ C_3 \\ D_3 \\ A_4 \\ B_4 \\ C_4 \\ D_4 \end{Bmatrix} = \begin{Bmatrix} 0 \\ 0 \\ 0 \\ 0 \end{Bmatrix} \qquad (3\text{-}26)$$

where $d_{11} = \cosh m_3\ell_4$

$d_{12} = \sinh m_3\ell_4$

$d_{13} = \cos m_3\ell_4$

$d_{14} = \sin m_3\ell_4$

$d_{15} = -\cosh m_4\ell_4$

$d_{16} = -\sinh m_4\ell_4$

$d_{17} = -\cos m_4\ell_4$

$d_{18} = -\sin m_4\ell_4$

$d_{21} = m_3\sinh m_3\ell_4$

$$d_{22} = m_3 \cosh m_3 \ell_4$$

$$d_{23} = -m_3 \sin m_3 \ell_4$$

$$d_{24} = m_3 \cos m_3 \ell_4$$

$$d_{25} = -m_4 \sinh m_4 \ell_4$$

$$d_{26} = -m_4 \cosh m_4 \ell_4$$

$$d_{27} = m_4 \sin m_4 \ell_4$$

$$d_{28} = -m_4 \cos m_4 \ell_4$$

$$d_{31} = -EI_3 m_3^2 \cosh m_3 \ell_4 - \omega^2 I' m_3 \sinh m_3 \ell_4$$

$$d_{32} = -EI_3 m_3^2 \sinh m_3 \ell_4 - \omega^2 I' m_3 \cosh m_3 \ell_4$$

$$d_{33} = EI_3 m_3^2 \cos m_3 \ell_4 + \omega^2 I' m_3 \sin m_3 \ell_4$$

$$d_{34} = EI_3 m_3^2 \sin m_3 \ell_4 - \omega^2 I' m_3 \cos m_3 \ell_4$$

$$d_{35} = EI_4 m_4^2 \cosh m_4 \ell_4$$

$$d_{36} = EI_4 m_4^2 \sinh m_4 \ell_4$$

$$d_{37} = -EI_4 m_4^2 \cos m_4 \ell_4$$

$$d_{38} = -EI_4 m_4^2 \sin m_4 \ell_4$$

$$d_{41} = EI_3 m_3^3 \sinh m_3 \ell_4$$

$$d_{42} = EI_3 m_3^3 \cosh m_3 \ell_4$$

$$d_{43} = EI_3 m_3^3 \cosh m_3 \ell_4$$

$$d_{44} = - EI_3 m_3^3 \sin m_3 \ell_4$$

$$d_{45} = - EI_4 m_4^3 \sinh m_4 \ell_4$$

$$d_{46} = - EI_4 m_4^3 \cosh m_4 \ell_4$$

$$d_{47} = - EI_4 m_4^3 \sin m_4 \ell_4$$

$$d_{48} = EI_4 m_4^3 \cos m_4 \ell_4$$

III.3.3.5 Boundary Conditions at $x = \ell_5$

The boundary conditions at $x = \ell_5$ are similar to those at $x = \ell_3$, except that a step change in diameter represents an abrupt decrease in diameter here rather than an increase. Therefore, the equations will be identical to those at $x = \ell_3$ if all the subscripts are changed accordingly, that is, subscripts 2 and 3 in eqs. (3-17) to (3-20) should be changed here to 4 and 5 respectively.

$$\begin{cases} y_4 = y_5 \\ \theta_4 = \theta_5 \\ M_4 = M_5 \\ V_4 = V_5 \quad \text{at } x = \ell_5. \end{cases}$$

Therefore, the equations will be similar to eq. (3-21) as below:

$$[E]\ \{\alpha_5\} = \{0\} \text{ or}$$

$$\begin{bmatrix} e_{11} & e_{12} & e_{13} & e_{14} & e_{15} & e_{16} & e_{17} & e_{18} \\ e_{21} & e_{22} & e_{23} & e_{24} & e_{25} & e_{26} & e_{27} & e_{28} \\ e_{31} & e_{32} & e_{33} & e_{34} & e_{35} & e_{36} & e_{37} & e_{38} \\ e_{41} & e_{42} & e_{43} & e_{44} & e_{45} & e_{46} & e_{47} & e_{48} \end{bmatrix} \begin{Bmatrix} A_4 \\ B_4 \\ C_4 \\ D_4 \\ A_5 \\ B_5 \\ C_5 \\ D_5 \end{Bmatrix} = \begin{Bmatrix} 0 \\ 0 \\ 0 \\ 0 \end{Bmatrix} \qquad (3\text{-}27)$$

where $e_{11} = \cosh m_4 \ell_5$

$e_{12} = \sinh m_4 \ell_5$

$e_{13} = \cos m_4 \ell_5$

$e_{14} = \sin m_4 \ell_5$

$$e_{15} = -\cosh m_5 \ell_5$$

$$e_{16} = -\sinh m_5 \ell_5$$

$$e_{17} = -\cosh m_5 \ell_5$$

$$e_{18} = -\sin m_5 \ell_5$$

$$e_{21} = m_4 \sinh m_4 \ell_5$$

$$e_{22} = m_4 \cosh m_4 \ell_5$$

$$e_{23} = -m_4 \sin m_4 \ell_5$$

$$e_{24} = m_4 \cos m_4 \ell_5$$

$$e_{25} = -m_5 \sinh m_5 \ell_5$$

$$e_{26} = -m_5 \cosh m_5 \ell_5$$

$$e_{27} = m_5 \sin m_5 \ell_5$$

$$e_{28} = -m_5 \cos m_5 \ell_5$$

$$e_{31} = EI_4 m_4^2 \cosh m_4 \ell_5$$

$$e_{32} = EI_4 m_4^2 \sinh m_4 \ell_5$$

$$e_{33} = -EI_4 m_4^2 \cos m_4 \ell_5$$

$$e_{34} = -EI_4 m_4^2 \sin m_4 \ell_5$$

$$e_{35} = -EI_5 m_5^2 \cosh m_5 \ell_5$$

$$e_{36} = -EI_5 m_5^2 \sinh m_5 \ell_5$$

$$e_{37} = EI_5 m_5^2 \cos m_5 \ell_5$$

$$e_{38} = EI_5 m_5^2 \sin m_5 \ell_5$$

$$e_{41} = EI_4 m_4^3 \sinh m_4 \ell_5$$

$$e_{42} = EI_4 m_5^3 \cosh m_4 \ell_5$$

$$e_{43} = EI_4 m_4^3 \sin m_4 \ell_5$$

$$e_{44} = -EI_4 m_4^3 \cos m_4 \ell_5$$

$$e_{45} = -EI_5 m_5^3 \sinh m_5 \ell_5$$

$$e_{46} = -EI_5 m_5^3 \cosh m_5 \ell_5$$

$$e_{47} = -EI_5 m_5^3 \sin m_5 \ell_5$$

$$e_{48} = EI_5 m_5^3 \cos m_5 \ell_5$$

III.3.3.6 Boundary Conditions at $x = \ell_6$

Conditions at $x = \ell_6$ are identical to those at $x = \ell_2$, (namely a "rigid support" point), except for subscripts. Therefore, we have

$$\left.\begin{aligned} y_5 &= 0 \\ y_6 &= 0 \\ \theta_5 &= \theta_6 \\ M_5 &= M_6 \end{aligned}\right\} \quad \text{at } x = \ell_6$$

This in matrix form will be:

$$[F]\ \{\alpha_6\} = \{0\} \text{ or}$$

$$\begin{bmatrix} f_{11} & f_{12} & f_{13} & f_{14} & 0 & 0 & 0 & 0 \\ 0 & 0 & 0 & 0 & f_{25} & f_{26} & f_{27} & f_{28} \\ f_{31} & f_{32} & f_{33} & f_{34} & f_{35} & f_{36} & f_{37} & f_{38} \\ f_{41} & f_{42} & f_{43} & f_{44} & f_{45} & f_{46} & f_{47} & f_{48} \end{bmatrix} \begin{Bmatrix} A_5 \\ B_5 \\ C_5 \\ D_5 \\ A_6 \\ B_6 \\ C_6 \\ D_6 \end{Bmatrix} = \begin{Bmatrix} 0 \\ 0 \\ 0 \\ 0 \end{Bmatrix} \qquad (3\text{-}28)$$

where

$$f_{11} = \cosh m_5\ell_6$$

$$f_{12} = \sinh m_5\ell_6$$

$$f_{13} = \cos m_5\ell_6$$

$$f_{14} = \sin m_5\ell_6$$

$$f_{25} = \cosh m_6\ell_6$$

$$f_{26} = \sinh m_6\ell_6$$

$$f_{27} = \cos m_6\ell_6$$

$$f_{28} = \sin m_6\ell_6$$

$$f_{31} = m_5 \sinh m_5 \ell_6$$

$$f_{32} = m_5 \cosh m_5 \ell_6$$

$$f_{33} = -m_5 \sin m_5 \ell_6$$

$$f_{34} = m_5 \cos m_5 \ell_6$$

$$f_{35} = -m_6 \sinh m_6 \ell_6$$

$$f_{36} = -m_6 \cosh m_6 \ell_6$$

$$f_{37} = m_6 \sin m_6 \ell_6$$

$$f_{38} = -m_6 \cos m_6 \ell_6$$

$$f_{41} = EI_5 m_5^2 \cosh m_5 \ell_6$$

$$f_{42} = EI_5 m_5^2 \sinh m_5 \ell_6$$

$$f_{43} = -EI_5 m_5^2 \cos m_5 \ell_6$$

$$f_{44} = -EI_5 m_5^2 \sin m_5 \ell_6$$

$$f_{45} = -EI_6 m_6^2 \cosh m_6 \ell_6$$

$$f_{46} = -EI_6 m_6^2 \sinh m_6 \ell_6$$

$$f_{47} = EI_6 m_6^2 \cos m_6 \ell_6$$

$$f_{48} = EI_6 m_6^2 \sin m_6 \ell_6$$

III.3.3.7 Boundary Conditions at $x = \ell_7$

The shaft has a "free end" condition at $x = \ell_7$. Therefore, the boundary conditions are similar to those at $x = \ell_1$, namely:

$$\left.\begin{aligned} M_6 &= 0 \\ V_6 &= 0 \end{aligned}\right\} \text{ at } x = \ell_7$$

These can be written in matrix form as below:

$$[G]\ \{\alpha_7\} = \{0\} \text{ or}$$

$$\begin{bmatrix} g_{11} & g_{12} & g_{13} & g_{14} \\ g_{21} & g_{22} & g_{23} & g_{24} \end{bmatrix} \begin{Bmatrix} A_6 \\ B_6 \\ C_6 \\ D_6 \end{Bmatrix} = \begin{Bmatrix} 0 \\ 0 \end{Bmatrix} \tag{3-29}$$

where
$$g_{11} = \cosh m_6\ell_7$$
$$g_{12} = \sinh m_6\ell_7$$
$$g_{13} = -\cos m_6\ell_7$$
$$g_{14} = -\sin m_6\ell_7$$
$$g_{21} = \sinh m_6\ell_7$$
$$g_{22} = \cosh m_6\ell_7$$
$$g_{23} = \sin m_6\ell_7$$
$$g_{24} = -\cos m_6\ell_7$$

III.3.3.8 Governing Equations for Critical Speeds

Combining eqs. (3-10), (3-16), (3-21), (3-26),(3.27), (3-28) and (3-29), these can be written in matrix form:

$[K]\ \{A\} = \{0\}$ or

$$
\begin{bmatrix}
a_{11}a_{12}a_{13}a_{14} & & & & & & & & & & & & & & & & & & & & & & & \\
a_{21}a_{22}a_{23}a_{24} & & & & & & & & & & & & & & & & & & & & & & & \\
b_{11}b_{12}b_{13}b_{14} & 0 & 0 & 0 & 0 & & & & & & & & & & & & & & & & & & & \\
0 & 0 & 0 & 0 & b_{25}b_{26}b_{27}b_{28} & & & & & & & & & & & & & & & & & & & \\
b_{31}b_{32}b_{33}b_{34} & b_{35}b_{36}b_{37}b_{38} & & & & & & & & & & & & & & & & & & & & & & \\
b_{41}b_{42}b_{43}b_{44} & b_{45}b_{46}b_{47}b_{48} & & & & & & & & & & & & & & & & & & & & & & \\
 & & c_{11}c_{12}c_{13}c_{14} & c_{15}c_{16}c_{17}c_{18} & & & & & & & & & & & & & & & & & & & & \\
 & & c_{21}c_{22}c_{23}c_{24} & c_{25}c_{26}c_{27}c_{28} & & & & & & & & & & & & & & & & & & & & \\
 & & c_{31}c_{32}c_{33}c_{34} & c_{35}c_{36}c_{37}c_{38} & & & & & & & & & & & & & & & & & & & & \\
 & & c_{41}c_{42}c_{43}c_{44} & c_{45}c_{46}c_{47}c_{48} & & & & & & & & & & & & & & & & & & & & \\
 & & & & d_{11}d_{12}d_{13}d_{14} & d_{15}d_{16}d_{17}d_{18} & & & & & & & & & & & & & & & & & & \\
 & & & & d_{21}d_{22}d_{23}d_{24} & d_{25}d_{26}d_{27}d_{28} & & & & & & & & & & & & & & & & & & \\
 & & & & d_{31}d_{32}d_{33}d_{34} & d_{35}d_{36}d_{37}d_{38} & & & & & & & & & & & & & & & & & & \\
 & & & & d_{41}d_{42}d_{43}d_{44} & d_{45}d_{46}d_{47}d_{48} & & & & & & & & & & & & & & & & & & \\
 & & & & & & e_{11}e_{12}e_{13}e_{14} & e_{15}e_{16}e_{17}e_{18} & & & & & & & & & & & & & & & & \\
 & & & & & & e_{21}e_{22}e_{23}e_{24} & e_{25}e_{26}e_{27}e_{28} & & & & & & & & & & & & & & & & \\
 & & & & & & e_{31}e_{32}e_{33}e_{34} & e_{35}e_{36}e_{37}e_{38} & & & & & & & & & & & & & & & & \\
 & & & & & & e_{41}e_{42}e_{43}e_{44} & e_{45}e_{46}e_{47}e_{48} & & & & & & & & & & & & & & & & \\
 & & & & & & & & f_{11}f_{12}f_{13}f_{14} & 0 & 0 & 0 & 0 & & & & & & & & & & & & \\
 & & & & & & & & 0 & 0 & 0 & 0 & f_{25}f_{26}f_{27}f_{28} & & & & & & & & & & & & \\
 & & & & & & & & f_{31}f_{32}f_{33}f_{34} & f_{35}f_{36}f_{37}f_{38} & & & & & & & & & & & & & & \\
 & & & & & & & & f_{41}f_{42}f_{43}f_{44} & f_{45}f_{46}f_{47}f_{48} & & & & & & & & & & & & & & \\
 & & & & & & & & & & g_{11}g_{12}g_{13}g_{14} & & & & & & & & & & & & & \\
 & & & & & & & & & & g_{21}g_{22}g_{23}g_{24} & & & & & & & & & & & & &
\end{bmatrix}
\begin{Bmatrix}
A_1 \\ B_1 \\ C_1 \\ D_1 \\ A_2 \\ B_2 \\ C_2 \\ D_2 \\ A_3 \\ B_3 \\ C_3 \\ D_3 \\ A_4 \\ B_4 \\ C_4 \\ D_4 \\ A_5 \\ B_5 \\ C_5 \\ D_5 \\ A_6 \\ B_6 \\ C_6 \\ D_6
\end{Bmatrix} = 0
$$

where all the elements are defined in the previous sections III.3.3.1 to III.3.3.7. Since this is a set of homogeneous equations, the determinant of the square matrix [K] should vanish for non-trivial soloutions of the constants $A_1, B_1, \ldots C_6$, and D_6.

$$\therefore \left|K\right| = 0 \text{ or}$$

$$\begin{vmatrix}
a_{11}a_{12}a_{13}\ 14 & & & & & & & & & \\
a_{21}a_{22}a_{23}a_{24} & & & & & & & & & \\
b_{11}b_{12}b_{13}b_{14} & 0\ 0\ 0\ 0 & & & & & & & & \\
0\ 0\ 0\ 0 & b_{25}b_{26}b_{27}b_{28} & & & & & & - 0 - & & \\
b_{31}b_{32}b_{33}b_{34} & b_{35}b_{36}b_{37}b_{38} & & & & & & & & \\
b_{41}b_{42}b_{43}b_{44} & b_{45}b_{46}b_{47}b_{48} & & & & & & & & \\
 & c_{11}c_{12}c_{13}c_{14}c_{15}c_{16}c_{17}c_{18} & & & & & & & & \\
 & c_{21}c_{22}c_{23}c_{24}c_{25}c_{26}c_{27}c_{28} & & & & & & & & \\
 & c_{31}c_{32}c_{33}c_{34}c_{35}c_{36}c_{37}c_{38} & & & & & & & & \\
 & c_{41}c_{42}c_{43}c_{44}c_{45}c_{46}c_{47}c_{48} & & & & & & & & \\
 & & d_{11}d_{12}d_{13}d_{14}d_{15}d_{16}d_{17}d_{18} & & & & & & & \\
 & & d_{21}d_{22}d_{23}d_{24}d_{25}d_{26}d_{27}d_{28} & & & & & & & = 0 \quad (3\text{-}30) \\
 & & d_{31}d_{32}d_{33}d_{34}d_{35}d_{36}d_{37}d_{38} & & & & & & & \\
 & & d_{41}d_{42}d_{43}d_{44}d_{45}d_{46}d_{47}d_{48} & & & & & & & \\
 & & & e_{11}e_{12}e_{13}e_{14}e_{15}e_{16}e_{17}e_{18} & & & & & & \\
 & & & e_{21}e_{22}e_{23}e_{24}e_{25}e_{26}e_{27}e_{28} & & & & & & \\
 & & & e_{31}e_{32}e_{33}e_{34}e_{35}e_{36}e_{37}e_{38} & & & & & & \\
 & - 0 - & & e_{41}e_{42}e_{43}e_{44}e_{45}e_{46}e_{47}e_{48} & & & & & & \\
 & & & & f_{11}f_{12}f_{13}f_{14} & 0\ 0\ 0\ 0 & & & & \\
 & & & & 0\ 0\ 0\ 0 & f_{25}f_{26}f_{27}f_{28} & & & & \\
 & & & & f_{31}f_{32}f_{33}f_{34} & f_{35}f_{36}f_{37}f_{38} & & & & \\
 & & & & f_{41}f_{42}f_{43}f_{44} & f_{45}f_{46}f_{47}f_{48} & & & & \\
 & & & & & & g_{11}g_{12}g_{13}g_{14} & & & \\
 & & & & & & g_{21}g_{22}g_{23}g_{24} & & &
\end{vmatrix}$$

At this point, it is worthwhile examining eq. (3-30) closely because there are many items which deserve further discussion and physical appreciation:

1) Equation (3-30) is the governing equation of the system for the critical speeds. Though it looks bulky and complicated, it is analytically complete in the sense that there is no approximations such as mass-lumping or numerical approximations, etc.

2) The particular speeds, ωs, which satisfy Eq. (3-30) are the critical speeds of the system.

3) The ωs appear in two kinds of terms in Eq. (3-30), namely

   i) in the terms, m_is

   ($m_i = [\frac{w_i}{gEI_i}\omega^2]^{\frac{1}{4}}$ where w_i = weight of shaft per unit length);

   ii) explicitly in the gyroscopic term, $\omega^2 I'\theta_i$ at the station of the disc.

4) The m_is appear in Eq. (3-30) in hyperbolic and trigonometric functions such as sinh $m_i\ell_i$, cosh $m_i\ell_i$, cos $m_i\ell_i$, sin $m_i\ell_i$, etc.

5) Therefore, the main variable, ω, appears in Eq. (3-30) in highly non-linear fashion. As a result, Eq. (3-30) cannot be solved for ω explicitly. However, it can be solved numerically.

6) The matrix [K] is a "banded" matrix with majority of its elements being zeros. This suggests that there is a potential for economized numerical algorithms for actual calculations of critical speeds.

7) The matrix [K] can be seen as a "partitioned" matrix as shown in Fig. 3-4.

Now it can easily be seen that each rectangular partitioned matrix corresponds to a "boundary point" of the shaft. That is, the matrix [A] is from the "free end" boundary conditions, [B] from "rigid support", [C] from the "step change" conditions, etc. (Fig. 3-4 and 3-5).

This leads to an automatic structured construction of the matrix [K] in computer programming. The computer programs listed in Appendices A and B include the features of automatic generation of the overall matrix [K].

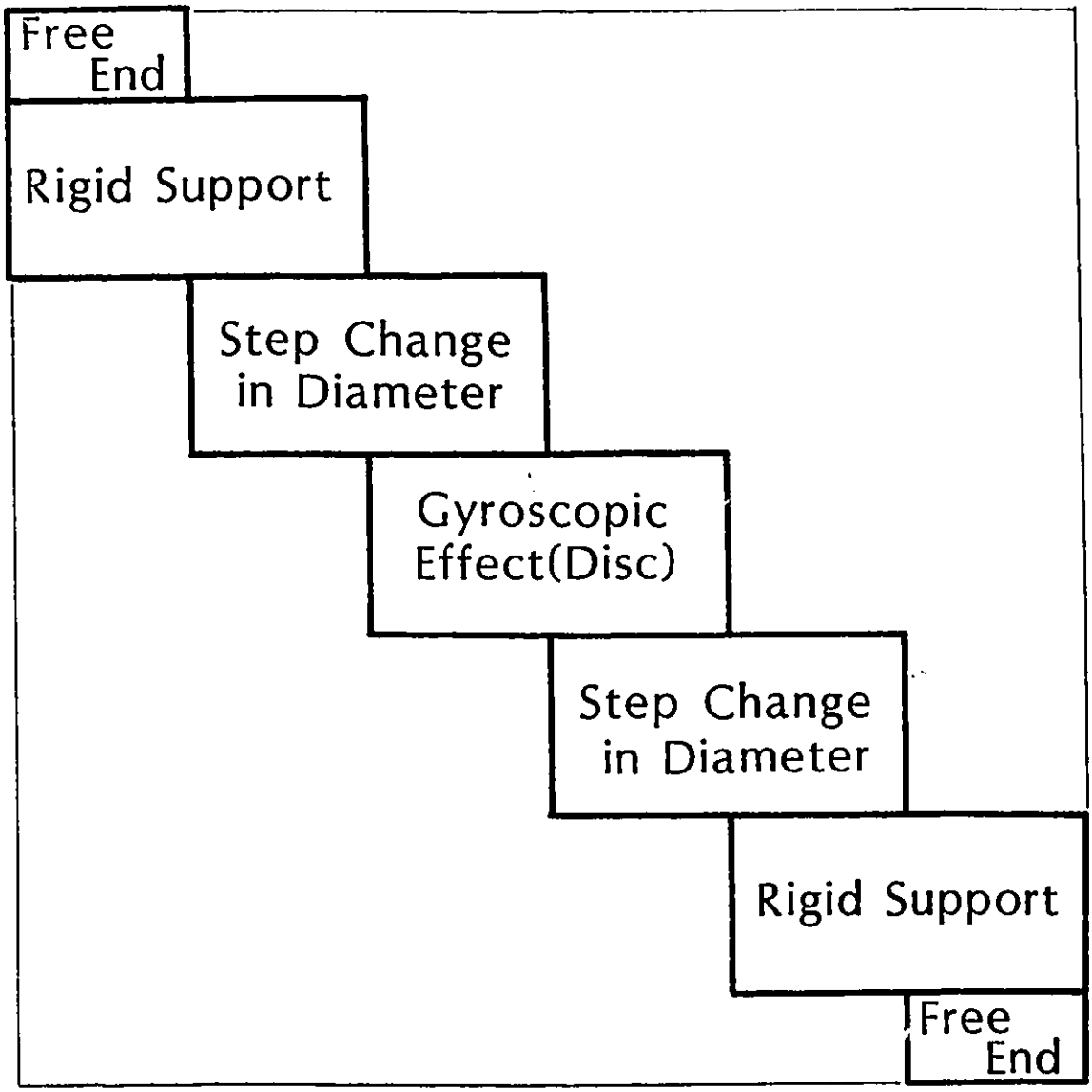

Fig. 3-5 Physical Meaning of Partitions in the Overall Matrix (Single Disc System)

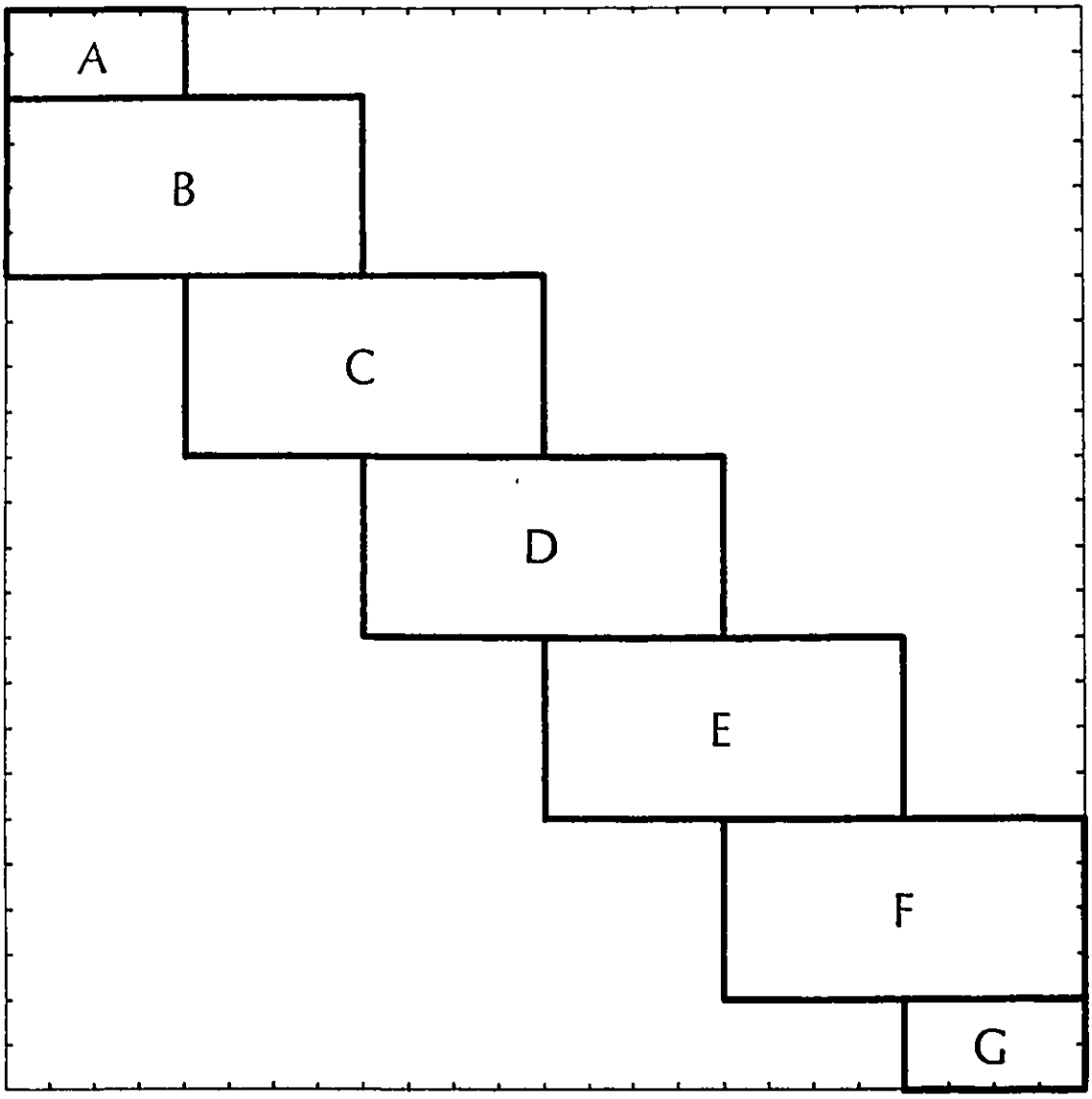

Fig. 3-4 General Layout of Overall Matrix with Partitions (Single Disc System)

III.3.3.9 Generalized Procedure

As illustrated in the previous sections, all the individual equations composing the final set of governing equation (3-30) were generated from "boundary conditions". When there are "n" boundaries in a rotor-bearing system the final set of matrix equation will contain 4(n-1) individual equations in itself. For example, there are seven boundaries in the system shown in Fig. 3-2. As a result, there are 24 individual equations included in the final governing equations (3-30).

Although there seems to be many individual equations involved, there are at most twelve (12) types of basic equations which can generate all kinds of shaft systems. That is, any meaningful boundary conditions can be generated out of these 12 "basic" equations. As will be discussed in detail later in this section, although there are 12 possible basic equations, only four of them are essential. Therefore, only if those four essential equations are stored in the computer program, all the required boundary conditions can be generated.

Another remarkable fact is that there are not very many boundary conditions occurring in the critical speed calculation. As shown in table 3-1, page 107, there seems to be only six end conditions and nine "mid-section" conditions being physically meaningful at present. Among them, less than eight conditions seem to be essential in practice. Therefore, all the boundary conditions as well as all the basic equations can be stored in the computer program.

Once they are formulated and stored in a computer program, any rotor-bearing system can be analysed for its undamped synchronous critical speeds by simply specifing the type of boundary (and the physical data) for the given rotor. This is exactly what has been done in the analyses of the two-disc rotor and Prohl's rotor, which will be discussed later in this thesis. This particular feature of the "simplicity" in use is one of the essential contribution of this thesis.

As mentioned previously there are only a finite number of "basic" equations which are physically meaningful in the critical speed calculation of rotor-bearing systems. For example, in the sections III.3.3.1 to III.3.3.7, the moment M entered in the analysis in only three types, namely

i) $M_i = 0$ in sections III.3.3.1 and III.3.3.7,

ii) $M_i = M_{i+1}$ in sections III.3.3.2, III.3.3.3, III.3.3.5, and III.3.3.6,

iii) $M_{i+1} - M_i = SF$ in section III.3.3.4,

where subscripts i and (i+1) stand for segment numbers, and SF stands for "Some Finite value". Strictly speaking, the third item above is the most general form which includes the first and second as special cases. That is, the second form above is a special case of the third item when SF = 0. Similarily, the first form above is another special case when both M_{i+1} and SF vanish. This means when the memory capacity of the computer is a critical factor, only one basic equation for the moment M needs to be stored in the computer.

Similar situations can be observed regarding the shear force V, the slope θ, and the deflection y. Therefore, at most 12 basic equations need to be stored in the computer. In case the memory capacity of the computer is a critical factor such as in micro-computers, only four basic equations need to be stored, namely

$$y_{i+1} - y_i = SF$$
$$\theta_{i+1} - \theta_i = SF$$
$$M_{i+1} - M_i = SF$$
$$V_{i+1} - V_i = SF$$

Then, these four basic equations can generate any type of boundary conditions. Table 3-1 lists a total of 15 boundary conditions which can occur in rotor dynamic analyses. It should be noted that the elemental equations listed in Table 3-1 are treated as "specific" or "detailed" in the sense that the case of $M_i = M_{i+1}$ is treated as independent of the case of $M_{i+1} - M_i = SF$. It is also worth noting that the "specific" basic equation, $y_{i+1} - y_i = SF$ is never invoked by any boundary conditions listed in Table 3-1 on account of requirements of compatibility.

Once the basic equations and the boundary conditions are stored in the form of a subroutine program, the general procedure consists of two steps, namely

i) calling in the main program, in the order of its occurrence, the relevant subroutine programs corresponding to the boundary conditions in the rotor-bearing systems, and

ii) placing them in the right locations in the overall matrix [K].

Table 3-1 Boundary Conditions Normally Encountered

Boundary Conditions \ Elemental Equations	y			θ			M			V		
	$y_i = 0$	$y_i = y_{i+1}$	$y_{i+1} - y_i = SF$	$\theta_i = 0$	$\theta_i = \theta_{i+1}$	$\theta_{i+1} - \theta_i = SF$	$M_i = 0$	$M_i = M_{i+1}$	$M_{i+1} - M_i = SF$	$V_i = 0$	$V_i = V_{i+1}$	$V_{i+1} - V_i = SF$
i) End Conditions:												
Free End							X			X		
Overhung Disc									X			X
Bearing:												
Rigid-Short	X						X					
Rigid-Long	X			X								
Compliant-Short							X					X
Compliant-Long				X								X
ii) Mid-Section Conditions:												
Step Change (Diameter)		X			X			X			X	
Disc:												
Shrunk-fit		X			X				X		X	
Non-Shrunk-fit		X			X				X			X
Bearing:												
Rigid-Short	X	X			X			X				
Rigid-Long	X	X		X	X							
Compliant-Short		X			X			X				X
Compliant-Long		X		X	X							X
Coupling:												
Flexible (Diaphragm)		X				X		X			X	
Gear		X					X	X			X	

The second item above is carried out by locating the first element of the partitioned sub-matrix at the right place in the overall matrix. This can be included at the beginning of each boundary condition subroutine so that the "locating" can be adjusted automatically as is the case with the computer programs listed in Appendices A and B.

III.3.3.10 The Mode Shape

In this section, two of the simplest cases of rotor-bearing systems are analysed to illustrate the fact that the mode shapes found in the present method are continuous curves.

The first case is that of a uniform shaft rotating on two rigid short bearings. This is the simplest case where analytical solutions are available for the critical speeds and the mode shapes. The second case is a rotor-bearing system with a single disc on its mid-point of the span.

1) The Uniform Cross-Sectional Shaft Without Disc

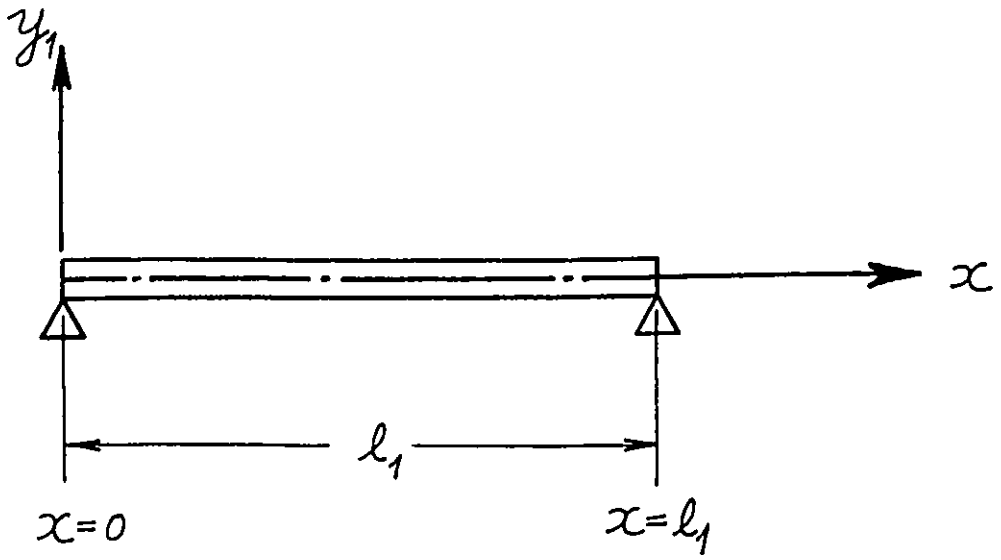

Fig. 3-6

A rotor-bearing system with a single segment is shown in Fig. 3-6. When rigid short bearings are assumed at the supports, the boundary conditions are:

$$\text{i) at } x = 0, \quad \begin{cases} y_1 = 0 \\ M_1 = 0 \end{cases}$$

$$\text{ii) at } x = \ell_1 \quad \begin{cases} y_1 = 0 \\ M_1 = 0 \end{cases}$$

This generates the governing equations as below:

$$\begin{bmatrix} 1 & 0 & 1 & 0 \\ 1 & 0 & -1 & 0 \\ \cosh m\ell_1 & \sinh m\ell_1 & \cos m\ell_1 & \sin m\ell_1 \\ \cosh m\ell_1 & \sinh m\ell_1 & -\cos m\ell_1 & -\sin m\ell_1 \end{bmatrix} \begin{Bmatrix} A_1 \\ B_1 \\ C_1 \\ D_1 \end{Bmatrix} = \begin{Bmatrix} 0 \\ 0 \\ 0 \\ 0 \end{Bmatrix}$$

The overall matrix is of the form:

$$\begin{bmatrix} a_{11} & a_{12} & a_{13} & a_{14} \\ a_{21} & a_{22} & a_{23} & a_{24} \\ b_{11} & b_{12} & b_{13} & b_{14} \\ b_{21} & b_{22} & b_{23} & b_{24} \end{bmatrix}$$

or

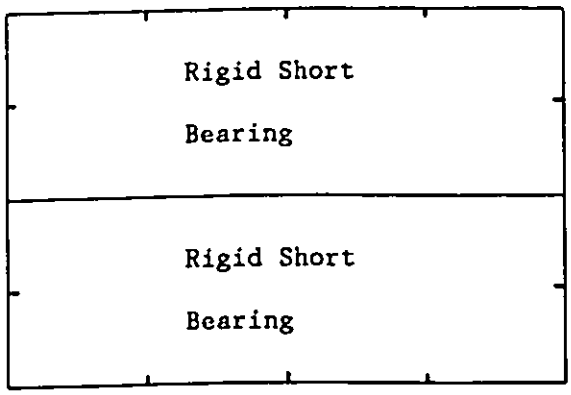

Carrying out the triangulation illustrated in Appendix C, we have

$$\begin{bmatrix} 1 & 1 & 0 & 0 \\ 0 & -2 & 0 & 0 \\ 0 & 0 & \sinh m\ell_1 & \sin m\ell_1 \\ 0 & 0 & 0 & -2\sin m\ell_1 \end{bmatrix} \begin{Bmatrix} A_1 \\ C_1 \\ B_1 \\ D_1 \end{Bmatrix} = \begin{Bmatrix} 0 \\ 0 \\ 0 \\ 0 \end{Bmatrix}$$

For non-trivial solution, the value of the determinant of the overall matrix should vanish, namely,

$$(1)\cdot(-2)\cdot(\sinh m\ell_1)\cdot(-2\sin m\ell_1) = 0$$

$$\therefore m\ell_1 = n\cdot\pi \ , \quad n = 1,2,3,\cdots$$

where n is the critical speed number.

In order to find the mode shape of, say, the first critical speed, the "back substitution" process is carried out with the value of D_1 fixed as the unit value (=1). As a result, we have,

$$A_1 = B_1 = C_1 = 0$$

$$D_1 = 1$$

Therefore, the mode shape is:

$$y_1 = \sin m\ell_1, \quad (0 \le x \le \ell_1)$$

2) The Uniform Cross-Sectional Shaft with Disc

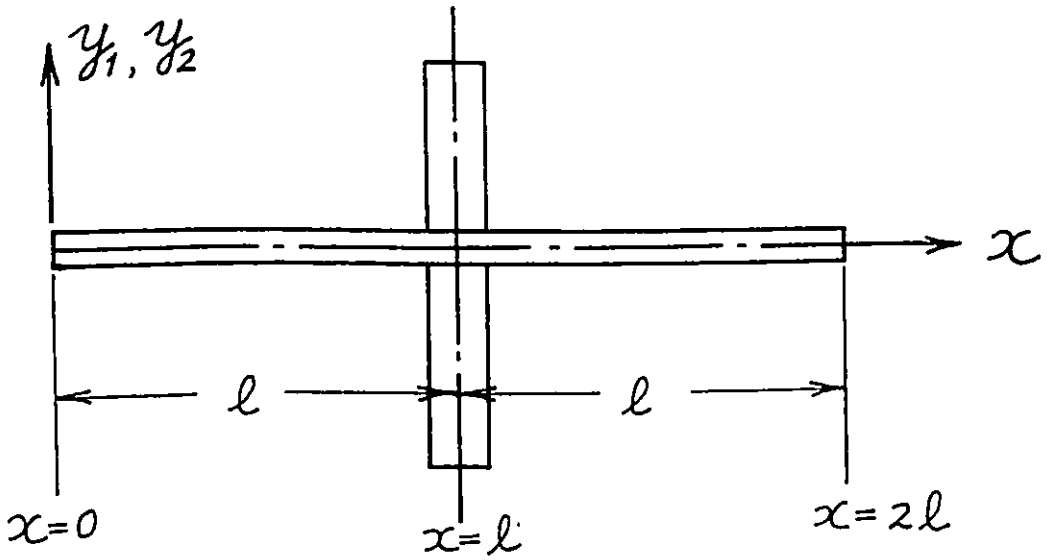

Fig. 3-7

The rotor-bearing system shown in Fig. 3-7 is assumed to have

i) a uniform cross-section over the entire length of the shaft,

ii) the disc which is non-shrunk fit at the mid-span, and

iii) rigid short bearings.

Therefore, the boundary conditions are:

i) at $x = 0$, $\begin{cases} y_1 = 0 \\ M_1 = 0 \end{cases}$

ii) at $x = \ell$ $\begin{cases} y_1 = y_2 \\ \theta_1 = \theta_2 \\ M_2 - M_1 = \omega^2 I' \theta_1 \\ V_2 - V_1 = \omega^2 m_D y_1 \end{cases}$

iii) at $x = 2\ell$ $\begin{cases} y_2 = 0 \\ M_2 = 0 \end{cases}$

The shape of the overall matrix is:

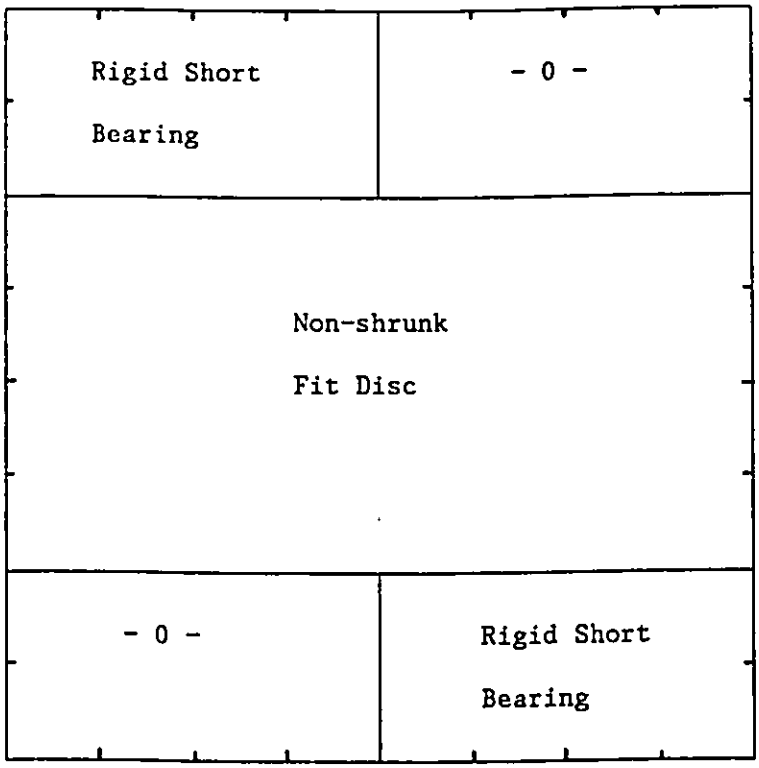

or

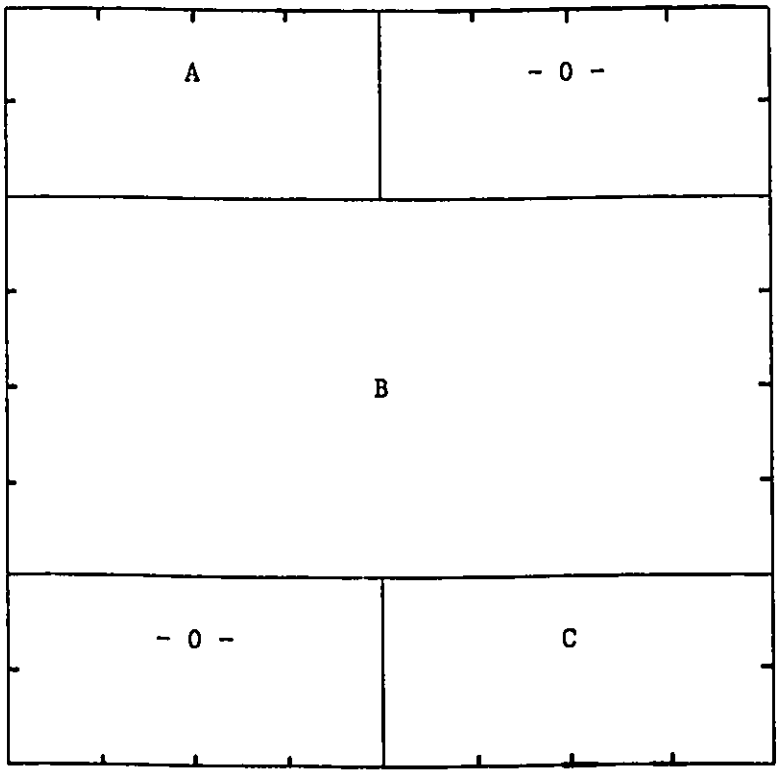

The matrix equation, $[K]\cdot\{A\} = \{0\}$, takes the form:

$$\begin{bmatrix} a_{11} & a_{12} & a_{13} & a_{14} & 0 & 0 & 0 & 0 \\ a_{21} & a_{22} & a_{23} & a_{24} & 0 & 0 & 0 & 0 \\ b_{11} & b_{12} & b_{13} & b_{14} & b_{15} & b_{16} & b_{17} & b_{18} \\ b_{21} & b_{22} & b_{23} & b_{24} & b_{25} & b_{26} & b_{27} & b_{28} \\ b_{31} & b_{32} & b_{33} & b_{34} & b_{35} & b_{36} & b_{37} & b_{38} \\ b_{41} & b_{42} & b_{43} & b_{44} & b_{45} & b_{46} & b_{47} & b_{48} \\ 0 & 0 & 0 & 0 & c_{11} & c_{12} & c_{13} & c_{14} \\ 0 & 0 & 0 & 0 & c_{21} & c_{22} & c_{23} & c_{24} \end{bmatrix} \begin{Bmatrix} A_1 \\ B_1 \\ C_1 \\ D_1 \\ A_2 \\ B_2 \\ C_2 \\ D_2 \end{Bmatrix} = \begin{Bmatrix} 0 \\ 0 \\ 0 \\ 0 \\ 0 \\ 0 \\ 0 \\ 0 \end{Bmatrix} \qquad (3\text{-}31)$$

The values of the elements can be found from the actual overall matrix given below:

1	0	1	0	0	0	0	0
1	0	-1	0	0	0	0	0
cosh mℓ	sinh mℓ	cos mℓ	sin mℓ	-cosh mℓ	-sinh mℓ	-cos mℓ	-sin mℓ
sinh mℓ	cosh mℓ	-sin mℓ	cos mℓ	-sinh mℓ	-cosh mℓ	sin mℓ	-cos mℓ
-cosh mℓ $-\beta$ sinh mℓ	-sinh $-\beta$ cosh mℓ	cos mℓ $+\beta$ sin mℓ	sin mℓ $-\beta$ cos mℓ	cosh mℓ	sinh mℓ	-cos mℓ	-sin mℓ
-sinh mℓ $-\alpha$ cosh mℓ	-cosh mℓ $-\alpha$ sinh mℓ	-sin mℓ $-\alpha$ cos mℓ	cos mℓ $-\alpha$ sin mℓ	sinh mℓ	cosh mℓ	sin mℓ	-cos mℓ
0	0	0	0	cosh 2mℓ	sinh 2mℓ	cos 2mℓ	sin 2mℓ
0	0	0	0	cosh 2mℓ	sinh 2mℓ	-cos 2mℓ	-sin 2mℓ

where $\alpha = \omega^2 m_D/(m^3 EI)$ and $\beta = \omega^2 I'/(mEI)$.

After a triangulation procedure is completed, equation (3-31) takes the form shown below:

$$\begin{bmatrix} 1 & 1 & 0 & 0 & 0 & 0 & 0 & 0 \\ & -2 & 0 & 0 & 0 & 0 & 0 & 0 \\ & & \gamma_{33} & \gamma_{34} & \gamma_{35} & \gamma_{36} & \gamma_{37} & \gamma_{38} \\ & & & \gamma_{44} & \gamma_{45} & \gamma_{46} & \gamma_{47} & 0 \\ & & & & \gamma_{55} & 0 & 0 & \gamma_{58} \\ & & -0- & & & \gamma_{66} & \gamma_{67} & 0 \\ & & & & & & \gamma_{77} & \gamma_{78} \\ & & & & & & & \gamma_{88} \end{bmatrix} \begin{Bmatrix} A_1 \\ C_1 \\ B_1 \\ D_1 \\ C_2 \\ D_2 \\ A_2 \\ B_2 \end{Bmatrix} = \begin{Bmatrix} 0 \\ 0 \\ 0 \\ 0 \\ 0 \\ 0 \\ 0 \\ 0 \end{Bmatrix} \qquad (3\text{-}32)$$

where $\gamma_{33} = \cosh m\ell$

$\gamma_{34} = \cos m\ell$

$\gamma_{35} = -\sinh m\ell$

$\gamma_{36} = -\cos m\ell$

$\gamma_{37} = \sin m\ell$

$\gamma_{38} = -\cosh m\ell$

$\gamma_{44} = -\dfrac{\cos m\ell \cdot \sinh m\ell - \sin m\ell \cdot \cosh m\ell}{\cosh m\ell}$

$\gamma_{45} = -\dfrac{1}{\cosh m\ell}$

$$\gamma_{46} = -\gamma_{44}$$

$$\gamma_{47} = -\frac{\cos m\ell \cdot \cosh m\ell + \sin m\ell \cdot \sinh m\ell}{\cos m\ell \cdot \sinh m\ell - \sin m\ell \cdot \cosh m\ell}$$

$$\gamma_{55} = \cosh 2m\ell = \cosh^2 m\ell + \sinh^2 m\ell$$

$$\gamma_{58} = \sinh 2m\ell = 2 \cosh m\ell \cdot \sinh m\ell$$

$$\gamma_{66} = \sin 2m\ell = 2 \cos m\ell \cdot \sin m\ell$$

$$\gamma_{67} = \cos 2\, m\ell = \cos^2 m\ell - \sin^2 m\ell$$

$$\gamma_{77} = \frac{-2 \sinh m\ell}{\cos m\ell \sinh m\ell - \sin m\ell \cosh m\ell} + \frac{\beta}{2 \cdot \sin m\ell}$$

$$\gamma_{78} = \frac{\cosh m\ell}{\cosh^2 m\ell + \sinh^2 m\ell}\left[-\beta + \frac{4 \sin m\ell \cdot \sinh m\ell}{\cos m\ell \cdot \sinh m\ell - \sin m\ell \cdot \cosh m\ell}\right]$$

$$\gamma_{88} = \frac{\sinh m\ell}{\cosh^2 m\ell + \sinh^2 m\ell}\left[\alpha + \frac{4 \cos m\ell \cdot \cosh m\ell}{\cos m\ell \cdot \sinh m\ell - \sin m\ell \cdot \cosh m\ell}\right]$$

$$+ \frac{\gamma_{78}}{\gamma_{77}}\left[\frac{2 \cosh m\ell}{\cos m\ell \cdot \sinh m\ell - \sin m\ell \cdot \cosh m\ell} + \frac{\alpha}{2 \cos m\ell}\right]$$

Since the determinant of the overall matrix vanishes at any critical speed, the constants, A_1, B_1, C_1,$\cdots$,D_2, cannot be determined uniquely. However, they can be available as a "one-parameter family" of solutions (Ref. 14). This leads to the mode "shape" at the particular critical speed. The procedure is given as follows.

Let $B_2 = 1$, then, by back-substitution using eq. (3-32), the constants are:

$$A_2 = \frac{-\gamma_{78}}{\gamma_{77}}$$

$$D_2 = \gamma_{67} \cdot A_2/\gamma_{66} = \frac{2\cos m\ell \cdot \sin m\ell}{\cos^2 m\ell - \sin^2 m\ell} \frac{\gamma_{78}}{\gamma_{77}}$$

$$C_2 = -\gamma_{58}/\gamma_{55} = \frac{-2\cosh\ m\ell \cdot \sinh\ m\ell}{\cosh^2\ m\ell + \sinh^2\ m\ell}$$

$$D_1 = -(\gamma_{45} \cdot C_2 + \gamma_{46} \cdot D_2 + \gamma_{36} \cdot \gamma_{47} \cdot A_2)/\gamma_{44}$$

$$B_1 = -(\gamma_{34} \cdot D_1 + \gamma_{35} \cdot C_2 + \gamma_{36} \cdot D_2 + \gamma_{37} \cdot A_2)/\gamma_{33}$$

$$C_1 = 0$$

$$A_1 = 0$$

Once the constants A_1, B_1, $C_1, \cdots$, D_2, are evaluated at the critical speed, the mode shape is available as a continuous curve as follows:

$$y_1 = A_1\cosh mx + B_1\sinh mx + C_1\cos mx + D_1\sin mx$$

$$= B_1\sinh mx + D_1\sin mx$$

where $0 \leq x \leq \ell$.

$$y_2 = A_2\cosh mx + \sinh mx + C_2\cos mx + D_2\sin mx$$

where $\ell \leq x \leq 2\ell$.

CHAPTER IV

EVALUATION OF NEW METHOD

IV.1 Introduction

In this chapter, in order to verify and evaluate the effectiveness of the new method, a rotor-bearing system with two-shrunk fit discs, shown in Fig. 4-1, will be evaluated both experimentally and analytically. And then, the results will be presented along with other analytical results obtained by using an independent computer program based on the Transfer Matrix Method.

After detailed descriptions on the experimental two-disc rotor system and the related instrumentation setup are given, the measurement results of the first critical speed of the system will be presented. For the analytical side of this evaluation, the identical system will be converted into a mathematical model. That is, the two-disc rotor system will be divided by imaginary lines into many segments with boundaries. Then the shape of overall matrix for this particular rotor-bearing system will be presented in the form of partitioned matrices. The overall matrix [K] will be solved for up to the third critical speeds and the results will be compared with those found by the Transfer Matrix Method.

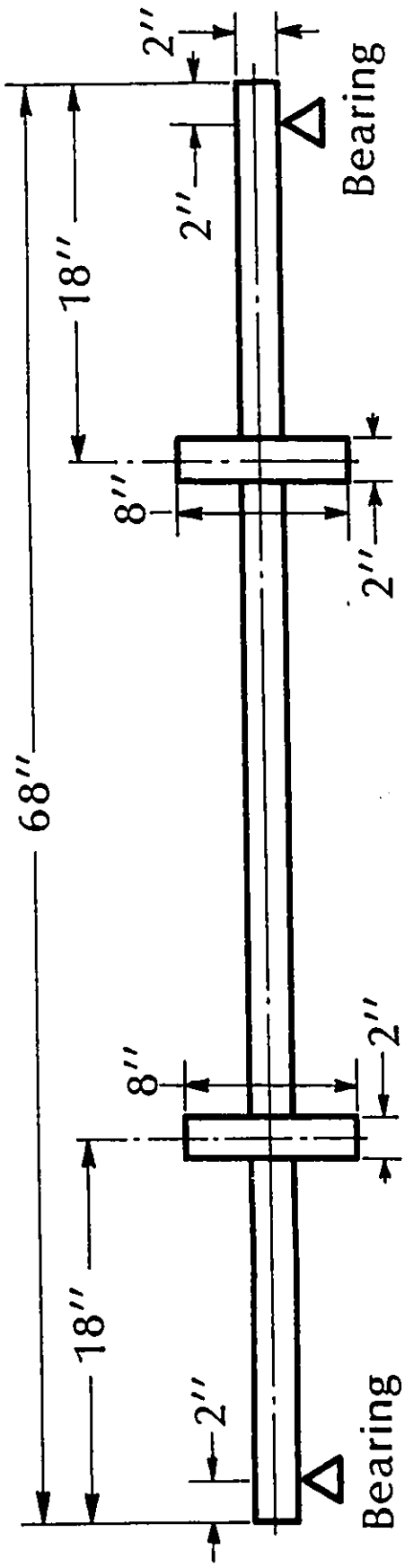

Fig. 4-1 Two-Disc Rotor-Bearing System

IV.2 Overview of Experimental Program and Runout

IV.2.1 Program Overview

A special rotor-bearing system has been designed and manufactured such that the configuration of the rotor is suitable for both experimental and analytical evaluation. The two-disc rotor-bearing system chosen for this study is a result of many generations of experimental evolutions through which virtually all the parts have been re-designed many times. The selection criteria for the experimental rotor-bearing system were:

i) The configuration of the rotor should be reasonably complicated, yet simple enough to manufacture identical rotors repeatedly, in case the rotor is damaged during experiments.

ii) The second critical speed of the rotor should be lower than 6000 RPM which is the maximum RPM of the existing drive system.

iii) The critical speeds should not be close causing possible interference amongst the principal modes.

Originally, a three-disc rotor system was selected. However, the final version of the two-disc rotor-bearing system emerged through many stages of progressive adjustments throughout the test program. Five specific problems encountered in the course of this experimental study are worth noting because they may prove enlightening for future students of Rotor Dynamics. These problems also took place over the

entire period of the experimental program representing a fair overview and highlighting the chronological progress of the overall experimental program.

The first problem was related to the disc installed on the shaft. In order to study the critical speeds of rotors, the rotor should be balanced to ultra-precision grade so that the rotor can run up and run down safely through the critical speed without being destroyed due to its resonant whirling at the critical speed. At this stage, a few milligrams of the correction weight which corresponds to approximately a quarter of one millionth of the total weight of the disc, would make noticeable difference in the whirling amplitude at a rotational speed near the critical speed. Every time the finely balanced rotor was run through the critical speed, a dramatic change in its dynamic characteristics, in terms of balancing parameters and whirling amplitude, was observed. A phenomenon of "re-settling" or "re-sitting" of the correction weights and the disc was suspected due to the violent whirling when the rotor was passing through the critical speed. Therefore, the disc was re-designed to eliminate this problem. The following changes were implemented:

i) The disc thickness was changed from 7/8 inches to 2 inches to provide more area of "sitting" and more leverage against tilting.

ii) All the discs were shrunk-fit to make sure that the "re-sitting" of the disc can be minimized.

iii) "Re-sitting" of the correction weights was prevented within reason by installing the correction weights using cap screws. Both faces of discs were drilled and tapped for the cap screws at the interval of ten degrees forming a circle of 36 holes around the circle of 7.5 inch diameter.

The second is still related to the dynamic characteristics of the rotors. Everytime the tests were stopped over a night, changes in dynamic characteristics were noticed. The most noticeable was the fact that the rotor could not run through the critical speed safely because somehow the fine grade of balancing was changed overnight. Therefore, this required a fresh balancing every time the rotor was stopped overnight. This presented some problems.

i) It takes time and effort to balance a rotor so that it can run through a critical speed safely. It takes usually two to four times of consecutive balancing operation to achieve a "smooth" running through a critical speed.

ii) Whenever a rotor is re-balanced, its characteristics change accordingly. That is, the rotor becomes a "new" or "different" rotor in a sense. Therefore, sometimes this causes a loss of continuity in a series of tests.

After much trial and error, the problem was minimized by leaving the rotor rotating at a lower speed, usually in the range 120 to 200 RPM. The sagging of the rotor was suspected as the main cause.

The third was the interference between the particular probes in use. Eddy current proximity transducers were used in pairs in this study. They were installed on right-angle brackets such that one probe observes the rotor movement in the vertical direction, and the other in horizontal direction so that its "orbit" can be observed during the tests. In order to avoid their interference the shaft diameter was changed from one inch to two inches. This, in turn, caused a series of changes in other related parts such as the discs, probe holders, bearings, bearing retainers, etc.

The fourth was the inconsistency or lack of similarity between the signals from the vertical probe and the horizontal probe. When a rotor is rotating at such a low RPM that there is no discernible dynamic phenomenon at all in the rotating system, it is reasonable to expect identical waveform signals from both vertical and horizontal probes. That is, since the probes were installed on a right-angle bracket, 90 degrees apart, observing the surface of the "quietly" rotating shaft at an imaginary cross-sectional plane, the waveform signals from the probes should be identical but 90 degrees apart in phase.

When identical waveform signals were not observed, a series of tests in search of possible causes, correctional measures, or justifications was started. Many types of supporting systems, driving systems, torque/bending isolation systems, rolling element bearings and fluid film bearings were tested until a set of self-aligning fluid film bearings started to give exactly identical waveform signals, 90 degrees phase shifted from each other. The self-aligning spherical fluid film

bearings were designed by the author and manufactured by the Manufacturing Technology Center, Division of Mechanical Engineering, National Research Council Canada. The manufacturing tolerance in diameters of the spherical parts and the bearing was four tenths of one thousand of an inch. All the rolling element bearings were purchased from outside vendors. Therefore, apart from the manufacturing tolerance of the in-house bearing, real mechanisms or parameters for the dissimilar signals remain unknown.

The fifth concerned the waveform signal itself. By the time the "right" type of signals started to appear consistently in a "repeatable" manner, one of the most fundamental questions was raised, namely the question of validity - "How do we know for sure that what we measure is what is really taking place dynamically in the rotor-bearing system?" To answer to this question, a precision dial indicator was installed at the plane of measurement of the proximity probes, to observe its readings and compare them with those from the proximity transducer signals. The rotor was rotated at as low as 30 RPM in order to make easy readings of the dial indicator and at the same time to minimise dynamic effects as much as possible. The results were astonishing. While the total indicator reading was less than one tenth of one thousandth of an inch, the proximity transducer signals presented a level of amplitude of one and one half thousandths of an inch. This led to a re-examination of the whole experimental setup and the test program to ensure the "initial runout compensation". Detailed discussions on how to compensate and an example of the compensation have been given later in section IV.4.2.

IV.2.2 Runout

The runout, or more specifically the circular runout, is defined by ANSI (American National Standards Institute) as "the surface variation at any fixed point during one complete rotation of the part about the datum axis" (Ref. 65). Although it is clearly specified as the rotation about the "datum axis", the common workshop practices are to represent the amount of runout as the T.I.R. (Total Indicator Reading) while the part is placed on V-blocks and slowly rotated on the blocks. This definition can be suitable for small parts with "coaxial features", where some variations in loction of the V-blocks and the location of the dial indicator do not make noticeable differences in the measured values. However, in the case of rotating shafts such as turborotors, the measurement values can be dramatically different according to the locations of measurement and bearings, for example a bent or bowed shaft.

Although ISO (International Standard Organization) deals in its Standards with the machinery vibration severity and rotor balancing, there is no established standard on the rotor runout regarding its definition, its means of measurements, procedures for its reduction or compensation. Since a detailed study on the runout is beyond the scope of this thesis, the runout is loosely defined as out-of-roundness of a rotor. When measured using eddy current proximity transducers, the overall runout signals can be contributed to two types of runout signals, namely mechanical runout and electrical runout (Ref. 66). The mechanical runout can be caused by bent or bowed shafts, and surface

imperfections or irregularities. Electrically induced runout can be due to the presence of residual magnetism in the rotor, metallurgical segregation of the rotor material, and the residual stress concentrations existing on the rotor surface area.

The electrical runouts illustrate the fact that the eddy current proximity transducers can generate erroneous signals even though the shaft surface is machined perfectly round and at the same time the shaft is rotated about its true axis.

Regardless of its sources, the overall runout should be compensated in order to find true dynamic motion of the rotor. This has been achieved in this experimental study by utilizing an encoder as described in detail in section IV.4.2. To the authors knowledge, this type of general, yet extremely rigorous, scheme of initial runout compensation has been neither published in the open literature nor is it available commercially in the market at present.

IV.3 Description of Experimental Arrangement

All the experimental work described in this thesis has been carried out at the Rotor Dynamics Research Facility, Engine Laboratory, Division of Mechanical Engineering, National Research Council. The facility consists of the control room and the test area. The control room accommodates the instrumentation system and the computer system which contains the A/D converters and related data acquisition system as an integral part.

The test area accommodates a rolling element bearing health monitoring test rig, a soft-bearing type balancing rig, and the rotor dynamics test rig. The experimental arrangement directly related to the work described in this thesis consists of the rotor dynamics test rig, the instrumentation system, and the comuter system. A schematic diagram for the general arrangement is shown in Fig. 4-2.

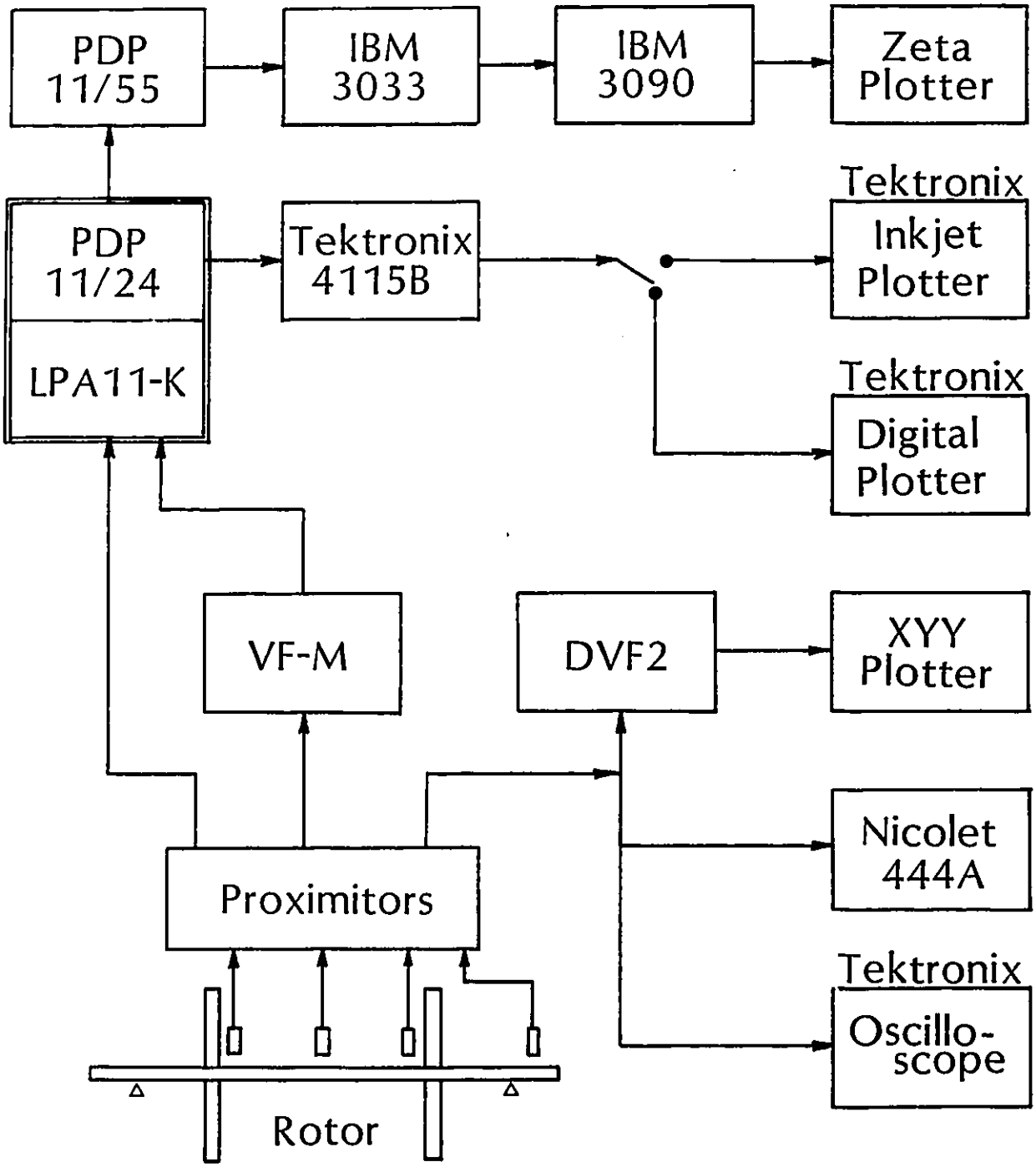

Fig. 4-2 Schematic Diagram for Experimental Arrangement

IV.3.1 Rotor Dynamics Test Rig

The rotor dynamics test rig consists of four major components, namely the rotor, the bearings, the foundation, and the drive system (Fig. 4-3).

1) The Rotor

The rotor consists of a shaft and two discs. The discs were shrunk-fit onto the shaft as shown in Fig. 4-3. The details of the shaft and the discs are as follows:

a) Shaft

diameter: $2.0000 \begin{smallmatrix} + 0.0000 \\ - 0.0003 \end{smallmatrix}$ in.

length: 68.00 ± 0.01 in.

material: Case-hardened alloy steel

hardness: Rc 60 to 65

b) Disc

diameter: 8.00 ± 0.01 in.

thickness: 2.00 ± 0.01 in.

material: mild steel

weight: 26.7 lbs.

2) The Bearings

The bearings are self-aligning spherical fluid film bearing.

material: brass

bearing I.D.: 2.0008 ± 0.0002 in.

length: 0.500 ± 0.005 in.

lubricant: SAE 5

Fig.4-3 Rotor Dynamics Test Rig

3) The Foundation

The foundation consists of a steel plate on a reinforced concrete block.

a) Steel Plate

length: 68.00 ± 0.05 in.

width: 30.00 ± 0.05 in.

thickness: 2.00 ± 0.005 in.

material: mild steel

b) Concrete Block

length: 84 in.

width: 48 in.

height: 20 in.

4) Drive System

The drive system consists of a D.C. motor and a speed controller.

a) Motor

type: D.C. stepless motor

power: 1.5 hp

max. RPM: 2400 RPM

b) Speed Controller

type: BEEL Model 10B-1

SCR Adjustable Speed Drive

IV.3.2 Instrumentation System

The instrumentation system consists of the following items:

i) eddy current proximity transducers

ii) proximitor

iii) DVF2 (Digital Vector Filter 2)

iv) VF-M (Multichannel Vector Filter)

v) HP 7046B XYY Plotter

vi) Nicolet 444A Spectrum Analyzer, and

vii) Bently Nevada/Tektronix Model 5110 Oscilloscope

(1) Eddy Current Proximity Transducer

The eddy current proximity transducer is a non-contacting displacement probe. It is composed of an epoxy-encased winding of silver wire around a fiber resin core. The probe receives a high frequency AC signal from the oscillator/demodulator, thus creating a magnetic field of flux lines around the tip of the probe. The electromagnetic waves, emitted from the probe tip, are partially dissipated as eddy currents when they reach the surface of the shaft. This dissipation is measured and converted into a voltage which is proportional to the distance between the probe and the shaft (Refs. 67 and 68). A special calibration rig for the probes was designed and manufactured at the NRC. A typical calibration curve for the Bently Nevada 7200 series probes using the rig and the particular shaft material is shown in Fig. 4-4.

(2) The Proximitor

The proximitor is also called the oscillator/demodulator. It has essentially two functions to perform: first, to generate the high

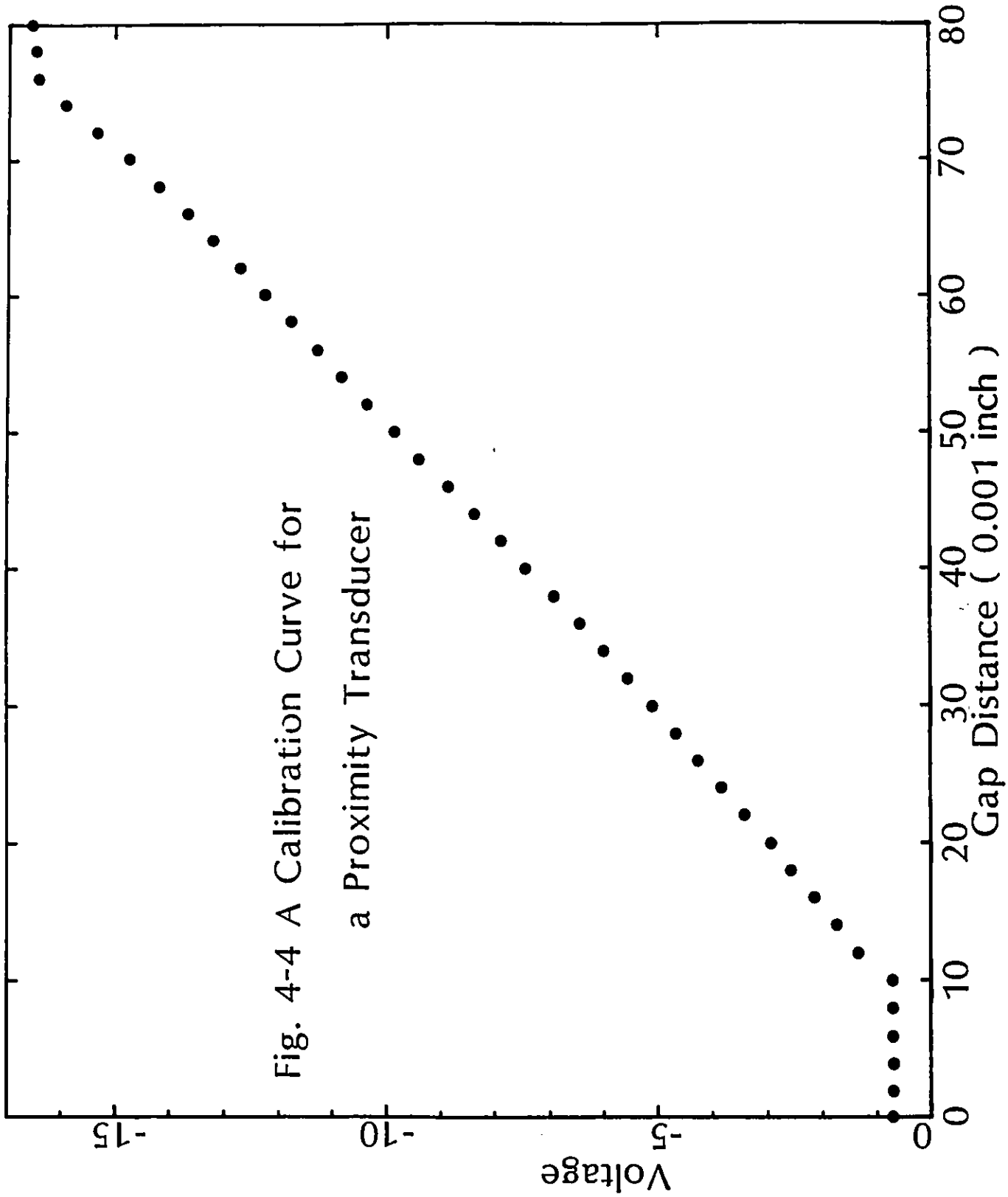

Fig. 4-4 A Calibration Curve for a Proximity Transducer

frequency AC signal being sent to the probe; and second, to demodulate the returning signal in such a way that it creates a direct relationship between the output voltage of the probe and the distance from the probe to the observed object (Ref. 67). The 7200 series proximitors manufactured by Bently Nevada Corp. were used in this experimental study.

(3) DVF2 (Digital Vector Filter 2)

The DVF2 is a two channel instrument that measures the amplitude and phase (with respect to a synchronizing reference signal) of a filtered vibration signal. Since it is one of the most effective and versatile pieces of equipment for balancing and rotating machinery diagnosis available, it was utilized throughout the tests as the real-time condition monitoring instrument. Following are some of its major features:

input: i) reference pulse (once-per-revolution signal)
ii) two channel, waveform signals

output: i) RPM
ii) two channel, amplitudes and phase angles
iii) two channel, in-phase and quadrature signals

miscellaneous: 120 or 12 RPM bandwidth tracking filter

accuracy for RPM: ±0.01% of full sclae ± 1 RPM

(4) VF-M (Vector Filter - Multichannel)

The VF-M is a 20 channel vector filter manufactured by Bently Nevada Corp. Comparing with DVF2, it is less versatile but has the advantage of multichannel capacity. Its accuracy in RPM reading is 0.1% or better (Ref. 69).

(5) HP 7046B XYY Plotter

The XYY plotter is usually connected to the DVF2 for real-time monitoring of the system as a whole.

(6) Nicolet 444A Spectrum Analyzer

This analyzer is a single channel narrow band spectrum analyzer. It is used along with the DVF2 for the purpose of real-time condition monitoring throughout test periods.

(7) Bently Nevada/Tektronix Model 5110 Oscilloscope

This oscilloscope was originally manufactured by TEKTRONIX, and modified by Bently Nevada Corp. as a special purpose oscilloscope for rotating machinery. It is basically a Tektronix oscilloscope 5110 with two 5A19N differential amplifiers and a 5B10N time-base module. The basic model has been modified for several tasks. One of the most significant modifications is that of the "dot" or bright spot when a reference signal through the "Z-axis" input comes in as an impulse signal. This provides users a capability to recognize forward or backward whirling and the phase or angular location of the reference (impulse) signal in the course of "orbit analysis".

The capability of this oscilloscope was practically enhanced from single channel to double channel oscilloscope by installation of an "in-house" switch box so that "filtered" as well as "non-filtered" orbit signals could be monitored throughout test periods as an additional means of real-time condition monitoring.

(8) Miscellaneous

In addition to the equipment mentioned above, many instruments were borrowed from other research groups for temporary use, for example,

B&K Accelerometer Type 4367, B&K Accelerometers Type 4369, B&K Accelerometers Type 8309, B&K Charge Amplifiers Type 2635, strain gages and strain gage conditioning amplifiers (Measurements Group, 2300 System), function generators, digital volt meters, B&K Motion Analyzer Type 4911, etc.

IV.3.3 Computer System

The computer system includes the LPA11-K data acquisition subsystem, PDP11/24 minicomputer, a Decwriter III terminal, a Tektronix 4115B graphics terminal, a Tektronix 4695 inkjet plotter, and a Tektronix 4662 Interactive Digital Plotter. The PDP 11/24 minicomputer is connected via a DECnet to a PDP 11/55, an IBM 3033, and an IBM 3090 at the Computation Center, NRC as shown in Fig. 4-2.

The LPA11-K (Laboratory Peripheral Accelerator) data acquisition subsystem and the PDP 11/24 minicomputer were configured and purchased as an integral system from the Digital Equipment Corp. (Fig. 4-5). The LPA11-K has 128 channel capacity and its maximum A/D conversion rate is 111 K Hz for a single channel. The resolution in its digitization is 25 micro-inches, that is one fortieth of a thousandth of an inch.

The PDP11/24, minicomputer has RSX11M multi-user operational system. It is connected to two terminals, namely Decwriter III and the high performance graphics terminal Tektronix 4115B. The graphics terminal, in turn, is connected to either the inkjet plotter, Tektronix 4695, or the digital plotter, Tektronix 4662 so that hard copy can be available promptly. Very high quality plots are also available from Zeta plotters located at the Computation Center, NRC, by transferring the data from the PDP 11/24 to the IBM 3090 via DECnet.

One of the most significant features of this computer system is the fact that only the "raw" signals need be stored. That is, the raw signals from the proximitors are stored in the computer, and then all the calculations and data processing are carried out later by using

Fig. 4-5 Data Acquisition System for Rotor Dynamics Test Rig

"in-house" software. Therefore, except for the probes and proximitors, all the instrumentation system can be bypassed. However, this is not practical because, firstly, many dynamic parameters should be monitored in "real-time" mode for safety of personnel and the test facility throughout the test periods; and secondly, it was essential to carry out some of the data processing in analogue mode using the "hard-wired" instruments to maintain effectiveness of experimental studies, for example, tracking filters, phase angles, etc.

IV.4 Experimental Measurements

Measurement of the critical speed can be achieved by measuring the motion of the rotor while the rotational speed of the shaft is varied. Data collection during the runup or rundown test can be carried out in many ways, however, two particular procedures have been adopted in this thesis work. One is data acquisition during the rundown of the rotor with a constant deceleration. This is referred to as "dynamic" testing in the sense that the rotational speed of the rotor is changing all the time during the data acquisition. The second is called "quasi-static" testing because data collection is carried out while the rotor is held at a constant speed. That is, the rotor speed is reduced by a preset amount, then the speed is held constant until the rotor-bearing system attains a steady state. The data are then recorded and the speed reduction/wait process is repeated. This is performed over the full speed range of the test.

The choice of rundown instead of runup is purely a matter of convenience.

As shown in Fig. 4-3, there are ten locations along the shaft length where the transducers are installed to measure the motion of the rotor. Three of them are used extensively in this study. They are designated as location #1, #2, and #3 as shown in Fig. 4-6. At each location, two proximity transducers are installed, one measures displacement of the rotor in vertical direction and the other in the horizontal direction.

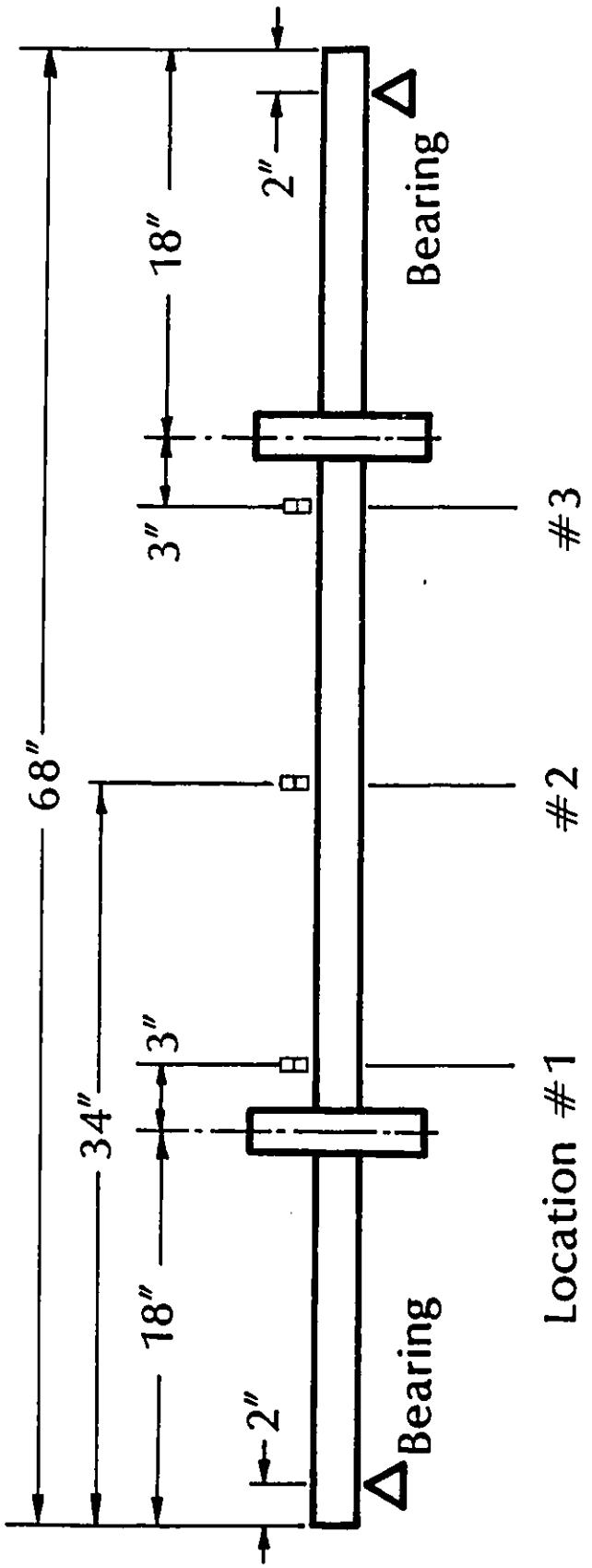

Fig. 4-6 Orbit Measurement Locations

IV.4.1 Dynamic Testing

A schematic diagram of the dynamic testing setup is shown in Fig. 4-7. There are three sampling/control programs involved in the dynamic rundown testing package, any combination of which can be run concurrently. One of the programs controls the rotor speed, another records filtered data from the VF-M, and the third records raw or unfiltered data directly from the displacement transducer.

The data recorded directly from the transducers are processed for the generation of cascade diagrams. The time series are Hanning weighted, transformed via an FFT algorithm, and the amplitude components of the transformed results are saved and plotted as shown in Fig. 4-8. The current sampling/processing algorithm produces a 200 line transform with a 50 cpm bandwidth. This results in a spectrum covering a frequency range from 0 to 10000 cpm. It can be seen in Fig. 4-8 that the first critical speed appears at approximately 1725 RPM. It should be noted that no compensation for the initial runout of the shaft was incorporated in the cascade diagram shown in Fig. 4-8.

The filtered data recorded from the VF-M are used for the generation of Bode/Nyquist diagrams. The original signals are narrow-band filtered by the tracking filters in the VF-M. The VF-M filters are normally set to track the synchronous (or once-per-revolution) component of the signal. Outputs from the VF-M are in "in-phase" and "quadrature" components for each input. They are converted to the amplitude and phase angle components when necessary.

The motion of the rotor whirling have been measured while the rotational speed of the rotor is slowly reduced from 3500 RPM to

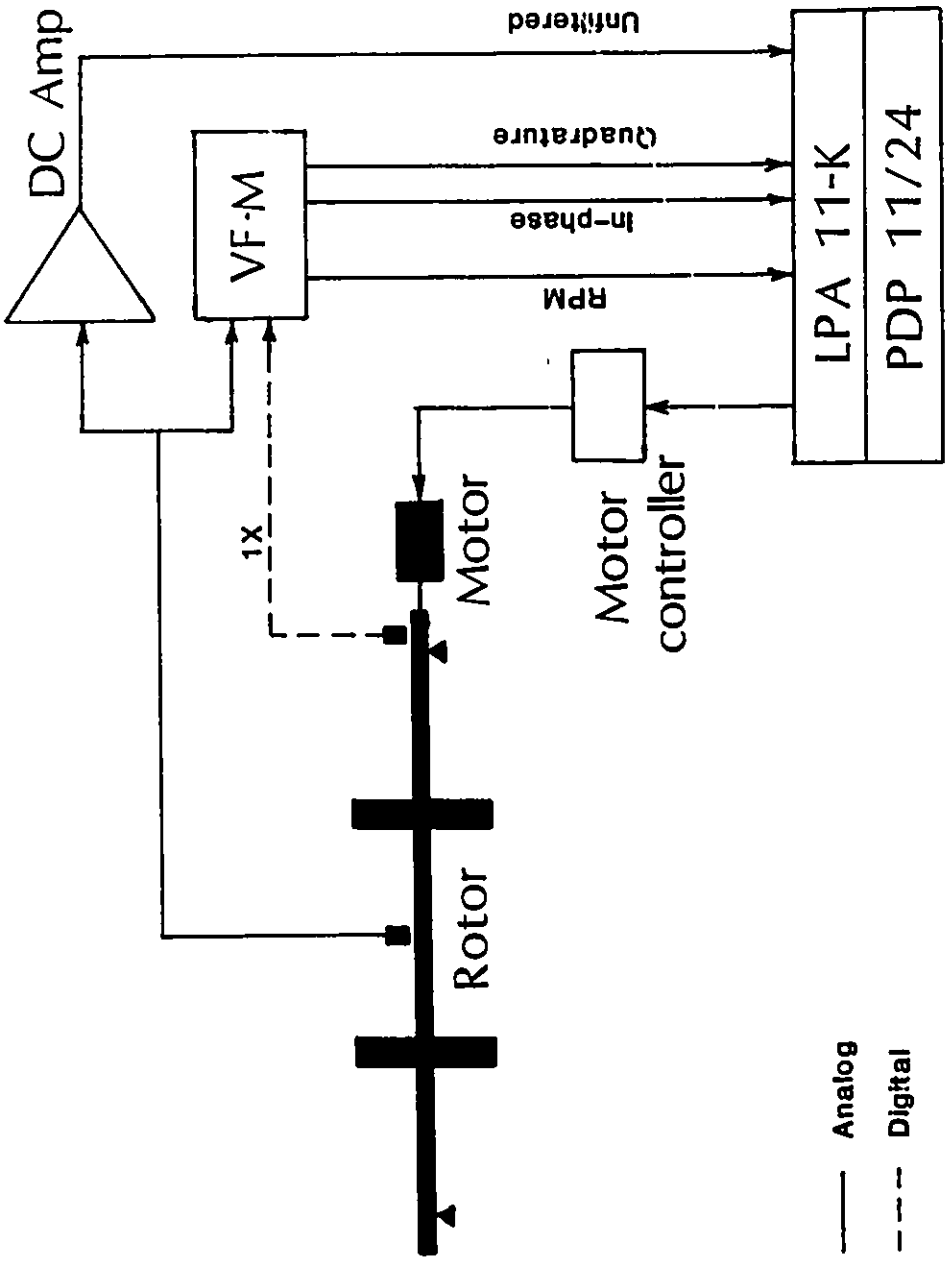

Fig. 4-7 Dynamic Rundown Test Setup

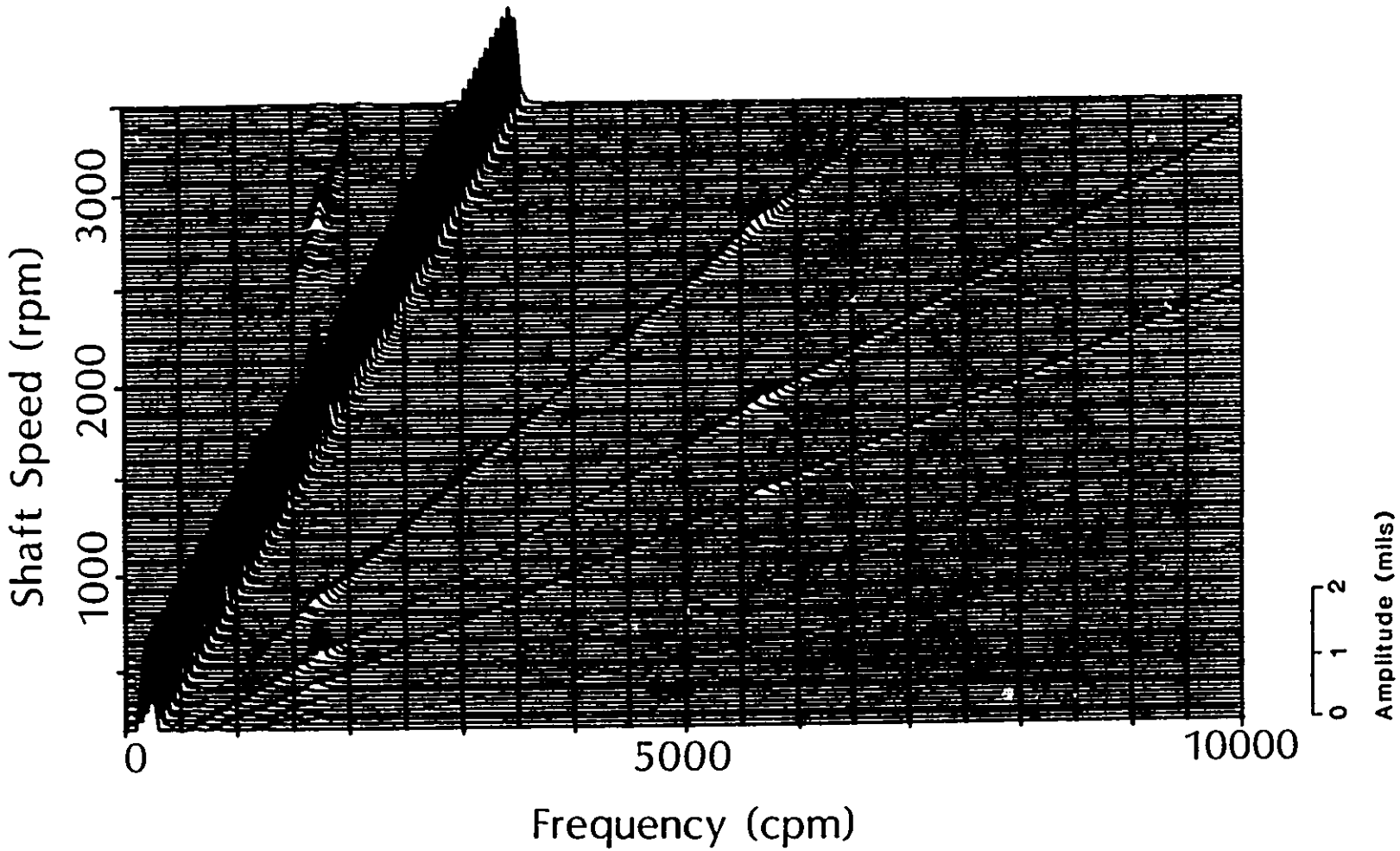

Fig.4-8 Cascade Diagram (Dynamic Rundown Test)
(Location#2,Vertical Probe)

approximately 100 RPM. The rate of rundown is controlled by the computerized data acquisition system and kept constant as shown in Fig. 4-9. The actual rundown rate for the particular case was 138.32 RPM/min, that is, it took approximately 25 minutes for the rotor to come down from 3500 RPM to 100 RPM.

The compensation for initial runout was carried out by subtracting the filtered data at approximately 100 RPM from the filtered data at any running speed.

The results of the dynamic rundown tests at the location #2 are shown in Fig. 4-10 and 4-11. As shown in the Bode diagram (Fig. 4-10), the first critical speed of the two-disc rotor system is 1719 RPM. It is worth noting that VF-M has its accuracy of measurement of RPM at 0.1% of the full scale of 1000 RPM. That is, the instruments can measure the rotational speed of the rotor within the accuracy of 10 RPM. Therefore, the critical speed during the dynamic testing is 1719 ± 10 RPM.

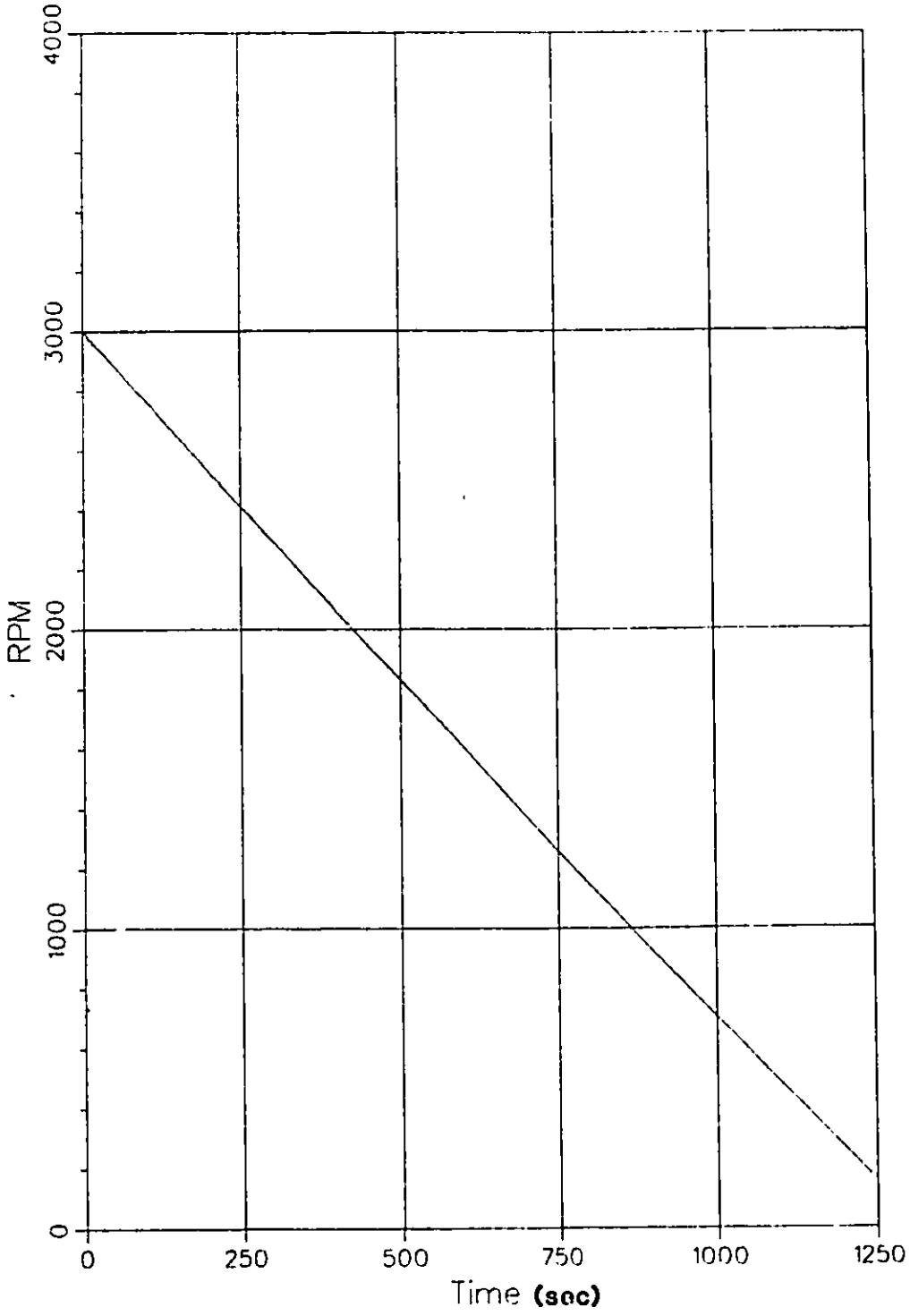

Fig. 4-9 Rundown Rate during Measurement of First Critical Speed

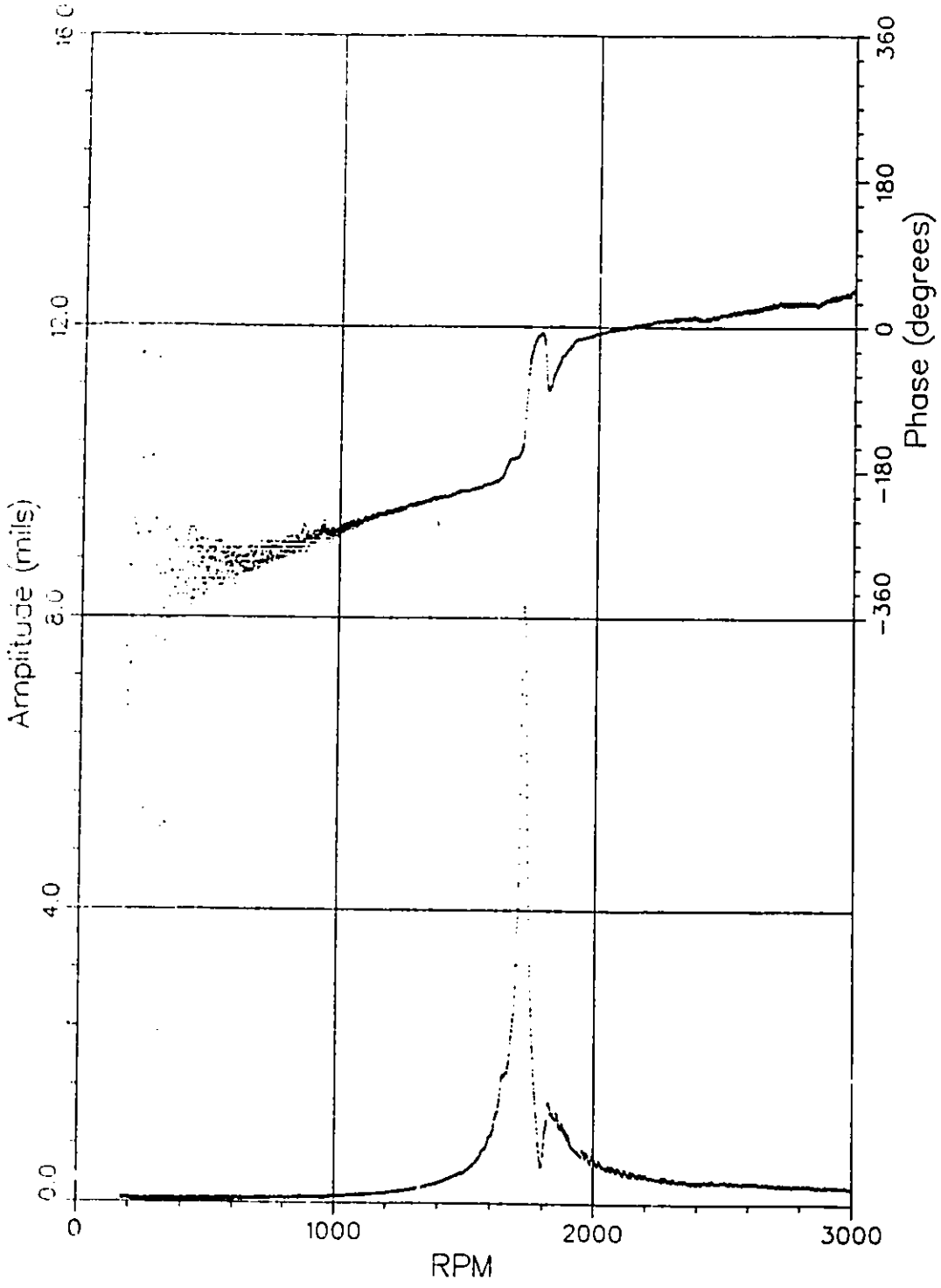

Fig. 4-10 Bode Diagram (Dynamic Rundown Test)

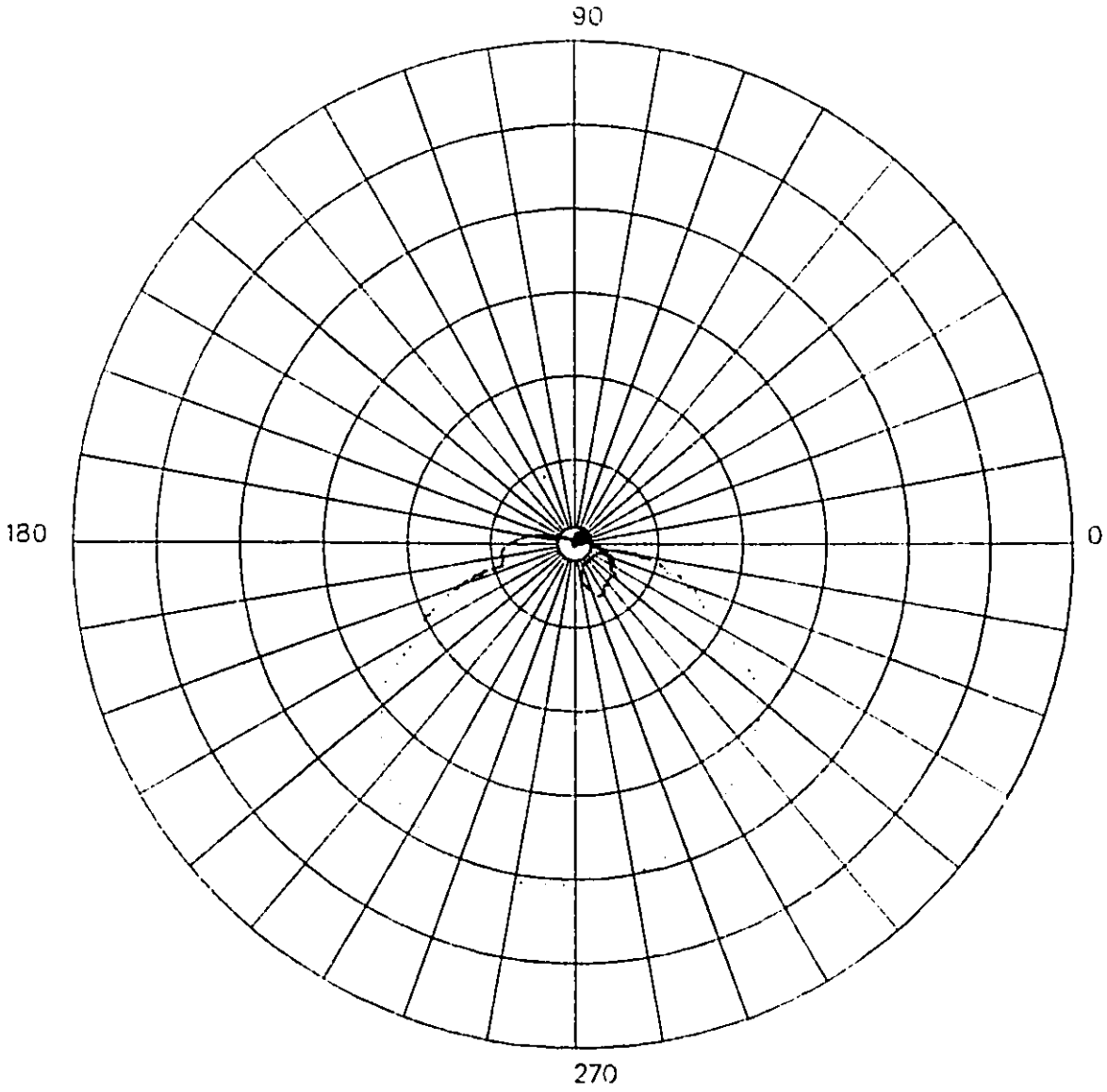

Probe: 15
Radial: 2.00 mils/div
Data locks out at: 0.02 mils

Fig. 4-11 Nyquist Diagram
(Dynamic Rundown Test)

IV.4.2 Quasi-Static Test

In the quasi-static testing, unlike the dynamic testing, all waveform data is sampled directly from the displacement transducers only, and all the signal manipulations are performed by the software in the minicomputer. Figure 4-12 shows an overview of the test system.

The orbits of the rotor are recorded by pairs of displacement transducers, one in the vertical and the other in the horizontal direction, at a number of discrete speeds as the rotational speed of the rotor is reduced in a stepwise fashion. Data are recorded only when the rotor speed is considered steady.

In the dynamic rundown testing, data sampling was carried out under the control of a time-based clock residing in the minicomputer. For the present quasi-static rundown test, an entirely different "clocking" system is introduced. The new clocking function is performed by an encoder installed at one end of the shaft. The encoder is synchronized to a reference point on the shaft so that it allows the data sampling once every half a degree of the rotor rotation. This is equivalent to installation of 720 triggering points for data sampling around the shaft periphery at a constant angular interval of half a degree. Therefore, regardless of the rotational speed of the rotor, there are 720 sampled data per revolution of the rotor.

One significant advantage of this encoder controlled data acquisition is that it allows for runout compensation of the displacement signals. That is, the orbit signal at a "slow roll" speed

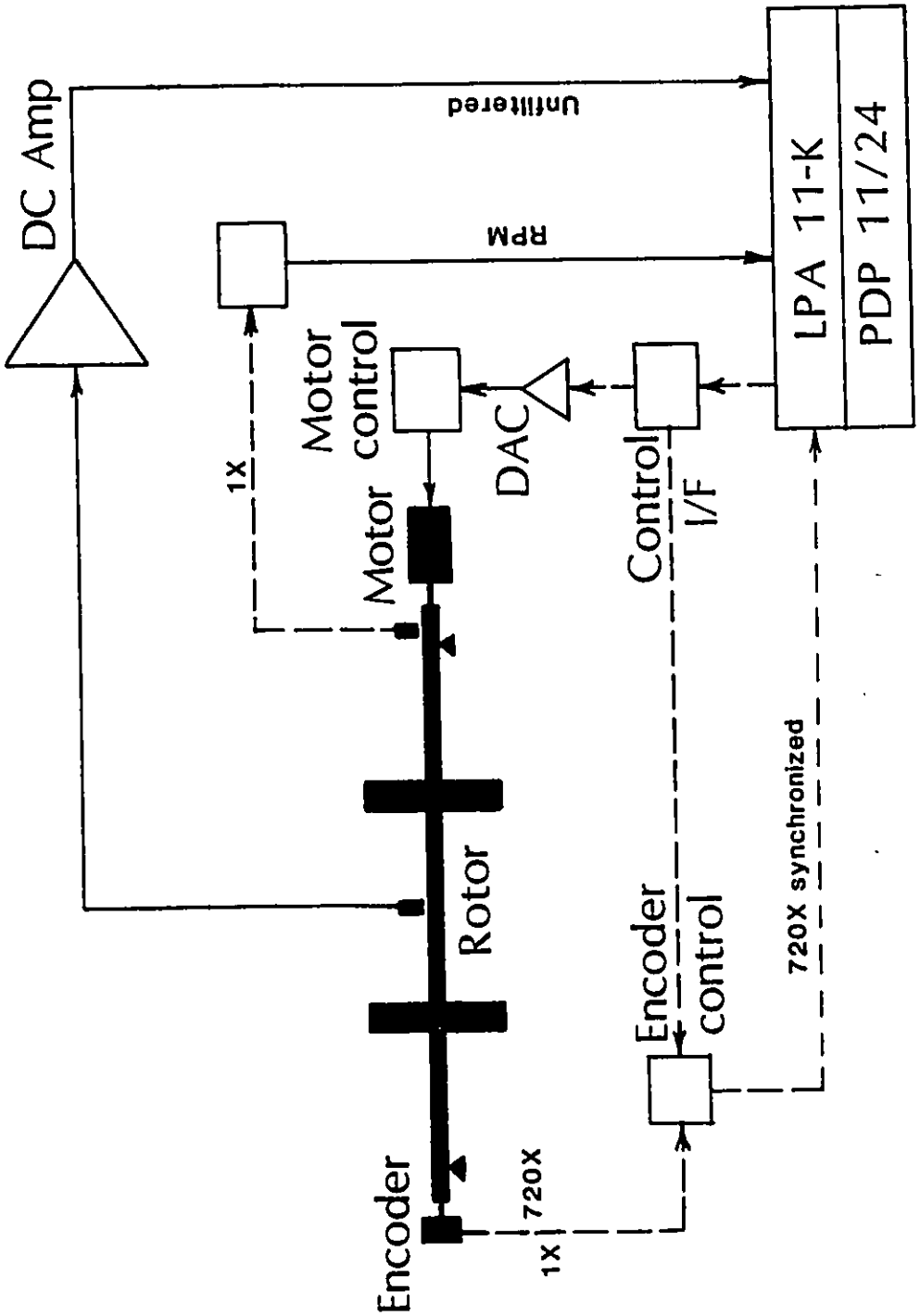

Fig. 4-12 Quasi-Static Rundown Test Setup

may be stored away, and then it can be subtracted from the "as is" orbit signals recorded at higher speeds, to yield runout compensated orbits as shown in Figs. 4-13 to 4-15. Figure 4-13 shows the orbit of the rotor whirling at slow roll speed of 102 RPM. Figure 4-14 shows "as is" orbit of the same rotor at 1008 RPM. When the slow roll data of Fig. 4-13 are subtracted from the "as is" data of Fig. 4-14, the runout compensated orbit can be found as shown in Fig. 4-15. All the data subsequently mentioned hereafter are runout compensated as described above.

All the runout compensated data are processed through a Fourier transform so that the synchronous components to the rotational speed can be extracted. The shaft orbit plotted out of the extracted synchronous components is often called as a "filtered orbit", and the runout compensated (but not processed any further) orbit is called a "raw orbit". The filtered and raw orbits at locations #1, #2, and #3 during a quasi-static rundown test, are shown in Figs. 4-16 to 4-20. The orbits are plotted at five consecutive steps of RPM, namely at 1680, 1702, 1730, 1756, and 1783 RPM.

Bode diagrams constructed from the quasi-static rundown tests at various locations are shown in Figs. 4-21 to 4-26. Figures 4-21 and 4-22 are Bode diagrams obtained from horizontal and vertical probes, respectively, at location #1, Figs. 4-23 and 4-24 are those at location #2, and Figs. 4-25 and 4-26 are those at location #3. The amplitude of Fig. 4-24 is re-plotted in Fig. 4-27 with its scales magnified. As can be seen from Figs. 4-17, 4-18, 4-19 and 4-27, the first critical speed is 1730 RPM $^{+26}_{-28}$ RPM.

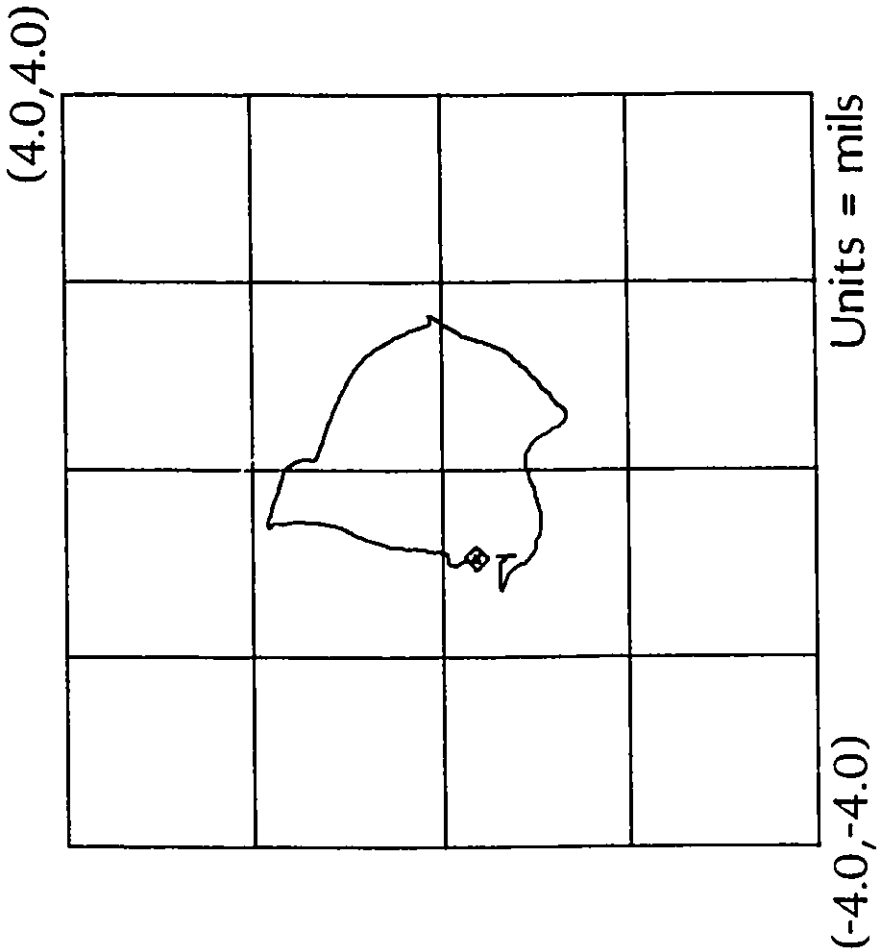

Fig. 4-13 Runout Orbit at Slow Roll Speed

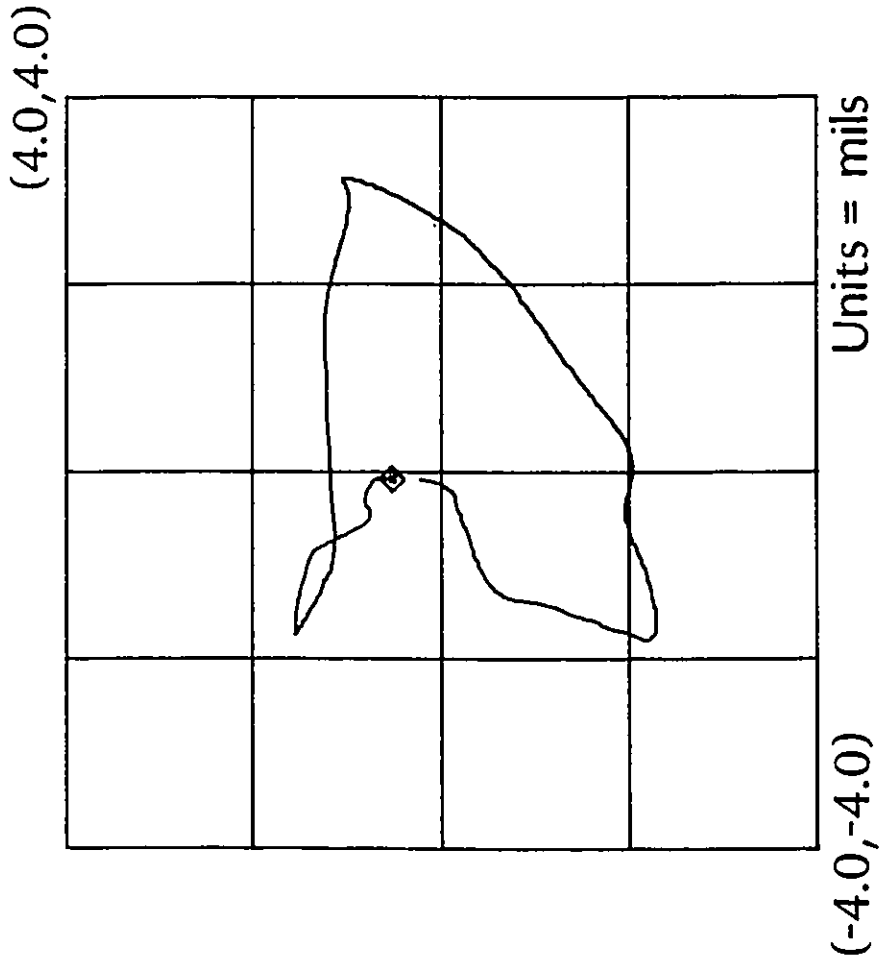

Fig. 4-14 Uncompensated Orbit (running speed)

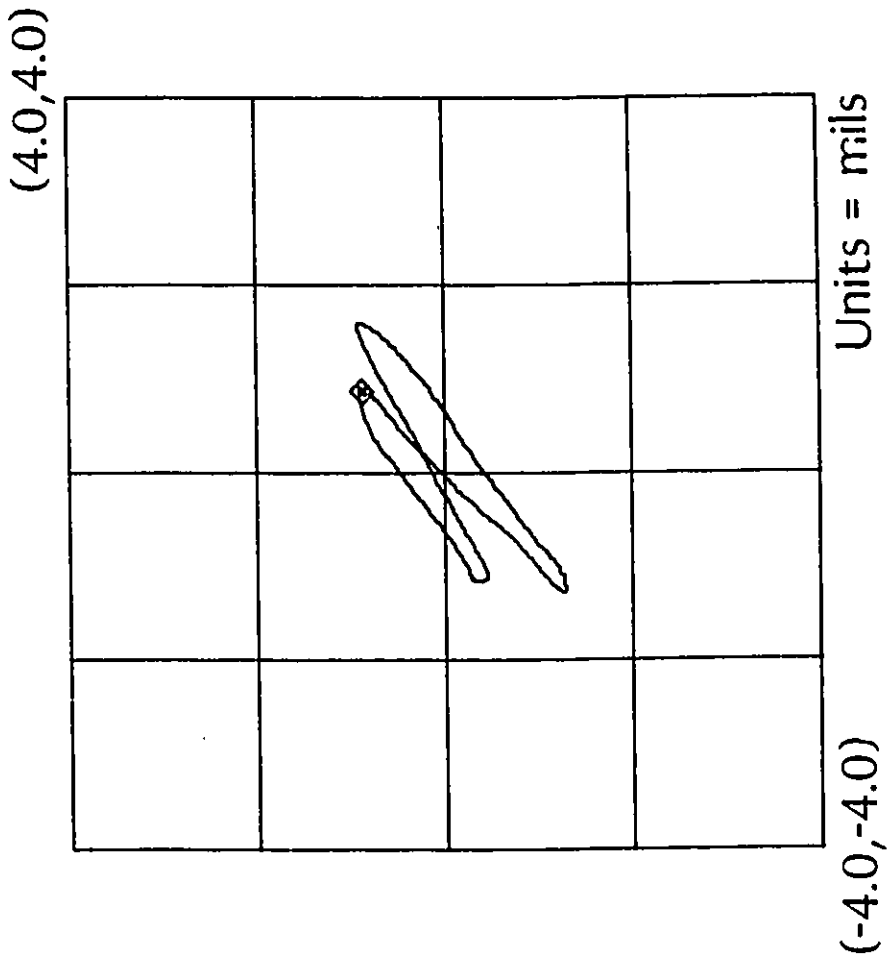

Fig. 4-15 Runout Compensated Orbit (running speed)

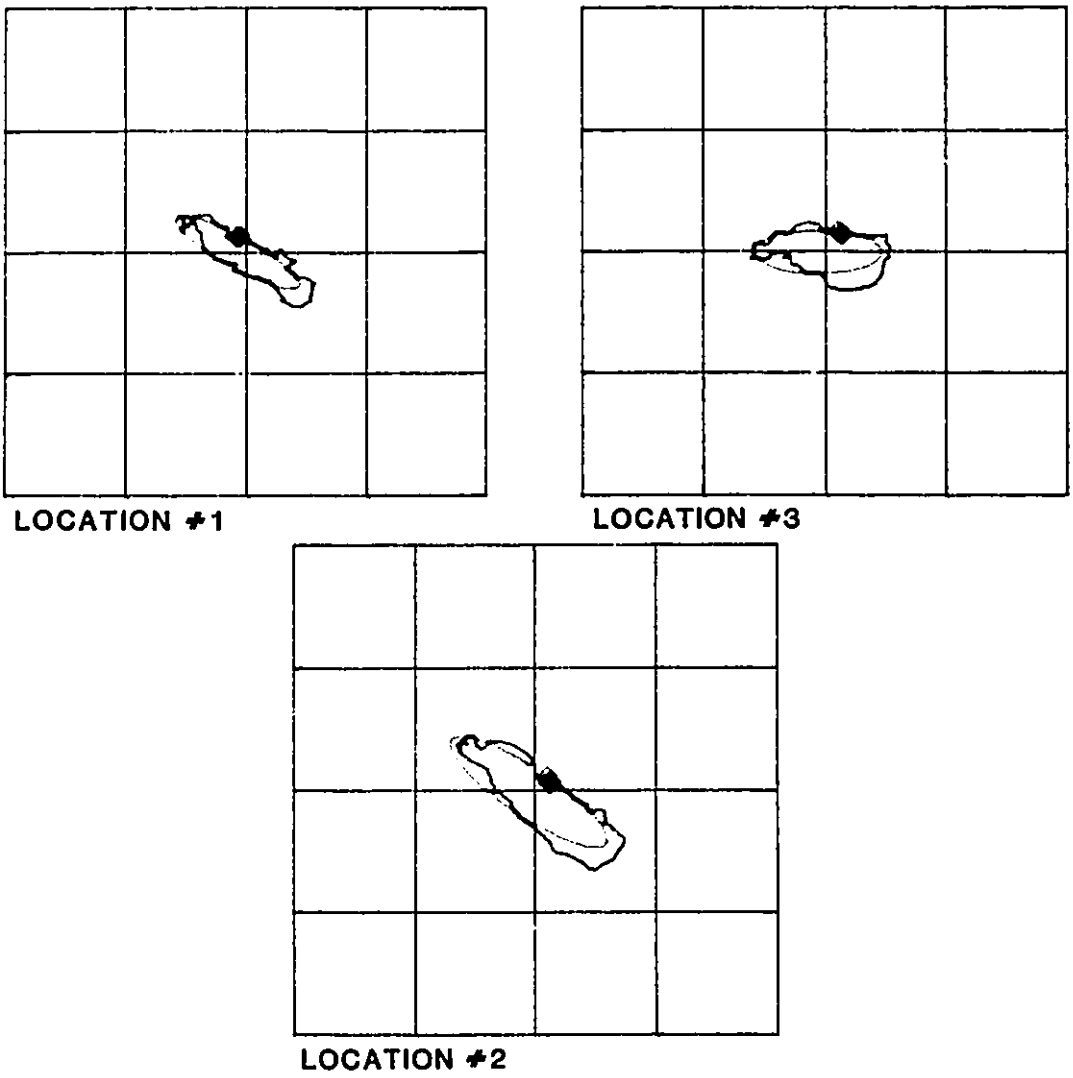

Fig. 4-16 Rotor Orbits at 1680 RPM
(Quasi-Static Rundown Test)
(Blue: Unfiltered Orbit)
(Red: Filtered Orbit)

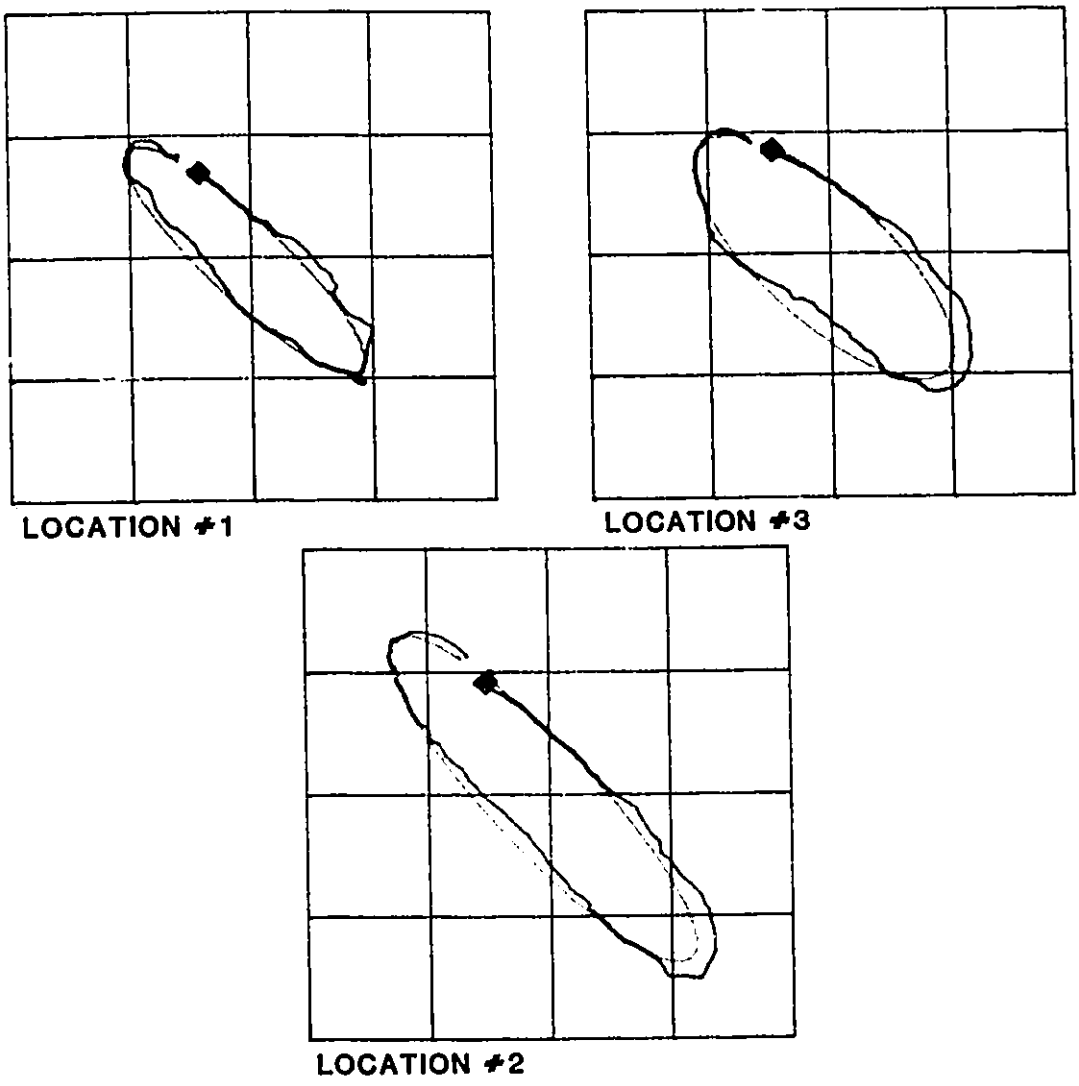

Fig. 4-17 Rotor Orbits at 1702 RPM
(Quasi-Static Rundown Test)
(Blue: Unfiltered Orbit)
(Red: Filtered Orbit)

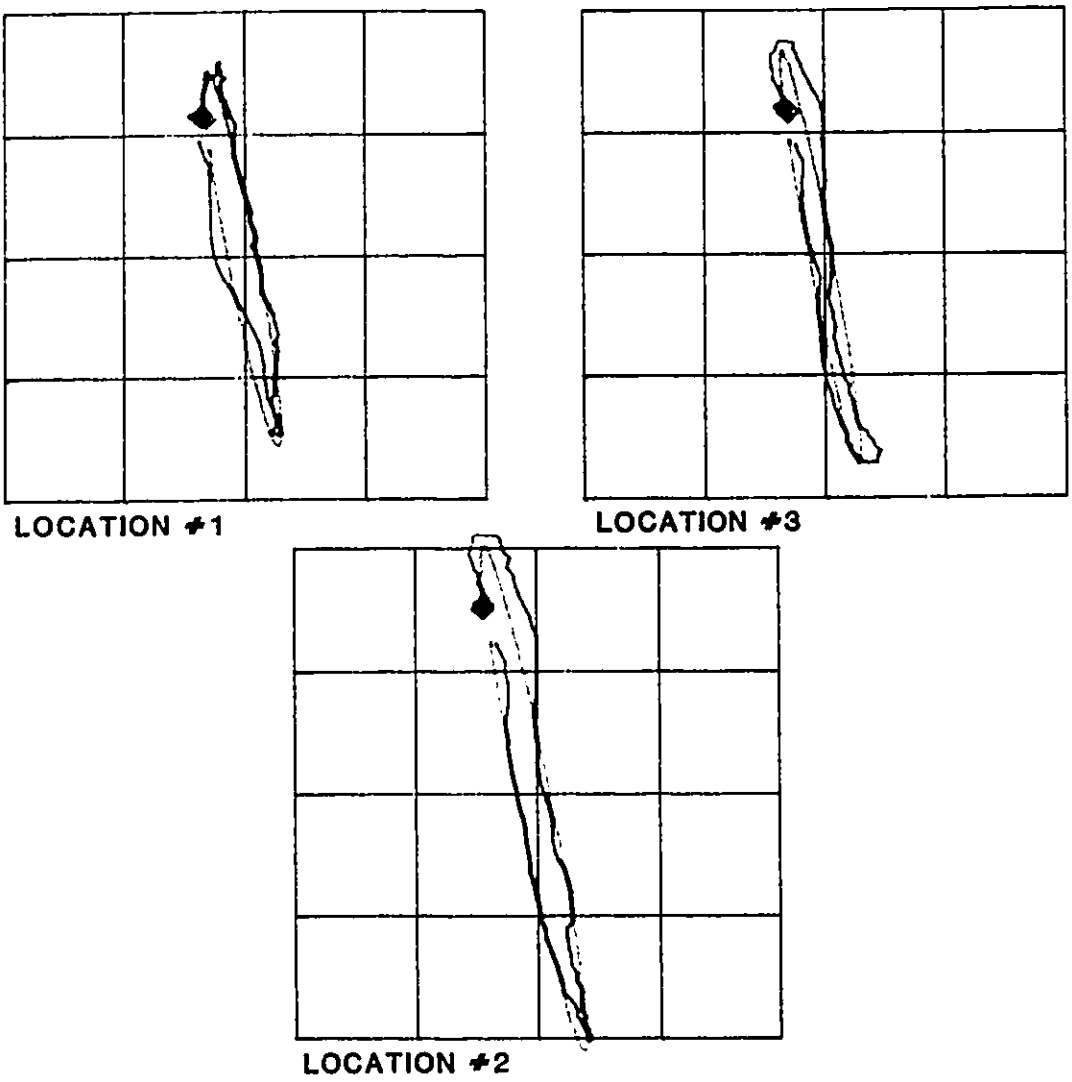

Fig. 4-18 Rotor Orbits at 1730 RPM
(Quasi-Static Rundown Test)
(Blue: Unfiltered Orbit)
(Red: Filtered Orbit)

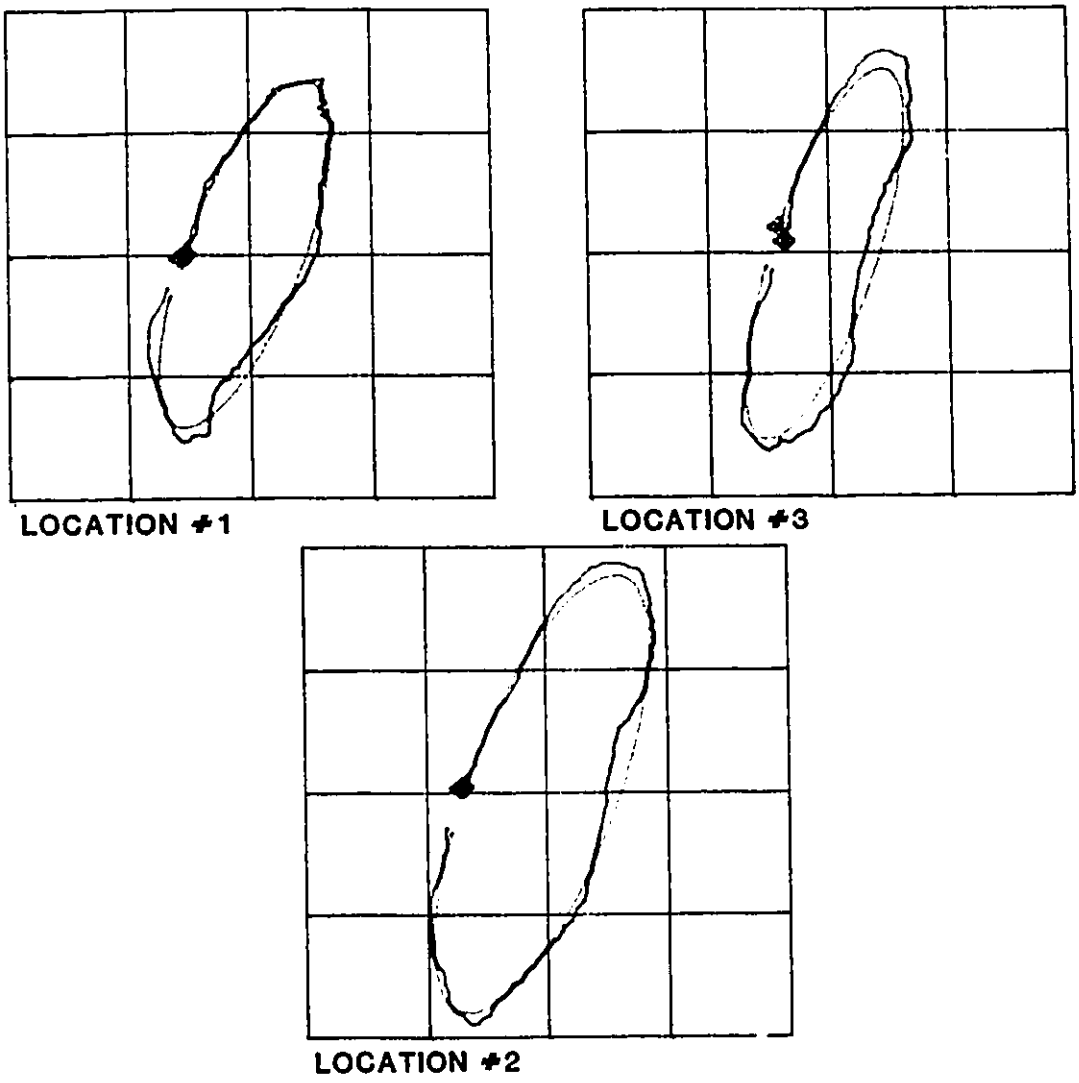

Fig. 4-19 Rotor Orbits at 1756 RPM
(Quasi-Static Rundown Test)

(Blue: Unfiltered Orbit)
(Red: Filtered Orbit)

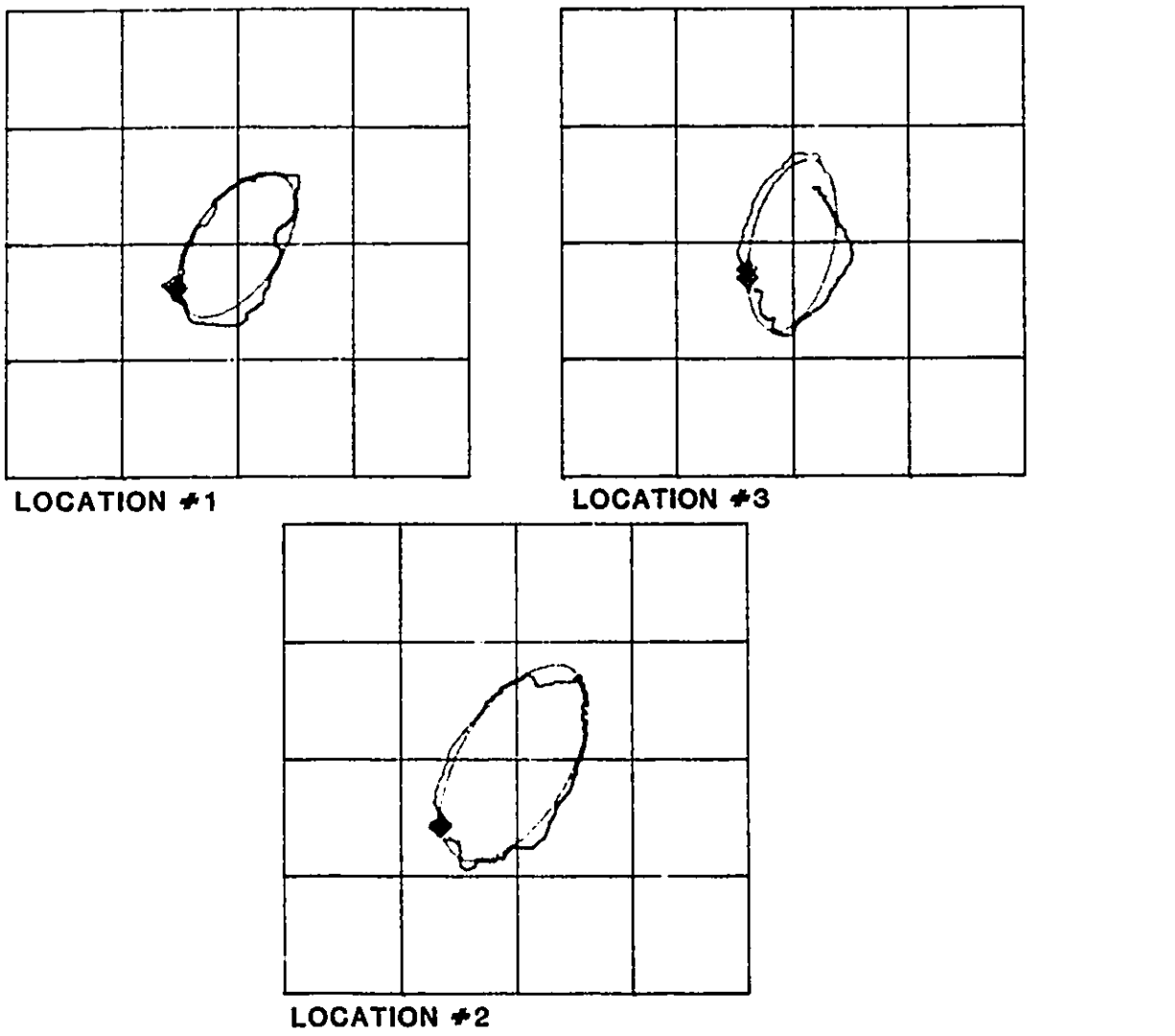

Fig. 4-20 Rotor Orbits at 1783 RPM
(Quasi-Static Rundown Test)
(Blue: Unfiltered Orbit)
(Red: Filtered Orbit)

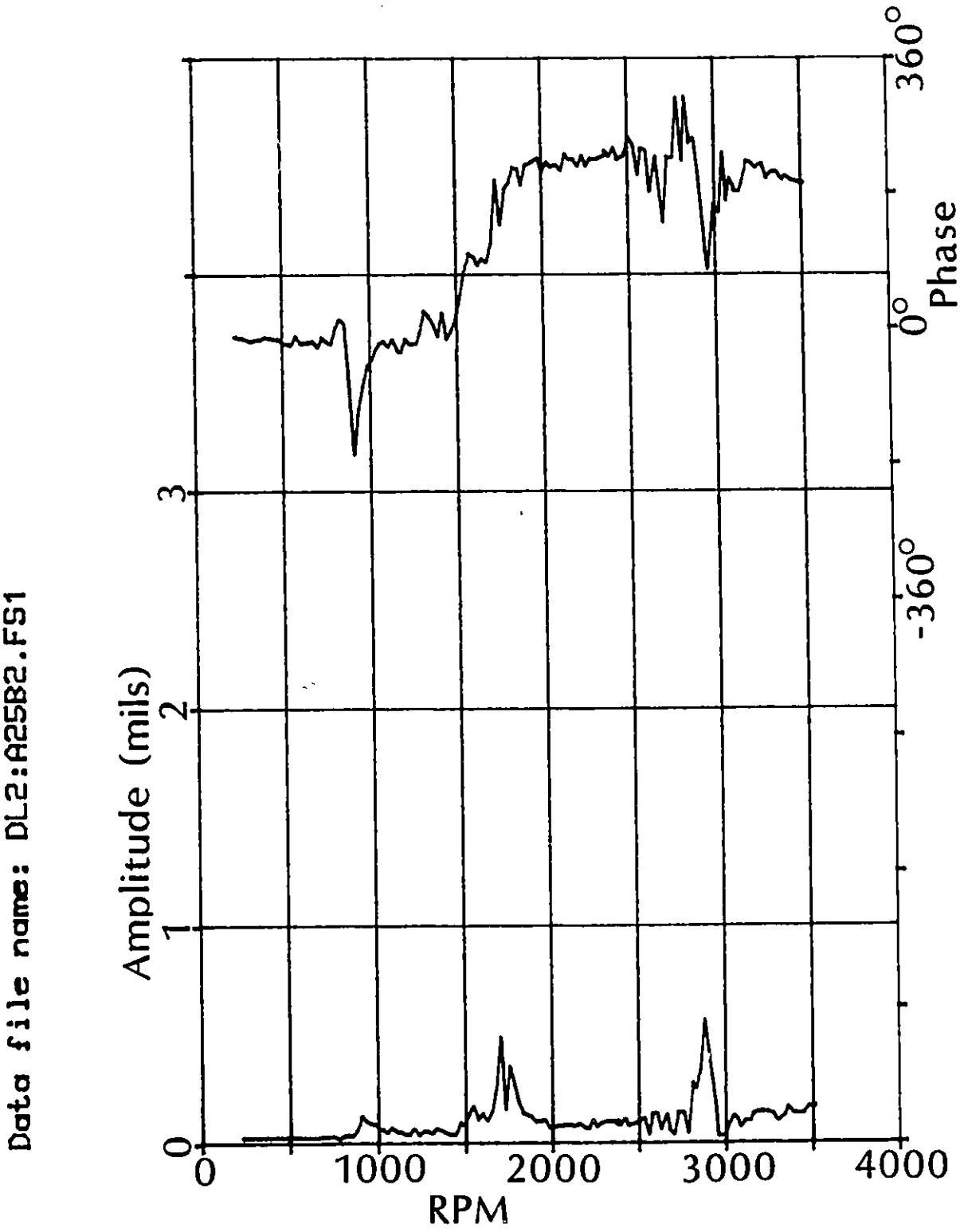

Fig. 4-21 Bode Diagram (Location#1, Horizontal Probe)

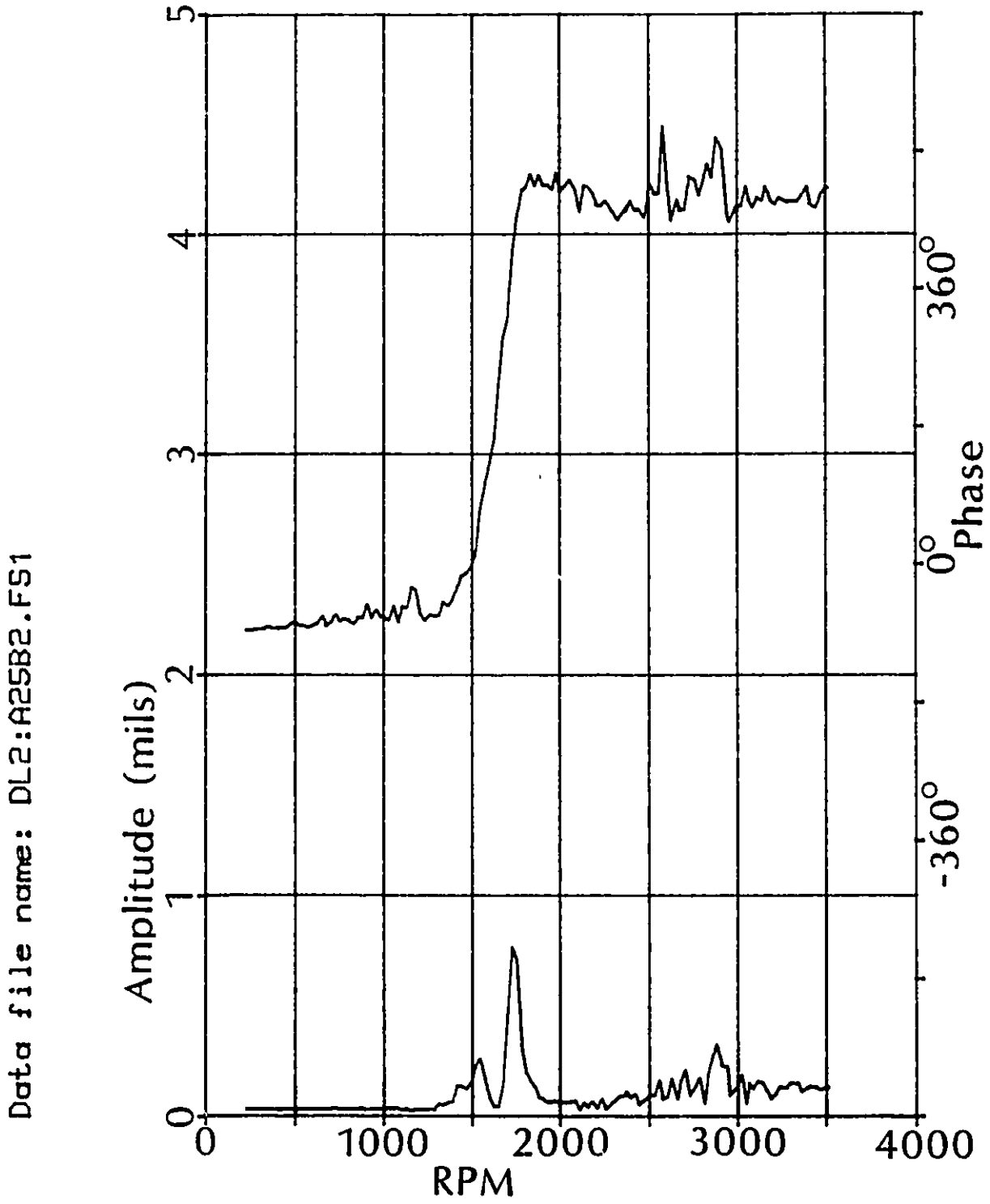

Fig. 4-22 Bode Diagram
(Location #1,Vertical Probe)

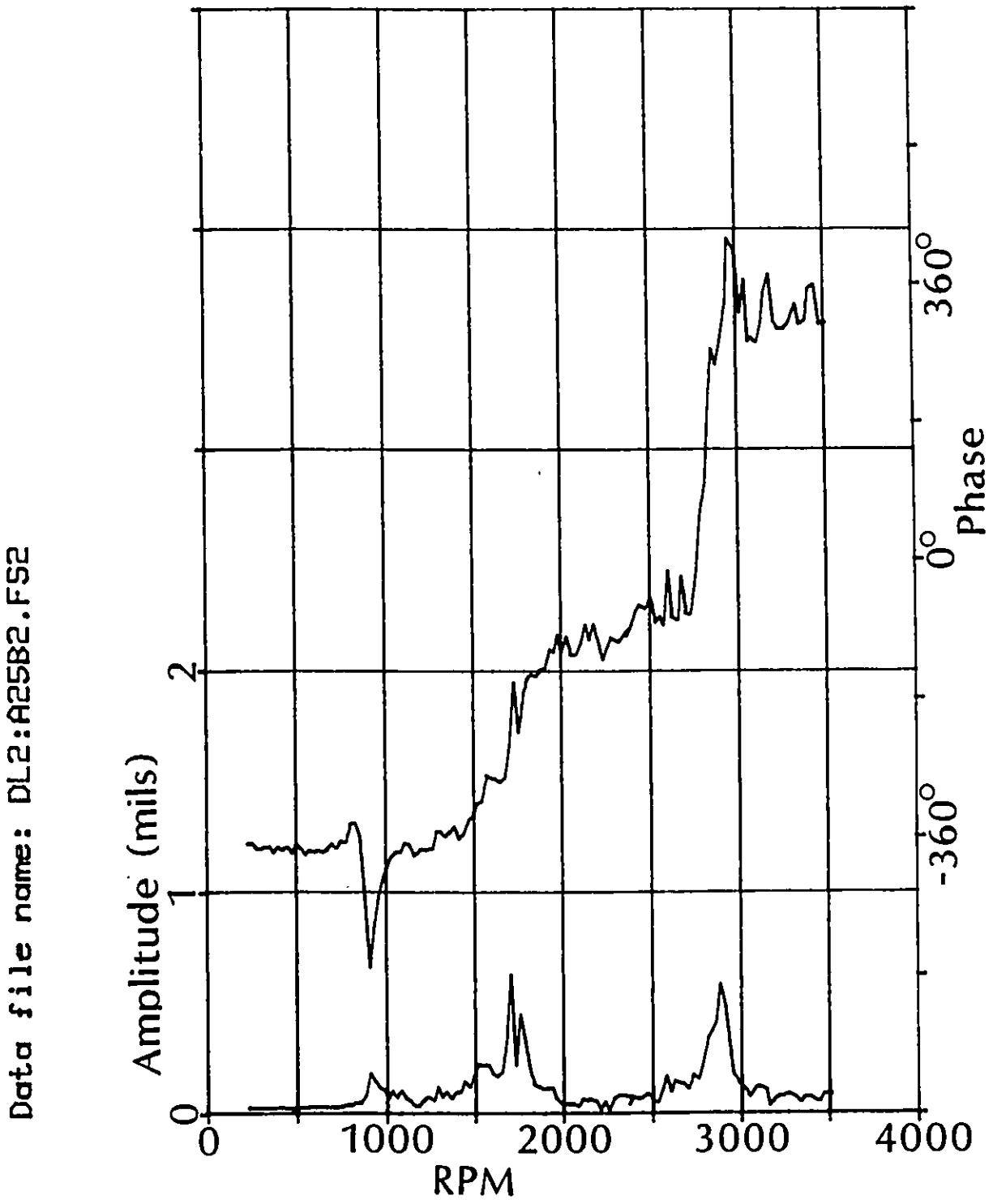

Fig. 4-23 Bode Diagram (Location #2, Horizontal Probe)

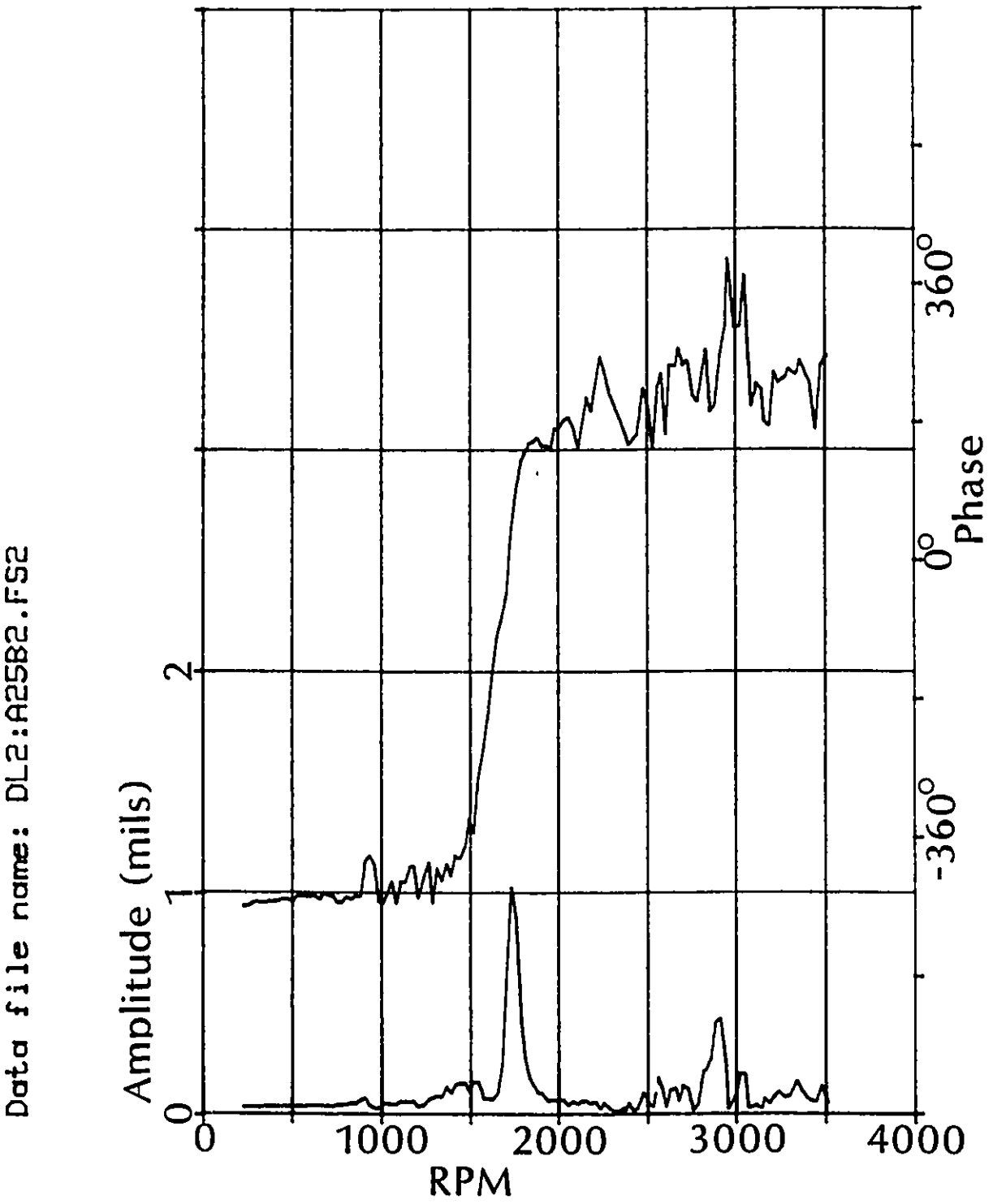

Fig. 4-24 Bode Diagram (Loation #2, Vertical Probe)

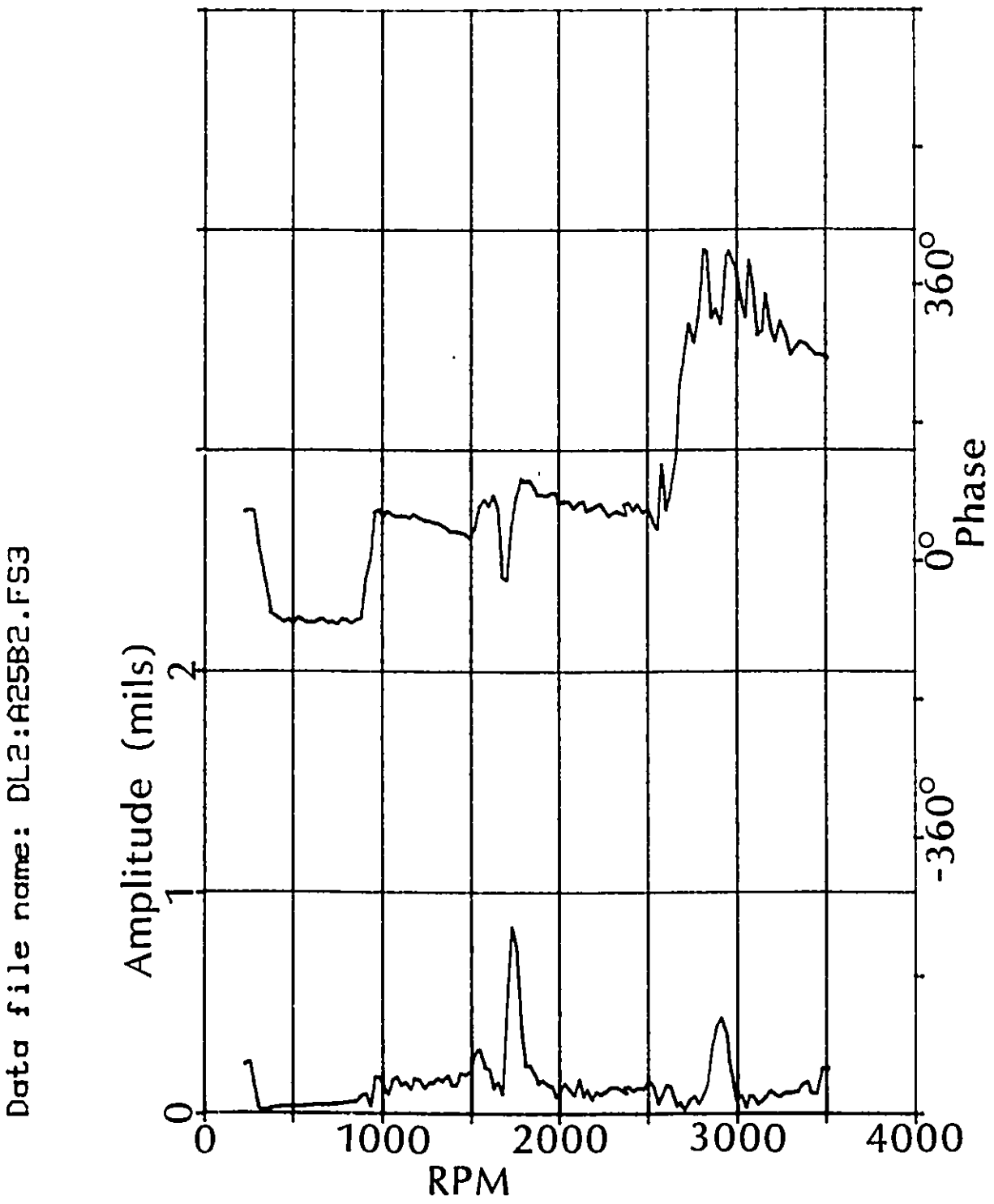

Fig. 4-26 Bode Diagram (Location #3, Vertical Probe)

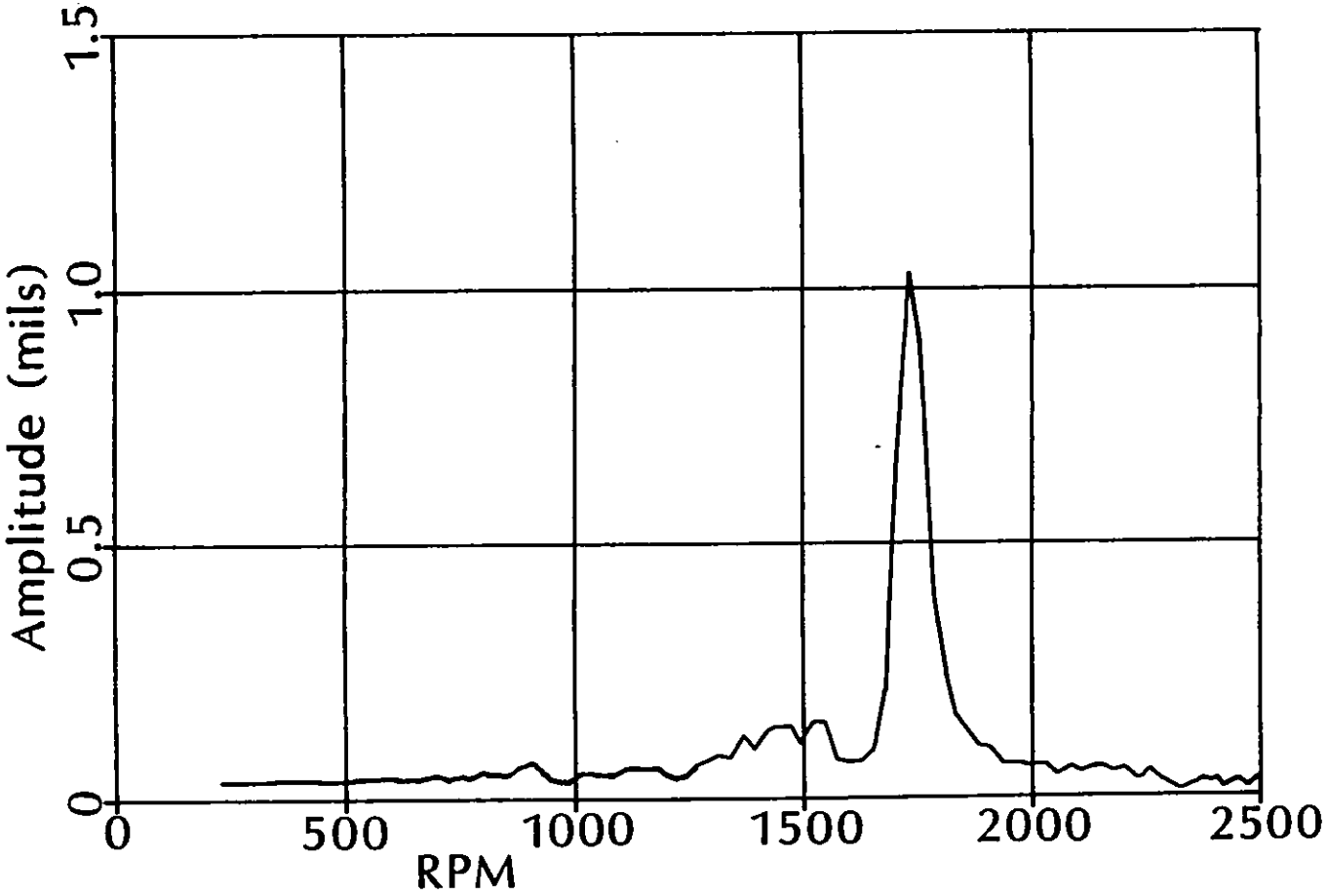

Fig. 4-27 Amplitude vs. RPM (Location #2,Vertical Probe)

IV.5 Analytical Evaluation

In this section, the proposed method will be applied to the two-disc rotor-bearing system. After a detailed description of the mathematical model, some features of the overall system matrix will be discussed, and then, the analytical results will be presented. Comparison with other results will be presented in the next section.

IV.5.1 Modelling of the Two-Disc Rotor System

The rotor-bearing system shown in Fig. 4-1, has been divided by imaginary stations into a series of shaft segments as shown in Fig. 4-28. Since the discs were shrunk-fit, they are "modelled" as thick shaft segments with concentrated gyroscopic effects at the intersection of the center lines of the shaft and the discs as indicated in Fig. 4-28. The bearings are treated as "rigid" in the analysis because of the minimal bearing clearance and the sturdy construction of the bearing housing.

It is worth noting that the station numbers in Fig. 4-28 can start from the left end with either zero (0) or one (1). This is a matter of convenience in computer programming and end conditions of the shaft.

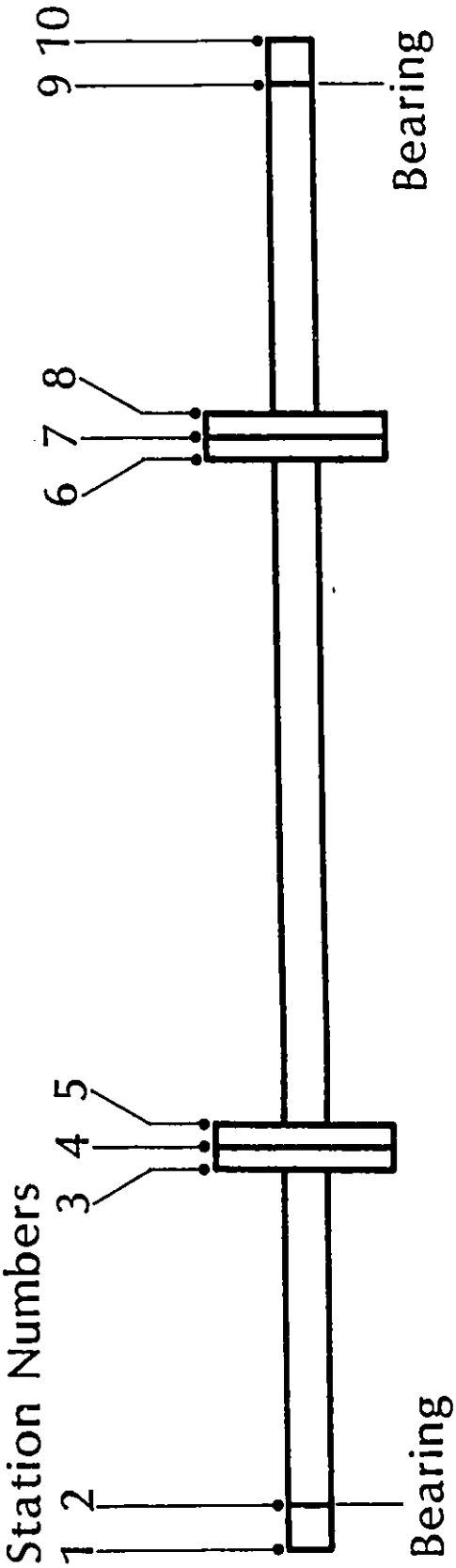

Fig. 4-28 Computer Model for Two-Disc Rotor-Bearing System

IV.5.2 Analytical Results

The two-disc rotor-bearing system described in the previous section (Figs. 4-1 and 4-28) has been analysed for its critical speeds using the present method. The computer program listing as well as the actual computer run itself are given in Appendix A.

The physical difference between the one-disc rotor and the two-disc rotor manifests itself in the overall matrix of the system. The general form of the matrix shown in Fig. 4-29 is the overall matrix of the two-disc rotor, which corresponds to that shown in Fig. 3-4 for the one-disc rotor system in the previous chapter.

The difference between the two overall matrices can be noted in the sense that the partitioned matrices, C, D and E in Fig. 3-4 have been repeated in the manner of C_I, D_I, E_I, C_{II}, D_{II}, and E_{II} in Fig. 4-29. This is due to the fact that the shaft has two discs (Fig. 4-29) instead of one (Fig. 3-4). This can be seen more clearly in Fig. 4-30 in comparison with Fig. 3-5. In Fig. 3-5 there is one group of partitioned sub-matrices namely "Step Change in Diameter", "Gyroscopic Effect of Disc", and "Step Change in Diameter", which represent one disc.

In the case of the two-disc rotor, such a group appears twice. These two groups of partitioned sub- matrices in Fig. 4-30 represent two shrunk-fit discs. Recapitulating, all the boundary conditions appear diagonally in the overall matrix in the form of partitioned sub-matrices in the order of the physical appearance from the ends of the rotor.

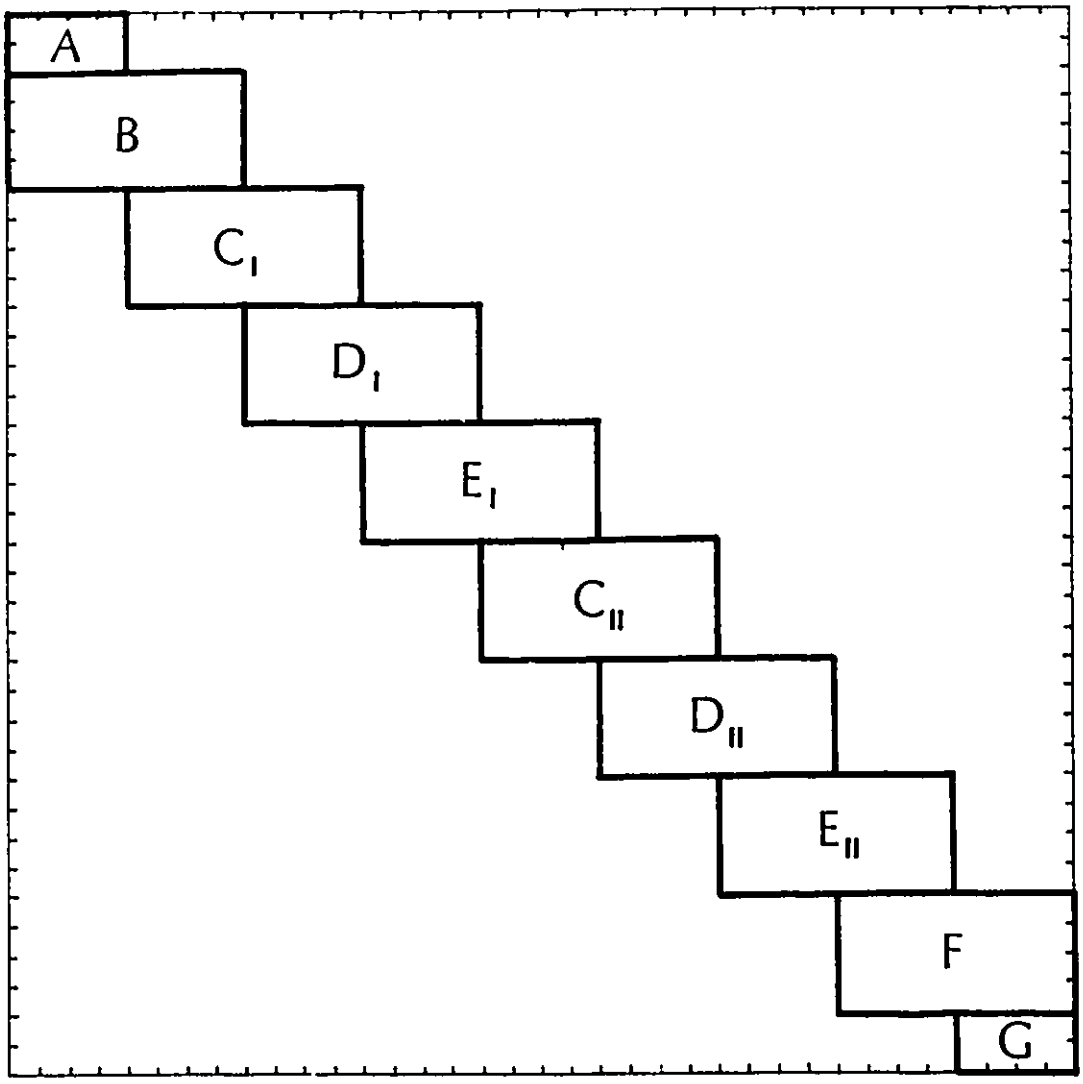

Fig. 4-29 General Layout of Overall Matrix with Partitions (Two-Disc System)

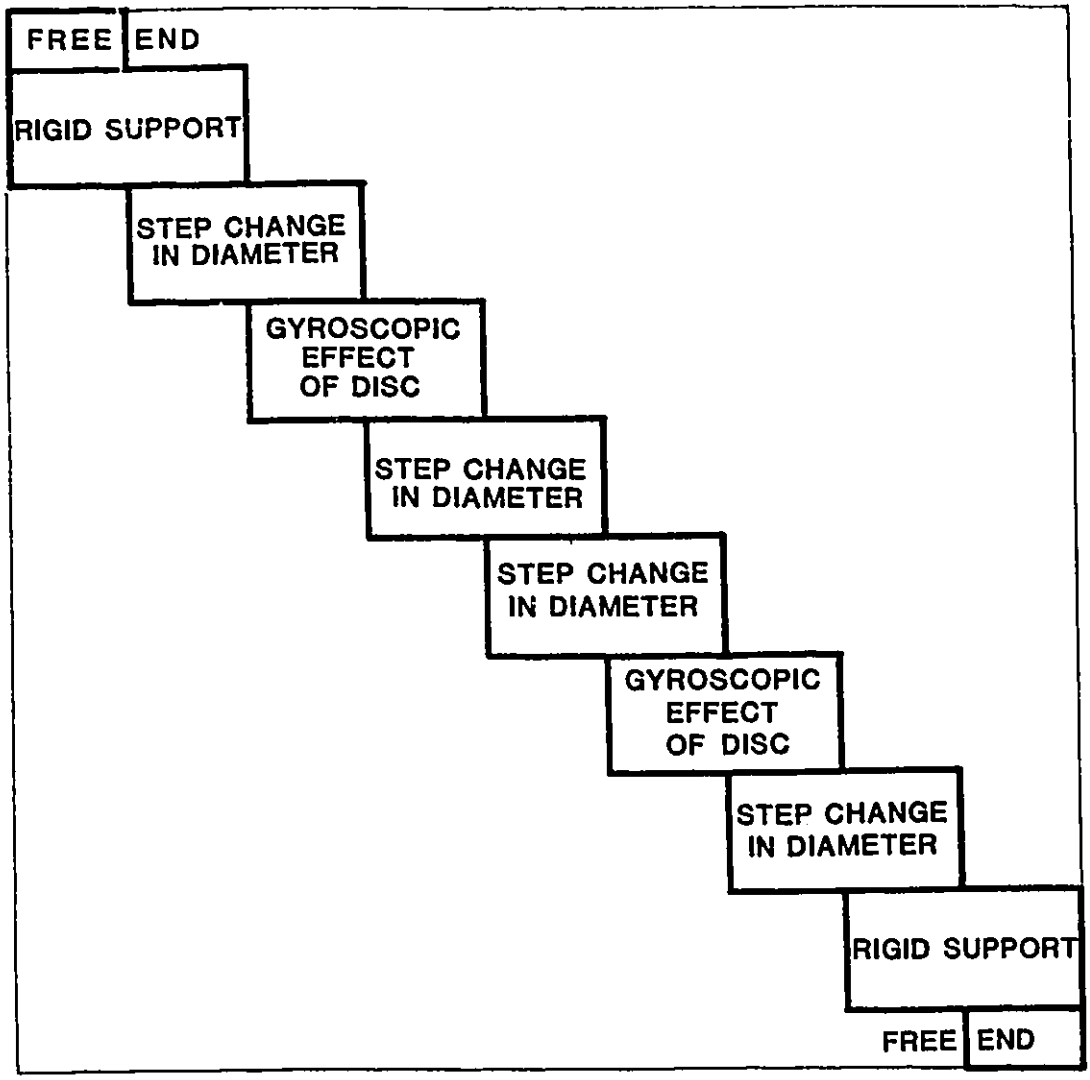

Fig. 4-30 Physical Meaning of Partitions in the Overall Matrix (Two-Disc System)

When the determinant of the overall matrix is solved numerically for the particular values of the rotational speeds of the rotor, ω_i, such that the numerical value of the determinant vanishes, the critical speeds of the rotor are found as those particular values of ω_i.

The results are:

i) the first critical speed (ω_1)

ω_1 = 1,733 RPM

ii) the second critical speed (ω_2)

ω_2 = 5,951 RPM

iii) the third critical speed (ω_3)

ω_3 = 17,797 RPM

It should be noted that higher critical speeds can be computed. However, for this study, computations have been limited to the first three critical speeds.

Results are plotted in Figs. 4-31 to 4-35. In order to control the magnitude of the determinant from overflowing, the elements are divided by the square root of the RPM, and the values of the determinant are plotted as a function of RPM. In Fig. 4-31, the value of the determinant is plotted from 100 to 18,000 RPM. The ranges of magnitude of the determinant are so vastly different that the scale of ordinate has been changed three times along the axis of RPM. Figure 4-32 shows exactly the same information as in Fig. 4-31 but in "modified" semi-log scale to accommodate all the values in one graph without changing the scale of the ordinate. Figures 4-33 to 4-35 are close-up plotting of the determinant values in the vicinities of the first, second, and third critical speeds, respectively.

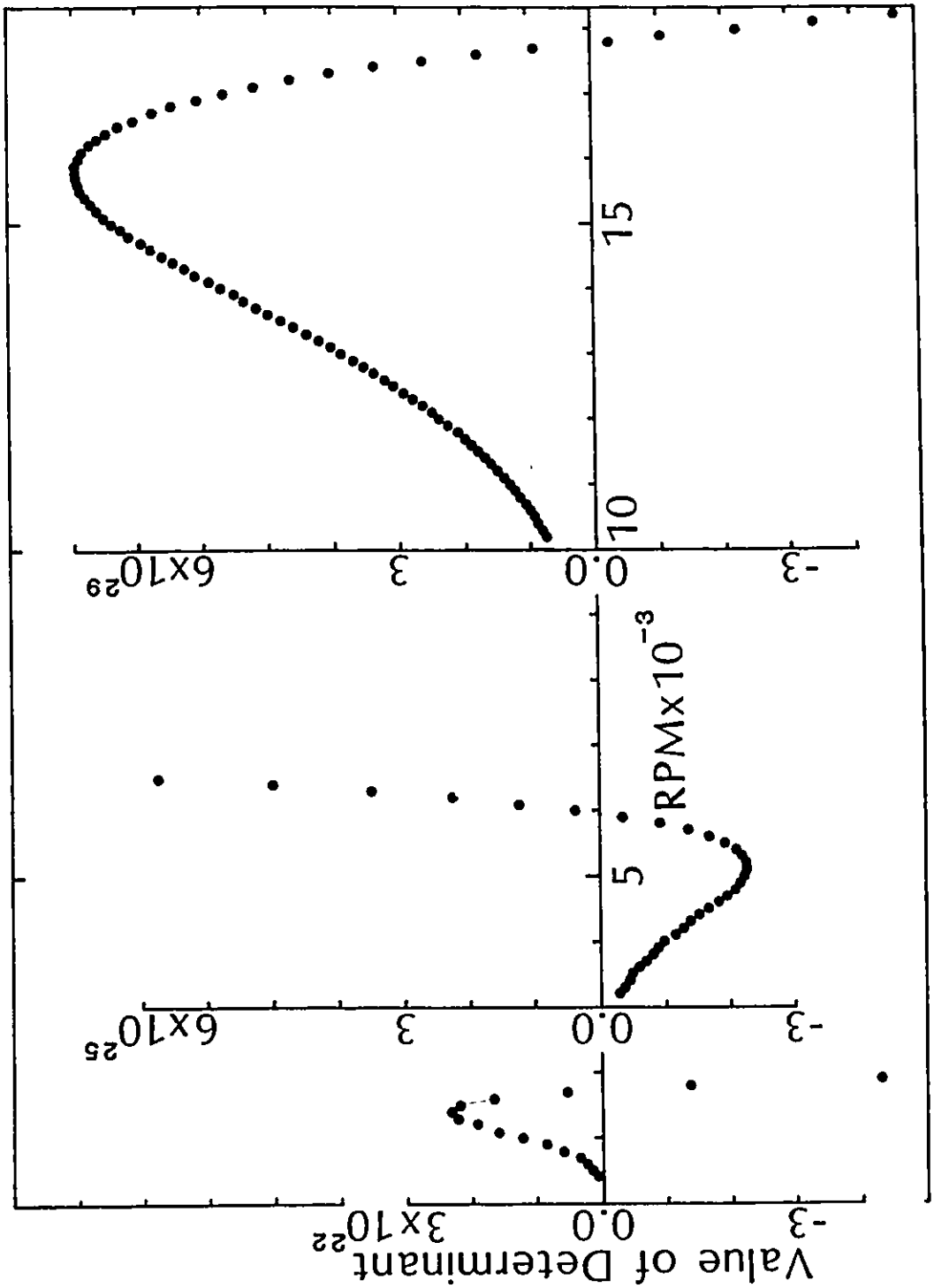

Fig. 4-31 Value of Determinant as a Function of Rotor RPM
(Two-Disc Rotor)

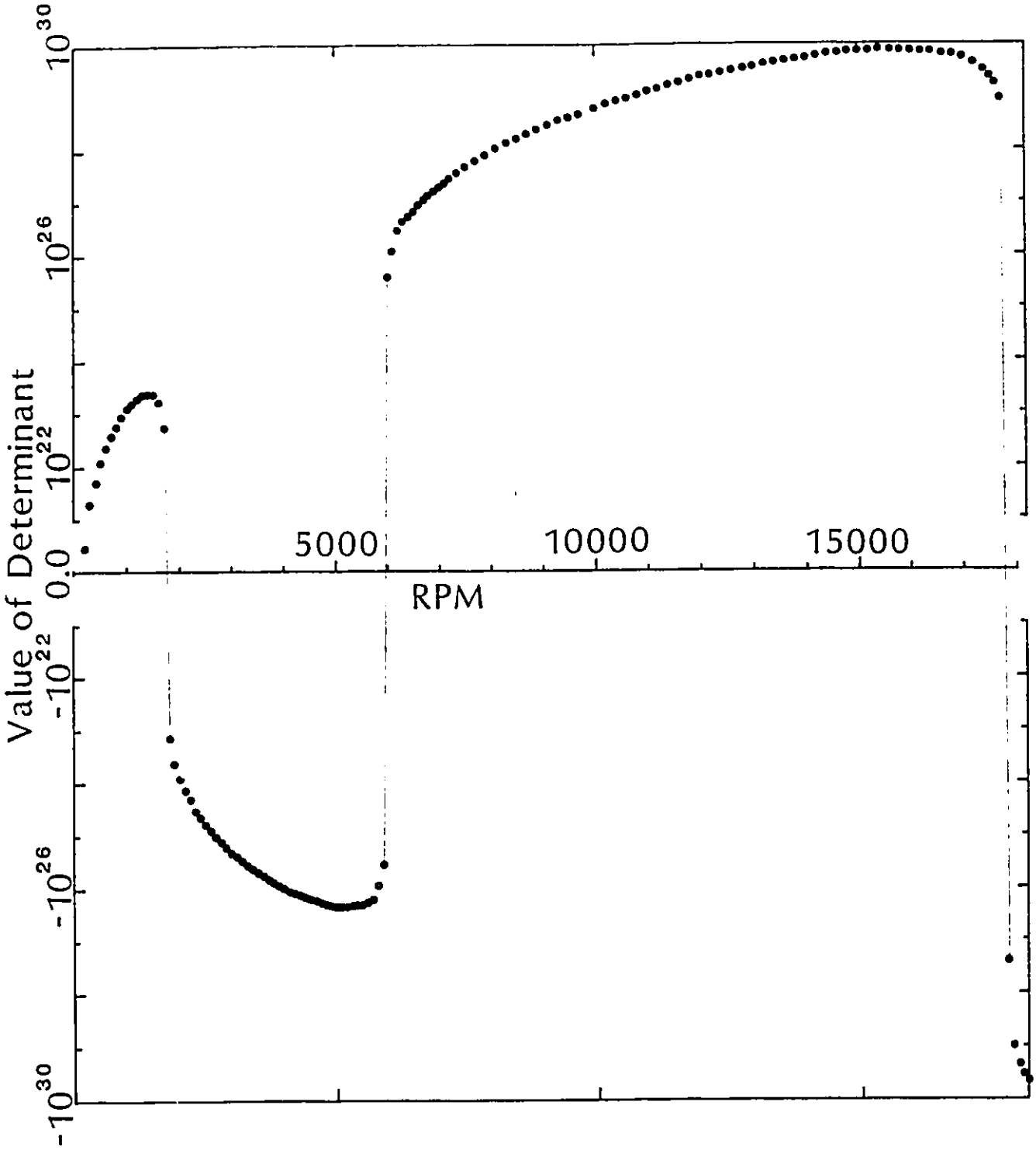

Fig. 4-32 Value of Determinant as a Function of RPM in ""Modified" Semi-Log Scale (Two-Disc Rotor)

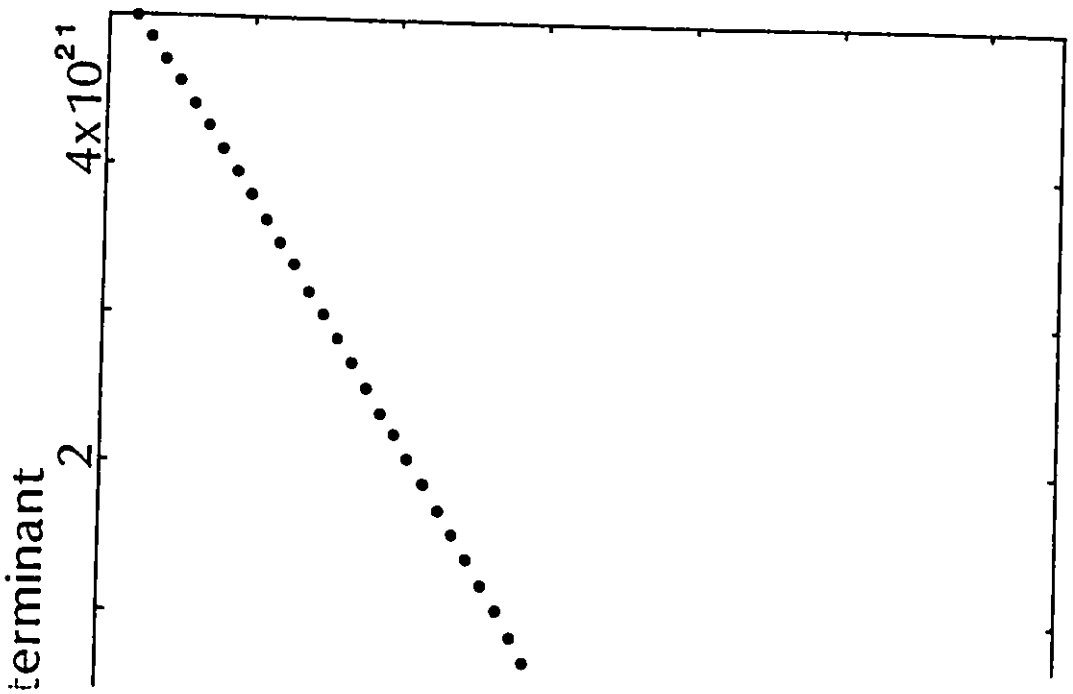
4x10^21
2
terminant

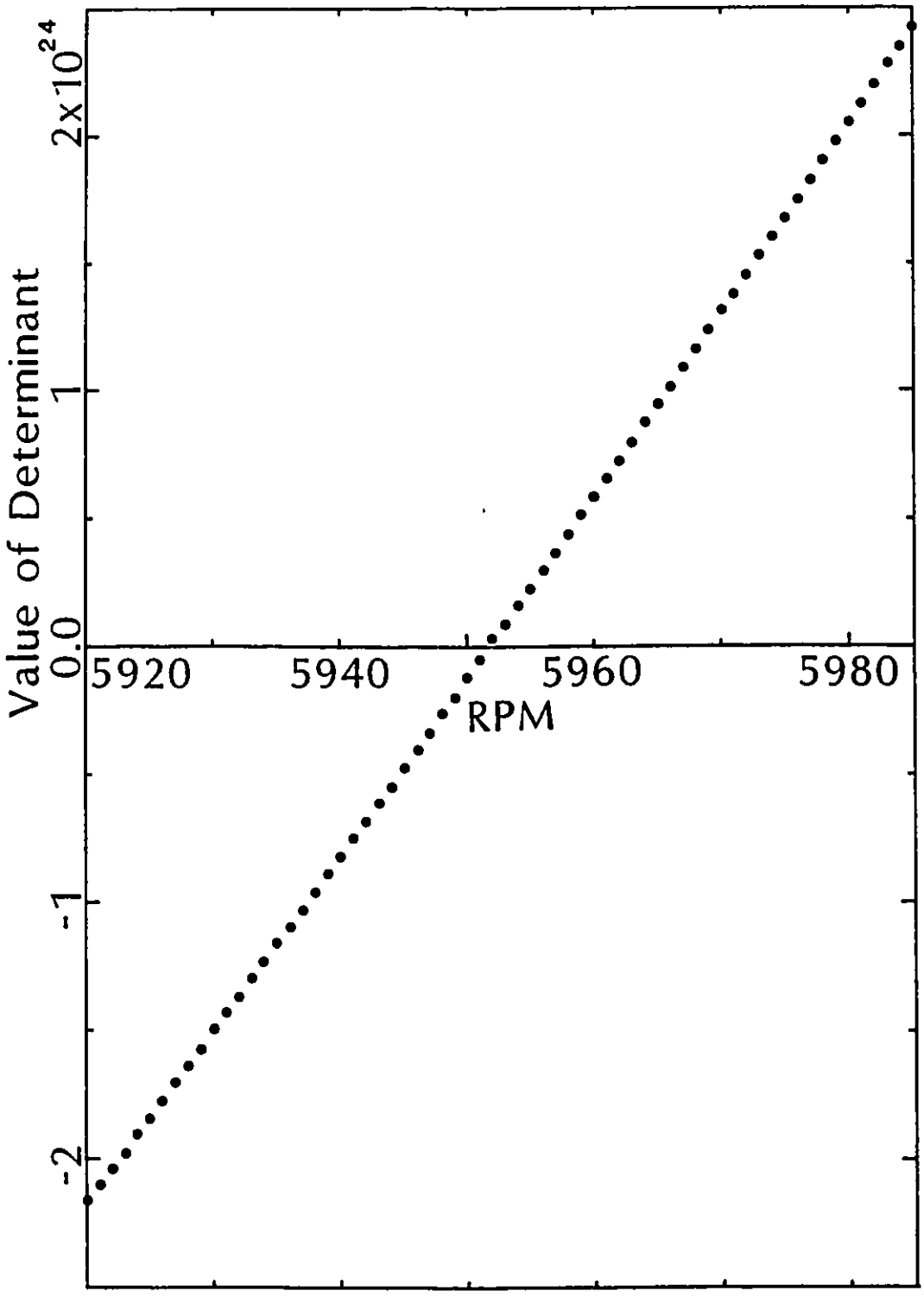

Fig. 4-34 Value of Determinant in the Vicinity of the Second Critical Speed (Two-Disc Rotor)

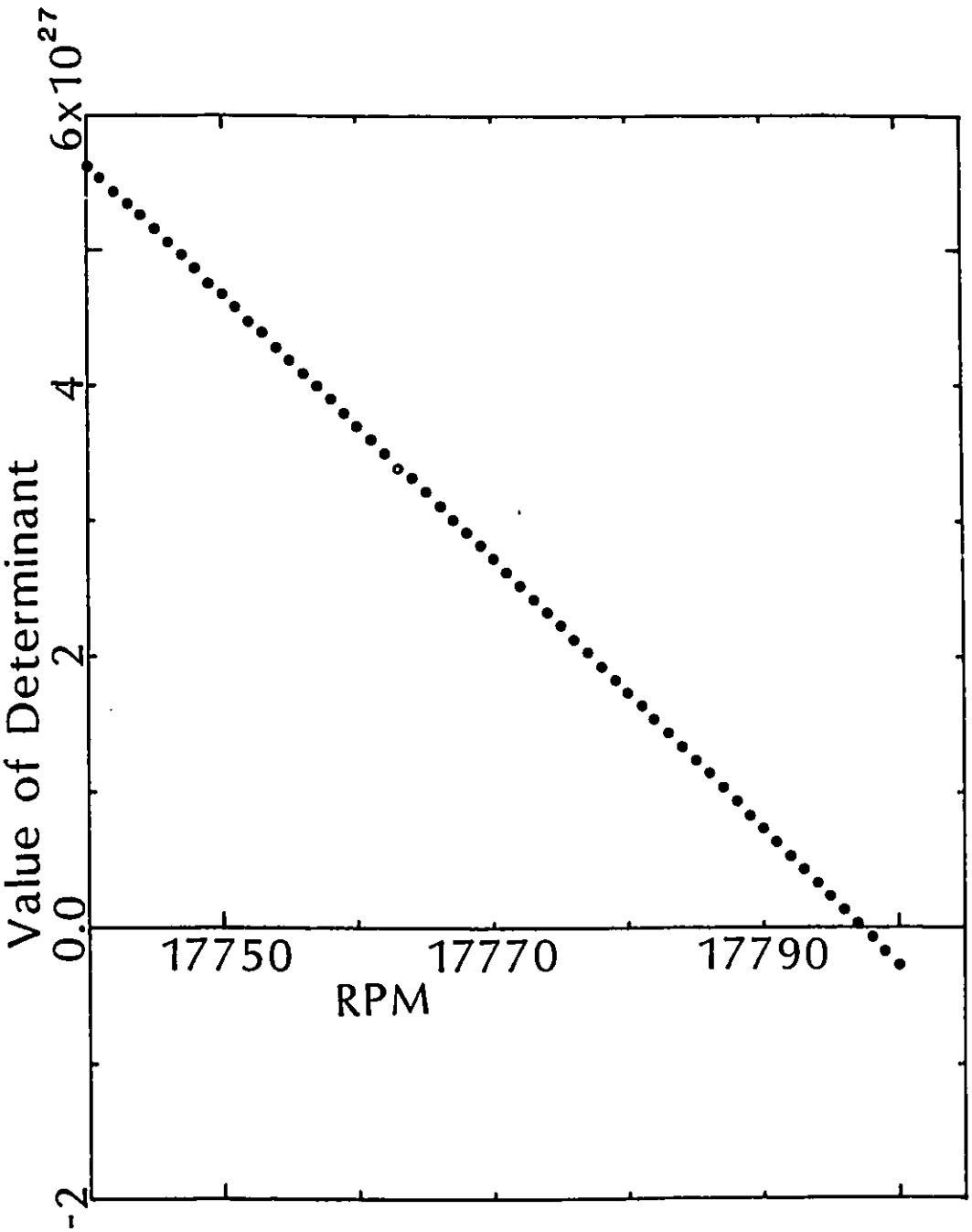

Fig. 4-35 Value of Determinant in the Vicinity of the Third Critical Speed (Two-Disc Rotor)

IV.6 Comparison with Other Methods

The model shown in Fig. 4-28 has been analysed by two different computer programs, one is based on the new method presented in this thesis and the other based on the Transfer Matrix Method. The independent computer program for rotor critical speed calculation based on the Transfer Matrix Method has been programmed originally in 1968 by then research officer, Mr. E.H. Dudgeon (Ref. 70). It has been used many times over the period of almost two decades, and its validity has been well established through applications to numerous projects at NRC. All the physical input parameters and characteristics were kept identical for both computer programs. That is, used are identical input parameters such as the configuration of stations and segments, physical constants, etc.

The rotor model has been solved for up to the third critical speed using both methods. The results from the new simplified method are compared with those from the Transfer Matrix Method. The comparison is given in Table 4-1 in terms of percentage difference.

When we compare with the results from the Transfer Matrix Method, the results from the present method are within 1% for the first and the second critical speeds, and within 3% for the third critical speed. This is an excellent agreement considering the fact that the results are based on two completely different methods.

Table 4-1: Critical Speeds of Two-Disc Rotor-Bearing System (Analytical Results)

(unit: RPM)

Critical Speeds	Transfer Matrix Method	Present Method	Difference %
1st critical speed ($=\omega_1$)	1732	1733	0.06
2nd critical speed ($=\omega_2$)	5912	5951	0.66
3rd critical speed ($=\omega_3$)	18315	17797	2.83

IV.7 Conclusions

A two-disc rotor-bearing system has been successfully analysed for its critical speeds using the method proposed in this thesis.

The results were compared with those from a different computer program based on the Transfer Matrix Method which has been well established as one of the most successful methods since 1944.

Percentage differences in the numerical values of the critical speeds from the two independent methods are:

i) within 0.1% in case of the first critical speed,

ii) within 1% for the second critical speed, and

iii) within 3% for the third critica speed.

When all the experimental and analytical results are compared, the maximum difference in percentage in case of the first critical speed is 0.81% as shown in Table 4-2. This illustrates the validity of the present method for critical speed prediction of rotor-bearing systems.

Table 4-2: Critical Speeds of Two-Disc Rotor-Bearing System (Overall Results)

(Unit: RPM)

Critical Speed	Experimental		Analytical		Maximum Difference (%)
	Dynamic Testing	Quasi-Static Testing	Transfer Matrix Method	Present Method	
ω_1	1719	1730	1732	1733	0.81
ω_2	-	-	5912	5951	0.66
ω_3	-	-	18315	17797	2.83

CHAPTER V

APPLICATION TO A GENERAL CONFIGURATION - PROHL'S ROTOR-BEARING SYSTEM

V.1 Introduction

The rotor-bearing system solved in the previous chapter has a rather simple physical configuration compared with that of general industrial turbo-rotors. As discussed earlier, this is because a test rotor of this simple configuration was set up for the experimental confirmation.

As an illustration of the sound capability of the new method in dealing with any "general" rotor, a rotor with complicated geometry has been selected from the open literature to be analysed by the new method. The rotor selected is that of Prohl. Prohl analysed this rotor and his results were published in 1944 [Ref. 48]. Later in 1958, Urban analysed the same rotor again and compared his results with Prohl's. Detailed physical dimensions and material characteristics of the rotor are available in Urban's thesis [Ref. 48] and are also given in the next section along with a sketch of the rotor.

V.2 Description of Prohl's Rotor

A sketch of Prohl's rotor is shown in Fig. 5-1. This is reproduced from his paper of 1944 (Ref. 48). Prohl's paper, however, did not present material characteristics of the discs and some of the fine details of physical dimensions. A complete set of data on the physical dimensions and material characteristics of Prohl's rotor has been given by Urban (Ref. 48). This is reproduced in Tables 5-1 and 5-2.

As shown in Fig. 5-1, the physical configuration of Prohl's rotor is quite "general" in the sense that it has complicated geometry, a total of eight discs, ten different shaft diameters, and one overhung end-condition. The complexity of actual industrial rotors is therefore reflected in this rotor system.

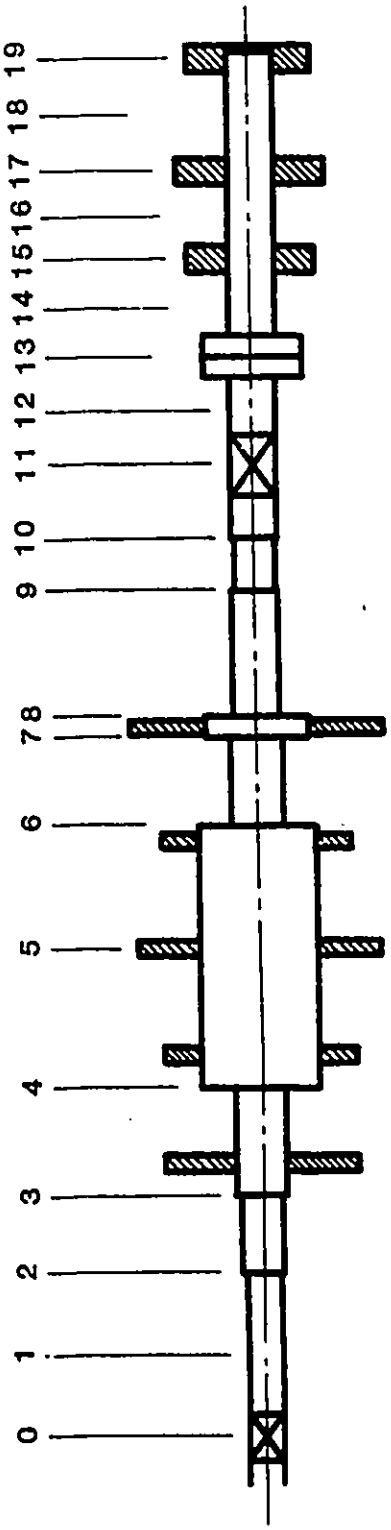

Fig. 5-1 Prohl's Rotor (Ref. 48)

Table 5-1: Shaft Parameters Defining Prohl's Rotor [Ref. 48]

Segment	L (in.)	d (in.)	a (in.^{2})	I (in.^{4}) *	EI (lb-in.^{2})	K(10^{11}) $[\frac{sec^2}{in.^4}]$ **
1	8.1250	1.6562	2.1543	0.3693	1.1079(10^7)	14.2046
2	3.6250	2.0625	3.3410	0.8883	2.6659(10^7)	9.1595
3	1.5626	2.3437	4.3141	1.4811	4.4433(10^7)	7.0933
4	3.6250	2.3437	4.3141	1.4811	4.4433(10^7)	7.0933
5	1.5938	5.7813	26.2507	54.8368	1.6451(10^9)	1.1658
6	5.2813	5.7813	26.2507	54.8368	1.6451(10^9)	1.1658
7	5.2500	5.7813	26.2507	54.8368	1.6451(10^9)	1.1658
8	0.7500	5.7813	26.2507	54.8368	1.6451(10^9)	1.1658
9	4.2500	2.3437	4.3141	1.4811	4.4433(10^7)	7.0933
10	0.5000	5.0000	19.6350	30.6796	9.2039(10^8)	1.5585
11	0.5000	5.0000	19.6350	30.6796	9.2039(10^8)	1.5585
12	6.1250	2.1875	3.7583	1.1240	3.3720(10^7)	8.1425
13	2.3750	2.0000	3.1416	0.7854	2.3562(10^7)	9.7409
14	3.6875	2.1875	3.7583	1.1240	3.3720(10^7)	8.1425
15	5.2500	2.1875	3.7583	1.1240	3.3720(10^7)	8.1425
16	2.0000	4.9375	19.1472	29.1742	8.7523(10^8)	1.5982
17	4.8125	2.1875	3.7583	1.1240	3.3720(10^7)	8.1425
18	4.2500	2.1875	3.7583	1.1240	3.3720(10^7)	8.1425
19	5.5625	2.1875	3.7583	1.1240	3.3720(10^7)	8.1425
20	0.4375	2.1875	3.7583	1.1240	3.3720(10^7)	8.1425

* $I = \frac{\pi d^4}{64}$

** $K = \frac{w_s a}{gEI} = \frac{\mu}{EI}$

Table 5-2: Disk Parameters Defining Prohl's Rotor [Ref. 48]

Section	W (lbs)	m $[\frac{lb\text{-}sec^2}{in.}]$ *	h (in.)	D_d (in.) **	I_d (lb-in-sec^2) ***
1	0	0	0	0	0
2	0	0	0	0	0
3	12.12	0.0314	0.75	10.41	0.2235
4	0	0	0	0	0
5	7.76	0.0201	0.75	9.97	0.1668
6	16.80	0.0435	0.75	13.27	0.570
7	7.76	0.0201	0.75	9.97	0.1668
8	0	0	0	0	0
9	0	0	0	0	0
10	20.18	0.0523	0.75	14.01	0.723
11	0	0	0	0	0
12	0	0	0	0	0
13	0	0	0	0	0
14	0	0	0	0	0
15	0	0	0	0	0
16	0	0	0	0	0
17	7.85	0.0203	1.00	7.40	0.0757
18	11.15	0.0289	1.00	8.70	0.1454
19	7.01	0.0182	1.00	7.03	0.0615
20	0	0	0	0	0

* $m = \frac{W}{g}$

** $D_d = \sqrt{\frac{4W}{\pi h w_d}}\, d^2$

*** $I_d = \frac{\pi h w_d}{64g} [D_d^4 - d^4]$

V.3 Results

Prohl's rotor shown in Fig. 5-1 had been analysed originally by Prohl (Ref. 48) in 1944, and then by Urban (Ref. 49) in 1958. Although they examined the identical rotor, their methods of dividing the rotor into a series of rotor segments were different. That is, Urban divided the rotor into twenty segments while Prohl divided it into nineteen. Prohl divided the rotor in a subjective manner so that an identical rotor can be divided in many different ways. Urban introduced a "station" whenever there was some geometric discontinuity such as a step change in the shaft diameter, or whenever there was a dynamic discontinuity such as an external shear force. The rotor is divided in this thesis in the manner used by Urban. Figure 5-2 represents the rotor along with all the station numbers depicting the manner in which the rotor segments are established.

Prohl's rotor shown in Fig. 5-2 is analysed using the computer program based on the general procedure described in Section III.3.3.9. The computer program listing as well as the actual computer run itself are given in Appendix B.

The results found are as follows:

i) the first critical speed (ω_1)

ω_1 = 2,059 RPM

ii) the second critical speed (ω_2)

ω_2 = 4,141 RPM

iii) the third critical speed (ω_3)

ω_3 = 12,883 RPM

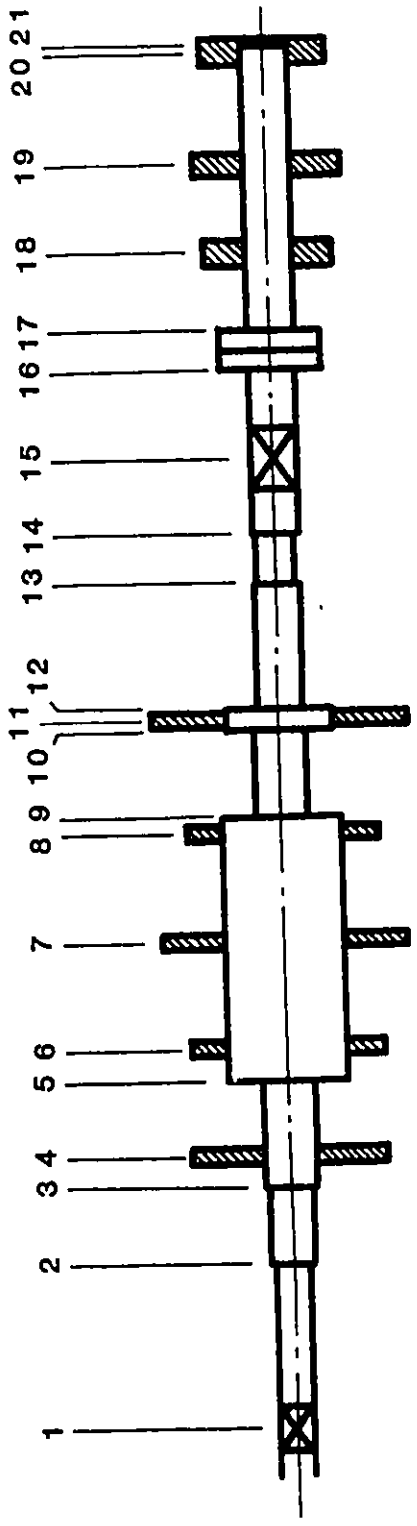

Fig. 5-2 Prohl's Rotor with Its Stations Adjusted

Again, the elements of the final matrix were divided by five times the RPM value, to control the overflow problem. The values of the determinant was plotted as a function of the rotational speed of the rotor. In Fig. 5-3, the value of the determinant is plotted with the scale of the ordinate changed. This was necessary to accommodate all the values of reasonable magnitude in one graph. The same information is plotted in Fig. 5-4 in a "modified" semi-logarithmic scale without changing the scale of ordinate. Figures 5-5 to 5-7 are close-up plots of the determinants value in the vicinities of the first, second, and third critical speeds, respectively.

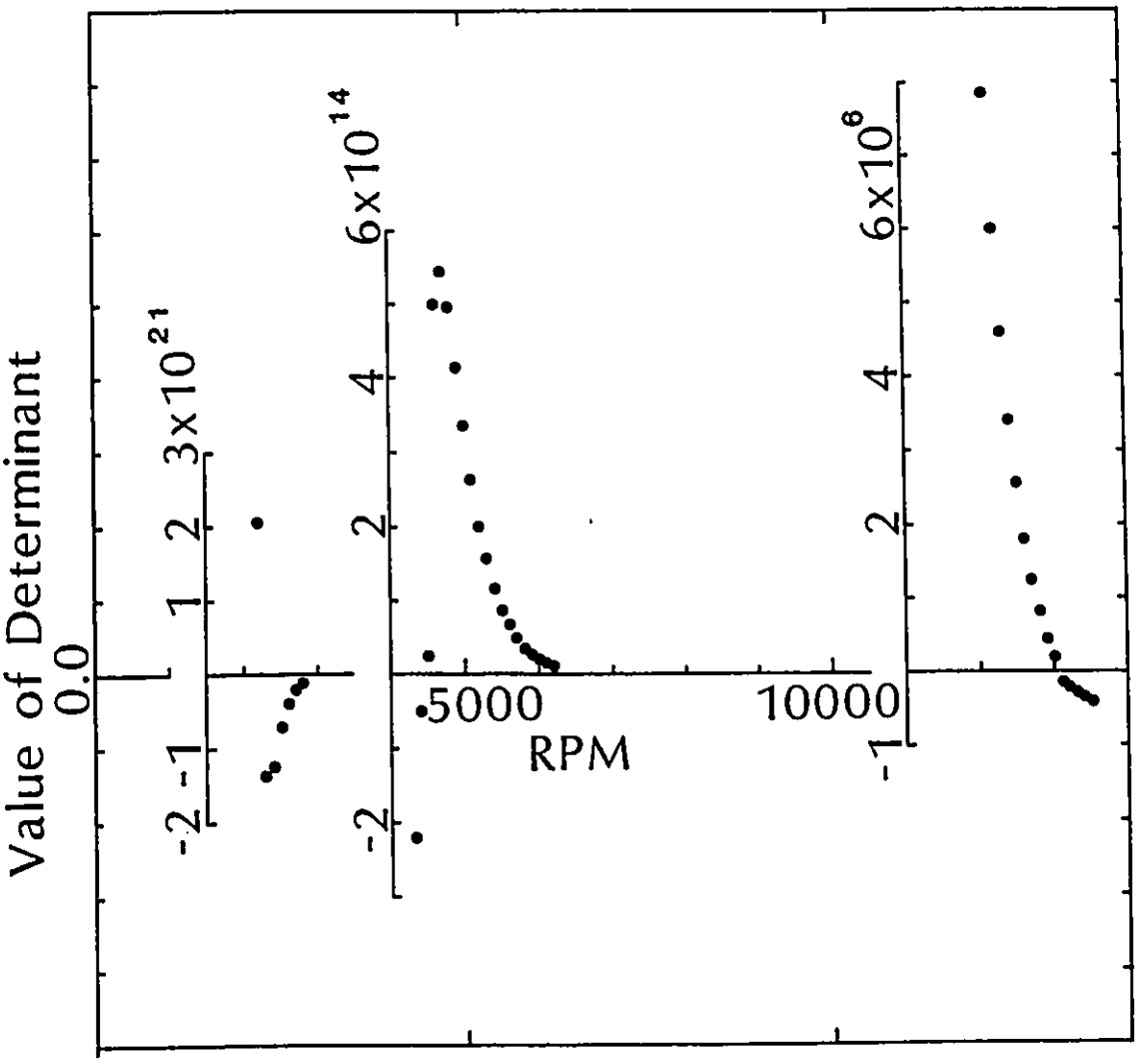

Fig. 5-3 Value of Determinant as a Function of Rotor RPM (Prohl's Rotor)

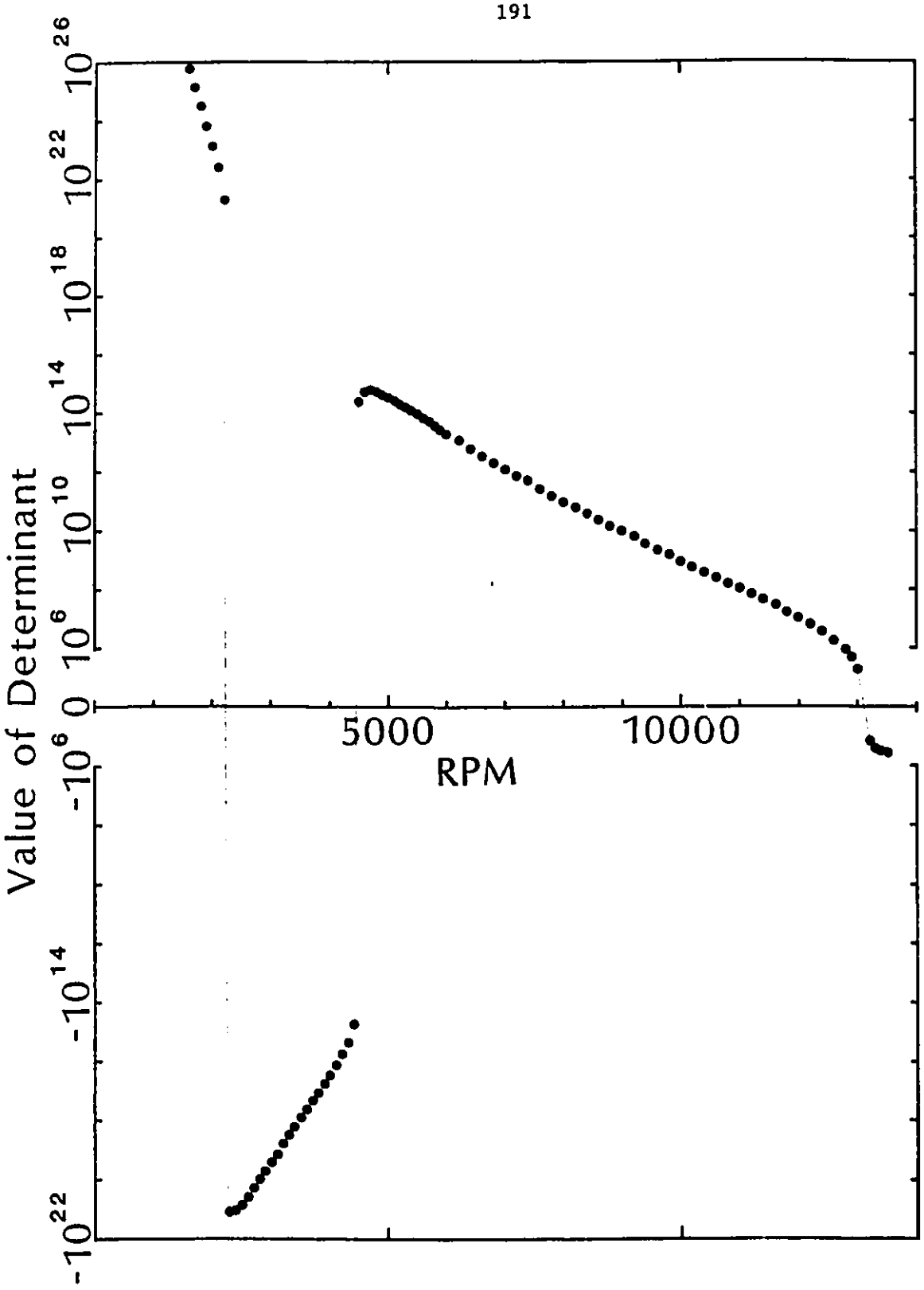

Fig. 5-4 Value of Determinant as a Function of RPM in "Modified" Semi-Log Scale (Prohl's Rotor)

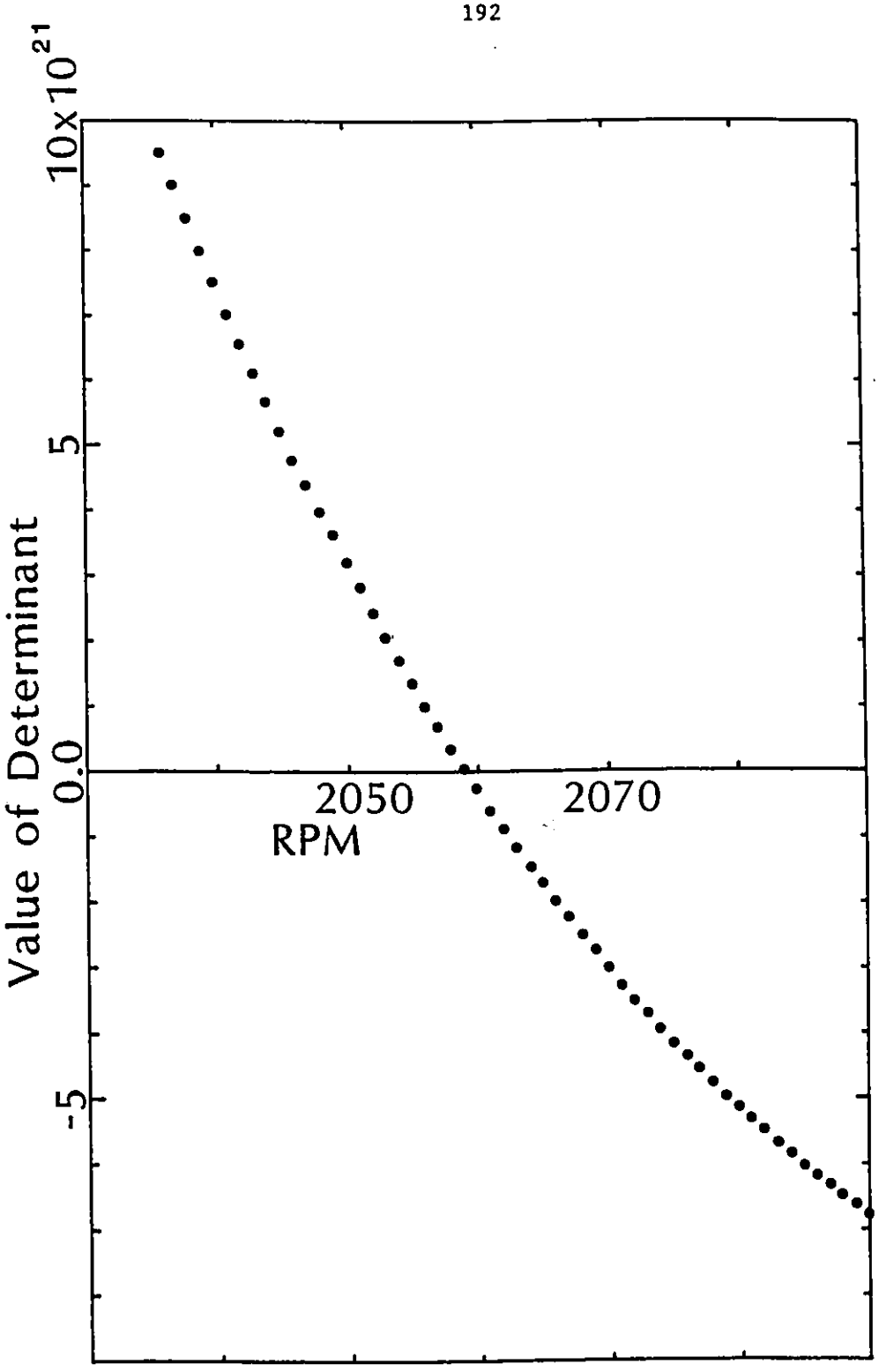

Fig. 5-5 Value of Determinant in the Vicinity of the First Critical Speed (Prohl's Rotor)

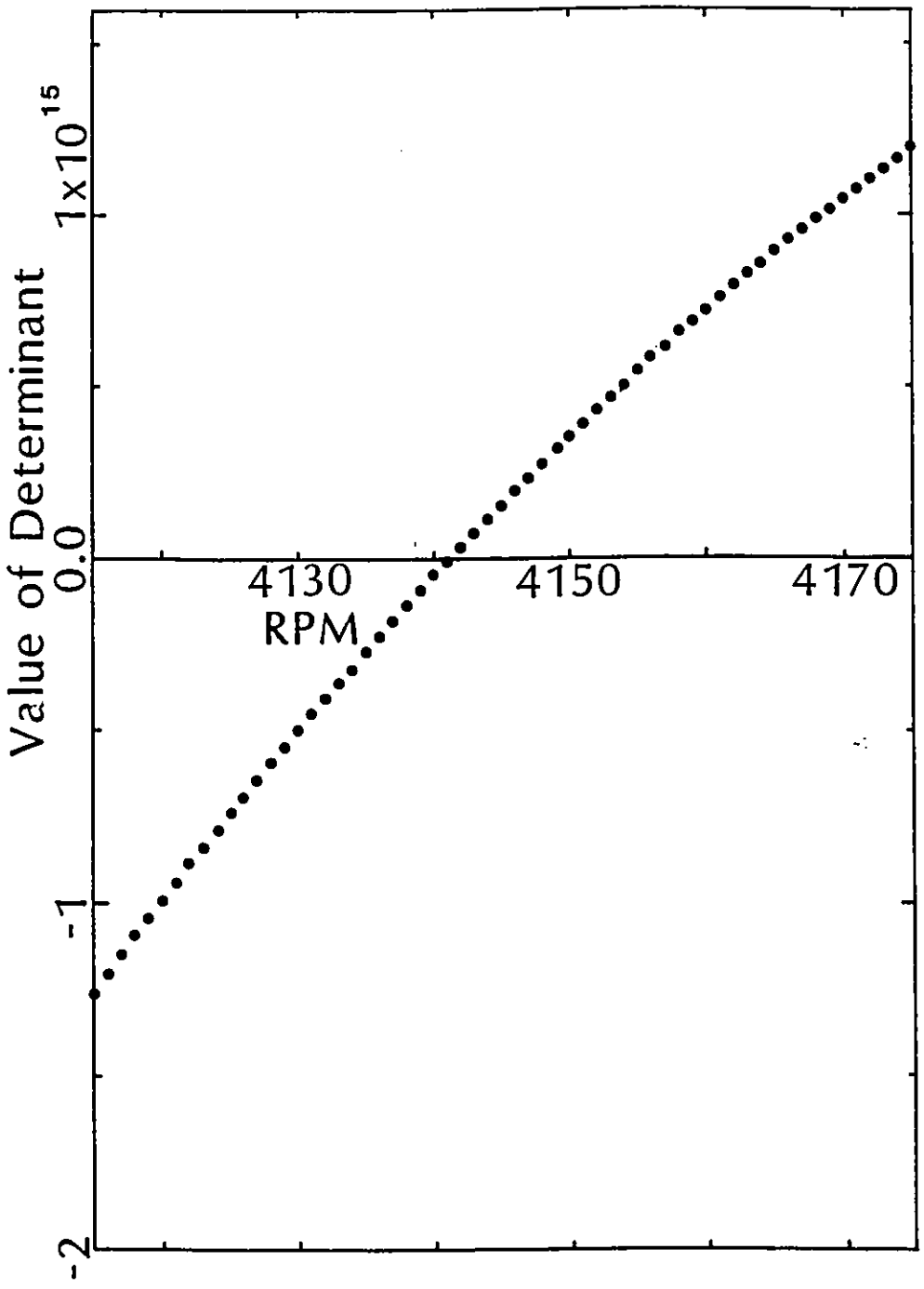

Fig. 5-6 Value of Determinant in the Vicinity of the Second Critical Speed (Prohl's Rotor)

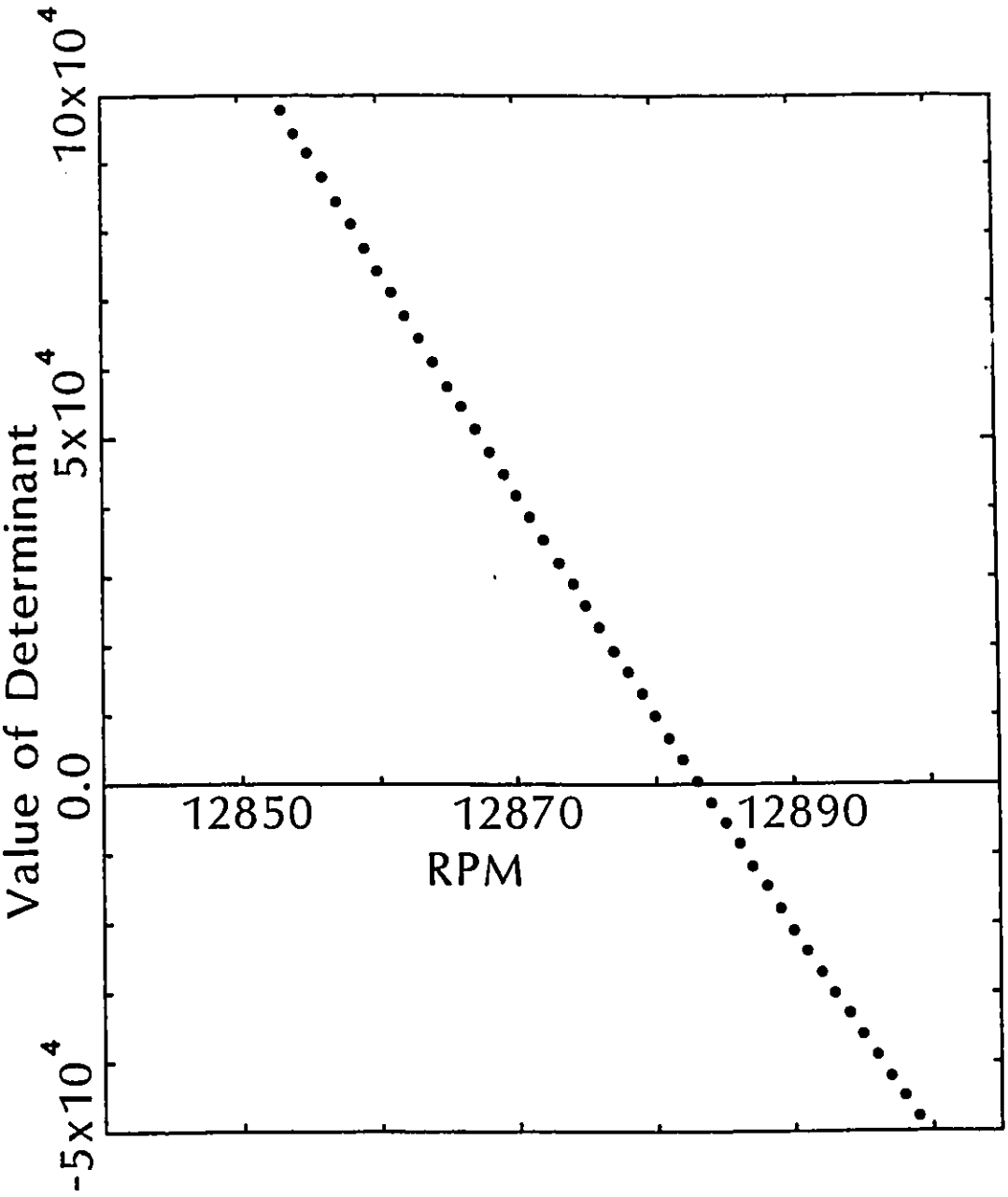

Fig. 5-7 Value of Determinant in the Vicinity of the Third Critical Speed (Prohl's Rotor)

V.4 Comparison with Other Methods

For the purpose of comparison, Prohl's rotor shown in Fig. 5-2 has been analysed using two different computer programs based on the Transfer Matrix Method and the new method presented in this thesis. The results from these two methods and those of Urban (Ref. 48) are given in Table 5-3 for comparison.

When the results from the present method are compared with those of Urban, the first critical speeds are within 1%, the second critical speeds within 0.025%, the third critical speeds within 0.11%.

When the results from the present method are compared with those from the Transfer Matrix Method, the first and second critical speeds are within 0.05%, and the third critical speed within 0.04%.

This is an excelent agreement considering the fact that the results are based on completely different methods.

Table 5-3: Critical Speeds of Prohl's Rotor

(unit: RPM)

Methods / Critical Speeds	Urban [Ref. 48]	Transfer Matrix Method	Present Method
ω_1	2040	2058	2059
ω_2	4140	4139	4141
ω_3	12870	12878	12883

V.5 Conclusions

As an example of a general rotor configuration, Prohl's rotor-bearing system has been selected and successfully analysed for its critical speeds using the new simplified method proposed in this thesis. The physical configuration of Prohl's rotor is indeed "general" in the sense that its geometry is complicated, that is, it has a total of eight discs, ten different shaft diameters, and one overhung end-condition.

The results were compared with those from a different computer program based on the Transfer Matrix Method, and those available in the open literature.

When the results from the new method and the Transfer Matrix Method are compared, percentage differences in the numerical values of the critical speeds are consistently less than 0.05% at the first, second and third critical speeds. This proves the validity of the new simplified method as a general method for critical speed analysis for practical rotors with complicated geometry.

CHAPTER VI

CONCLUSIONS

VI.1 Merits and Advantages of the Present Method

A number of merits and advantages of the present method are listed below:

1) The theory and procedures necessary in the development of this method are straightforward. The Euler beam solution was applied to a rotor-bearing system. This generates a set of governing equations for the critical speeds of the system in the form of a sparse and banded determinant. By solving for specific values of ω (the rotational speed of the shaft) which makes the value of the determinant vanish, the critical speeds of the rotor-bearing system are found. The analysis is exact within the limits of the inherent assumptions of the Euler beam solution. The method can be applied to other analytical approaches with closed-form general solutions.
2) The overall matrix, representing any rotor system, can be readily generated by the computer program. Once boundary conditions are defined, they are directly applicable to general rotor-bearing systems. Further, by simply storing them in computer memory, the overall matrix can be generated by calling appropriate boundary conditions.
3) A numerical algorithm for calculation of the determinant of the overall matrix has been developed and illustrated in Appendix C. The computing procedures are based on "pivoting" and a recurrence

characteristic of the banded matrix. The basic recurrence numerical scheme deals with a pivoting process of a six-by-eight (6×8) matrix only. Thus, micro-computers with limited memory capacity can be used in the calculation of critical speeds of complex rotor-bearing systems.

4) Further, due to the ease of overflow control, micro-computers can be used without compromise in accuracy. Since a large number of calculations are involved in the process of critical speed calculation, the numbers in the computer often "overflow", that is, the numbers become too large to be handled by the computer. Without overflow control, it is extremely difficult to create computer code for mini- or micro-computers. Although the "Dynamic Reduction Technique", in conjunction with the Finite Element Method, can be used, this introduces some compromise in accuracy. With the method proposed in this thesis, it is easy to eliminate the occurence of overflow since the governing equations for the critical speeds are a set of homogeneous equations, and can be divided by a constant without affecting the final results. Thus, normalization of the matrix (as a whole or as a local partition) can be directly achieved.

5) The mode shape of the rotor is directly available as a continuous curve rather than discrete points. Therefore, the deflection, slope, bending moment and shear are available at any location along the rotor length without establishing a station at the location.

6) Different end conditions do not affect the entire set of equations. In the Transfer Matrix Method, an entirely different set of equations result if the end conditions change. For example, the final equations to be solved in the case of a "free end" are different from that for "clamped" or "hinged" ends. In the new method, boundary conditions do not affect anything beyond the local partitioned matrix which corresponds to that particular boundary. This renders to the present method the exceptional capability to accommodate any type and number of couplings. That is, at least in theory, the present method can accommodate any finite number of couplings without changes in its general procedure.

VI.2 Conclusions

A number of rotor-bearing systems have been analyzed and the governing equations of the system have been derived. The analytical expression for the governing equations were shown to be a set of homogeneous equations forming a sparse, banded matrix.

For non-trivial solutions, the determinant of the banded matrix must vanish. Based on the direct relationships between the boundary conditions of the rotor-bearing system and the banded partitions of the overall matrix, a unique and simplified method of critical speed prediction has been developed. A basic recurrence numerical scheme to calculate the determinant of the overall matrix has been formulated.

A computer program based on this new method has been developed, and two examples have been analysed, namely a two-disc rotor and a rotor of "general" configuration.

An experimental study on the two-disc rotor-bearing system has been carried out and presented. A unique experimental scheme of the initial runout compensation using an encoder system has been utilized, and the results from the dynamic and the quasi-static testing are presented.

All the results from analytical and experimental studies show excellent agreement substantiating the validity of the new method proposed in this thesis.

REFERENCES

1. Rankine, W.J.M., On the Centrifugal Force of Rotating Shafts, The Engineer, Vol. 27, April 1869, p. 249.
2. Eshleman, R.L., Flexible Rotor-Bearing System Dynamics - Part I: Critical Speeds and Response of Flexible Rotor Systems, ASME Publication No. H42, New York, N.Y., 1972.
3. Lowey, R.G., Piarulli, V.J., The Dynamics of Rotating Shafts, SVM, No. 4, The Shock and Vibration Information Center, Washington, D.C. 1970.
4. Lund, J.W., Rotor-Bearing Dynamics Design Technology, Part III: Design Handbook for Fluid-Film Type Bearings, Mechanical Technology Incorporated, Technical Report AFAPL-TR-65-45, Part 3, May 1965.
5. Johnes, A.B., McGrew, J.M. Jr., Rotor-Bearing Dynamics Technology Design Guide, Part III: Ball Bearings, Shaker Research Corp., Technical Report AFAPL-TR-78-6, Part II, February 1978.
6. Rieger, N.F., Flexible Rotor-Bearing System Dynamics - III, Unbalance Response and Balancing of Flexible Rotors in Bearings, ASME Publication, New York, N.Y. 1973.
7. Tse, F.S., Morse, I.E., Hinkle, R.T., Mechanical Vibrations Theory and Application, 2nd ed. Allyn & Bacon Inc., Boston, 1963.
8. Crandall, S.H., Engineering Analysis, McGraw-Hill Book Co., 1956.
9. Willem, N., Holzer, S.M., Critical Speeds of Rotating Shaft Subjected to Axial Loading and Tangential Torsion, Trans. ASME, J. Engrg. Ind., Vol. 89, No. 2, May 1967, pp. 259-264.

10. Dunkerley, S., On the Whirling and Vibration of Shafts, Trans. Roy. Soc. (London), Vol. 185, Series A, 1894, pp. 279-360.

11. Stodola, A., Steam and Gas Turbines, McGraw-Hill Book Company Inc., New York, N.Y., 1927.

12. Den Hartog, J.P., Mechanical Vibrations, 4th Ed., McGraw-Hill Book Co. Inc., New York, N.Y., 1956.

13. Church, A.H., Mechanical Vibrations, John Wiley, 1957.

14. Hildebrand, F.B., Methods of Applied Mathematics, 2nd ed., Prentice-Hall, 1965.

15. Plunkett, R., Introduction to Mechanical Impedance Methods for Vibration Problems, Colloquium on Mechanical Impedance Methods for Mechanical Vibrations, presented at the ASME Annual Meeting, New York, N.Y., December 2, 1958, pp. 1-4.

16. Caruso, W.J., Prediction of Critical Speeds of Steam Turbines by Dynamic Stiffness Method, Colloquium on Mechanical Impedance Methods for Mechanical Vibrations, presented at the ASME Annual Meeting, New York, N.Y., December 2, 1958, pp. 137-145.

17. Ludwig, G.A., Vibration Analysis of Large High-Speed Rotating Equipment, Trans. ASME, J. Eng. Ind., May 1966, pp. 201-210.

18. Wright, D.V., Impedance Analysis of Distributed Mechanical Systems, Colloquium on Mechanical Impedance Methods for Mechanical Vibrations, presented at the ASME Annual Meeting, New York, N.Y., December 2, 1958, pp. 19-42.

19. Gladwell, G.M.L. and Bishop, R.E.D., The Vibration of Rotating Shafts Supported in Flexible Bearings, J. Mech. Engrg. Sci. Vol. 1, No. 3, 1959, pp. 195-206.

20. Lund, J.W., Modal Response of a Flexible Rotor in Fluid-Film Bearings, Trans. ASME, J. Eng. Ind., Vol. 96, No. 1, 1974, p. 525.

21. Lund, J.W., Stability and Damped Critical Speeds of a Flexible Rotor in Fluid-Film Bearings, Trans. ASME, J. Eng. Ind., Vol. 96, No. 1, 1974, p. 509.

22. Hashish, E., Sankar, T.S., Finite Element and Modal Analysis of Rotor-Bearing Systems Under Stochastic Loading Conditions, Trans. ASME, J. Vib. Acoustics Stress Rel. in Design, Vol. 106, January 1984.

23. Bishop, R.E.D., The Vibration of Rotating Shafts, J. Mech. Engrg. Sci., Vol. 1, No. 1, 1959, pp. 50-65.

24. Gladwell, G.M.L., Bishop, R.E.D., The Receptances of Uniform and Non-uniform Rotating Shafts, J. Mech. Engrg. Sci., Vol. 1, 1959, pp. 78-91.

25. Bishop, R.E.D, Gladwell, G.M.L., The Vibration and Balancing of an Unbalanced Flexible Rotor, J. of Mech. Engrg. Sci., Vol. 1, 1959, pp. 66-77.

26. Bishop, R.E.D, Unbalanced and Initially Bent Shafts, Engineering, Vol. 190, December 23, 1960, pp. 848-849; Vol. 191, March 3, 1961, pp. 312-313.

27. Bishop, R.E.D., Parkinson, A.G., On the Isolation of Modes in The Balancing of Flexible Shafts, Proc. Instn. Mech. Engrs., Vol. 177, No. 16, 1963, pp. 407-423.

28. Bishop, R.E.D., Parkinson, A.G., Second-Order Vibration of Flexible Shafts, Phil. Trans. Roy. Soc. (London) (A), Math. Phys. Sc., Vol. 259, No. 1095, 1965, pp. 619-649.

29. Bishop, R.E.D, An Introduction to the Balancing of Flexible Rotors, Engng. Mat. Des., Vol. 9, 1966, pp. 1468-1474.

30. Bishop, R.E.D., Mahalingam, S., Some Experiments in the Vibration of a Rotating Shaft, Proc. Roy. Soc. A, Vol. 292, 1966, pp. 537-561.

31. Bishop, R.E.D, Parkinson, A.G., Vibration and Balancing of Flexible Shafts, Applied Mechanics Reviews, Vol. 21, No. 5, May 1968, pp. 439-451.

32. Bishop, R.E.D, Parkinson, A.G., On the Use of Balancing Machines for Flexible Rotors, J. Eng. Ind., Trans. ASME, Vol. 94, Series B, No. 2, May 1972, pp. 561-576.

33. Lindley, A.L.G., Bishop, R.E.D., Some Recent Research on the Balancing of Large Flexible Rotors, Proc. I. Mech. E., Vol. 177, No. 30, 1963, pp. 811-825.

34. Parkinson, A.G., Bishop, R.E.D., Vibration and Balancing of Rotating Continuous Shafts, J. Mech. Eng. Sci. Vol. 3, No. 3, 1961, pp. 200-213.

35. Parkinson, A.G., Jackson, K.L., Bishop, R.E.D., Some Experiments on the Balancing of Small Flexible Rotors: Part I - Theory, J. Mech. Eng. Sci., Vol. 5, No. 1, 1963, pp. 114-130.

36. Parkinson, A.G., Jackson, K.L., Bishop, R.E.D., Some Experiments on the Balancing of Small Flexible Rotors; Part II - Experiments, J. Mech. Eng. Sci. Vol. 5, No. 2, 1963, pp. 133-145.

37. Parkinson, A.G., The Vibration and Balancing of Shafts Rotating in Asymmetric Bearings, J. Sound Vib., Vol. 2, No. 4, p. 477, 1965.

38. Parkinson, A.G., The Vibration and Balancing of Rotating Shafts, Ph.D. Thesis, University of London, 1965.

39. Parkinson, A.G., Bishop, R.E.D., Residual Vibration in Modal Balancing, J. Mech. Eng. Sci., Vol. 7, No. 1, 1965, pp. 33-39.

40. Parkinson, A.G., On the Balancing with Axial Asymmetry, Proc. Roy. Soc., 294, Series A, 1966, p. 66.

41. Parkinson, A.G., An Introduction to the Vibration of Rotating Flexible Shafts, Bull. Mech. Engng. Educ., Vol. 6, 1967, p. 47.

42. Parkinson, A.G., Balancing of Flexible Shafts Rotating in Massive Flexible Bearings, J. Mech. Eng. Sci. Vol. 15, No. 6, December 1973, pp. 430-438.

43. Parkinson, A.G., The Balancing of Flexible Rotors, Dynamics of Rotors, IUTAM Symposium, Lyngby, Denmark, 1974, (Sponsored by International Union of Theoretical and Applied Mechanics), pp. 413-435.

44. Parkinson, A.G., The Modal Interpretation of the Vibration of a Damped Rotating Shaft, I. Mech. E. Conference, Vibrations in Rotating Machinery, University of Cambridge, England, 15-17 Sept. 1976, pp. 263-267.

45. Eshleman, R.L., Critical Speeds and Response of Flexible Rotors, Proceedings of Third Turbo Mechanics Seminar, Toronto, Canada, 19 September 1974, Sponsored by Turbo Mechanics Sub-Committee, Associate Committee on Propulsion, National Research Council, Canada.

46. Lund, J.W., Orcutt, F.K., Calculations and Experiments on the Unbalance Response of a Flexible Rotor, Trans. ASME, J. Eng. Ind., Vol. 89, No. 4, November 1967, pp. 785-796.

47. Prohl, M.A., A General Method for Calculating Critical Speeds of Flexible Rotors, Trans. ASME, J. Appl. Mech., Vol. 12, No. 3, September 1945, pp. A142-A148.

48. Urban, R.L., Extension of Holzer-Myklestad-Prohl Calculation of Turbo-Rotor Critical Speeds, M.S. Thesis, Illinois Institute of Technology, January 1958.

49. Urban, R.L., Extension of Holzer-Myklestad-Prohl Calculation of Turbo-Rotor Critical Speeds, ASME, Paper 58-A-246, 1958.

50. Ruhl, R.L., Dynamics of Distributed Parameter Turbo-Rotor Systems: Transfer Matrix and Finite Element Techniques, Ph.D. Thesis, Cornell University, Ithaca, New York, January 1970.

51. Thomson, W.T., Matrix Solution for the Vibration of Non-Uniform Beams, J. Appl. Mech., Vol. 17, No. 3, 1950, pp. 337-339.

52. Wolfe, W.A., Wong, P.Y., On the Transfer Matrix for Rotor Dynamics, Trans. CSME, Vol. 2, No. 3, 1973-74, pp. 129-135.

53. Thomson, W.T., Vibration Theory and Applications, Prentice-Hall Inc., 1965.

54. Ekong, I.E., Eshleman, R.L., Bonthron, R.J., Dynamics of Continuous Multi-Mass Rotor Systems, ASME Paper 69-VIBR-51, 1969.

55. Miller, D.F., Forced Lateral Vibration of Beams on Damped Flexible End Supports, Trans. ASME, Vol. 75, J. Appl. Mech. Vol. 20, 1953, pp. 167-172.

56. Koenig, E.C., Analysis for Calculating Lateral Vibration Characteristics of Rotating Systems with Any Number of Flexible Supports; Part I, Method of Analysis, Trans. ASME, J. Appl. Mech. Vol. 28, 1961, pp. 585-590.

57. Ruhl, R.L., Booker, J.F., A Finite Element Model for Distributed Parameter Turbomotor Systems, Trans. ASME, J. Eng. Ind., February 1972, pp. 128-132.

58. Nelson, H.D., McVaugh, J.M., The Dynamics of Rotor-Bearing Systems Using Finite Elements, Trans. ASME, J. Eng. Ind., Vol. 98, No. 2, 1976, pp. 593-600.

59. Zorgi, E.S., Nelson, H.D., Finite Element Simulation of Rotor-Bearing Systems with Internal Damping, Trans. ASME, J. Eng. Power, Vol. 99, No. 1, 1977, pp. 71-76.

60. Nelson, H.D., A Finite Rotating Shaft Element Using Timoshenko Beam Theory, Trans. ASME, J. Mech. Design. Vol. 102, October 1980, p. 793.

61. Rouch, K.E., Kao, J.S., A Tapered Beam Finite Element for Rotor Dynamics Analysis, J. Sound Vib., Vol. 66, No. 1, 1979, pp. 119-140.

62. Rouch, K.E., Kao, J.S., Dynamic Reduction in Rotor Dynamics by the Finite Element Method, Trans, ASME, J. Mech. Design, Vol. 102, 1980, p. 360, (ASME Paper 79-DET-70).

63. Ozguven, H.N., Ozkan, N.L., Whirl Speeds and Unbalance Response of Multibearing Rotors Using Finite Elements, Trans. ASME, J. Vib. Acoustics Stress Rel. in Design, Vol. 106, January 1984, pp. 72-79.

64. Huebner, K.H., The Finite Element Method for Engineers, John Wiley & Sons, New York, 1975.

65. Dimensioning and Tolerancing for Engineering Drawings, OMC Drawing Standards, Reference ANSI Y145.5-1966, Outboard Marine Corporation, Marine Engineering Engine Section, 300 Sea Horse Drive, Waukegan, Illinois 60085, U.S.A.

66. "Glitch": Definition of and Methods for Correction, Including Shaft Burnishing to Remove Electrical Runout, Application Note, Bently Nevada Corp., Minden, Nevada, U.S.A., Aug. 1978.

67 Prentice, J.S., Smith, S.E. and Virtue, L.S., Safety in Polyethylene Plant Compressor Areas, Chemical Engineering Progress, Vol. 70, No. 9, Sept. 1974.

68. Stuart, J.W., Retrofitting Gas Turbines and Centrifugal Compressors with Proximity Vibration Probes, BNC-43-PUBS, Bently Nevada Corp., Minden, Nevada, U.S.A., 1974.

69. Operation and Maintenance Manual, Multichannel Vector Filter (VF-M), Bently Nevada Corp., Minden, Nevada, U.S.A., July 1979 (Revision A Nov. 1980).

70. Dudgeon, E.H., A Computer Program to Calculate the Critical Speeds of Flexible Rotors, Laboratory Memorandum GD-182, Division of Mechanical Engineering, National Research Council, May 1968.

71. Dudgeon, E.H., The Critical Speeds of Compound Flexible Rotors, Laboratory Memorandum GD-192, Division of Mechanical Engineering, National Research Council, April 1970.

72. Tang, T.M., Trumpler, P.R., Dynamics of Synchronous-Precessing Turborotors with Particular Reference to Balancing. Part 1 - Theoretical Foundations, Trans. ASME, J. Appl. Mech., Vol. 31, No. 1, March 1964, pp. 115-122.

73. Tang, T.M., Trumpler, P.R., Dynamics of Synchronous-Precessing Turborotors with Particular Reference to Balancing. Part 2 - Application, Trans. ASME, J. Appl. Mech., Vol. 35, No. 1, March 1968, pp. 25-28.

74. Pestel, E.C., Leckie, F.A., Matrix Methods in Elastomechanics, McGraw-Hill Book Co., Inc., New York, 1963.

APPENDIX A

Computer Program for the Two-Disc Rotor

```
C     RPMST  STARTING RPM
C     RPMEND END RPM
C     RPMDEL DELTA RPM
C     A      WORKING MATRIX A(I,J) USED IN SUBROUTINE DTMNT
C            DIMENSION =(4*NSEG,11)
C            DATA = 44*NSEG*11
C     WL     WORKING SPACE USED IN SUBROUTINE DTMNT
C            DIMENSION = 4**NSEG
C     L      LENGTH OR C-COORD OF SHAFT SEGMENTS MEASURED FROM LEFT END
C     ML     = M*L = ONE OF THE MAIN VARIABLES
C     DSHAFT DIAMETER OF THE SHAFT
C     DDISC  DIAMETER OF DISC
C     WDISC  WIDTH OR THICKNESS OF DISC
C     NSEG   NUMBER OF SEGMENT = (DIMENSION - 1)
C     NEND   STATION NUMBER AT THE END = DIMENSION OF L
C            (STATION NUMBER #1 STARTS FROM THE LEFT END, IE. 0.0)
C     M
C     PI      3.141592D0
C     G      GRAVITATIONAL CONSTANT (386.4D0 IN/SEC**2)
C
C     ********************************************************************
C     INET   NET (POLAR MASS) MOMENT OF INERTIA OF DISC.
C     E      YOUNG'S MODULUS(PSI)
C     IA     DIAMETRAL MOMENT OF INERTIA OF (CROSS SECTIONAL) AREA OF
C            SHAFT (IN**4)
C     MU     LINEAR SPECIFIC MASS OF SHAFT MATERIAL(UNITS PER UNIT LENGTH)
C                                          = (LB*SEC**2/IN**2)
C     RHOW   SPECIFIC WEIGHT OF SHAFT MATERIAL (LB/IN**3)
C     RHO    SPECIFIC  MASS  OF SHAFT MATERIAL  (LB*SEC**2/IN**4)
C     ********************************************************************
C
C
      IMPLICIT REAL*8(A-H,M,O-Z)
      REAL*8 IA,INET,L
      INTEGER RPMST,RPMEND,RPMDEL
C
C
C
      DIMENSION A(36,11)
      DIMENSION L(10),ML(10),NML(10)
      DIMENSION DDISC(10), WDISC(10), MDISC(10)
      DIMENSION DSHAFT(10)
C                           DIA. OF SHAFT IS 'SEGMENTAL',
C                                HOWEVER,DSHAFT(SEG)=DSHAFT(NEND)
      DIMENSION X(10),INET(10),ALPHA(10),BETA(10)
      DIMENSION EI(10), EIM(10), EI2(10), EI4(10)
      DIMENSION MU(10)
      DIMENSION WL(216)
C                              DIMENSION OF WL = 4 * 9 * NSEG
C                        ********** WL IS USED IN SUBROUTINE DTMNT ***
C                        ********** AS A WORKING SPACE             ***
C
C
```

```
      C
      C
   12         DATA A/396*0.0D0/
   13         DATA RHOW/0.284D0/
      C
      C
   14         DATA NSEG/9/
   15         DATA E/30.0D6/
   16         DATA RPMST/1700/, RPMEND/17800/, PRINCL /
   17         DATA L/0.0D0,2.0D0,17.0D0,18.0D0,19.0D0,
     +          50.0D0,51.0D0,66.0D0,68.0D0/
   18         DATA DSHAFT/2*3.0D0,3.0D0,2.0D0,2*3.0D0,3*2.0D0
      C                           DSHAFT(NEND)=DSHAFT(NEND-1)
   19         DATA DDISC/3*1.0D0,8.0D0,2*0.0D0,3.0D0,3*0.0D0/
   20         DATA WDISC/3*0.0D0,2.0D0,2*0.0D0,3.0D0,3*0.0D0/
      C                            WDISC IS "STATIONAL",
      C                            HOWEVER, IT SHOULD BE SET TO ZERO AT THE "CENTER
      C                            LINE STATION".
   21         PI=3.14159265D0
   22         G=32.2D0*12.0D0
   23         RHO=RHOW/G
   24         NEND=NSEG+1
   25         N=NSEG*4
      C                                        N IS USED IN A(N,11)
      C                                         REASON FOR "11" ------ LAMB
      C                                      ALGORITHM FOR BAND MATRIX
   26         NDUMMY=N*6
      C                                        NDUMMY IS USED IN DETM
      C                      PURPOSE OF THIS DO LOOP - TO DEFINE EI(I) AND
      C                           FROM 1 TO NEND.
      CC           DO 3 I=1,NSEG
   27              DO 3 I=1,NEND
   28              DSHFT2=DSHAFT(I)*DSHAFT(I)
   29              MU(I)=RHO*PI*DSHFT2/4.0D0
   30              DSHFT4=DSHFT2*DSHFT2
   31              IA=PI*DSHFT4/64.0D0
   32              EI(I)=E*IA
   33        3     CONTINUE
      C
      C
      C
      C
   34              DO 5 I=1,NEND
   35              DDISC2=DDISC(I)*DDISC(I)
      C                            MDISC IS NEEDED FOR ALPHA (DELTA W, NON-SYNCH)
   36              MDISC(I)=PI*RHO*WDISC(I)*(DDISC2-DSHFT2)/4.0D0
   37              DDISC4=DDISC2*DDISC2
   38              WDISC2=WDISC(I)*WDISC(I)
      C                            INET IS NEEDED FOR BETA (DELTA M)
   39              INET(I)=PI*RHO*WDISC(I)*((DDISC4-DSHFT4)-4.0D0*WDISC2*
     +          (DDISC2-DSHFT2)/3.0D0)/64.0D0
   40        5     CONTINUE
      C
      C
      C
      C
   41         ICOUNT=0
      C2    FORMAT(1X,I10,2F20.1,3X,E20.6)
   42     2  FORMAT(1X,I10,2F20.1,5X,E20.6)
   43     7  FORMAT(1X,11E11.4,/)
```

```
      DO 1 I=RPMST,RPMEND,RPMDEL
      ICOUNT=ICOUNT+1
      RPM=I
      OMEGA=RPM*2.0*PI/60.0
                                  CONVERSION RPM TO OMEGA(RAD/SEC)


      OMEGA2=OMEGA*OMEGA
            DO 10 J=1,NEND
            M(J)=(WT(J)*OMEGA2/EI(J))/9.2500
            ALPHA(J)=NDISC(J)*OMEGA2/(M(J)*M(J)*E(J)*EI(J))
C                       ALPHA IS NECESSARY ONLY FOR
C                             DELTA U (NON-SYMMETRIC)
            BETA(J)=OMEGA2*INET(J)/(M(J)*EI(J))
C                     BETA IS NECESSARY FOR DELTA W (SYMMETRIC)
            BETA1(J)=OMEGA2*INET(J)*M(J)
            ML(J)=M(J)*L(J)
            EIM(J)=EI(J)*M(J)
            EIM2(J)=EIM(J)*M(J)
            EIM3(J)=EIM2(J)*M(J)
C                 EIM IS FOR THE SEGMENT AND LEFT HAND STATION
   10       CONTINUE
C
            DO 11 J=2,NEND
            JM1=J-1
            MML(J)=M(JM1)*L(J)
   11       CONTINUE
C           ********************CALLING NULL MATRIX; INITIALIZATION
C           * MATRIX A(I,J) IS DESTROYED BY 'LEQT1B' IN SUBROUTINE DETNT.********
C           * THEREFORE, IT WAS ABSOLUTELY NECESSARY TO INITIALIZE A(I,J)
C           * TO CLEAN UP THE POLUTED ELEMENTS.
C           ************************************************************
C
C
C           ************** NULLING THE MATRIX A    ***************************
            CALL NULL(N,A)
            CALL MATRIX(N,NEND,M,MML,ML,EIM2,EIM3,A,ALPHA,BETA1,
C                                                CONSTRUCT TOTAL MATRIX FROM INFO C
C           IF(I.EQ.1)WRITE(6,4)
            IF (I .EQ. 10) WRITE(6,7)((A(J,JJ),JJ=1,11),J=1,36)
         DO 6 III=1,N
         DO 6 JJJ=1,11
         A(III,JJJ)=A(I+I,JJJ)/DSQRT(OMEGA)
    6    CONTINUE
         IF(I .EQ. 10) WRITE(6,7)((A(J,JJ),JJ=1,11),J=1,36)
            CALL  DETNT(N,A,XL,DET,NDUMMY)
C
C
C
            IF(ICOUNT .EQ. 1) WRITE(6,4)
C           WRITE(6,2) ICOUNT,RPM,OMEGA,DET
            WRITE(6,2) ICOUNT,RPM,OMEGA,DET
    1       CONTINUE
         STOP
C$REFOFF
         END
C

         SUBROUTINE NULL (N,A)
```

```
      IMPLICIT REAL*8(A-H,M,O-Z)
      DIMENSION A(N,11)
      DO 1 I=1,N
      DO 1 J=1,11
      A(I,J)=0.0D0
    1 CONTINUE
      RETURN
      END

C

      SUBROUTINE MATRIX(N,NEND,M,MML,ML,EIM2,EIM3,A,ALPHA,BETA)
      IMPLICIT REAL*8(A-H,M,O-Z)
      DIMENSION A(N,11)
      DIMENSION ALPHA(NEND), BETA(NEND)
      DIMENSION M(NEND),ML(NEND),MML(NEND),EIM2(NEND),EIM3(NEND)
CCC           THE DIMENSION 7 SHOULD BE LINKED TO M
      K=1
      CALL FREEND(N,ML(K),A,K)
      CALL RIGIDS(N,M(K-1),M(K),MML(K),ML(K),EIM2(K-1),EIM2(K),A,K)
      CALL STEP(N,M(K-1),M(K),MML(K),ML(K),EIM2(K-1),EIM2(K),
     +          EIM3(K-1),EIM3(K),A,K)
      CALL DISCM (N,NEND,M(K-1),M(K),MML(K),ML(K),A,K,BETA(K),
     +          EIM2(K-1),EIM2(K),EIM3(K-1),EIM3(K))
      CALL STEP(N,M(K-1),M(K),MML(K),ML(K),EIM2(K-1),EIM2(K),
     +          EIM3(K-1),EIM3(K),A,K)
      CALL STEP(N,M(K-1),M(K),MML(K),ML(K),EIM2(K-1),EIM2(K),
     +          EIM3(K-1),EIM3(K),A,K)
      CALL DISCM (N,NEND,M(K-1),M(K),MML(K),ML(K),A,K,BETA(K),
     +          EIM2(K-1),EIM2(K),EIM3(K-1),EIM3(K))
      CALL STEP(N,M(K-1),M(K),MML(K),ML(K),EIM2(K-1),EIM2(K),
     +          EIM3(K-1),EIM3(K),A,K)
      CALL RIGIDS(N,M(K-1),M(K),MML(K),ML(K),EIM2(K-1),EIM2(K),A,K)
      CALL FREEND(N,ML(K),A,K)
      RETURN
      END
C

      SUBROUTINE DETNT(N,A,XL,DET,NDUMMY)
      IMPLICIT REAL*8(A-H,M,O-Z)
      INTEGER NDUMMY
      DIMENSION A(N,11),XL(NDUMMY)
      DIMENSION BDUMMY(1,1)
      IBDUM=1
      CALL LEQT1B(A,N,5.5,N,BDUMMY,NDUMMY,IBDUM,1,XL,IER)
      DET=1.0D0
      NLC=5
      IXL=NLC*N
      DO 10 J=1,N
      IXL=IXL+1
      IP=XL(IXL)
      DET=DET*A(J,1)
      IF(IP .NE. I)DET=-DET
   10 CONTINUE
      RETURN
      END
C

      SUBROUTINE FREEND(N,ML,K)
```

```
      IMPLICIT REAL*8(A-H,O-Z)
      DIMENSION A(N,11)
      CALL LOCATE(K,I,J)
      CALL   YEQ0(I,J,ML,A,N)
      CALL   YEQ0(I+1,J+1,ML,A,N)
      K=K+1
      RETURN
      END

      SUBROUTINE STEP(N,MM,M,MML,ML,A,K,BETA1M,EIMM2,EIM2,EIMMM3,EIM3)
      IMPLICIT REAL*8(A-H,O-Z)
      DIMENSION A(N,11)
      CALL LOCATE(K,I,J)
      CALL EQDIS2(I,J,MML,ML,A,N)
      CALL EQANG2(I+1,J-1,MM,M,MML,ML,A,N)
      CALL EQMOM2(I+2,J-2,MML,ML,EIMMM2,EIM2,A,N)
      CALL EQSHR2(I+3,J-3,MML,ML,EIMMM3,EIM3,A,N)
      K=K+1
      RETURN
      END
C

      SUBROUTINE RIGIDS(N,MM,M,MML,ML,EIMMM2,EIM2,A,K)
      IMPLICIT REAL*8(A-H,M,O-Z)
      DIMENSION A(N,11)
      CALL LOCATE(K,I,J)
      CALL   YEQ0(I,J,MML,A,N)
      JODD=J+3
      CALL   YEQ0(I+1,JODD,ML,A,N)
      CALL EQANG2(I+2,J-2,MM,M,MML,ML,A,N)
      CALL EQMOM2(I+3,J-3,MML,ML,EIMMM2,EIM2,A,N)
      K=K+1
      RETURN
      END
C

      SUBROUTINE DISCM (N,NEND,MM,M,MML,ML,A,K,BETA1M,EIMMM2,
     +                  EIM2,EIMMM3,EIM3)
      IMPLICIT REAL*8(A-H,M,O-Z)
      DIMENSION A(N,11)
C     DIMENSION  BETA(NEND)
      CALL LOCATE(K,I,J)
      CALL EQDIS2(I,J,MML,ML,A,N)
      CALL EQANG2(I+1,J-1,MM,M,MML,ML,A,N)
      CALL DELM2 (I+2,J-2,MML,ML,BETA1M,EIMMM2,EIM2,A,N)
C     CALL DELTAV(I+3,J-3,ML,A,ALPHA,N)
      CALL EQSHR2(I+3,J-3,MML,ML,EIMMM3,EIM3,A,N)
      K=K+1
      RETURN
      END
C

      SUBROUTINE EQDIS2(I,J,MML,ML,A,N)
      IMPLICIT REAL*8(A-H,M,O-Z)
      DIMENSION A(N,11)
      A(I+1,J+1)= DCOSH(MML)
      A(I+1,J+2)= DSINH(MML)
      A(I+1,J+3)=  DCOS(MML)
```

```
      A(I+1,J+4) =  DSIN(ML)*EIMMM3
      A(I+1,J+5)=-DCOSH(ML)*EIMMM3
      A(I+1,J+6)=-DSINH(ML)*EIMMM3
      A(I+1,J+7) = -DCOS(ML)*EIMMM3
      A(I+1,J+8) =  DSIN(ML)*EIMMM3
      RETURN
      END

      SUBROUTINE EQANG3(I,J,NM,A,EIMM,ML,L)
      IMPLICIT REAL*8(A-H,M,O-Z)

      DIMENSION A(M,11)
      A(I+1,J+1)= DSINH(ML)*EIMMM3
      A(I+1,J+2)= DCOSH(ML)*EIMMM3
      A(I+1,J+3)= -DSIN(ML)*EIMMM3
      A(I+1,J+4)=  DCOS(ML)*EIMMM3
      A(I+1,J+5)=-DSINH(ML)*EIMMM3
      A(I+1,J+6)=-DCOSH(ML)*EIMMM3
      A(I+1,J+7)=  DSIN(ML)*EIMMM3
      A(I+1,J+8)= -DCOS(ML)*EIMMM3
      RETURN
      END
C

      SUBROUTINE EQANG4(I,J,NM,ML,L,EIMM,A)
      IMPLICIT REAL*8(A-H,M,O-Z)
      DIMENSION A(M,11)
      A(I+1,J+1)= DCOSH(MML)*EIMMM3
      A(I+1,J+2)= DSINH(MML)*EIMMM3
      A(I+1,J+3)= -DCOS(MML)*EIMMM3
      A(I+1,J+4)= -DSIN(MML)*EIMMM3
      A(I+1,J+5)=-DCOSH(ML)*EIMM3
      A(I+1,J+6)=-DSINH(ML)*EIMM3
      A(I+1,J+7)=  DCOS(ML)*EIMM3
      A(I+1,J+8)=  DSIN(ML)*EIMM3
      RETURN
      END
C

      SUBROUTINE EQSHR2(I,J,MML,ML,L,EIMMM3,MM3,A)
      IMPLICIT REAL*8(A-H,M,O-Z)
      DIMENSION A(M,11)
      A(I+1,J+1)= DSINH(MML)*EIMMM3
      A(I+1,J+2)= DCOSH(MML)*EIMMM3
      A(I+1,J+3)=  DSIN(MML)*EIMMM3
      A(I+1,J+4)= -DCOS(MML)*EIMMM3
      A(I+1,J+5)=-DSINH(ML)*EIMM3
      A(I+1,J+6)=-DCOSH(ML)*EIMM3
      A(I+1,J+7)= -DSIN(ML)*EIMM3
      A(I+1,J+8)=  DCOS(ML)*EIMM3
      RETURN
      END
C

      SUBROUTINE DELM2(I,J,MML,ML,L,EIMMM3,MM3,A)
      IMPLICIT REAL*8(A-H,M,O-Z)
      DIMENSION A(M,11)
      A(I+1,J+1)=-EIMMM3*DCOSH(MML)-EIMM3*DCOSH(ML)
```

```
      A(I+1,J+2)=-EIMNM2*DSINH(ML)-EETA1*DCOSH(ML)
      A(I+1,J+3)= EIMNM2*DCOS(ML)+EETA1*DSIN(ML)
      A(I+1,J+4)= EIMNM2*DSIN(ML)-EETA1*DCOS(ML)
      A(I+1,J+5)= EIM2*DCOSH(ML)
      A(I+1,J+6)= EIM2*DSINH(ML)
      A(I+1,J+7)=-EIM2*DCOS(ML)
      A(I+1,J+8)=-EIM2*DSIN(ML)
      RETURN
      END
C
C
      SUBROUTINE   MEQQ(I,J,ML,A,N)

      IMPLICIT REAL*8(A-H,M,O-Z)
      DIMENSION A(N,11)
      A(I+1,J+1)= DCOSH(ML)
      A(I+1,J+2)= DSINH(ML)
      A(I+1,J+3)= -DCOS(ML)
      A(I+1,J+4)= -DSIN(ML)
      RETURN
      END
C
      SUBROUTINE   VEQQ(I,J,ML,A,N)
      IMPLICIT REAL*8(A-H,O,Q-Z)
      DIMENSION A(N,11)
      A(I+1,J+1)= DSINH(ML)
      A(I+1,J+2)= DCOSH(ML)
      A(I+1,J+3)=  DSIN(ML)
      A(I+1,J+4)= -DCOS(ML)
      RETURN
      END
C
      SUBROUTINE   YEQQ(I,J,ML,A,N)
      IMPLICIT REAL*8(A-H,M,O-Z)
      DIMENSION A(N,11)
      A(I+1,J+1)= DCOSH(ML)
      A(I+1,J+2)= DSINH(ML)
      A(I+1,J+3)=  DCOS(ML)
      A(I+1,J+4)=  DSIN(ML)
      RETURN
      END
C
      SUBROUTINE LOCATE(N,I,J)
      I=(N-2)*4+2
      J=3
      IF(N .EQ. 1) I=2
      IF(N .EQ. 1) J=5
      RETURN
      END
C
C

C$ENTRY
C$OPTIONS NOLIST
```

1	17700.0	1853.5	0.[illegible]
2	17701.0	1853.6	[illegible]
3	17702.0	1853.7	0.9220734D 28
4	17703.0	1853.8	[illegible]
5	17704.0	1853.9	[illegible]
6	17705.0	1854.0	[illegible]
7	17706.0	1854.1	[illegible]
8	17707.0	1854.2	[illegible]
9	17708.0	1854.3	[illegible]
10	17709.0	1854.4	0.8650660D 28
11	17710.0	1854.5	0.8507520 28
12	17711.0	1854.6	0.8464360 28
13	17712.0	1854.7	0.8371120 28
14	17713.0	1854.8	0.8277800 28
15	17714.0	1854.9	0.8184390 28
16	17715.0	1855.0	0.8090910 28
17	17716.0	1855.1	0.7997340 28
18	17717.0	1855.2	0.7903690 28
19	17718.0	1855.3	0.7809950 28
20	17719.0	1855.4	0.7716140 28
21	17720.0	1855.5	0.7622240 28
22	17721.0	1855.6	0.7528260 28
23	17722.0	1855.7	0.7434200 28
24	17723.0	1855.8	0.7340060 28
25	17724.0	1855.9	0.7245830 28
26	17725.0	1856.0	0.7151530 28
27	17726.0	1856.1	0.7057140 28
28	17727.0	1856.2	0.6962660 28
29	17728.0	1856.3	0.6868110 28
30	17729.0	1856.4	0.6773470 28
31	17730.0	1856.5	0.6678750 28
32	17731.0	1856.6	0.6583950 28
33	17732.0	1856.7	0.6489060 28
34	17733.0	1856.8	0.6394100 28
35	17734.0	1856.9	0.6299050 28
36	17735.0	1857.0	0.6203910 28
37	17736.0	1857.1	0.6108700 28
38	17737.0	1857.2	0.6013400 28
39	17738.0	1857.3	0.5918020 28
40	17739.0	1857.4	0.5822550 28
41	17740.0	1857.5	0.5727010 28
42	17741.0	1857.6	0.5631380 28
43	17742.0	1857.7	0.5535660 28
44	17743.0	1857.8	0.5439970 28
45	17744.0	1857.9	0.5343990 28
46	17745.0	1858.0	0.5248020 28
47	17746.0	1858.1	0.5151920 28
48	17747.0	1858.3	0.5055850 28
49	17748.0	1858.4	0.4959640 28
50	17749.0	1858.5	0.4863340 28
51	17750.0	1858.6	0.4766960 28
52	17751.0	1858.7	0.4670500 28
53	17752.0	1858.8	0.4573950 28
54	17753.0	1858.9	0.4477330 28
55	17754.0	1859.0	0.4380610 28
56	17755.0	1859.1	0.4283820 28
57	17756.0	1859.2	0.4186940 28
58	17757.0	1859.3	0.4089970 28
		1859.4	0.3992920 28

59	17758.0	1859.6	0.389579D 28
60	17759.0	1859.7	0.379858D 28
61	17760.0	1859.8	0.370128D 28
62	17761.0	1859.9	0.360390D 28
63	17762.0	1860.0	0.350643D 28
64	17763.0	1860.1	0.340888D 28
65	17764.0	1860.2	0.331124D 28
66	17765.0	1860.3	0.321352D 28
67	17766.0	1860.5	0.311572D 28
68	17767.0	1860.6	0.301783D 28
69	17768.0	1860.7	0.291986D 28
70	17769.0	1860.8	0.282181D 28
71	17770.0	1860.9	0.272367D 28
72	17771.0	1861.0	0.262544D 28
73	17772.0	1861.1	0.252714D 28
74	17773.0	1861.2	0.242874D 28
75	17774.0	1861.3	0.233026D 28
76	17775.0	1861.4	0.223170D 28
77	17776.0	1861.5	0.213306D 28
78	17777.0	1861.6	0.203433D 28
79	17778.0	1861.7	0.193551D 28
80	17779.0	1861.8	0.183661D 28
81	17780.0	1861.9	0.173762D 28
82	17781.0	1862.0	0.163855D 28
83	17782.0	1862.1	0.153940D 28
84	17783.0	1862.2	0.144016D 28
85	17784.0	1862.3	0.134084D 28
86	17785.0	1862.4	0.124143D 28
87	17786.0	1862.5	0.114193D 28
88	17787.0	1862.7	0.104235D 28
89	17788.0	1862.8	0.942687D 27
90	17789.0	1862.9	0.842938D 27
91	17790.0	1863.0	0.743103D 27
92	17791.0	1863.1	0.643183D 27
93	17792.0	1863.2	0.543178D 27
94	17793.0	1863.3	0.443087D 27
95	17794.0	1863.4	0.342911D 27
96	17795.0	1863.5	0.242650D 27
97	17796.0	1863.6	0.142303D 27
98	17797.0	1863.7	0.418706D 26
99	17798.0	1863.8	-0.586475D 26
100	17799.0	1863.9	-0.159251D 27
101	17800.0	1864.0	-0.259940D 27

STATEMENTS EXECUTED= 1023804

CORE USAGE OBJECT CODE= 26288 BYTES,ARRAY AREA= 6258 BYTES,TOTAL AREA AVAILABLE

DIAGNOSTICS NUMBER OF ERRORS= 0, NUMBER OF WARNINGS= 0, NUMBER OF EXTE

COMPILE TIME 0.85 SEC,EXECUTION TIME= 11.11 SEC, 15.40.54 FRIDAY 18 /

C*STOP

EXEC: CESEX005 EXEC OF WATFIV COMPLETE WITH RETURN CODE OF 0000.

APPENDIX B

Computer Program for Prohl's Rotor

```
WARNING MODULE(PRIM) NOT FOUND
EXEC: CESSP30V  PROCEEDING: NON-ZERO RETURN CODE FROM SYP.

)          C$JOB          XREF
           C
           C
           C  PROHL3              DISCWT(I),INET(I) DATA INITIALIZATION ADDED
           C                      DO LOOP 5 CC'ED
           C                                                              86-3-19
           C  PROHL4              L'S CORRECTED AT STATIONS 15 & 17       86-3-19
           C
           C  PROHL5              DISCMV  AND FOLLOWING SUBROUTINES ADDED
           C                      DELM2
           C                      DELV2
           C                      DISC, DELTAM, DELTAV ERASED
           C                      ALPHA, BETA CHANGED TO ALPHA1,BETA1
           C                      OVERFLOW-CONTROL FACTOR CHANGED
           C                           WAS SQRT(OMEGA)*2.0D0
           C                           = OMEGA                            86-3-20
           C  PROHL6                   = OMEGA*4                          86-3-20
           C  PROHL7                   = OMEGA*2                          86-3-20
           C                           - DSQRT(OMEGA)                     86-3-20
           C                           = OMEGA*5.0D0                      86-3-20
           C                      E=30.0D0              FROM 29.0D0       86-3-21
           C                      RHO = 0.729881D-3     FROM 0.733D-3     86-3-21
           C                      G = 386.0D0           FROM 12.D0*32.2D0 86-3-21
           C                      L(15) & L(17)  TO OLD VALUES            86-3-21
           C
           C
           C     RPMST  STARTING RPM
           C     RPMEND END RPM
           C     RPMDEL DELTA RPM
           C     A      WORKING MATRIX A(I,J) USED IN SUBROUTINE DTMNT
           C            DIMENSION =(4*NSEG,11)
           C            DATA = 4*NSEG*11
           C     XL     WORKING SPACE USED IN SUBROUTINE DTMNT
           C            DIMENSION = 4*6*NSEG
           C     L      LENGTH OR X-COORD OF SHAFT SEGMENTS MEASURED FROM LEFT END
           C     ML     = M*L ; ONE OF THE MAIN VARIABLES
           C     DSHAFT DIAMETER OF THE SHAFT
           C     DDISC  DIAMETER OF DISC
           C     WDISC  WIDTH OR THICKNESS OF DISC
           C     NSEG   NUMBER OF SEGMENT = (DIMENSION - 1)
           C     NEND   STATION NUMBER AT THE END = DIMENSION OF L
           C            (STATION NUMBER #1 STARTS FROM THE LEFT END, IE. X=0.)
           C     N
           C     PI     =3.141592D0
           C     G      GRAVITATIONAL CONSTANT (386.4D0 IN/SEC**2)
           C
           C     ********************************************************************
           C     INET   NET (POLAR MASS) MOMENT OF INERTIA OF DISC.
           C     E      YOUNG'S MODULUS(PSI)
           C     IA     DIAMETRAL MOMENT OF INERTIA OF (CROSS SECTIONAL) AREA OF
           C            SHAFT (IN**4)
           C     MU     LINEAR SPECIFIC MASS OF SHAFT MATERIAL(MASS PER UNIT LENGTH)
           C                                          ( (LB*SEC**2/IN)/IN  )
           C     RHOW   SPECIFIC WEIGHT OF SHAFT MATERIAL (LB/IN**3)
           C     RHO    SPECIFIC  MASS  OF SHAFT MATERIAL  (LB*SEC**2/IN**4)
           C     ********************************************************************
```

```
      C
      C
      IMPLICIT REAL*8(A-H,M,O-Z)
      REAL*8 IA,INET,L


      INTEGER RPMST,RPMEND,RPMDEL
      C
      C
      C
      DIMENSION A(80,11)
      DIMENSION L(21),ML(21),MML(21)
      DIMENSION DDISC(21), WDISC(21), MDISC(21)
      DIMENSION DISCWT(21)
      DIMENSION DSHAFT(21)
      C     +                     **DIA. OF SHAFT IS 'SEGMENTAL'.
      C     +                       HOWEVER,DSHAFT(SEG)=DSHAFT(NEND)
      DIMENSION M(21),INET(21),ALPHA1(21),BETA1(21)
      DIMENSION EI(21), EIM(21), EIM2(21), EIM3(21)
      DIMENSION MU(21)
      DIMENSION XL(480)
      C                           **DIMENSION OF XL = 4 * 6 * NSEG
      C                           **XL IS USED IN SUBROUTINE DTMNT  **
      C                             AS A WORKING SPACE    **
      C
      C
      C
      C
      DATA A/880*0.0D0/
      DATA NSEG/20/
      DATA E/30.0D6/
      DATA RPMST/2100/, RPMEND/2300/, RPMDEL/1/
      DATA L/0.0D0, 8.1250D0,11.7500D0,13.3125D0,16.9375D0,18.5313D0,
     +             23.8126D0,29.0626D0,29.8126D0,34.0626D0,34.5626D0,
     +             35.0626D0,41.1876D0,43.5626D0,47.2501D0,51.5001D0,
     +             53.5001D0,57.3126D0,61.5626D0,63.1251D0,67.5626D0/
      DATA DSHAFT/  1.6562D0,2.0625D0, 2*2.3437D0,
     +              4*5.7813D0,2.3437D0,2*5.0D0,
     +              2.1875D0,2.0D0,2*2.1875D0,4.9375D0,
     +              5*2.1875D0/
      C                          DSHAFT(NEND)=DSHAFT(NSEG-1)
      DATA DISCWT/3*0.0D0,12.12D0,0.0D0,7.76D0,16.80D0,7.71D0,
     +            2*0.0D0,20.18D0,6*0.0D0,7.85D0,11.15D0,7.01D0,
     +            0.0D0/
      DATA INET/3*0.0D0,0.2235D0,0.0D0,0.1668D0,0.57D0,0.1663D0,
     +          2*0.0D0,0.723D0,6*0.0D0,0.0757D0,0.1454D0,
     +          0.0615D0,0.0D0/
      DATA RHO/0.72981D-3/
      PI=3.1415926D0
      G=386.0D0
      NEND=NSEG+1
      N=NSEG*4
      C     +                   ** N IS USED IN  A(N,11)
      C     +                   ** REASON FOR '11' ------ COMPACTING
      C     +                      ALGORITHM FOR BAND MATRIX
      NDUMMY=N*6
      C                         ** NDUMMY IS USED IN SETM
      C                         ** PURPOSE OF THIS LOOP - TO DEFINE
      C                            MU(I),EI(I),MDISC(I) FROM 1 TO NEND.
      DO 3 I=1,NEND
```

```
      DSHFT2=DSHAFT(I)*DSHAFT(I)
      MU(I)=RHO*PI*DSHFT2/4.0D0
      DSHFT4=DSHFT2*DSHFT2
      IA=PI*DSHFT4/64.0D0
      EI(I)=E*IA
      MDISC(I)=DISCWT(I)/G

    3 CONTINUE
      ICOUNT=0
    2 FORMAT(1X,I10,2F20.1,5X, E20.6)
    7 FORMAT(1X,11E11.3,//)
    4 FORMAT('1')
      DO 1 I=RPMST,RPMEND,RPMDEL
      ICOUNT=ICOUNT+1
      RPM=I
      OMEGA=RPM *2.0D0*PI/60.0D0
C     +                          ** CONVERSION RPM TO OMEGA(RAD/SEC))
      OMEGA2=OMEGA*OMEGA
            DO 10 J=1,NEND
            M(J)=(MU(J) *OMEGA2/EI(J))**0.25D0
            ALPHA1(J)=MDISC(J)*OMEGA2
            BETA1(J)=OMEGA2*INET(J)*M(J)
            ML(J)=M(J)*L(J)
            EIM(J)=EI(J)*M(J)
            EIM2(J)=EIM(J)*M(J)
            EIM3(J)=EIM2(J)*M(J)
   10       CONTINUE
C                                  ** EIM IS A 'SEGMENTAL' PROPERTY
C                                     FOR THE 'SEGMENT' AND '
C                                     THE LEFT HAND 'STATION'
C
C
            DO 11 J=2,NEND
            JM1=J-1
            MML(J)=M(JM1)*L(J)
   11       CONTINUE
C     ********************CALLING NULL MATRIX; INITIALIZATION
C     * MATRIX A(I,J) IS DESTROYED BY 'LEQT1B' IN SUBROUTINE DETNT.*********
C     * THEREFORE, IT WAS ABSOLUTELY NECESSARY TO INITIALIZE A(I,J)
C     * TO CLEAN UP THE POLUTED ELEMENTS.
C     ************************************************************
C     +
C     +
C     +                            ** NULLING THE MATRIX A **   *
      CALL NULL(N,A)
C     +                            ** CONSTRUCT TOTAL MATRIX **OF SECTIONS
C     +
      CALL MATRIX(N,NEND,M,MML,ML,EIM2,EIM3,A,ALPHA1,BETA1)
C     +
C     +
C     IF(ICOUNT .EQ. 10) WRITE(6,7)((A(J,JJ),JJ=1,11),J=1,36)
            DO 6 III=1,N
            DO 6 JJJ=1,11
            A(III,JJJ)=A(III,JJJ)/OMEGA**5.0D0
    6       CONTINUE
C     IF(ICOUNT .EQ. 10) WRITE(6,7)((A(J,JJ),JJ=1,11),J=1,36)
      CALL  DETNT(N,A,XL,DET,NDUMMY)
      IF(ICOUNT .EQ. 1) WRITE(6,4)
      WRITE(6,2) ICOUNT,RPM,OMEGA,DET
```

```
      1         CONTINUE
            STOP
      C*XREFOFF
            END
      C
      C
      C
      '


      C
      C
      C
*WARNING** FORMAT STATEMENT      7 IS UNREFERENCED

      SUBROUTINE NULL (N,A)
      IMPLICIT REAL*8(A-H,M,O-Z)
      DIMENSION A(N,11)
      DO 1 I=1,N
      DO 1 J=1,11
      A(I,J)=0.0D0
    1 CONTINUE
      RETURN
      END
      C

      SUBROUTINE MATRIX(N,NEND,M,MML,ML,EIM2,EIM3,A,ALPHA1,BETA1)
      IMPLICIT REAL*8(A-H,M,O-Z)
      DIMENSION A(N,11)
      DIMENSION ALPHA1(NEND),BETA1(NEND)
      DIMENSION M(NEND),ML(NEND),MML(NEND),EIM2(NEND),EIM3(NEND)
      C                              **  K IS STATION NUMBER **
      K=1
      CALL RGDEND(N,ML(K),A,K)
      CALL STEP(N,M(K-1),M(K),MML(K),ML(K),EIM2(K-1),EIM2(K),
     +          EIM3(K-1),EIM3(K),A,K)
      CALL STEP(N,M(K-1),M(K),MML(K),ML(K),EIM2(K-1),EIM2(K),
     +          EIM3(K-1),EIM3(K),A,K)
      CALL DISCMV(N,NEND,M(K-1),M(K),MML(K),ML(K),A,K,ALPHA1(K),
     +          BETA1(K),EIM2(K-1),EIM2(K),EIM3(K-1),EIM3(K))
      CALL STEP(N,M(K-1),M(K),MML(K),ML(K),EIM2(K-1),EIM2(K),
     +          EIM3(K-1),EIM3(K),A,K)
      CALL DISCMV(N,NEND,M(K-1),M(K),MML(K),ML(K),A,K,ALPHA1(K),
     +          BETA1(K),EIM2(K-1),EIM2(K),EIM3(K-1),EIM3(K))
      CALL DISCMV(N,NEND,M(K-1),M(K),MML(K),ML(K),A,K,ALPHA1(K),
     +          BETA1(K),EIM2(K-1),EIM2(K),EIM3(K-1),EIM3(K))
      CALL DISCMV(N,NEND,M(K-1),M(K),MML(K),ML(K),A,K,ALPHA1(K),
     +          BETA1(K),EIM2(K-1),EIM2(K),EIM3(K-1),EIM3(K))
      CALL STEP(N,M(K-1),M(K),MML(K),ML(K),EIM2(K-1),EIM2(K),
     +          EIM3(K-1),EIM3(K),A,K)
      CALL STEP(N,M(K-1),M(K),MML(K),ML(K),EIM2(K-1),EIM2(K),
     +          EIM3(K-1),EIM3(K),A,K)
      CALL DISCMV(N,NEND,M(K-1),M(K),MML(K),ML(K),A,K,ALPHA1(K),
     +          BETA1(K),EIM2(K-1),EIM2(K),EIM3(K-1),EIM3(K))
      CALL STEP(N,M(K-1),M(K),MML(K),ML(K),EIM2(K-1),EIM2(K),
     +          EIM3(K-1),EIM3(K),A,K)
      CALL STEP(N,M(K-1),M(K),MML(K),ML(K),EIM2(K-1),EIM2(K),
     +          EIM3(K-1),EIM3(K),A,K)
      CALL STEP(N,M(K-1),M(K),MML(K),ML(K),EIM2(K-1),EIM2(K),
     +          EIM3(K-1),EIM3(K),A,K)
```

```
      CALL RIGIDS(N,M(K-1),M(K),MML(K),ML(K),EIM2(K-1),EIM2(K),A,K)
      CALL STEP(N,M(K-1),M(K),MML(K),ML(K),EIM2(K-1),EIM2(K),
     +          EIM3(K-1),EIM3(K),A,K)
      CALL STEP(N,M(K-1),M(K),MML(K),ML(K),EIM2(K-1),EIM2(K),
     +          EIM3(K-1),EIM3(K),A,K)
      CALL DISCMV(N,NEND,M(K-1),M(K),MML(K),ML(K),A,K,ALPHA1(K),
     +          BETA1(K),EIM2(K-1),EIM2(K),EIM3(K-1),EIM3(K))
      CALL DISCMV(N,NEND,M(K-1),M(K),MML(K),ML(K),A,K,ALPHA1(K),
     +          BETA1(K),EIM2(K-1),EIM2(K),EIM3(K-1),EIM3(K))
      CALL DISCMV(N,NEND,M(K-1),M(K),MML(K),ML(K),A,K,ALPHA1(K),
     +          BETA1(K),EIM2(K-1),EIM2(K),EIM3(K-1),EIM3(K))
      CALL FREEND(N,ML(K),A,K)
      RETURN
      END
C

      SUBROUTINE DETNT(N,A,XL,DET,NDUMMY)
      IMPLICIT REAL*8(A-H,M,O-Z)
      INTEGER MDUMMY
      DIMENSION A(N,11),XL(NDUMMY)
      DIMENSION BDUMMY(1,1)
      IBDUM=1
      CALL LEQT1B(A,N,5,5,N,BDUMMY,MDUMMY,IBDUM,1,XL,IER)
      DET=1.0D0
      NLC=5
      IXL=NLC*N
      DO 10 J=1,N
      IXL=IXL+1
      IP=XL(IXL)
      DET=DET*A(J,1)
      IF(IP .NE. J)DET=-DET
   10 CONTINUE
      RETURN
      END
C

      SUBROUTINE SGOEND(N,ML,A,K)
      IMPLICIT REAL*8(A-H,M,O-Z)
      DIMENSION A(N,11)
      CALL LOCATE(K,I,J)
      CALL   YE00(I,J,ML,A,N)
      CALL   ME00(I+1,J-1 ,ML,A,N)
      K=K+1
      RETURN
      END
C

      SUBROUTINE FREEND(N,ML,A,K)
      IMPLICIT REAL*8(A-H,M,O-Z)
      DIMENSION A(N,11)
      CALL LOCATE(K,I,J)
      CALL   ME00(I,J,ML,A,N)
      CALL   VE00(I+1,J-1 ,ML,A,N)
      K=K+1
      RETURN
      END
C
```

```
      SUBROUTINE STEP(N,MM,M,MML,ML,EIMM2,EIM2,EIMM3,EIM3,A,K)
      IMPLICIT REAL*8(A-H,M,O-Z)
      DIMENSION A(N,11)
      CALL LOCATE(K,I,J)
      CALL EQDIS2(I,J,MML,ML,A,N)
      CALL EQANG2(I+1,J-1,MM,M,MML,ML,A,N)
      CALL EQMOM2(I+2,J-2,MML,ML,EIMM2,EIM2,A,N)
      CALL EQSHR2(I+3,J-3,MML,ML,EIMM3,EIM3,A,N)
      K=K+1
      RETURN
      END
C

      SUBROUTINE RIGIDS(N,MM,M,MML,ML,EIMM2,EI2,A,K)
      IMPLICIT REAL*8(A-H,M,O-Z)
      DIMENSION A(N,11)
      CALL LOCATE(K,I,J)
      CALL   YEQ0(I,J,MML,A,N)
      JODD=J+3
      CALL   YEQ0(I+1,JODD,ML,A,N)
      CALL EQANG2(I+2,J-2 ,MM,M,MML,ML,A,N)
      CALL EQMOM2(I+3,J-3 ,MML,ML,EIMM2,EIM2,A,N)
      K=K+1
      RETURN
      END
C

      SUBROUTINE EQDIS2(I,J,MML,ML,A,N)
      IMPLICIT REAL*8(A-H,M,O-Z)
      DIMENSION A(N,11)
      A(I+1,J+1)= DCOSH(MML)
      A(I+1,J+2)= DSINH(MML)
      A(I+1,J+3)=  DCOS(MML)
      A(I+1,J+4)=  DSIN(MML)
      A(I+1,J+5)=-DCOSH(ML)
      A(I+1,J+6)=-DSINH(ML)
      A(I+1,J+7)= -DCOS(ML)
      A(I+1,J+8)= -DSIN(ML)
      RETURN
      END
C

      SUBROUTINE EQANG2(I,J,MM,M,MML,ML,A,N)
      IMPLICIT REAL*8(A-H,M,O-Z)
      DIMENSION A(N,11)
      A(I+1,J+1)= DSINH(MML)*MM
      A(I+1,J+2)= DCOSH(MML)*MM
      A(I+1,J+3)= -DSIN(MML)*MM
      A(I+1,J+4)=  DCOS(MML)*MM
      A(I+1,J+5)=-DSINH(ML)*M
      A(I+1,J+6)=-DCOSH(ML)*M
      A(I+1,J+7)=  DSIN(ML)*M
      A(I+1,J+8)= -DCOS(ML)*M
      RETURN
      END
C

      SUBROUTINE EQMOM2(I,J,MML,ML,EIMM2,EIM2,A,N)
      IMPLICIT REAL*8(A-H,M,O-Z)
```

```
194         DIMENSION A(N,11)
195         A(I+1,J+1)= DCOSH(MML)*EIMMM2
196         A(I+1,J+2)= DSINH(MML)*EIMMM2
197         A(I+1,J+3)= -DCOS(MML)*EIMMM2
198         A(I+1,J+4)= -DSIN(MML)*EIMMM2
199         A(I+1,J+5)=-DCOSH(ML)*EIM2
200         A(I+1,J+6)=-DSINH(ML)*EIM2
201         A(I+1,J+7)=  DCOS(ML)*EIM2
202         A(I+1,J+8)=  DSIN(ML)*EIM2
203         RETURN
204         END
      C
205         SUBROUTINE EQSHR2(I,J,MML,ML,EIMMM3,EIM3,A,N)

206         IMPLICIT REAL*8(A-H,M,O-Z)
207         DIMENSION A(N,11)
208         A(I+1,J+1)= DSINH(MML)*EIMMM3
209         A(I+1,J+2)= DCOSH(MML)*EIMMM3
210         A(I+1,J+3)=  DSIN(MML)*EIMMM3
211         A(I+1,J+4)= -DCOS(MML)*EIMMM3
212         A(I+1,J+5)=-DSINH(ML)*EIM3
213         A(I+1,J+6)=-DCOSH(ML)*EIM3
214         A(I+1,J+7)= -DSIN(ML)*EIM3
215         A(I+1,J+8)=  DCOS(ML)*EIM3
216         RETURN
217         END
      C
218         SUBROUTINE   MEQ0(I,J,ML,A,N)
219         IMPLICIT REAL*8(A-H,M,O-Z)
220         DIMENSION A(N,11)
221         A(I+1,J+1)= DCOSH(ML)
222         A(I+1,J+2)= DSINH(ML)
223         A(I+1,J+3)= -DCOS(ML)
224         A(I+1,J+4)= -DSIN(ML)
225         RETURN
226         END
      C
227         SUBROUTINE   VEQ0(I,J,ML,A,N)
228         IMPLICIT REAL*8(A-H,M,O-Z)
229         DIMENSION A(N,11)
230         A(I+1,J+1)= DSINH(ML)
231         A(I+1,J+2)= DCOSH(ML)
232         A(I+1,J+3)=  DSIN(ML)
233         A(I+1,J+4)= -DCOS(ML)
234         RETURN
235         END
      C
236         SUBROUTINE   YEQ0(I,J,ML,A,N)
237         IMPLICIT REAL*8(A-H,M,O-Z)
238         DIMENSION A(N,11)
239         A(I+1,J+1)= DCOSH(ML)
240         A(I+1,J+2)= DSINH(ML)
241         A(I+1,J+3)=  DCOS(ML)
242         A(I+1,J+4)=  DSIN(ML)
243         RETURN
```

```
244         END
      C
245         SUBROUTINE LOCATE(N,I,J)
246         I=(N-2)*4+2
247         J=3
248         IF(N .EQ. 1) I=0
249         IF(N .EQ. 1) J=5
250         RETURN
251         END
      C
      C
      C
252         SUBROUTINE DELM2 (I,J,MML,ML,BETA1M,EIMMM2,EIM2,A,N)
253         IMPLICIT REAL*8(A-H,M,O-Z)

254         DIMENSION A(N,11)
255         A(I+1,J+1)=-EIMMM2*DCOSH(MML)-BETA1M*DSINH(MML)
256         A(I+1,J+2)=-EIMMM2*DSINH(MML)-BETA1M*DCOSH(MML)
257         A(I+1,J+3)= EIMMM2*DCOS(MML)+BETA1M* DSIN(MML)
258         A(I+1,J+4)= EIMMM2*DSIN(MML)-BETA1M* DCOS(MML)
259         A(I+1,J+5)= EIM2*DCOSH(ML)
260         A(I+1,J+6)= EIM2*DSINH(ML)
261         A(I+1,J+7)=-EIM2*DCOS(ML)
262         A(I+1,J+8)=-EIM2*DSIN(ML)
263         RETURN
264         END
      CC
265         SUBROUTINE DELV2 (I,J,MML,ML,ALPHA1,EIMMM3,EIM3,A,N)
266         IMPLICIT REAL*8(A-H,M,O-Z)
267         DIMENSION A(N,11)
268         A(I+1,J+1)= -EIMMM3*DSINH(MML)-ALPHA1*DCOSH(MML)
269         A(I+1,J+2)= -EIMMM3*DCOSH(MML)-ALPHA1*DSINH(MML)
270         A(I+1,J+3)=  -EIMMM3*DSIN(MML)-ALPHA1* DCOS(MML)
271         A(I+1,J+4)=   EIMMM3*DCOS(MML)-ALPHA1* DSIN(MML)
272         A(I+1,J+5)= EIM3*DSINH(ML)
273         A(I+1,J+6)= EIM3*DCOSH(ML)
274         A(I+1,J+7)=  EIM3*DSIN(ML)
275         A(I+1,J+8)= -EIM3*DCOS(ML)
276         RETURN
277         END
      C
      C
278         SUBROUTINE DISCMV(N,NEND,MM,M,MML,ML,A,K,ALPHA1,BETA1M,
           +                  EIMMM2,EIM2,EIMMM3,EIM3)
279         IMPLICIT REAL*8(A-H,M,O-Z)
280         DIMENSION A(N,11)
281         CALL LOCATE(K,I,J)
282         CALL EQDIS2(I,J,MML,ML,A,N)
283         CALL EQANG2(I+1,J-1,MM,M,MML,ML,A,N)
284         CALL DELM2 (I+2,J-2,MML,ML,BETA1M,EIMMM2,EIM2,A,N)
285         CALL DELV2 (I+3,J-3,MML,ML,ALPHA1,EIMMM3,EIM3,A,N)
286         K=K+1
287         RETURN
288         END
```

APPENDIX C

Numerical Alogrithm

APPENDIX C

Numerical Algorithm

A numerical algorithm for calculation of the critical speeds has been developed and presented in detail in this section. The major process involved in the new method is that of calculation of the the determinant given in eq. (3-30). The process is basically based on "pivoting" and a recurrence characteristic of the banded matrix.

A series of pivoting will be applied to the determinant given in eq. (3-30) in order to triangulate the determinant. When the pivoting is carried out four times consecutively, it will be seen that the pattern can be repeated since the remaining portion of the determinant takes the same form as it started. For the sake of simplicity in counting the number of calculations, one division will be counted as equivalent to one multiplication in the following presentation.

The major process of calculation involved in the Transfer Matrix Method is that of multiplications of four by four matrices. The number of matrix multiplication is identical to the number of segments in the shaft.

Tang and Trumpler (Ref. 73), Wolfe (Ref. 52), or Pestel (Ref. 75) utilized different station vectors so that their matrix dimensions are larger than (4×4). This means their operations require considerably larger number of multiplications. For example, Wolfe used (8×8) matrices.

The top left hand corner of the determinant (eq. 3-30) is shown in Fig. C1. The first pivoting starts with the element a_{11}.

In case a_{11} is zero, the elements should be re-arranged so that the new a_{11} will be non-zero.

The first row is divided by a_{11}, then multiplied by $-a_{21}$, and then added to the second row, term by term, so that the first term in the second row will become zero. Repeating similar operations on the third, fourth, fifth and sixth rows, the determinant becomes as shown in Fig. C2.

Substituting the following terms into the determinant,

$$a'_{2j} = a_{2j} - \frac{a_{21}}{a_{11}} a_{1j}, \quad (j = 2,3,4)$$

$$b'_{ij} = b_{ij} - \frac{b_{i1}}{a_{11}} a_{1j}, \quad (j = 2,3,4;$$

$$i = 1,2,3,4)$$

the determinant becomes as shown in Fig. C3.

$$
\begin{array}{cccc}
a_{11} & a_{12} & a_{13} & a_{14} \\
a_{21} & a_{22} & a_{23} & a_{24} \\
b_{11} & b_{12} & b_{13} & b_{14} \\
b_{21} & b_{22} & b_{23} & b_{24} \\
b_{31} & b_{32} & b_{33} & b_{34} \\
b_{41} & b_{42} & b_{43} & b_{44}
\end{array}
\qquad - 0 -
$$

$$
\begin{array}{cccccccc}
b_{15} & b_{16} & b_{17} & b_{18} \\
b_{25} & b_{26} & b_{27} & b_{28} \\
b_{35} & b_{36} & b_{37} & b_{38} \\
b_{45} & b_{46} & b_{47} & b_{48}
\end{array}
$$

$$
\begin{array}{cccccccc}
c_{11} & c_{12} & c_{13} & c_{14} & c_{15} & c_{16} & c_{17} & c_{18} \\
c_{21} & c_{22} & c_{23} & c_{24} & c_{25} & c_{26} & c_{27} & c_{28} \\
c_{31} & c_{32} & c_{33} & c_{34} & c_{35} & c_{36} & c_{37} & c_{38} \\
c_{41} & c_{42} & c_{43} & c_{44} & c_{45} & c_{46} & c_{47} & c_{48}
\end{array}
$$

- 0 -

Fig. C1

$$
\begin{array}{cccccccccccc}
a_{11} & a_{12} & & a_{13} & & a_{14} & & & & & & \\
0 & a_{22}-\frac{a_{21}}{a_{11}}a_{12} & & a_{23}-\frac{a_{21}}{a_{11}}a_{13} & & a_{24}-\frac{a_{21}}{a_{11}}a_{14} & & & & & & -0- \\
0 & b_{12}-\frac{b_{11}}{a_{11}}a_{12} & & b_{13}-\frac{b_{11}}{a_{11}}a_{13} & & b_{14}-\frac{b_{11}}{a_{11}}a_{14} & b_{15} & b_{16} & b_{17} & b_{18} & & \\
0 & b_{22}-\frac{b_{21}}{a_{11}}a_{12} & & b_{23}-\frac{b_{21}}{a_{11}}a_{13} & & b_{24}-\frac{b_{21}}{a_{11}}a_{14} & b_{25} & b_{26} & b_{27} & b_{28} & & \\
0 & b_{32}-\frac{b_{31}}{a_{11}}a_{12} & & b_{33}-\frac{b_{31}}{a_{11}}a_{13} & & b_{34}-\frac{b_{31}}{a_{11}}a_{14} & b_{35} & b_{36} & b_{37} & b_{38} & & \\
0 & b_{42}-\frac{b_{41}}{a_{11}}a_{12} & & b_{43}-\frac{b_{41}}{a_{11}}a_{13} & & b_{44}-\frac{b_{41}}{a_{11}}a_{14} & b_{45} & b_{46} & b_{47} & b_{48} & & \\
 & & & & & & c_{11} & c_{12} & c_{13} & c_{14} & c_{15} & c_{16} \\
 & & & & & & c_{21} & c_{22} & c_{23} & c_{24} & c_{25} & c_{26} \\
 & & & -0- & & & c_{31} & c_{32} & c_{33} & c_{34} & c_{35} & c_{36} \\
 & & & & & & c_{41} & c_{42} & c_{43} & c_{44} & c_{45} & c_{46}
\end{array}
$$

Fig. C2

$$
\begin{array}{cccc|cccc|cccc}
a_{11} & a_{12} & a_{13} & a_{14} & & & & & & & & \\
0 & a'_{22} & a'_{23} & a'_{24} & & & & & & & & \\
0 & b'_{12} & b'_{13} & b'_{14} & b_{15} & b_{16} & b_{17} & b_{18} & & & & \\
0 & b'_{22} & b'_{23} & b'_{24} & b_{25} & b_{26} & b_{27} & b_{28} & & - 0 - & & \\
0 & b'_{32} & b'_{33} & b'_{34} & b_{35} & b_{36} & b_{37} & b_{38} & & & & \\
0 & b'_{42} & b'_{43} & b'_{44} & b_{45} & b_{46} & b_{47} & b_{48} & & & & \\
\hline
 & & & & c_{11} & c_{12} & c_{13} & c_{14} & c_{15} & c_{16} & c_{17} & c_{18} \\
 & & & & c_{21} & c_{22} & c_{23} & c_{24} & c_{25} & c_{26} & c_{27} & c_{28} \\
 & - 0 - & & & c_{31} & c_{32} & c_{33} & c_{34} & c_{35} & c_{36} & c_{37} & c_{38} \\
 & & & & c_{41} & c_{42} & c_{43} & c_{44} & c_{45} & c_{46} & c_{47} & c_{48}
\end{array}
$$

Fig. C3

This is the first pivoting with respect to a_{11}. It can be seen in Fig. C3 that all the element in the first column, except for a_{11}, became zero.

The minimum number of multiplication during the above pivoting is 18. The first operation can be a_{12}/a_{11} (= β). Then, there are five more operations for the second column, namely $\beta \times a_{21}$, $\beta \times b_{11}$, $\beta \times b_{21}$, $\beta \times b_{31}$, and $\beta \times b_{41}$. Therefore, a total of six operations are necessary for the second column. This should be repeated on the third and fourth column. That is, a total of 18 multiplications are needed.

Similar process of pivoting with respect to the term, a_{22}, results in a determinant shown in Fig. C4.

Substituting the following terms,

$$b''_{ij} = b'_{ij} - \frac{b'_{i2}}{a'_{22}} a'_{2j}, \quad (j = 3,4, \text{ and } i = 1,2,3,4)$$

into the determinant shown in Fig. C4, we find the form as shown in Fig. C5. The number of multiplication involved in the second pivoting is 10. Similarly, another pivoting with respective to the term, b''_{13}, will result in a determinant shown in Fig. C6.

$$
\begin{array}{cccccccccc}
a_{11} & a_{12} & a_{13} & a_{14} & & & & & & \\
0 & a'_{22} & a'_{23} & a'_{24} & - 0 - & & & - 0 - & & \\
0 & 0 & b'_{13} - \frac{b'_{12}}{a'_{22}} a'_{23} & b'_{14} - \frac{b'_{12}}{a'_{22}} a'_{24} & b_{15} & b_{16} & b_{17} & b_{18} & & \\
0 & 0 & b'_{23} - \frac{b'_{22}}{a'_{22}} a_{23} & b'_{24} - \frac{b_{22}}{a'_{22}} a'_{24} & b_{25} & b_{26} & b_{27} & b_{28} & & \\
0 & 0 & b'_{33} - \frac{b'_{32}}{a'_{22}} a'_{23} & b'_{34} - \frac{b'_{32}}{a'_{22}} a'_{24} & b_{35} & b_{36} & b_{37} & b_{38} & & \\
0 & 0 & b'_{43} - \frac{b'_{42}}{a'_{22}} a'_{23} & b'_{44} - \frac{b'_{42}}{a'_{22}} a'_{24} & b_{45} & b_{46} & b_{47} & b_{48} & & \\
 & & & & c_{11} & c_{12} & c_{13} & c_{14} & c_{15} & c_{16} & c_{17} & c_{18} \\
 & & & & c_{21} & c_{22} & c_{23} & c_{24} & c_{25} & c_{26} & c_{27} & c_{28} \\
 & & - 0 - & & c_{31} & c_{32} & c_{33} & c_{34} & c_{35} & c_{36} & c_{37} & c_{38} \\
 & & & & c_{41} & c_{42} & c_{43} & c_{44} & c_{45} & c_{46} & c_{47} & c_{48}
\end{array}
$$

Fig. C4

$$
\begin{array}{cccc|cccc|cccc|c}
a_{11} & a_{12} & a_{13} & a_{14} & & & & & & & & & \\
0 & a'_{22} & a'_{23} & a'_{24} & \multicolumn{4}{c|}{- 0 -} & \multicolumn{4}{c|}{- 0 -} & & \\
0 & 0 & b''_{13} & b''_{14} & b_{15} & b_{16} & b_{17} & b_{18} & & & & & \\
0 & 0 & b''_{23} & b''_{24} & b_{25} & b_{26} & b_{27} & b_{28} & \multicolumn{4}{c|}{- 0 -} & \\
0 & 0 & b''_{33} & b''_{34} & b_{35} & b_{36} & b_{37} & b_{38} & & & & & \\
0 & 0 & b''_{43} & b''_{44} & b_{45} & b_{46} & b_{47} & b_{48} & & & & & \\
\hline
 & & & & c_{11} & c_{12} & c_{13} & c_{14} & c_{15} & c_{16} & c_{17} & c_{18} & \\
 & \multicolumn{2}{c}{- 0 -} & & c_{21} & c_{22} & c_{23} & c_{24} & c_{25} & c_{26} & c_{27} & c_{28} & \multicolumn{1}{c}{- 0 -} \\
 & & & & c_{31} & c_{32} & c_{33} & c_{34} & c_{35} & c_{36} & c_{37} & c_{38} & \\
 & & & & c_{41} & c_{42} & c_{43} & c_{44} & c_{45} & c_{46} & c_{47} & c_{48} &
\end{array}
$$

Fig. C5

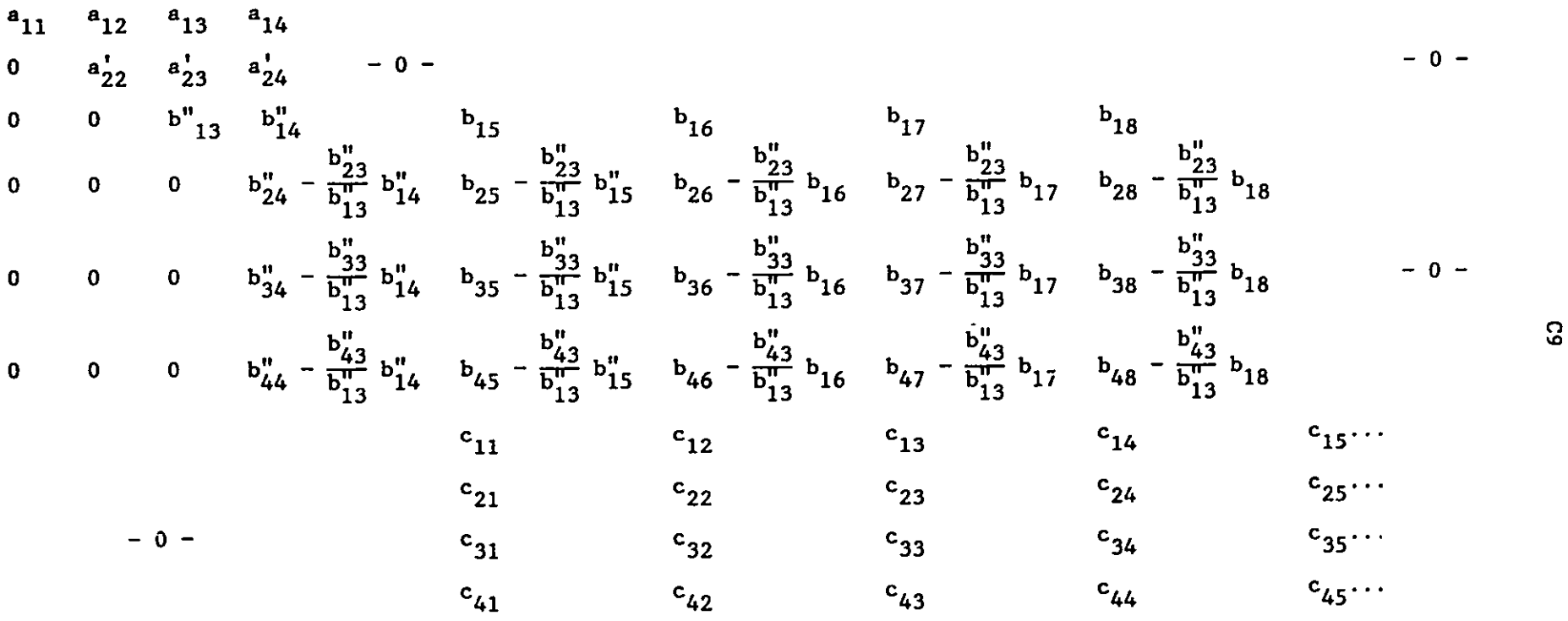

Fig. C6

Again, substituting the following terms into the determinant of Fig. C6,

$$b''_{ij} = b''_{ij} - \frac{b''_{i3}}{b''_{13}} b''_{1j}, \qquad (j = 4, \text{ and } i = 2,3,4)$$

$$b'_{ij} = b_{ij} - \frac{b''_{i3}}{b''_{13}} b_{1j}, \qquad (j = 5,6,7,8 \text{ and } i = 2,3,4)$$

we have the determinant shown in Fig. C7. A total of 18 multiplications were necessary in the process of the third pivoting with respect to the term, b''_{13}.

Once again, pivoting with respect to b'''_{24} will result in a determinant shown in Fig. C8. The number of multiplications carried out during this operation (It is the fourth pivoting) is ten.

Therefore, we have a total of 56 multiplications in four pivoting operations.

$$
\begin{array}{cccc|cccc}
a_{11} & a_{12} & a_{13} & a_{14} & 0 & 0 & 0 & 0 \\
0 & a'_{22} & a'_{23} & a'_{24} & 0 & 0 & 0 & 0 \\
0 & 0 & b''_{13} & b''_{14} & b_{15} & b_{16} & b_{17} & b_{18} \\
0 & 0 & 0 & b'''_{24} & b'_{25} & b'_{26} & b'_{27} & b'_{28} \\
0 & 0 & 0 & b''''_{34} & b'_{35} & b'_{36} & b'_{37} & b'_{38} \\
0 & 0 & 0 & b''''_{44} & b'_{45} & b'_{46} & b'_{47} & b'_{48} \\
\multicolumn{4}{c|}{\multirow{4}{*}{- 0 -}} & c_{11} & c_{12} & c_{13} & c_{14} \\
\multicolumn{4}{c|}{} & c_{21} & c_{22} & c_{23} & c_{24} \\
\multicolumn{4}{c|}{} & c_{31} & c_{32} & c_{33} & c_{34} \\
\multicolumn{4}{c|}{} & c_{41} & c_{42} & c_{43} & c_{44}
\end{array}
\qquad
\begin{array}{cccc}
c_{15} & c_{16} & c_{17} & c_{18} \\
c_{25} & c_{26} & c_{27} & c_{28} \\
c_{35} & c_{36} & c_{37} & c_{38} \\
c_{45} & c_{46} & c_{47} & c_{48}
\end{array}
\qquad \text{- 0 -}
$$

Fig. C7

$$
\begin{array}{cccc|cccccc|cc}
a_{11} & a_{12} & a_{13} & a_{14} & 0 & 0 & 0 & 0 & 0 & 0 & \\
0 & a'_{22} & a'_{23} & a'_{24} & 0 & 0 & 0 & 0 & 0 & 0 & - 0 - \\
0 & 0 & b''_{13} & b''_{14} & b15 & b_{16} & b_{17} & b_{18} & 0 & 0 & \\
0 & 0 & 0 & b'''_{24} & b'_{25} & b'_{26} & b'_{27} & b'_{28} & 0 & 0 & \\
0 & 0 & 0 & 0 & b'_{35} - \frac{b'''_{34}}{b'''_{24}} b'_{25} & b'_{36} - \frac{b'''_{34}}{b'''_{24}} b'_{26} & b'_{37} - \frac{b'''_{34}}{b'''_{24}} b'_{27} & b'_{38} - \frac{b'''_{34}}{b'''_{24}} b'_{28} & 0 & 0 & \\
0 & 0 & 0 & 0 & b'_{45} - \frac{b'''_{44}}{b'''_{24}} b'_{25} & b'_{46} - \frac{b'''_{44}}{b'''_{24}} b'_{26} & b'_{47} - \frac{b'''_{44}}{b'''_{24}} b'_{27} & b'_{48} - \frac{b'''_{44}}{b'''_{24}} b'_{28} & 0 & 0 & \\
\hline
 & & & & c_{11} & c_{12} & c_{13} & c_{14} & c_{15} & c_{16}\cdots & \\
 & & & & c_{21} & c_{22} & c_{23} & c_{24} & c_{25} & c_{26}\cdots & \\
 & - 0 - & & & c_{31} & c_{32} & c_{33} & c_{34} & c_{35} & c_{36}\cdots & \\
 & & & & c_{41} & c_{42} & c_{43} & c_{44} & c_{45} & c_{45}\cdots &
\end{array}
$$

C12

Fig. C8

$$
\begin{array}{cccccccccccc}
a_{11} & a_{12} & a_{13} & a_{14} & & & & & & & & \\
 & a'_{22} & a'_{23} & a'_{24} & & & - 0 - & & & & & \\
 & & b''_{13} & b''_{14} & b_{15} & b_{16} & b_{17} & b_{18} & & & & \\
 & & & b'''_{24} & b'_{25} & b'_{26} & b'_{27} & b'_{28} & & & & \\
 & & & & b''_{35} & b''_{36} & b''_{37} & b''_{38} & & - 0 - & & \\
 & & & & b''_{45} & b''_{46} & b''_{47} & b'_{48} & & & & \\
 & & & & c_{11} & c_{12} & c_{13} & c_{14} & c_{15} & c_{16} & c_{17} & c_{18} \\
 & - 0 - & & & c_{21} & c_{22} & c_{23} & c_{24} & c_{25} & c_{26} & c_{27} & c_{28} \\
 & & & & c_{31} & c_{32} & c_{33} & c_{34} & c_{35} & c_{36} & c_{37} & c_{38} \\
 & & & & c_{41} & c_{42} & c_{43} & c_{44} & c_{45} & c_{46} & c_{47} & c_{48}
\end{array}
$$

Fig. C9

Substituting the terms,

$$b''_{ij} = b'_{ij} - \frac{b'''_{i4}}{b'''_{24}} b'_{2j}, \qquad (j = 5,6,7,8 \text{ and } i = 3,4)$$

into the determinant shown in Fig. C8, we have a determinant shown in Fig. C9.

Now, it is obvious that the shape of the remaining portion to be pivoted is identical to that of Fig. C1. That is, b''_{35} of Fig. C9 corresponds to a_{11} in Fig. C1, and a_{14} and b_{48} in Fig. C1 correspond to b''_{38} and C_{48} in Fig. C9.

This completes one round of the recurrence scheme. That is, we started with the partitioned matrices A and B; and fifty-six multiplications later, we have to start the same scheme all over again with the similar matrices B" and C (see Fig. C10).

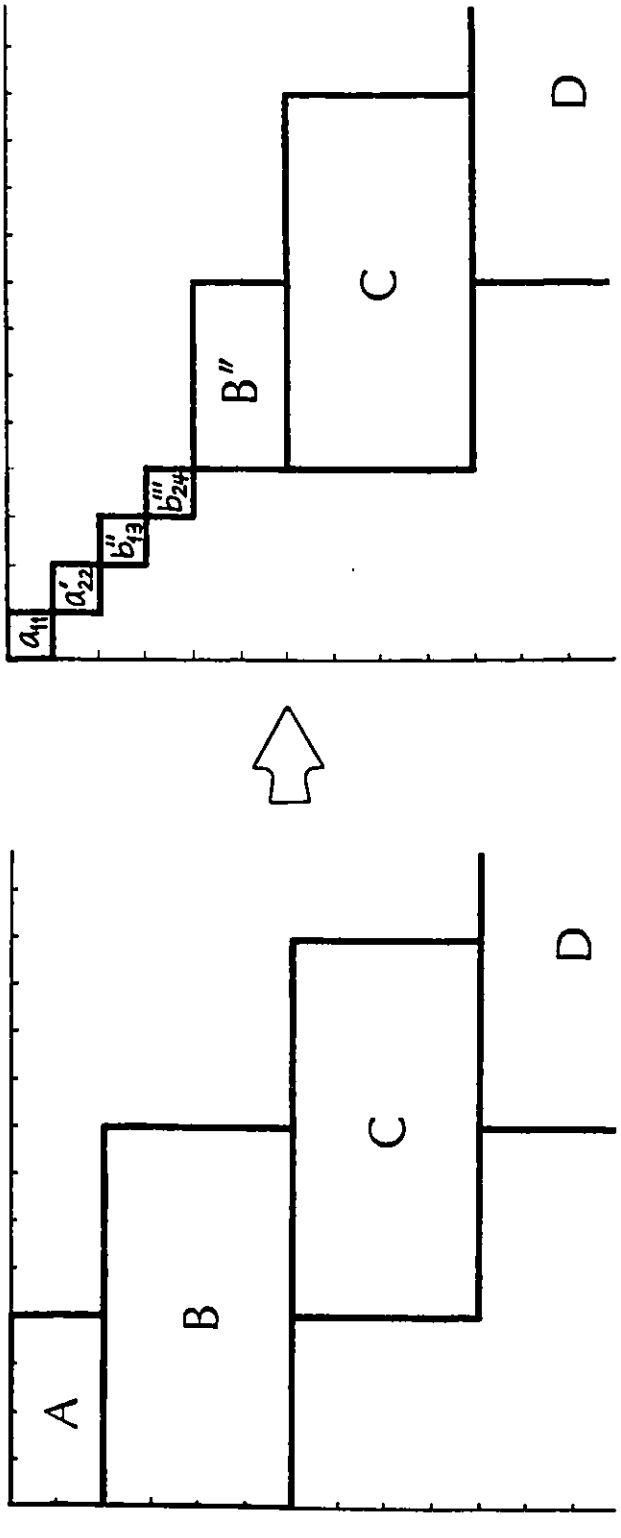

Fig. C10

At the end of the repeated operations, there will be a 4×4 matrix, the determinant of which can be calculated as usual way. The final operation with the 4×4 matrix can be seen easily when the [C] matrix in the previous page become a 2×4 matrix, ie. one of the "end conditions".

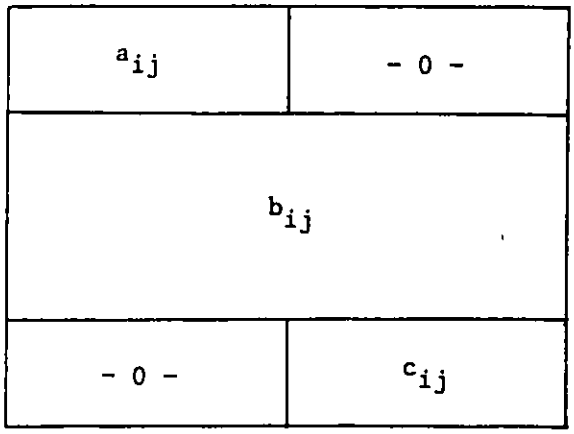

After the first series of "pivoting" operations, the above matrix becomes

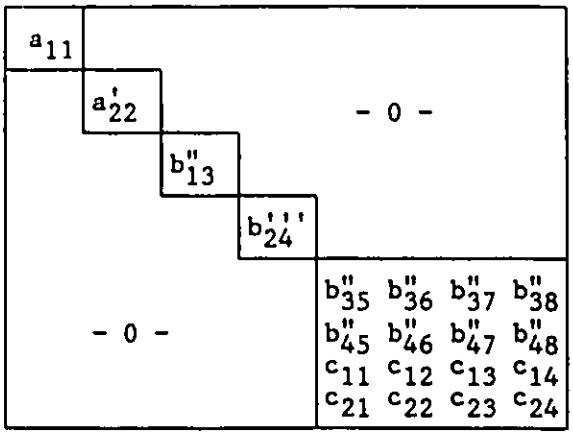

Triangulation of this four by four determinant is similar to previous operation and straightforward.

Once the triangulation of the determinant is accomplished, the value of the determinant is merely the product of all the diagonal terms. Since the task at hand is to find such an ω (the rotational speed of the shaft) that it makes the value of the determinant a zero, a series of ω's are substituted in orderly manner until the value of the corresponding determinant becomes a zero or smaller. Various types of root searching technique can be adopted once the method of calculation of the determinant is resolved.

It is recapitulated that the number of multiplications necessary in this new method is 56 per segment of the shaft.

UNIVERSITÉ D'OTTAWA
UNIVERSITY OF OTTAWA